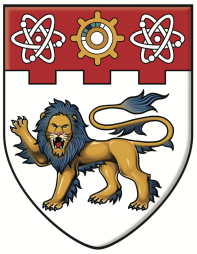

NANYANG TECHNOLOGICAL UNIVERSITY

Mechanisms regulating adult neurogenesis in the hypothalamus using a genetic inducible-approach to label and optogenetically stimulate hypothalamic neural progenitors

RAHUL LEKHRAJ PESWANI

WARWICK-NTU Neuroscience PhD Programme

School of Biological Sciences

2018

Acknowledgments

I would like to thank my supervisors, Professor Nicholas Dale and Asst. Prof Ayumu Tashiro for giving me the opportunity to work in their labs and pursue my interest in Neuroscience. The practical experience I have gained throughout this project will undoubtedly benefit me in my future career as a research scientist, for which I am very grateful. I would like to express my deep gratitude for their undivided attention toward my provision and support through every step of my project, experimentally and academically. Their generosity in patience and effort is greatly appreciated and respected.

I would also like to extend my thanks to the past and present members of the Dale and Tashiro labs for their warm reception and keen support when required. I would particularly like to thank my colleagues, Mehdi Fallahnezad and Vanja Knops for helping me to look at the humorous side of my hardships, Eric Pollatzek and Matei Bolborea for his dedication to always answering my questions, Joe van der Wiel and Daniel Cooper for their assistance in other matters.

I would like to acknowledge and thank the following people for their contribution toward my PhD project; Sandhya Kamath for her assistance in blinding immunostained sections, Paul Anderson for his assistance in surgical procedures (optic fibre implantation), animal facility staff from the Biological Research Centre of A*STAR (Singapore) and University of Warwick (United Kingdom) for their assistance in genotyping transgenic mice pertaining to my project.

Table of contents

List of figures

Chapter 1:

Chapter 2:

Chapter 3:

Chapter 4:

List of Table

Abbreviations

3V	3rd ventricle
4-OHT	4-hydroxy tamoxifen
Ace-K	Acesulfame-K
aCSF	aritifical CSF
AgRP	Agouti-related protein
ANOVA	Analysis of variance
Ara-C	Arabinosylcytosine
Arc	Arcuate nucleus
ATP	Adenosine triphosphate
BBB	Blood-brain barrier
BDNF	Bone-derived neurotrophic factor
BLBP	Brain lipid-binding protein
BrdU	5-Bromo-2′-deoxyuridine
CAG	CMV early enhancer/chicken β-actin
CatCh	Calcium translocating channelrhodopsin
ChR	Channelrhodopsin
CNS	Central nervous system
CNTF	Cilliary neurotrophic factor
CSF	Cerebrospinal fluid
DAPI	Diamidino-2-phenylindole-dihydrochloride
Dcx	Doublecortin
DG	Dentate Gyrus
DMH	Dorsomedial nucleus
DMSO	Dimethyl sulfoxide
DNA	Deoxyribonucleic acid
EGF	Epidermal growth factor
eGFP	Enhanced green fluorescent protein
FGF-10	Fibroblast growth factor-10
FGF-2	Fibroblast growth factor-2
GFAP	Glial fibrillary acidic protein

GLAST	Glutamate aspartate transporter
GLUT-1/2	Glucose transporter 1/2
Hes-5	Hes Family BHLH Transcription Factor 5
HFD	High-fat diet
HPA	Hypothalamic-pituitary axis
i.c.v.	intracerebroventricular
i.p.	intraperitoneal
IGF-1	Insulin-like growth factor 1
IKKβ	Inhibitor of nuclear factor kappa-B kinase beta
LED	Light-emitting diode
LH	Lateral hypothalamus
LHA	Lateral hypothalamic area
MAP-2	Microtubule-associated protein 2
ME	Median eminence
NeuN	Neuronal nuclei
NF-κB	Nuclear factor kappaB
NG2	Neural/glial antigen 2
NPY	Neuropeptide Y
NSC	Neural stem cell
NTPDase-2	Ectonucleotidase-2
OB	Olfactory buld
OPC	oligodendrocytic progenitor cell
P2X	Purinoreceptor X
P2Y	Purinoreceptor Y
PB	Phosphate buffer
PCNA	Proliferating cell nuclear antigen
PCR	Polymerase chain reaction
PDGFRα	Platelet-derived growth factor receptor α
Pe	Periventricular nucleus
PeA	Periventricular area
PFA	Paraformaldehyde
POMC	Pro-opiomelanocortin

Prox-1	Prospero homeobox protein 1
PSA-NCAM	Polysialylated-neural cell adhesion molecule
PVA-DABCO	Polyvinyl - 1,4-diazabicyclo[2.2.2]octane
PVN	Paraventricular nucleus
PZ	parenchymal zone
Rax	retina and anterior neural fold homeobox
ROI	Region of interest
RTN	Retrotrapezoid nucleus
SEM	Standard error of the mean
SGZ	Subgranular zone
Sox-2	SRY (sex determining region Y)-box 2
SSC	Saline sodium citrate
STAT3	Signal transducer and activator of transcription 3
SVZ	Subventricular zone
TAM	Tamoxifen
Tas1r2/3	Taste receptor type 1 member 2/3
TBS	Tris-buffered saline
VMH	Ventromedial nucleus
VZ	Ventricular zone
YFP	Yellow fluorescent protein

Abstract

Adult neurogenesis is defined as the generation of newborn functional neurons during adulthood. In addition to the canonical neurogenic niches in the hippocampus and lateral ventricles, the hypothalamus has recently been shown to exhibit adult neurogenesis. We first aimed to elucidate the regulation of adult hypothalamic neurogenesis by investigating the effect of novel external factors on hypothalamic cell proliferation: physical exercise, antidepressant (fluoxetine) and non-nutritive artificial sweetener, acesulfame-K (Ace-K). Short/mid-term (14-21 days) exposure of Ace-K, but not physical exercise or fluoxetine induced changes in the number of newly generated cells: a decrease in the dorsomedial nucleus at 7 days, and an increase in the ventromedial nucleus at 14 days. Next, although the exact identity of the neural stem/progenitor cells underlying hypothalamic neurogenesis is still under debate, tanycytes have been proposed as an attractive candidate. However, the cellular/molecular mechanism underlying their neurogenic role has yet to be elucidated. We hypothesized that the intracellular calcium signalling induced by their chemosensory role might also be linked to their neurogenic role. We used a Cre-inducible genetic-labelling approach (nestin-CreERT2:Rosa-YFP) to characterize hypothalamic nestin+ stem/progenitor cells as part of validating this strategy for *in vivo* optogenetic stimulation of tanycytes. The vast majority (97%) of labelled cells were found at the ependymal layer and identified as tanycytes and ependymocytes. A small percentage of parenchymal cells were also labelled, which resembled neuronal and glial cells. Over time, an increasing trend in parenchymal labelled cells was seen, indicating a slow basal rate of neurogenesis. We then generated a transgenic line (nestin-CreERT2:Rosa-ChR2-YFP) in which tanycytes expressed Channelrhodopsin-2. Optogenetic stimulation of tanycytes in mouse brain slices induced strong and reproducible intracellular calcium waves. *In vivo* optogenetic stimulation of hypothalamic cells specified by nestin expression induced an increase in newly generated cells in close proximity to optically-responsive tanycytes, whilst long-term optogenetic stimulation indicated an increasing trend in labelled tanycytes and hypothalamic neurons. We have thus, successfully generated an optogenetic mouse model and validated its use in the hypothalamus to stimulate tanycytes (and potentially other putative neural progenitors). Although we cannot determine if the observed effects were solely due to tanycyte stimulation, we speculate that adult hypothalamic neurogenesis is regulated slowly, requiring long-term stimulation (optogenetically or by external/environmental stimuli). Further investigation using this optogenetic approach would prove helpful in elucidating the role/contribution of tanycytes in the regulation of adult hypothalamic neurogenesis.

Chapter 1: Review of adult neurogenesis in the hypothalamus

Neurogenesis is defined as the process by which functionally integrated neurons are generated from progenitor cells, referred to as neural stem cells [Ming & Song, 2005]. It was long believed that this process was limited to the embryonic and perinatal stages of mammalian development, and that the adult central nervous system was incapable of regenerating [Ramon y Cajal, 1913]. However, this notion was challenged five decades ago, and has since been disproven with accumulating evidence for a plastic, adaptable and regenerative adult brain.

Stem cells generally refer to progenitor cells responsible for the initiation of a lineage and retain two key characteristics; the ability to amplify and self-renew through cell division, and generate specialized cell-types through differentiation [Ming & Song, 2011]. Atlhough neural stem cells (NSCs) are a more specialized subset of stem cells, pertaining to neural tissue, they still retain these cardinal properties; they are multipotent and are able to commit to a range of neural lineages (including neurons and glia) whilst being able to self-renew for extended periods of time [Gage, 2000].

Historical overview of adult neurogenesis

The first study to suggest the occurrence of neurogenesis after birth and in adulthood came from a pioneering study that made use of the [^{3}H]-thymidine radiolabelling technique to identify proliferating cells [Altman and Das, 1965]. [^{3}H]-thymidine is permanently incorporated into the DNA of dividing cells in S-phase, which can be detected with autoradiography [Sidman et al, 1959]. Using this technology, Altman and colleagues were able to provide anatomical evidence for the generation of cells *de novo* in the dentate gyrus of the hippocampus [Altman & Das, 1965], neocortex [Altman 1963], and in the olfactory bulb [Altman, 1969]. The results of these studies were only substantiated later by Kaplan and colleagues, using electron microscopy to reveal typical neuronal structures in [^{3}H]-thymidine-labelled cells, including axons, dendrites and the presence of synapses [Kaplan & Hinds, 1977; Kaplan & Bell, 1984; Kaplan et al, 1985]. Soon after, the first studies emerged providing evidence for functional roles of adult neurogenesis, in this case, in the seasonal learning of new songs involved in courtship behaviour in songbirds [Goldman & Nottebohm, 1983; Paton and Nottebohm, 1984;

Alvarez-Buylla & Nottebohm, 1988]. In these studies, it was shown that there was a substantial seasonal replacement of neurons in the high vocal centre (a structure critical for song production) with newly generated neurons that originated from the lateral ventricle walls. Indeed, the increase in neuronal replacement in this region correlated with the peak season in learning new songs [Nottebohm, 2004].

Progress in the field of adult neurogenesis accelerated upon the development and use of a simpler labelling technique that uses the same premise as [^{3}H]-thymidine labelling. 5-bromo-2'-deoxyuridine (BrdU) is a thymidine analogue that permanently incorporates into the DNA of S-phase dividing cells and has thus, been used to identify newborn cells and/or neural progenitors [Taupin, 2007]. In addition, the cellular fate of these BrdU-labelled cells can also be determined through immunohistochemical/phenotypic analysis (e.g. BrdU co-localization with neuronal/cell fate markers) at later time-points. Furthermore, the extent of newborn cells' survival can be examined by quantitative comparison of BrdU+ cells between two different time points [Kuhn et al, 1996; Taupin, 2007]. Thus, this tool has since allowed for robust analysis of cell proliferation, cell survival and differentiation. However, a key limitation of using BrdU as a labelling tool is its progressive dilution in rapidly-dividing stem cells [Kiel et al, 2007]; because the BrdU label is shared between daughter cells, after multiple proliferation events, the levels of BrdU becomes undetectable by immunohistochemistry. Another one of the major pitfalls is the fact that BrdU is a toxic and mutagenic substance, which can trigger a range of ectopic/detrimental effects on cells that incorporate it (and hence, on neurogenesis) [Taupin, 2007]. As a result more recent studies have made use of genetic markers via viral-mediated or transgenic approaches (e.g. inducible cre-recombinase) to permanently label, lineage-trace and/or manipulate putative adult neural stem cells *in vivo* [Solek & Ekker, 2012; Dhaliwal & Lagace, 2011]. Indeed, using combined labelling and electrophysiological techniques (such as patch-clamp recording of retroviral GFP-labelled adult-born neurons), studies have provided irrefutable evidence that newborn neurons in the adult brain are indeed functionally and synaptically integrated [van Praag et al, 2002, Belluzzi et al, 2003].

Finally, the identification of growth factors that render mitogenic and trophic effects in neural tissue, such as epidermal growth factor (EGF) and fibroblast growth factor 2 (FGF-

2), allowed the successful isolation and culture of neural stem cells *in vitro* [Reynolds and Weiss, 1992]. As a result, a novel 'neurosphere' assay was developed and has since been used as the definitive experimental test for *bona fide* NSCs [Reynolds & Rietze, 2005]. In this assay, isolated cells that were able to form neurospheres *in vitro* (proliferate), whose progeny could also form neurospheres (self-renew) and differentiate into tissue-specific cell-types, were granted as *bona fide* NSCs [Reynolds & Weiss, 1996; Weiss et al, 1996; Reynolds & Rietze, 2005]. Using this assay, both human embryonic and adult neural stem cells have subsequently been isolated and studied [Kukekov et al, 1999; Vescovi et al, 1999]. However, the neurosphere assay has recently been criticized for its lack of stringency to isolate *bona fide* NSCs due to the lack of markers that allow discrimination between 'true' NSCs and transit-amplifying neural progenitors [Pastrana et al, 2011]. As a result, neurospheres may constitute of a heterogeneous cell population (that may consist of different lineage-committed progenitors and not multipotent NSCs) instead of a homogenous clonal population [Gil-Perotin et al, 2013]

Studies have since indicated the evolutionary conservation of postnatal and adult neurogenesis across several species of higher vertebrates, including in humans (although the latter is still highly debated; see below) [Lledo et al, 2006; Eriksson et al, 1998; Kempermann, 2012, Grandel & Brand, 2013]. It is now widely accepted that neurogenesis occurs in distinct regions of the adult mammalian brain [Ming and Song, 2005]. Two canonical neurogenic niches have since been identified, namely, the subgranular zone (SGZ) of the dentate gyrus in the hippocampus and the subventricular zone (SVZ) lining the lateral ventricles, and until very recently, the vast majority of research in the field has focused on these two brain regions due to the robust level of neurogenesis observed [Gage, 2000; Ming and Song, 2011].

The canonical neurogenic niches

In the SGZ of the rodent dentate gyrus, adult-born cells have been seen to briefly migrate (as neuroblasts) into the inner granule cell layer, where they further differentiate and mature into excitatory granule neurons that project into the CA3 region of the hippocampus within 1 to 3 weeks from their birth (in rodents) [Lledo et al, 2006; Zhao et al, 2008]. The functional integration of these newborn neurons into the hippocampal

neural circuitry has been confirmed and characterized using electrophysiological recordings [van Praag, 2002]. It has been suggested that SGZ neurogenesis plays a role in hippocampus-dependent learning and memory formation [Zhao et al, 2008].

In the SVZ of rodents, adult-born cells acquire a migratory phenotype (expressing markers such as doublecortin; DCX, and polysialylated neural-cell-adhesion molecule; PSA-NCAM) and travel as neuroblasts to the olfactory bulb via the rostral migratory stream [Lledo et al, 2006; Whitman & Greer, 2009]. Unlike hippocampal adult-born cells, those of the SVZ migrate over a great distance, and hence are highly regulated by diffusible factors and scaffolding structures [Kaneko et al, 2017]. Chemoattractants Prokineticin-2, Netrin-1 and glial cell line-derived neurotrophic factor are released from the rostral olfactory bulb [Murase & Horwitz 2002; Ng et al. 2005; Paratcha et al, 2006], and the chemorepellant Slit2 secreted from the septum [Wu et al, 1999] to provide directional (caudal-to-rostral) migration for SVZ neuroblasts, whilst being kept along the migratory pathway by the attractant Hepatocyte growth factor [Garzotto et al. 2008; Wang et al. 2011a]. Neuroblasts migrate along the RMS as chains [Lois et al, 1996], enabled through dynamic regulation of PSA-NCAM-mediated adhesion [Hu et al, 1996]. Interestingly, neuroblasts also express matrix metalloproteinases (proteolytic enzymes well-known for their role in tumorigenesis and cancer-cell migration [Nabeshima et al, 2002]), which were proven essential for cytokine-mediated migration [Barkho et al, 2008]. Upon arrival at the olfactory bulb, neuroblasts detach from their chain, which is regulated by extracellular matrix proteins such as Reelin and Prokineticin-2 [Hack et al, 2002; Ng et al, 2005], and migrate radially into the olfactory bulb where they differentiate into one of two inhibitory (granule or periglomerular) interneurons [Kaneko et al, 2017]. Adult-born neurons in the olfactory bulb exhibited a lower activation threshold for novel odors and/or for odors involved in reward-associated memories, thereby implicating SVZ neurogenesis in perceptual learning, olfactory discrimination and ultimately, olfactory-dependent memory formation [Magavi et al, 2005; Lazarini & Lledo, 2011; Lepousez & Lledo, 2013].

Both neurogenic canonical niches share some broad similarities. Firstly, the NSCs underlying neurogenesis in both regions have been identified as radial glia-like cells that express astrocytic features/genes [Doetsch et al, 1999; Seri et al, 2001]. Whilst these cells are predominantly quiescent [Morshead et al, 1994; Doetsch et al, 1999; Seri et al,

2001], these cells are capable of long-term self-renewal and generating several lineages (astrocytes, oligodendrocytes and neurons), both being hallmarks of NSCs [Ge et al, 2007; Kriegstein & Alvarez-Buylla, 2009]. It should be noted however, that it has been debated if the SVZ may harbour a heterogeneous population of NSCs, in which ependymal cells may also partake in neurogenesis [Chojnacki et al, 2009]. Secondly, although both niches comprise of different cell-types and generate different neuronal cell-types, their lineage hierarchy and expression profiles are somewhat mirrored; [Glial fibrillary acidic protein-positive (GFAP+), Sox-2+ and/or nestin+] NSCs of both niches give rise to highly proliferative (Sox-2+ and/or nestin+) intermediate progenitor cells (also referred to as transit amplifying cells), which are capable of developing into (Dcx+) migrating immature neurons (neuroblasts) and differentiating further into (Prox1+, NeuN+ or other specific neuronal marker+) mature, functionally integrated neurons [Ming & Song, 2011] (Figure 1.1). Thirdly, these neurogenic niches are also responsive/sensitive to changes in the peripheral environment. This is because they are in close proximity to, or in direct contact with the vasculature. Through the vasculature, fluctuations in circulating levels of neurotrophic factors and hormones can impose a regulatory effect. [Palmer et al, 2000; Tavazoie et al, 2008]. In the case of the SVZ, NSCs also contact the cerebrospinal fluid (CSF), which may further regulate their behaviour [Mirzadeh et al, 2008]. The cellular process of neurogenesis in the SGZ and SVZ, their components and their lineage hierarchies have been highlighted in Figure 1.1.

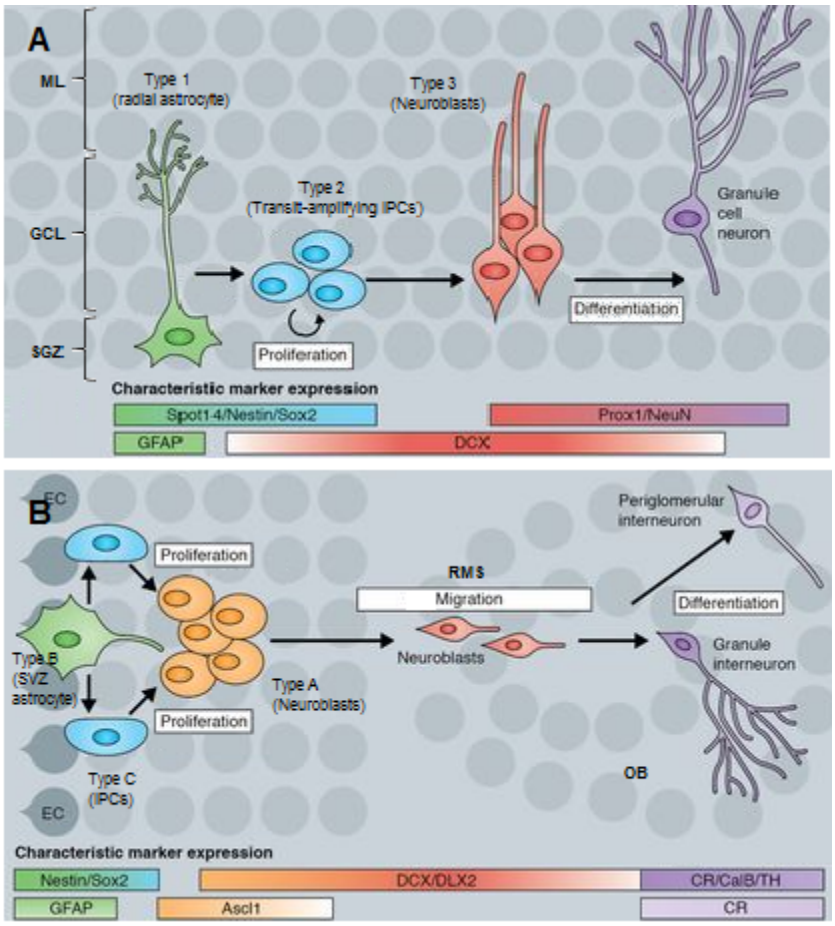

Figure 1.1 Adult neurogenesis in the canonical neurogenic niches. A) SGZ NSCs (type I cells) generate transit amplifying intermediate progenitor cells (type 2 cells), which develop into neuroblasts (type 3 cells) that differentiate into hippocampal granule cells. **B)** SVZ NSCs (type B cells) give rise to intermediate progenitor cells (type C cells), which develop into neuroblasts (type A cells) that migrate into the olfactory bulb and differentiate into olfactory interneurons. Characteristic gene expression profiles for each different developmental stage during neurogenesis is underlined below. EC, ependymal cell (layer); ML, molecular layer; GCL, granule cell layer; GFAP, Glial fibrillary acidic protein; Sox-2, sex-determining region Y-box 2; DCX, doublecortin; Ascl1, Achaete-scute homolog 1; NeuN, Neuronal nuclei; CR, Calretinin. Adapted from Braun & Jessberger (2014).

Although the phenotype and functional role of adult-born neurons generated may differ between these two neurogenic niches, it has been suggested that adult neurogenesis provides an adaptive mechanism to encode contextual or olfactory information and optimize discrimination between similar and/or ambiguous stimuli [Sahay et al, 2011; Brennan & Keverne, 2015]. Indeed, ablation of hippocampal and bulbar neurogenesis resulted in decreased discriminatory capability between similar spatial locations and olfactory stimuli, respectively [Clelland et al, 2009; Mouret et al, 2009] (although some

compensatory effects were seen in the long-term [Breton-Provencher et al, 2009; Singer et al, 2011]).

The refinement of these circuits is regulated by programmed cell death/apoptosis, whereby newborn neurons that fail to receive sufficient synaptic input or neurotrophic factors do not survive [Kim & Sun, 2011; Kuhn, 2015]. Accordingly, high levels of apoptosis have been mostly observed in the neurogenic regions (including the subventricular zone, the dentate gyrus, then rostral migratory stream and in the olfactory bulb), in which the majority of apoptotic cells were identified as immature neurons [Biebl et al, 2000; Dayer et al, 2003; Kuhn et al, 2005]. Thus, the equilibrium between adult neurogenesis and apoptosis may collectively fulfill the common goal of enabling the optimal adaptation of the organism to the changing environment [Migaud et al, 2016]. Indeed, dysregulation of this balance has been linked to impaired synaptic activity and implicated in several neurodegenerative and psychiatric diseases [Santarelli et al, 2003; Grote & Hannan, 2007; Kim et al, 2009].

It should be noted that the occurrence of adult neurogenesis in humans has more recently been debated [Arellano et al, 2018; Kempermann et al, 2018; Snyder, 2018]. Although several studies have reported persisting adult neurogenesis in the human hippocampus (DG) [Eriksson et al, 1998; Spalding et al, 2013; Boldrini et al, 2018; reviewed in Kempermann et al, 2018], other recent studies have challenged this notion [Dennis et al, 2016; Cipriani et al, 2018; Sorrells et al, 2018]; one particular study suggested that hippocampal neurogenesis rapidly decreased, with none detected from adolescents older than 13 years [Sorrells et al, 2018]. However, it has been criticized that the lack of a positive observation may have been due to poor tissue preparation (long post-mortem delay, and varied duration/type of fixation) and lack of consideration for crucial factors in matching brain tissue from patients and controls for postmortem research, such as disease-phase of patients' brains, environmental (lifestyle) or tissue-based (angiogenesis, hormone levels and volume) parameters [Bao & Swaab, 2018; Kempermann et al, 2018].

Emerging sites of adult neurogenesis

It is now apparent that mammalian adult neurogenesis is not limited to the aforementioned regions; there is a growing number of reports of adult neurogenesis and newly-identified NSC-like populations in additional brain regions, including but not limited to the neocortex [Gould et al, 1999; Dayer et al, 2005], the striatum [Pencea et al, 2001; Bedard et al, 2002; Dayer et al, 2005], the amygdala [Bernier et al, 2002; Fowler et al, 2002], the substantia nigra [Lie et al, 2002; Zhao et al, 2003], the cerebellum [Lee et al, 2005; Klein et al, 2005; Ahlfeld et al, 2017], the entire ventricular system [Weiss et al, 1996; Chouaf-Lakhdar et al, 2003], and most notably, the hypothalamus [Pencea et al, 2001; Kokoeva et al, 2005; 2007; Migaud et al, 2010], although no definitive evidence has been provided in humans [Batailler et al, 2014]. However, due to the substantially lower levels of neurogenesis observed in these regions in comparison to the canonical niches (For example, the total number of newly-generated neurons in the hypothalamus was not even 2% or 0.1% of those generated in the dentate gyrus and olfactory bulb, respectively; estimated from [Matsuzaki et al, 2009; Kandasamy et al, 2015; Leuchtweis et al, 2014], the occurrence of neurogenesis in the majority of these 'non-canonical' regions has been met with scepticism and is still a topic of debate [Migaud et al, 2010; Lee & Blackshaw, 2012; Rojczyk-Gołębiewska et al, 2014]. Interestingly, it has been postulated that the conventional methods of detecting proliferating cells and adult-born neurons in more-vascularized brain regions (SGZ and SVZ) might not be adequate for these regions (with exception to the hypothalamic median eminence), which are less vascularized or may contain slow-dividing/quiescent progenitors [Lee & Blackshaw, 2012; Sousa-Ferreira et al, 2014a]. For instance, by using a different delivery method (intracerebroventricular; icv injection) for BrdU-labelling (conventionally via intraperitoneal; ip injection) in the hypothalamus, substantially more proliferative cells were identified, which differentiated into neurons [Kokoeva et al, 2007]. Furthermore, it can be argued that since only a small number of new-born neurons have been found to be critical in regulating functional outputs in the canonical regions, for example hippocampal memory formation/retention [Han et al, 2009], the low levels (or contribution) of neurogenesis to small brain regions (such as the hypothalamus), which may contain fewer but critical neurons, may be equally important [Lee & Blackshaw, 2012].

Many lines of evidence support the notion of the hypothalamus emerging as a third site of adult neurogenesis, including a constitutive capacity for cell proliferation and generation of neurons in various species, and a putative NSC niche highly reminiscent of that in the SVZ [Lee & Blackshaw, 2012; Haan et al, 2013; Migaud et al, 2016; Rojczyk-Gołębiewska et al, 2014]. Furthermore, the morphological plasticity exhibited by hypothalamic neurons in response to secreted neuropeptides and hormones [Theodosis et al, 2006; Prevot et al, 2010] further indicates the potential ease of integration of adult-born neurons in existing hypothalamic circuitry [Lee & Blackshaw, 2012]. Indeed, as a master regulator of neuroendocrine function and physiological homeostasis, further elucidation of the cellular processes and key players in adult hypothalamic neurogenesis would render extensive implications for therapeutic intervention for hypothalamic (particularly metabolic) disorders, and so has attracted substantial interest in the field of adult neurogenesis [Sousa-Ferreira et al, 2014a; Lee & Blackshaw, 2012].

Structure and functions of the hypothalamus

The hypothalamus is located directly below the thalamus, which together form the diencephalon of the forebrain. This diencephalic structure sits in between the cerebral hemispheres and the midbrain, and lies caudal to the basal forebrain and olfactory bulb [Yuan & Carrion, 2011] (Figure 1.2A). It also contains the lateral and ventral walls of the 3rd ventricle.

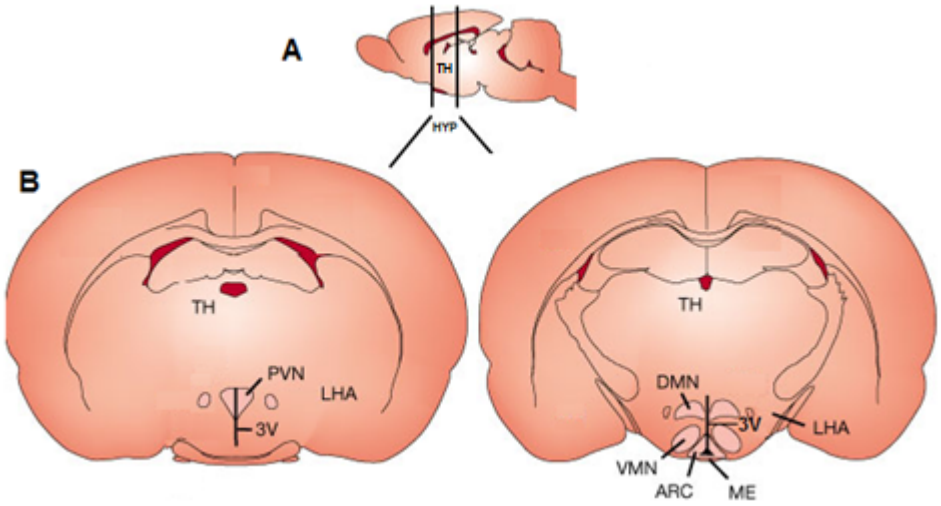

Figure 1.2 Location and anatomy of the rodent hypothalamus. A) Saggital plane: the hypothalamus is situated in the forebrain, on the ventral-most side, below the thalamus (TH). **B)** Coronal plane: rostral/anterior (left) and tuberal/mid- (right) sections of the hypothalamus. The 3rd ventricle (3V) spans along the length of the hypothalamus. The hypothalamic nuclei/regions that have been implicated in energy balance are indicated; paraventricular (PVN), arcuate (ARC), ventromedial (VMH) and dorsomedial (DMH) nuclei, the lateral (LHA) hypothalamic area, and the median eminence (ME). Image adapted from Schwartz (2000).

Although the hypothalamus occupies a relatively small volume of the total brain volume, it is an integral part of the limbic system and regulates a myriad of autonomous physiological processes essential for the organism's adaptation and survival to their environment [Migaud et al, 2016]. These include, thermoregulation, food and water intake, energy metabolism, sexual behaviour and reproduction, and circadian rhythms [Saper & Lowell, 2014]. Each of these processes is regulated by one or more anatomically distinct neuronal nuclei within the hypothalamic parenchyma, which can detect external signals and interface with (relay information to and from) other brain regions [Schwartz et al, 2000; Sousa-Ferreira et al, 2014a]. For instance, the arcuate, paraventricular, ventromedial and dorsomedial hypothalamic nuclei, in addition to the lateral hypothalamic area have been implicated in feeding regulation and energy homeostasis (Figure 1.2B) [Schwartz et al, 2000; Simpson et al, 2009].

The hypothalamus mediates its regulatory functions by forming the physical link between the nervous and endocrine systems via the pituitary gland. The ventral most hypothalamic structure, the median eminence (ME) is devoid of any blood-brain barrier by the presence

of fenestrated capillaries (a hallmark of circumventricular organs [Bennett et al, 2009]), allowing access of small molecules to and from the portal blood circulation [Johnson & Gross, 1993; Langlet, 2014]. This makes the ME an important site of information transfer between the blood circulation and hypothalamus, whereby blood-borne molecules can be detected by hypothalamic nuclei, which in turn can secrete hormones into the hypophysial portal blood circulation system to act on pituitary secretory cells [Migaud et al, 2010]. As well as the ME, information can also be attained from the circulating ventricular CSF to act on the hypothalamic parenchyma [Frayling et al, 2011; Bolborea & Dale, 2013]. Thus, the hypothalamus is able to detect changes from the peripheral environment (from both media, portal blood and ventricular CSF), integrate information received from other brain regions, and modulate secretion of pituitary hormones to regulate the aforementioned physiological processes [Rizzoti & Lovell-Badge, 2017].

Adult hypothalamic neurogenesis

The adult hypothalamus has been reported to exhibit constitutive cell proliferation and neurogenesis in a range of mammalian species, including mice [Kokoeva et al, 2005; 2007], rats [Pencea et al, 2001; Xu et al, 2005], hamsters [Huang et al, 1998], vole [Fowler et al, 2002], sheep [Migaud et al, 2010; 2011] and pigs [Raymond et al, 2006], but has yet to be decisively demonstrated in humans [Bakos et al, 2016]. These observations have been accompanied with the expression of several neural stem and/or progenitor cell markers, including nestin [Xu et al, 2005], musashi-1 [Haan et al, 2013], sox-2 [Haan et al, 2013], PSA-NCAM [Bonfanti, 2006] and hes-5 [Lee et al, 2012]. Studies have indicated that the basal levels of neurogenesis in the adult hypothalamus is substantially lower than that in the canonical neurogenic niches [Pencea et al, 2001; Kokoeva et al, 2007; Migaud et al, 2010; Lee & Blackshaw, 2012; Robins et al, 2013a], and decreases substantially with age, with post-natal ages exhibiting the highest levels [Lee et al, 2012; McNay et al, 2012; Haan et al, 2013].

Initial studies

One of the first pieces of evidence highlighting the occurrence of adult neurogenesis in the hypothalamus came from a study that investigated the effect of intracerebroventricular infusion (cannular administration into the CSF) of a growth factor, brain derived

neurotrophic factor (BDNF) on adult neurogenesis in a number of brain regions [Pencea, 2001]. In addition to those brains infused with BDNF, control brains (infused with PBS) also demonstrated newborn (BrdU+) cells in the hypothalamic parenchyma with increasing frequency towards the 3V. Furthermore, at later time points BrdU+ cells adopted a neuronal fate indicated by expression of the immature neuronal marker, βIII-tubulin. Indeed, both cell proliferation and neuronal differentiation of BrdU+ cells were enhanced upon infusion of BDNF, suggesting that the hypothalamus exhibits low basal levels of adult neurogenesis which could be up-regulated by growth factors [Pencea et al, 2001].

In vitro studies further supported the hypothalamus' neurogenic capacity. In primary hypothalamic cultures from adult rats, α-internexin+ neuroblasts were identified that were able to incorporate BrdU, express additional neuronal markers (βIII-tubulin, MAP-2, Tau) at later time-points and exhibit modest electrophysiological properties of neurons [Evans, 2002]. When cultured in monolayers, hypothalamic cells were able to differentiate into glia as well as a range of neuropeptide-expressing neurons typically found in the hypothalamus, as assessed by immunohistochemistry [Markakis et al, 2004]. Furthermore, isolated primary cells could form spheroid floating cell clusters (neurospheres), which could be passaged repeatedly and whose progeny could differentiate into several neural cell types (astrocytes, oligodendrocytes and neurons), reflecting their capacity for self-renewal and multipotency, respectively [Xu et al, 2005]. These results suggested that NSCs or neural stem-like progenitor cells exist in the adult hypothalamus and are capable of neurogenesis.

After the initial demonstration of adult neurogenesis in the hypothalamus, subsequent studies have further investigated several features of adult hypothalamic neurogenesis, including the source of and identity of adult newborn neurons, regulatory factors, and its functions.

Cell proliferation in the adult hypothalamus

Several regions of proliferative capacity have been identified, albeit differentially between studies (summarized in Table 1.1). These include the ependymal layer lining the 3rd ventricle walls, the underlying subependymal layer, the median eminence, and the

hypothalamic parenchyma [Migaud et al, 2010; Lee & Bradshaw, 2012; Sousa-Ferreira et al, 2014a; Rojczyk-Gołębiewska et al, 2014]. These proliferative regions can be classed into two main domains; the ventricular and the parenchymal zones (Figure 1.3).

Publication/ Author	**Observed location of BrdU+ cells**	**Survival period(s)**	**Species**	**BrdU injection method/ period**
Pencea et al, 2001	Parenchyma (PVN) and periventricular area (not specified)	28 days	Rat	i.c.v.; 12 days
Chouaf-Lakhdar et al, 2003	Periventricular area (subependymal, ependymal ependymocytes & tanycytes), ME	5 days	Rat	i.c.v.; 3 days
Xu et al, 2005	Ependymal layer (tanycytes but rare), but not in parenchyma	2 or 5 days (unclear)	Rat	i.p.; 2 days
Kokoeva et al, 2005	Parenchyma (not specified), periventricular area (not specified), ME	1, 20, 40, 60days	Mice	i.c.v.; 5 days
Kokoeva et al, 2007	Parenchyma (not specified), periventricular area (not specified), ME	1 or7, 14 days	Mice	i.c.v. 1 or 7 days, 14 i.p; 7 days
Perez-Martin et al, 2010	Parenchyma (rarely), periventricular (subependymal, ependymal tanycytes but not ependymocytes), ME	3 days	Rat	i.p.; 3 days
Cifuentes et al, 2011	I.P.; parenchymal (sparse), periventricular (not specified), ME. I.C.V; Parenchymal (including microglia and neurons), periventricular (subependymal astrocytes, microglia; ventral ependymal tanycytes but not ependymocytes)	7 days	Rat	i.c.v., i.p; 7 days

Migaud et al, 2011	Parenchyma (not specified), periventricular (subependymal, ependymal; not specified), ME	1 day, 4 weeks	Sheep	i.v.; 1 days, 2days
Robins et al, 2013a	Parenchyma (not specified), periventricular area (not specified)	7 days, 6 weeks	Mouse	i.c.v.; 7 days
Robins et al 2013b	Parenchyma (ARC, VMH, DMH), Periventricular (not specified), ME	1, 7, 28 days	Mouse	i.c.v.; 1,7 days, oral: 28 days
Haan et al, 2013	Parenchyma (not specified), ependymal (ventral tanycytes), ME	9, 15 days	Mouse	*Ad libitum* (drinking water) 9, 15 days

Table 1.1 BrdU-labelling studies reporting different hypothalamic regions of constitutive cell proliferation; ependymal layer, the periventricular area (here referring to the subependymal layer and adjacent parenchyma, unless specified in parenthesis) the parenchyma (PVN; paraventricular nucleus, ARC; arcuate nucleus, VMH; ventromedial nucleus, DMH; dorsomedial nucleus) and the median eminence (ME). BrdU was administered via intraperitoneal (i.p.), intravenous (i.v.), intracerebroventricular (i.c.v) injections, or *ad libitum* (*ad lib)* as drinking water. Survival period refers to time (days) from the first BrdU treatment until termination of experiment/brain fixation.

The ventricular zone

This zone collectively comprises structures and cellular layers surrounding the 3rd ventricle (Figure 1.3A). This mostly refers to the periventricular area (PeA), which is composed of the lateral ependymal layers, the subependymal layer and the adjacent proximal parenchyma [Perez-Martin et al, 2010]. However, the median eminence, albeit being a separate structure (as a circumventricular organ), is also included in this category due to its contact with the ventricular CSF. Both the PeA and the ME have been described to retain proliferative capacities and exhibit constitutive adult neurogenesis [Perez-Martin et al, 2010; Lee et al, 2012; Haan et al, 2013 Robins et al, 2013a; Sousa-Ferreira et al 2014a].

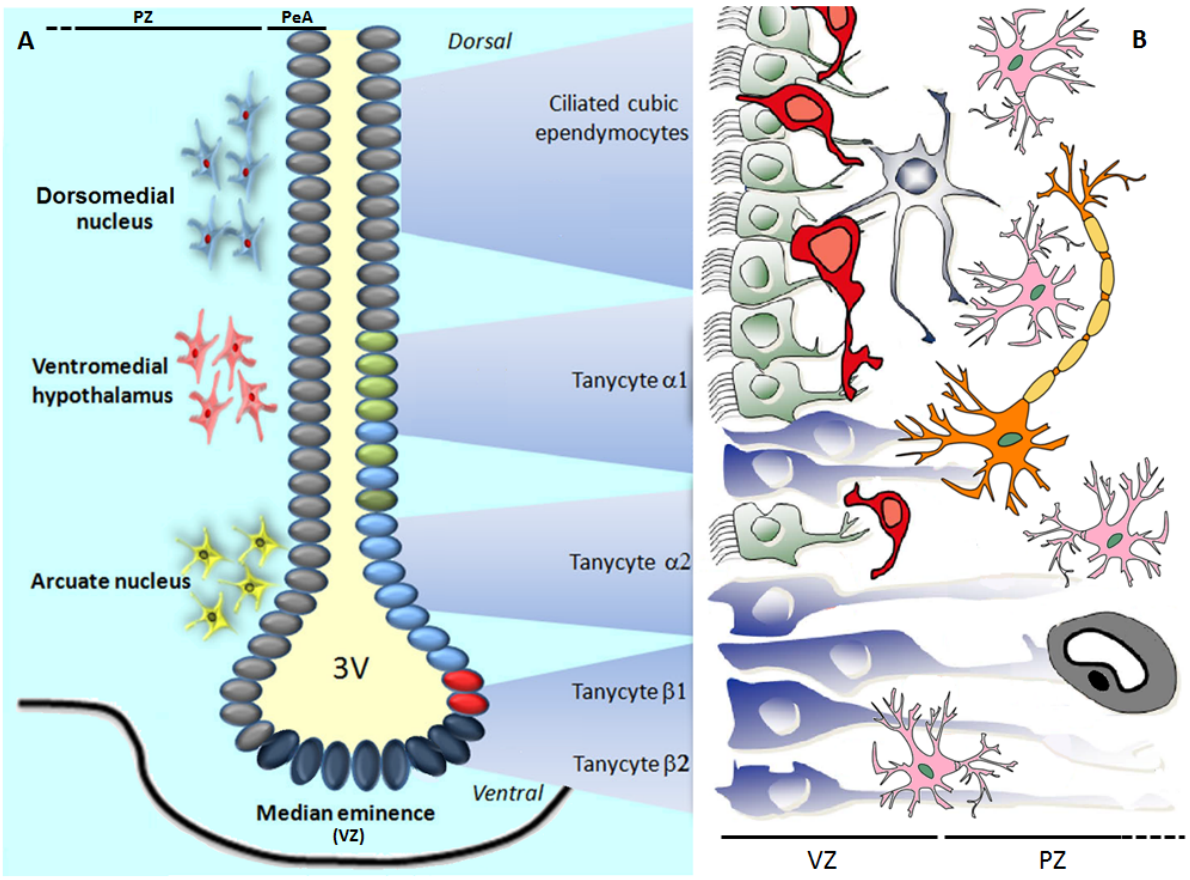

Figure 1.3 Location and cellular organization of the ventricular and parenchymal proliferative zones. A) Cellular architecture of the 3rd ventricle. Tanycytes are located within the ependymal layer (ovals); α1 (green) and α2 (blue), β1 (red) and β2 (dark blue) and project to the ventromedial nucleus (red), arcuate nucleus (yellow) and median eminence. **B)** Magnified representation of the cellular components of the ventricular and parenchymal proliferative (and neurogenic) zones. In the mediolateral periventricular area, tanycytes (blue; corresponding to α-subtypes from **A** and subependymal astrocytes (red) can proliferate. In the ME tanycytes (blue; indicated as β-subtypes from **A** are proliferative. Within the parenchymal zone, proliferative NG2+ glia (pink) as well as microglia (light grey), endothelial cells (dark grey), and neurons (orange) were seen. Parenchymal zone (PZ), ventricular zones (VZ), including the periventricular area (PeA) have been defined. Adapted from Yuan & Arrias-Carrion, 2011; Rojczyk-Gołębiewska et al, 2014.

The ependymal layer consists of two cell types; multiciliated cuboidal ependymocytes and non-ciliated, radial glia-like cells called tanycytes [Rodriguez et al, 2005]. Both cell-types contact the CSF, and are at the interface between the 3V and the hypothalamic parenchyma (Figure 1.3A). Tanycytes are characteristically identified by an elongated cell body and a long basal process (blue; Figure 1.3B). They are found at increasing

frequency dorsoventrally along the 3V, first appearing interspersed with ependymocytes along the mediolateral 3V walls before gradually becoming a contiguous layer ventrally, at the ME interface [Bolborea & Dale, 2013]. It should be noted that whilst the ependymal layer is a continuous lining of the 3rd ventricle, the ventral ependymal layer forms part of the ME, and is therefore collectively referred to here with/as the ME.

Within the mediolateral ependymal layer, BrdU+ tanycytes have been observed, although this was very rare under basal conditions [Xu et al, 2005]. However, upon infusion of growth factors, FGF-2 or insulin growth factor 1 (IGF-1), proliferation was robustly upregulated as seen by BrdU uptake in tanycytes visualized with astroglial (GFAP) [Xu et al, 2005] or ependymal (Vimentin) [Perez-Martin et al, 2010; Robins et al, 2013a] marker expression. As in the SVZ [Spassky et al, 2005; Chojnacki et al, 2009], ependymocytes have been reported to not having a proliferative capability [Perez-Martin et al, 2010; Cifuentes et al, 2011; Haan et al, 2013], although some conflicting BrdU-labelling data exists [Chouaf-Lakhdar, 2003].

In addition to the ependymal layer, subependymal astrocytes have been identified with a capability to proliferate [Perez-Martin et al, 2010; Cifuentes et al, 2011]. These cells are characteristically identified by GFAP expression and possession of a single apical process that contacts the ventricular interface, features reminiscent of SVZ astrocytes [Perez-Martin et al, 2010; Mathew, 2008]. A unique pinwheel structure was described for SVZ astrocytes in which the apical process would occupy the centre of a rosette formed by ependymal cells [Mirzadeh et al, 2008]. Although this has not been investigated for hypothalamic subependymal astrocytes, their close proximity to the ependymal layer is suggestive of a similar structure to that of the SVZ neurogenic niche [Perez-Martin et al, 2010; Rojczyk-Gołębiewska et al, 2014]. In summary, the microarchitecture and cellular components of the mediolateral PeA is very reminiscent of the SVZ niche; it contains a heterogeneous pool of quiescent or low-proliferative cells (subependymal astrocytes and radial glia-like tanycytes), some of which exhibit strong morphological and expressional similarities to type-B SVZ NSCs and whose proliferative state can be regulated by mitogenic/growth factors [Rojczyk-Gołębiewska et al, 2014; Migaud et al, 2016].

The ME, has been reported to exhibit a very high rate of basal proliferation relative to other hypothalamic proliferative zones, from postnatal periods and throughout adulthood, though a decline is seen with age [Lee et al, 2012; Haan et al, 2013]. Ventral tanycytes, unlike their mediolateral counterparts, are readily proliferative under basal conditions [Cifuentes et al, 2011; Lee et al, 2012; Haan et al, 2013], but are not responsive to IGF-1 or FGF-2 [Robins et al, 2013a; Perez-Martin et al, 2010]. Instead, environmental factors such as dietary signals can regulate ME cell proliferation. For instance, a high fat diet or low protein diet upregulates ME cell proliferation, whilst caloric restriction induced the opposite effect [Lee et al, 2014]. It should be noted that additional proliferative cells have been observed in the ME other than tanycytes. It can be speculated that, NG2+ glia residing in the ME [Djogo et al, 2016], may constitute proliferative capacities [Robins et al, 2013b].

The parenchymal zone

Whilst all studies (with the exception of Hawken et al, 2009) agree upon the existence of proliferative (BrdU+) cells in the hypothalamic parenchyma (Table 1.1), the levels of cell proliferation and distribution of these BrdU+ cells vary in the literature. Some studies saw few BrdU+ cells scattered evenly throughout the parenchyma [Xu et al, 2005; Perez-Martin et al, 2010; Migaud et al, 2011], whilst other studies saw a high number of BrdU+ cells whose density was inversely proportional to the distance from the 3rd ventricle [Pencea et al, 2001; Kokoeva et al, 2005; Haan et al, 2013; Robins et al, 2013a]. The potential causes for this disparity are discussed below.

Neural/glial antigen-2 (NG2)+ glia appear to comprise the majority of proliferative parenchymal cells, accounting for approximately 80% of parenchymal BrdU+ cells [Robins et al, 2013b]. In addition to NG2+ glia, proliferating microglia and endothelial cells have been reported, although the latter was only observed when IGF-1 was administered centrally [Cifuentes et al, 2011; Perez-Martin et al, 2010]. Whilst IGF-1 mostly induces periventricular cell proliferation [Perez-Martin et al, 2010], ciliary neurotrophic factor (CNTF) induces a significant (5-fold) increase in proliferation throughout the hypothalamic parenchyma [Kokoeva et al, 2005; Kokoeva et al, 2007].

Difficulties in assessing hypothalamic cell proliferation

The majority of discrepancies in the categorical identification of hypothalamic proliferative cells, their respective locations (Table 1.1), and their relative proliferative capacities is owed to some technical factors and endogenous limitations that require consideration when using BrdU as a proliferative marker in the hypothalamus [Sousa-Ferreira et al, 2014a].

Different BrdU-delivery techniques used reflect varying BrdU permeability by different regions of the hypothalamus [Lee & Blackshaw, 2012; Sousa-Ferreira et al, 2014a]; peripheral administration (intraperitoneal; i.p. injection) of BrdU appears to be preferentially incorporated in cells of the median eminence, which has its unrestricted access to circulating blood, whereas central (intracereboventricular; i.c.v) delivery of BrdU preferentially labels cells lining the 3rd ventricle and in the parenchyma, which have higher permeability across the ventricular interface [Kokoeva et al, 2007; Cifuentes et al, 2011]. This leads to question whether the observation of higher BrdU+ cells in the ME, relative to the PeA or distal parenchyma (when BrdU is administered peripherally) is due to an inherently higher proliferative capacity or due to higher accessibility to the ME [Lee et al, 2012]. Indeed, when delivered centrally, a more comparable BrdU+ cell density is seen between the PeA and ME [Kokoeva et al, 2007].

Further methodological differences in BrdU administration, such as the duration and frequency of delivery/injections, may account for additional variation in observations made [Sousa-Ferreira et al, 2014a]. For instance, when injected for short periods, BrdU+ cells are scarcely seen in the parenchyma [Xu et al, 2005; Perez-Martin et al, 2010], whereas longer delivery periods indicate otherwise [Robins et al, 2013b; Haan et al, 2013]. Equally, the disparity in survival periods (the time window from the first BrdU injection to tissue fixation and analysis) used between studies (Table 1.1) can affect the observed location of proliferation since, with increasing survival time, there is a greater likelihood of BrdU+ cell migration [Sousa-Ferreira, 2014a].

The properties of hypothalamic neural stem/progenitor cells, such as how frequently they enter the cell cycle and how long their cycles are, is not clear. Considering that the hypothalamus may comprise of a heterogeneous pool of neural stem/progenitor cells

[Haan et al, 2013; Robins et al, 2013a; 2013b], each of which may have different cell-cycle properties, as seen in other stem cell niches [Li & Clevers, 2010], it is not known whether BrdU may reliably labelled all, or just a proportion of this heterogeneous population. For instance, when BrdU is administered for discrete/short periods, neural stem/progenitor cells with an active cell-cycle (fast-dividing) are more likely to be labelled with BrdU, whereas longer BrdU administration increases the chances of 'capturing' neural stem/progenitor cells that may be in the cell-cycle infrequently (slow-dividing) [Sousa-Ferreira et al, 2014a].

Indeed, BrdU-studies in the SGZ and SVZ have conventionally used a single peripheral (i.p) pulse to label proliferating cells [Migaud et al, 2010; Lee & Blackshaw, 2012]. As explained, this methodology yields exceedingly low hypothalamic BrdU+ cells and thus, is not optimal for labelling dividing neural progenitors in the hypothalamus. Thus, multiple BrdU injections and/or central (i.c.v.) BrdU delivery has been used. However, an increase in the length and duration of BrdU delivery (and hence, the survival time) may compromise the unequivocal identification/location of proliferating cells and their discrimination from post-mitotic progeny. Furthermore, given the additional limitations of using BrdU as a proliferative marker, namely its potential incorporation in non-dividing cells (during DNA repair and/or apoptosis) when administered at high doses [Bauer & Patterson, 2005; Breunig et al, 2007], may render misleading. Alternative endogenous proliferative markers such as Ki67 and PCNA have previously been detected for to confirm the proliferative status/capacity of BrdU+ cells [Kokoeva et al, 2007; Pierce & Xu, 2010], but have not been used to as great an extent.

Assessing neurogenesis using transgenic lineage-tracing

In addition to BrdU, genetic labelling approaches have more recently been employed to lineage-trace and fate-map neural stem/progenitor cells [Imayoshi et al, 2011; Blanpain & Simons, 2013]. Lineage-tracing/fate-mapping entails the (visual) identification of a cell (population) and its progeny by a permanent labelling method [Kretzschmar & Watt, 2012]. A widely-used approach to lineage-trace cells in mice is the genetically inducible lineage-tracing approach (Fig 1.4), which makes use of the P1 bacteriophage-derived Cre-Lox recombination system [Hamilton & Abremski, 1984; Joyner & Zervas, 2006;

Imayoshi et al, 2011]. The Cre-Lox system was initially used to generate gene mutations (including knock-outs) in mice [Lakso et al, 1992; Orban et al, 1992; Nagy, 2000]; the site-specific recombinase, Cre acts on LoxP recognition sites to delete, insert or invert any DNA sequence flanked by these LoxP sites via homologous recombinaton [Nagy, 2000; Kretzschmar & Watt, 2012]. The yeast-derived FLP-FRT system is an alternative site-specific recombination system which has also been used for gene-targeting and lineage-tracing, including in mice [Dymecki, 1996; Golic & Lindquist, 1989; Kretzschmar & Watt, 2012].

Cre activity can be spatially and temporally controlled by insertion of a cell-type/tissue-specific promoter sequence upstream from the recombinase gene, and fusion with a mutated ligand-binding domain (with stronger affinity for a synthetic estrogen analogue such as tamoxifen or its metabolite, 4-hydroxy-tamoxifen) of the estrogen receptor to give the modified Cre-ERT, respectively [Feil et al., 1997, Indra et al, 1999, Metzger & Chambon, 2001]. Thus, in this system, Cre-ERT expression is restricted to cells that express the endogenous gene regulated by the same upstream promoter sequence as Cre-ERT, and can only translocate to the nucleus (where it can induce recombination) upon binding to Tamoxifen or 4-OHT.

In the lineage-tracing approach, a double-transgenic mouse is used, whereby one transgenic construct comprises of Cre-ERT under the control of a cell-type/tissue-specific promoter sequence (Fig 1.4). The second transgenic construct consists of a reporter gene under the control of a ubiquitous promoter, such as CAG or Rosa26, but interrupted by a floxed STOP cassette [Branda & Dymecki, 2004]. Thus, only upon tamoxifen (or 4-OHT) administration Cre-ERT is allowed to translocate to the nucleus and excise the STOP cassette, resulting in the permanent expression of the reporter. Daughter cells that derive from these recombined cells will inherit the excised reporter construct and thus, express the reporter as well. However, although the inducible Cre-ERT enables control of recombination in a specific cellular population, some instances of non-specific Cre-expression and ectopic activation have been noted, indicating potential caveats of using this lineage-tracing approach [Favaro et al, 2009; Chen et al, 2009; Imayoshi et al, 2011].

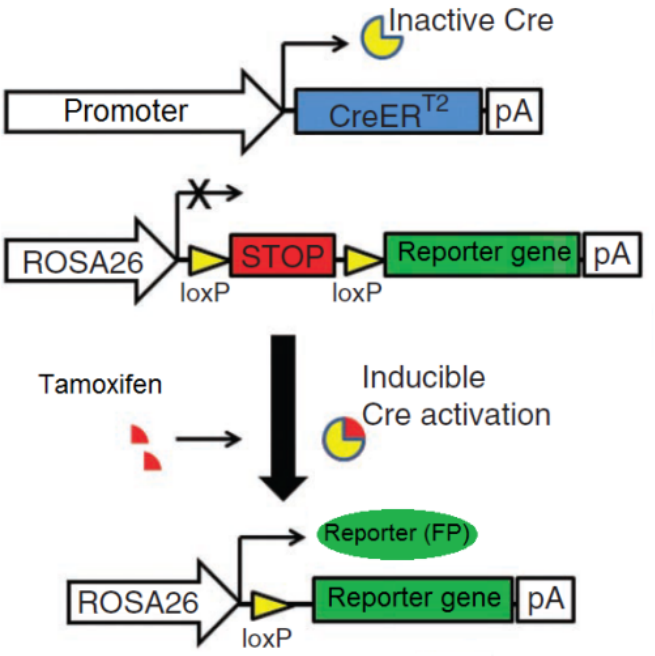

Figure 1.4 Cre-inducible transgenic approach for lineage-tracing. Double transgenic mice are used containing two separate constructs; one containing an inducible Cre-recombinase (CreER^{T2}) gene, and another containing a STOP cassette flanked by lox-P (recombinastion) sites followed by a reporter gene (usually a fluorescent protein). By using a tanycyte- or NSC-specific promoter, CreER^{T2} expression can be restricted to tanycytes or NSCs, respectively. Under normal conditions, CreER^{T2} is expressed in an inactive form. However, upon injection of tamoxifen, is translocated to the nucleus where it actively recombines lox-P sequences, resulting in the excision of the STOP cassette. This allows for permanent YFP expression (driven by a constitutive promoter in the Rosa26 locus) in tanycytes/NSCs and in their progeny. This approach allows temporal control of reporter-labelling and lineage-tracing. Adapted from Lee et al, 2012.

Hypothalamic neurons generated

Using BrdU-labelling and genetic lineage-tracing approaches, different neuronal cell-types associated with feeding behaviour are generated in the adult hypothalamus. These include orexigenic (stimulate feeding) Agouti-related peptide (AgRP), Neuropeptide Y (NPY), and Orexin A-expressing neurons [Xu et al, 2005; Kokoeva et al, 2005; Pierce & Xu, 2010; Li et al, 2012; McNay et al, 2012; Lee et al, 2012; Haan et al, 2013], as well as anorexigenic (inhibit feeding) Proopiomelanocortin (POMC)-expressing neurons [Pierce & Xu 2010; Li et al, 2012; McNay et al, 2012; Lee et al, 2012]. These newly-generated neurons were functionally integrated into the existing hypothalamic circuitry as indicated by expression of immediate-early genes (c-fos) or activation of early-response

transcription factor expression (STAT3) in response to acute or hormone-induced (leptin) fasting [Kokoeva et al, 2005; Pierce & Xu, 2010; Lee et al, 2012; Haan et al, 2013].

Tanycytes of the mediolateral ependymal layer were suggested to generate new-born cells which migrate along tanycytes processes into the hypothalamic parenchyma where they differentiate into mature neurons, indicated by NeuN or Hu expression [Xu et al, 2005; Robins et al, 2013a]. Similarly, another study implied that DCX+ neuroblasts migrated into the deeper parenchyma, where they adopted more neuronal morphologies and phenotypes; rounded shaped DCX+/Nestin+ cells were seen with no processes in the periventricular area, whilst bipolar/fusiform-shaped DCX+ cells were seen in the distal parenchyma co-expressing NeuN [Batailler et al, 2014]. The reported identity of adult-born neurons from the mediolateral PeA is limited, with only one study reporting the generation of Orexin-A-expressing neurons [Xu et al, 2005]. Whilst BrdU+ subependymal astrocytes were seen [Perez-Martin et al, 2010], their involvement in hypothalamic neurogenesis has yet to be elucidated.

Tanycytes of the ME have been shown to generate both neurons in the ME [Lee et al, 2012; 2014] and those that migrate to the hypothalamic parenchyma [Haan et al, 2013]. Newborn neurons (DCX+ neuroblasts) were observed in the ME albeit at lower levels respectively to the PeA and parenchyma [Batailler et al, 2014]. Tanycyte-derived progenies matured into ME and arcuate neurons as demonstrated by their Hu or NeuN expression, and was further characterized as NPY and POMC- peptidergic neurons [Lee et al, 2012; Haan et al, 2013].

NG2+ glia were identified as the predominant proliferative cell-type in the hypothalamic parenchyma, and were seen to retain neurogenic, gliogenic and self-renewal capabilities [Robins et al 2013b; 2013c]. However, although the authors identified the glial descendants as oligodendrocytes and astrocytes, they did not further investigate the identity of NG2+-derived neurons after confirming their neuronal fate with Hu [Robins et al, 2013b].

Functional implications of adult hypothalamic neurogenesis

In addition to the generation of appetite-regulating neurons, several studies have indicated further evidence for a role of adult hypothalamic neurogenesis in energy homeostasis and metabolic regulation and its functional relevance from induction/ablation studies [Bolborea & Dale, 2013; Sousa-Ferreira et al, 2014a; Migaud et al, 2016]. Application of CNTF induced increased neurogenesis associated with an increase in new-born diet-regulating (NPY and POMC) neurons [Kokoeva et al, 2005]. This was accompanied by a reduction in food intake and weight gain in obese mice, which could be reversed upon ablation of cell proliferation with the mitotic blocker, arabinosylcytosine (AraC) [Kokoeva et al, 2005]. In another study, a neurodegenerative mouse model for AgRP neurons exhibited a dependence on *de novo* neurogenesis for keeping intact food intake and body weight; when proliferation was inhibited with AraC, decreased food intake and body fat followed [Pierce & Xu, 2010], mirroring the effects seen upon acute ablation of AgRP neurons (severe anorexia and weight loss) [Gropp et al, 2005]. Similarly, in another study where neurogenesis was ablated in the ME using focal irradiation, changes in weight and basal metabolic activity were observed [Lee et al, 2012].

Several lines of evidence suggest that obesity induces hypothalamic injury and impairs neurogenesis in the hypothalamic parenchyma [Thaler et al, 2012; Sousa-Ferreira et al, 2014a]. HFD-induced obese mice indicate reduced cell proliferation and generation of hypothalamic (including NPY and POMC-expressing) neurons, further suppressing neuronal turnover by increasing apoptosis of new-born neurons in the arcuate nucleus [Moraes et al, 2009; Li et al, 2012; McNay et al, 2012]. The negative effect of HFD-induced obesity on neural stem/progenitor cell proliferation has been linked to an increase in pro-inflammatory signalling; overexpression of IKKβ in hypothalamic NSCs led to the onset of (diet-independent) obesity [Li et al, 2012]. It is interesting to note that hypothalamic IKKβ/NF-κB activation is also linked to ageing [Zhang et al, 2013], since ageing is associated with an increased risk of obesity and neuroinflammation [Yang et al, 2012]. Genetically (leptin-deficient) obese mice also exhibit diminished levels of neurogenesis, but notably due to a substantially smaller neural stem/progenitor population, since leptin signalling is required for NSC proliferation [Desai et al, 2011; McNay et al, 2012]. On the other hand, other studies have nevertheless indicated that HFD can positively regulate

postnatal and adult hypothalamic neurogenesis in the ME in a sexually dimorphic manner (in females only) [Lee et al, 2012; 2014]. Upon the onset of HFD, increased cell proliferation is observed, peaking at 3 days after introduction to HFD, followed by an increase in POMC neuron generation [Gouaze et al, 2013]. Inhibition of this HFD-induced neurogenesis resulted in an accelerated onset of obesity, suggesting an adaptive anorectic function. Indeed in mice exhibiting progressive AgRP neurodegeneration, a similar compensatory role is played, whereby the energy-balance is maintained by increased generation of AgRP neurons [Pierce & Xu, 2010]. These studies indicate that adult hypothalamic neurogenesis may serve as an early protective mechanism to maintain energy homeostasis under detrimental conditions [Sousa-Ferreira et al, 2014a].

In addition to nutritional cues, adult hypothalamic neurogenesis is also regulated by external environmental stimuli. Seasonal changes such as a shift in photoperiod (from long to short days) leads to increased hypothalamic cell proliferation [Huang et al, 1998; Migaud et al, 2011; 2014] and increased DCX+ neuroblast migration [Batailler et al, 2014]. Similarly, changes in social environment, such as exposure to the opposite sex, increased cell proliferation and neuronal differentiation [Fowler et al, 2002]. Thus, it appears that adult hypothalamic neurogenesis may exist as a physiological mechanism to respond and adapt to changing metabolic and environmental challenges, remodelling hypothalamic neuronal circuitry *de novo* throughout adult life [McNay et al, 2012; Sousa-Ferreira et al, 2014a].

Interestingly, inducers of hippocampal neurogenesis such as social enrichment and physical exercise [Kempermann et al, 1998; van Praag et al, 1999] and antidepressants (fluoxetine) [Santarelli et al, 2003; Sairanen et al, 2005] were reported to have an effect on some hypothalamic functions (Novak et al, 2012; McGuirk et al, 1992). However, it has yet to be determined if these external factors might also regulate (induce) hypothalamic neurogenesis.

Tanycytes

Tanycytes were first described in 1954 [Horstmann, 1954] and named accordingly due to their characteristic morphology of bearing a long basal process [Rodriguez et al, 2005; Goodman & Hajihosseini, 2015]. Although they were first identified lining the hypothalamic 3rd ventricle, tanycytes and/or tanycyte-like cells have been found lining the ventricular walls of additional circumventricular organs other than the ME, along the (dorsal) 3rd and 4th ventricles [Langlet et al, 2014; Mirzadeh et al, 2017].

Hypothalamic tanycytes have been suggested to arise from local glial cells in the median eminence, and are first observed during late-gestation after embryonic day 18 in rats [Rutzel & Schliebler, 1980], but undergo terminal differentiation postnatally [Bruni et al, 1983; Rodriguez et al, 2005]. Thus, due to their late development/ontogeny, tanycytes do not likely partake in embryonic neurogenesis. Interestingly, tanycytes and ependymocytes may share the same ancestral lineage, as deletion or downregulation of transcription factors, Lhx-2 or Rax in tanycytes resulted in the acquisition of ependymocyte features in tanycytes or the ectopic presence of ependymal cells in tanycyte regions, respectively [Miranda-Angulo, 2014; Salvatierra et al, 2014].

Tanycyte subtypes

Tanycytes have been classified into α and β subtypes, based on differences in their anatomical location, projection paths and distinguishing features (Figure 1.3) [Rodriguez et al, 2005]. α tanycytes are further subdivided into α1 and α2, as are β tanycytes into β1 and β2 tanycytes. α-tanycytes reside more dorsally to β tanycytes, along the mediolateral 3rd ventricular walls and project into the parenchyma where they proximate glucosensitive neurons (orange; Figure 1.3B) of the ventromedial (α1) and arcuate (α2) nuclei [Rodriguez et al, 2005; Bolborea & Dale, 2013; Langlet, 2014]. β tanycytes, on the other hand, line the infundibular recess and the ventral floor of the 3rd ventricle, where they project either into the arcuate nucleus (β1) to contact vascular endothelial cells (dark grey; Figure 1.3B) or ventrally into the ME (β2) to contact portal blood vessels [Rodriguez et al, 2005; Goodman & Hajihosseini, 2015]. Unlike β tanycytes, α tanycytes lack direct contact with the blood circulation.

Another key differentiating feature between α and β tanycytes entails the barrier properties that β tanycytes exclusively exhibit [Rodriguez et al, 2005; Langlet, 2014]. Due to the lack of a blood-brain barrier (BBB) at the ME (blood vessels are fenestrated), this gives β2 tanycytes direct access to the circulating blood and borne molecules [Bolborea & Dale, 2013]. Barrier properties are assigned to β2 tanycytes by expressing tight junction proteins along their apical cell bodies to form an impermeable 'belt' between the CSF and ME [Mullier et al, 2010; Langlet, 2014]. Interestingly, β1 tanycytes contact and ensheath parenchymal (arcuate) capillaries, but the barrier properties are retained in the endothelial cells expressing tight junctions to maintain the BBB [Mullier et al, 2010]. Instead, β1 tanycytes express zonula adherens along their lateral cell bodies to maintain the arcuate-CSF barrier [Rodriguez et al, 2005]. Interestingly, β2 tanycytes play additional exclusive roles in hypothalamic neuroendocrine functions, such as regulation of thryroid hormone synthesis and secretion [Sanchez et al, 2009; Bolborea & Dale, 2013] as well as modulation of gonadotropin-releasing hormone secretion, which is associated with reproductive function [Prevot et al, 2010; Rizzotti & Love-badge, 2016].

Indeed, α and β tanycytes exhibit differential gene expression profiles, although both express some common markers, such as Sox-2, vimentin and nestin [Haan et al, 2013; Bennett et al, 2009; summarized in Goodman & Hajihosseini et al, 2015]; α tanycytes express GLAST (Glutamate aspartate transporter), GFAP and S100β [Haan et al, 2013; Robins et al, 2013a; Goodman & Hajihosseini, 2015], whilst β tanycytes express BLBP, FGF10 and FGF receptors 1 and 2 [Gonzalez et al, 1994; Hajihosseini et al, 2008; Haan et al, 2013, Goodman & Hajihosseini, 2015]. As indicated by Goodman & Hajihosseini (2015), S100β expression represents a potential domain-marker that can distinguish between the α- and β- tanycyte domains along the ventricular wall.

Tanycytes as chemosensors

The location of tanycytes at the 3rd ventricle lining and in the ME gives them the ability to sense and integrate changes in metabolism and the peripheral environment [Sousa-Ferreira et al, 2014a]. As a result, tanycytes can sense changes in the CSF composition [Bolborea & Dale, 2013]. Indeed, β2 tanycytes have unrestricted access to the circulating blood from fenestrated capillaries [Rodriguez et al, 2005] and as a result, can sense a

range of metabolic signals, including glucose [Frayling et al, 2012] and hormones such as leptin [Balland et al, 2014]. Tanycytes can also respond to several neurotransmitters including ATP, histamine and acetylcholine, when applied exogenously [Frayling et al, 2011].

Several lines of evidence have implicated tanycytes as glucose sensors. Selective ablation of tanycytes impairs the feeding response to hypoglycaemia, which can be reversed when tanycytes were allowed to regenerate [Sanders et al, 2004]. Tanycytes express components of the glucosensing system adopted in pancreatic β-cells: GLUT-1 [Peruzzo et al, 2000], GLUT-2 [Garcia et al, 2003], glucokinase [Salgado; 2014], and ATP-sensitive potassium channels [Thomzig, 2005]. However, it has been debated on whether this glucosensing system is actually utilized by tanycytes [Bolborea & Dale, 2013]. More recently a new sweet-taste receptor (Tas1r2/Tas1r3)-mediated mechanism for glucosensing was identified in a substantial proportion of tanycytes [Benford et al, 2017]. However, since 40% of tanycytes were still glucosensitive, it can be speculated that a combination of receptors and or additional as-of-yet unknown mechanisms may exist.

Tanycytes have been shown to exhibit glucose sensitivity via ATP-mediated purinergic signalling [Frayling et al, 2011; Dale, 2011]; when glucose was directly applied onto tanycyte cell bodies, calcium influx is stimulated, causing a large intracellular calcium wave to propagate the tanycyte layer. This is brought about by two events; short-range propagation of intracellular calcium into neighbouring tanycytes via gap junctions [Orellana et al, 2012] and activation of intracellular signalling cascades that result in the release of ATP [Frayling et al, 2011]. Released ATP stimulates activation of the purinergic receptor, P2Y1R, causing further calcium influx along the tanycyte layer [Frayling et al, 2011]. This mode of glucosensing allows for tanycyte signalling at short ranges (via gap junctions) and long ranges (ATP release into the extracellular space, leading to P2Y1R stimulation) [Bolborea & Dale, 2013]. Tanycytes have also shown to respond to non-metabolizable glucose analogs and non-nutritive (artificial) sweeteners via the same mechanism [Frayling et al, 2011; Benford et al, 2017].

Tanycytes as neural stem/progenitor cells

During embryonic brain development, radial glia serve as neuronal progenitors and are thus considered to be the embryonic counterpart to adult neural stem cells (NSCs) [Alvarez-Buylla et al, 2001; 2002; Rodriguez et al, 2005]. Interestingly, tanycytes resemble radial glia and NSCs in more ways than one. Radial glia possess long basal extensions to support the migration of newborn neurons/progenitors [Kriegstein & Alvarez-Buylla, 2009]. Tanycytes possess a similar basal process and evidence has been shown to indicate a potentially analogous mechanism of progenitor guidance during adult hypothalamic neurogenesis [Xu et al, 2005]. As previously described, tanycytes are responsive to ATP amongst other molecules [Frayling et al, 2011]. The intracellular calcium waves evoked through the tanycyte layer is reminiscient of that seen in radial glia during proliferation [Weissman et al, 2004]. Furthermore, episodic bursts of ATP release result in autocrine and paracrine induction of NSC proliferation and inhibition of differentiation, by specifically acting on purinergic P2X and P2Y receptors [Scemes et al, 2003; Lin et al, 2007; Cavaliere et al, 2015]. In line with this, tanycytes also express NTPDase2, an enzyme typically expressed in some NSC populations that degrade extracellular ATP to enable a tight regulation of extracellular ATP levels [Braun et al, 2003; Gampe et al, 2015].

Tanycytes also express a wide variety of NSC/neural progenitor markers, some of which include nestin, vimentin and Sox-2 [Rodriguez et al, 2005; Lee & Bradshaw, 2012]. Furthermore, when isolated *in vitro*, tanycytes were able to form self-renewing neurospheres, which were able to differentiate into both, glia and neurons, indicating their parallel multipotency to NSCs [Xu et al, 2005, Robins et al, 2013a]. However, the physiological proliferative capacity of tanycytes is not well-established. Whilst BrdU+ tanycytes were seen in few studies, this occurrence was either very rare [Xu et al, 2005] or seen only under long survival periods after BrdU administration (9-15 days; no BrdU+ cells were seen at the ependymal layer after 6 days of BrdU) [Hajihosseini et al, 2008; Haan et al, 2013]. Other studies reporting tanycyte proliferation lacked any morphological characterization of BrdU+ cells at the ependymal layer to confirm that these cells were indeed tanycytes [Chouaf-Lakdar et al, 2003]. Finally, BrdU+ tanycytes were only abundantly seen upon infusion of growth factors such as FGF-2 and IGF-1 [Xu et al, 2005;

Perez-Martin et al, 2010; Robins et al, 2013a]. Given the low basal levels of adult hypothalamic neurogenesis it is reasonable to suggest that tanycytes may represent a quiescent population of NSCs [Morshead et al, 1994]. However, it could also be argued that the non-physiological levels of growth factors used in these studies may evoke ectopic proliferation not seen under physiological conditions, and more importantly, no conclusive evidence was provided to distinguish that tanycytes, and not other nearby proliferative cells, such as subependymal astrocytes had taken up BrdU. Thus, it is not clear if tanycytes are *bona fide* neural stem/progenitor cells capable of cell proliferation (and self-renewal).

Lineage-tracing of tanycytes

More recently, genetically inducible fate-mapping approaches have been used to investigate the contribution of tanycytes toward hypothalamic neurogenesis [Lee et al, 2012; Haan et al, 2013; Robins et al, 2013a] (Figure 1.4). In these studies, inducible Cre-recombinase (CreER) was under the control of promoter sequences specific for β-tanycytes (FGF10) [Hajihosseini et al, 2008; Haan et al, 2013] or α-tanycytes (GLAST) [Robins et al, 2013a]. Upon induction of recombination by tamoxifen, these particular tanycyte subpopulations were permanently labelled with a reporter, allowing studies to track the migration and map the cellular fate of these cells and their progeny.

Indeed, studies using this approach have indicated tanycytes as components of the hypothalamic neurogenic niche in both postnatal [Lee et al, 2012] and adult [Xu et al, 2005; Haan et al, 2013; Robins et al, 2013a] rodents. Lineage-traced β tanycytes were seen to mostly generate neurons of the parenchyma in several nuclei (Arcuate, VMH, DMH, lateral hypothalamus), but predominantly to the arcuate nucleus, where progeny developed into NPY+ neurons [Haan et al, 2013]. A rare contribution to parenchymal astrocytes was also noted. Conversely, lineage-traced α tanycytes generated GFAP+ astrocytes robustly, whilst few NeuN+ neurons were observed, of which only half I migrated into the parenchyma after an extended period of time (9 months) [Robins et al, 2013a]. Although specific neuronal descendants of α tancycytes were not identified in this study, adenoviral labelling of mediolateral (presumably α) tanycytes indicated newly generated Orexin A+ neurons [Xu et al, 2005]. Interestingly, lineage-tracing of α

tancycytes also indicated labelled tanycytes residing in the ventral 3V walls, suggesting their potential to generate β tanycytes [Robins et al, 2013a].

Some conflicting observations were made in these studies; lineage-traced β tanycytes were seen to amplify in number within the ependymal layer, suggestive of self-renewal [Haan et al, 2013]. However, Robins et al [2013a] suggested that, using the neurosphere assay, only neurospheres from sub-dissections of hypothalamic slices containing α2 tanycytes could self-renew for an extended period (over 7 generations), but not β tanycytes. These findings require further investigation to assess and confirm tanycyte self-renewal in alternative experimental paradigms, for instance, whether either tanycyte subpopulation can be restored upon genetic ablation. Further controversy is added to the matter as GLAST expression is not limited to tanycytes [Berger & Hediger, 2001], but is also expressed in parenchymal astrocytes [Hartfuss et al, 2001; Fuente-Martin et al, 2012]. Thus, the absolute contribution of GLAST-expressing α tanycytes to neurogenesis remains unclear.

Due to conflicting findings described above, it is unclear which subtype (α or β) is the predominant population contributing to hypothalamic neurogenesis. Indeed, since different promoters were used in these studies to drive Cre-mediated labelling of specific tanycyte subtypes, it is possible that the other tanycyte subtype and their role in adult neurogenesis may have been overlooked [Sousa-Ferreira et al, 2014a]. Thus, it is possible that α and β tanycytes may simply represent different neural stem cell/progenitor populations, or neural progenitors in sequential states of differentiation, given that α tanycytes may give rise to β tanycytes [Robins et al, 2013a; Sousa-Ferreira et al, 2014a].

Although accumulating evidence has supported tanycytes' contribution to adult hypothalamic neurogenesis, the current understanding of tanycytes and their involvement in neurogenesis is still rudimentary and many questions remain [Bolborea & Dale, 2013; Goodman & Hajihosseini, 2015]. For example, the intermediate steps by which tanycytes mediate their role in neurogenesis and the signalling pathway(s) regulating this role still remains unclear (Figure 1.5).

Given tanycytes' role as chemosensors and putative neural stem cells, it could be speculated that tanycytes may represent the cellular link between sensing changes in the

peripheral environment and integrating these changes via neurogenic remodelling of homeostatic circuitry [Sousa-Ferreira et al, 2014a]. Indeed, the molecular events involved in tanycyte-mediated glucosensing (induction of calcium influx, ATP release and subsequent P2Y1R activation) [Frayling et al, 2011; Benford et al, 2017] are also exhibited in radial glia and NSC proliferation [Weissman et al, 2004; Lin et al, 2007]. Thus, this very mechanism may well be associated in the stimulation of tanycyte proliferation and subsequent neurogenesis.

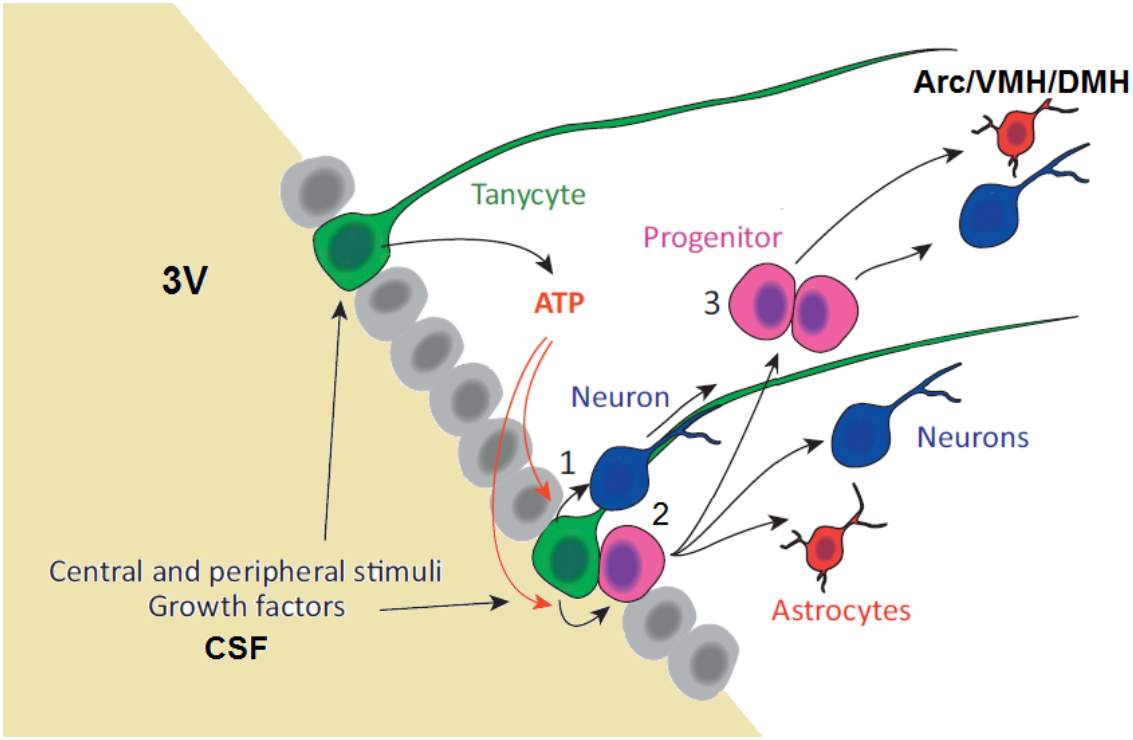

Figure 1.5 Potential intermediate steps by which tanycytes may mediate their neurogenic role. Upon stimulation by soluble factors (e.g. neurotrophic or metabolic molecules) in the CSF or blood circulation, tanycytes may release ATP to stimulate proliferation in neighbouring cells. Tanycytes may directly generate neurons (1) or indirectly via intermediate progenitor cells (2), which may amplify further (3) prior to committing to a cellular fate (neuronal or glial). Newly generated cells may either migrate along tanycyte's long processes into the relevant hypothalamic nuclei, or via other unknown means. Adapted from Bolborea & Dale, 2013.

Aims

The general aim of this project was to investigate the regulation of adult hypothalamic neurogenesis and elucidate the role that tanycytes play in this. This can be broken down into 3 specific aims.

1) Investigate external factors that regulate adult hypothalamic proliferation

Given that environmental stimuli can regulate hypothalamic neurogenesis, I hypothesized that external factors such as physical exercise, artificial sweeteners (Acesulfame-K) and antidepressant (fluoxetine) also influence hypothalamic neurogenesis to refine/adapt hypothalamic functions accordingly. Thus, the effect of these external factors on hypothalamic proliferation was assessed. BrdU-labelling and Ki67 immunodetection was used to assess hypothalamic cell proliferation. Null hypothesis: these stimuli do not have any effect on hypothalamic cell proliferation.

2) Characterize the identity of hypothalamic nestin-expressing cells and their progenies

Although the identity of all putative hypothalamic neural stem/progenitor cells is not clear, tanycytes have been implicated as potential candidates [Lee et al, 2012; Haan et al, 2013; Robins et al, 2013a]. Since nestin might be expressed by α and β tanycytes, an inducible genetic-labelling approach was used to characterize the identity of all putative stem/progenitor cells defined by a transgenic nestin promoter. This characterization was used as preliminary validation for optogenetic stimulation of tanycytes.

3) *Investigate the role of calcium signalling in adult hypothalamic neurogenesis*

In addition to neurogenesis, tanycytes have been demonstrated to have a chemosensing role, which is dependent on purinergic stimulation of intracellular calcium waves [Frayling et al, 2011]. Given that purinergic signalling and calcium waves have also been implicated in radial glia/NSC proliferation [Weissman et al, 2004; Tang & Illes, 2017], I hypothesized that this mechanism may underlie tanycytes' neurogenic function. Thus, optogenetic stimulation was used to induce intracellular calcium waves in tanycytes and assess any effect on hypothalamic neurogenesis. Null hypothesis: optogenetic stimulation does not have any effect on tanycyte cell proliferation and hypothalamic neurogenesis.

Chapter 2: Exposure to acesulfame-K, but not physical exercise or fluoxetine, showed variable effects on the number of newly-generated cells in the adult hypothalamus

Background

Adult hypothalamic neurogenesis can be modulated by changes in several external environmental factors, such as seasonal photoperiodic change [Huang et al, 1998; Migaud et al, 2011; 2014; Batailler et al, 2015], increased exposure to reproductive/social cues [Fowler et al, 2002], heat [Matsuzaki et al, 2009] and dietary changes [Gouaze et al, 2013; Lee et al, 2014]. Indeed, it has been proposed that similarly in the hippocampus, adult neurogenesis in the hypothalamus may serve as a physiological mechanism to respond and adapt to changing metabolic and environmental challenges throughout adulthood [Sousa-Ferreira et al, 2014a; Migaud et al, 2016]. Thus, it is reasonable to suggest that adult hypothalamic neurogenesis may be modulated by external/environmental stimuli.

Indeed, studies investigating the effects of factors that modulate adult hippocampal neurogenesis have revealed a potential link to hypothalamic function [Lee & Blackshaw, 2012]. More specifically, inducers of hippocampal neurogenesis were seen to affect several physiological features, homeostatic and behavioural processes governed by the hypothalamus. Physical activity, which positively regulates hippocampal neurogenesis [van Praag et al, 1999; Kempermann et al, 2000; Vivar et al, 2013], was also seen to affect several aspects of energy balance, including body weight and adiposity, food intake, and energy expenditure, as well as behaviours related to the stress response, mood, and reward [Novak et al, 2012]. Similarly, treatment with fluoxetine, a pharmaceutical drug developed to treat depression and previously identified as another positive modulator of hippocampal neurogenesis [Malberg et al, 2000; Santarelli et al, 2003; Sairanen et al, 2005], caused changes in food intake and body weight [McGuirk et al, 1992], aggressive [Datla et al, 1991] and reproductive [Maswood et al, 2008] behaviours, all of which are functions regulated by the hypothalamus. Furthermore, the hypothalamic-pituitary-adrenal (HPA) axis, an intricate stress-response signalling system, is disrupted in the pathogenesis of depression and can be reversed by antidepressant

treatment [Barden, 2004; Pariante & Lightman, 2008; Mendez-David et al, 2013]. Thus, both physical activity and fluoxetine can bring about long-term changes in several hypothalamic functions, but it has yet to be determined if these effects are mediated through modulation of adult hypothalamic neurogenesis.

Recently, another study indicated that changes in diet such as calorie-restriction and high-fat diet can regulate hypothalamic cell proliferation and adult neurogenesis [Lee et al, 2014]. Whilst high sugar/artificial sweetner-intake have been argued to be linked to weight gain and obesity [Berkey et al, 2004; Yang, 2010; Musselman et al, 2011; Bes-Rastrollo et al, 2016], it has not been determined whether this effect is also associated with changes in hypothalamic neurogenesis. It is interesting to note that tanycytes,, in addition to their neurogenic function, have demonstrated a sweet-tasting function and are able to detect both glucose and non-nutritive sweeteners, such as acesulfame-K [Frayling et al, 2011; Benford et al, 2017].

Given that several environmental stimuli/changes have been reported to regulate the levels of hypothalamic neurogenesis, I hypothesized that the reported changes in hypothalamus-related functions upon exposure to physical exercise, antidepressant administration or high artificial sweetner intake may reflect a modification of the hypothalamic neural circuitry via adult neurogenesis. Thus, this chapter aims to assess whether the aforementioned external stimuli can modulate hypothalamic cell proliferation and accordingly, neurogenesis.

Methods

Mice and treatments

Early-adult (5-6 weeks-old) C57BL/6NTac mice (male) were purchased and used from InVivos (Singapore). 5 mice were housed in each cage. Mice were given 10 days to acclimatize prior to starting any treatment.

Physical activity (Fig. 2.2); mice (n=8) were housed in cages with a running wheel (Bio-serv, K3250/K3328) for 14 days. These ‘Runner’ mice were visually monitored daily in order to ensure running wheels were operational and being used frequently. Control mice (n=10) were housed in cages under the same conditions except lacking a running wheel.

On day 7, all mice were injected i.p. with 50mg/kg BrdU (Sigma, T-5648; 10mg/ml stock in 0.9% saline). Brains were perfusion-fixed on day 14, and extracted for immunohistochemical analysis.

Antidepressant (Fig. 2.3); fluoxetine (Sequoia Research, SRP01950f; stock concentration of 4mg/ml in 0.9% saline/3% Tween20) was injected daily intraperitoneally into mice (n=10) for 21 consecutive days at a dose of 20mg/kg (of bodyweight). Control mice (n=8) were injected with 0.1ml 0.9% saline. On day 14, all mice were injected i.p. with 50mg/kg BrdU (Sigma, T-5648; 10mg/ml stock in 0.9% saline). Brains were perfusion-fixed after the last injection and extracted for immunohistochemical analysis.

Artificial sweetener (Fig 2.4); Mice (n=11) were given Acesulfame K (Ace-K; Sigma, 04054-25G) *ad libitum* (50mM in drinking water) for 14 days. The concentration of Ace-K resulting in the highest Ace-K intake was determined in a previous trial experiment; the concentration yielding the maximum intake of Ace-K was found to be 50mM. However, in this experiment, quantities of Ace-K consumed was not recorded. Control mice (n=10) were given drinking water. On day 7, all mice were injected i.p. with 50mg/kg BrdU (Sigma, T-5648; 10mg/ml stock in 0.9% saline). Brains were perfusion-fixed on day 14, and extracted for immunohistochemical analysis.

Tissue processing & immunohistochemistry

Mice were anesthetized with a lethal dose of pentobarbital and intracardially perfused with 4% paraformaldehyde (PFA; Sigma, P-6148) in 0.1M phosphate buffer (PB). Brains were immediately post-fixated in 4% PFA solution overnight at 4 °C, and subsequently cryoprotected in 30% sucrose in 0.1M PB for at least 48 hours. Cryoprotected brains were sectioned coronally at a thickness of 40µm using a freezing microtome at -30°C (Microm HM430, Thermo Scientific, USA). Serial coronal sections were collected along the anteroposterior axis (approx. from Bregma 0 to -3.0mm) covering the hypothalamus and stored in cryoprotective solution (20% Glycerin, 30% Ethylene Glycol in 0.1M PB) at -20 °C. For multiple immuohistochemisty, a total of 8 sections were used (1 every 4 serial sections). This was appropriate to capture the majority of the hypothalamus. The free-floating method [Bachman, 2013] was used; sections were rinsed 3 times for 10 minutes in 0.1M Tris-buffered saline (TBS), incubated in 50% Formamide at 65°C for 2 hours in a

shaking water bath, rinsed in 2X saline sodium citrate (SSC) for 15 min, incubated in 2N HCl al 37°C for 30 min, rinsed in 0.1M Borate Buffer for 10 min, rinsed 6 times with TBS for 15 min, incubated in blocking buffer, TBS++ (3% Donkey serum, 0.25% Triton-X100 in TBS) for 60min, prior to incubation with primary antibody in TBS++ at 4°C for 36 hours (two nights). Primary antibodies used: rabbit anti-Ki67 (1:500; Leica, NCL-Ki67p), mouse anti-NeuN (1:1200; Millipore, MAB377), rat anti-BrdU (1:400; AbD Serotec, OBT0030G). Following primary antibody incubation, sections were rinsed with TBS 2 times for 10min, blocked in TBS++ for 20 min, and incubated in secondary antibody in TBS++ for 4 hours at room temperature. Secondary antibodies used: donkey Anti-Rat Cy3 (1:250; Jackson Immuno., 712-165-153), donkey Anti-Rabbit 488 (1:250; Jackson Immuno., 711-545-152), donkey anti-mouse 647 (1:250; Jackson Immuno., 705-605-147). Nuclear staining was performed with incubation with 4',6-Diamidino-2-phenylindole-dihydrochloride (DAPI; 0.5µg/mL; Sigma, 28718-90-3) for 10 mins. Immunostained sections were rinsed with TBS 3 times for 10 minutes and mounted on glass slides with mounting medium, polyvinyl alcohol (PVA)-DABCO.

Analysis & quantification

From immunostained slides, 4-6 sections (at an interval of 1 in every 4 sections) were selected based on their location (mid-caudal hypothalamus), from Bregma -1.22mm to -2.18mm, and analysed for BrdU+ and Ki67+ cell quantification. Selected sections were imaged/viewed under the epifluorescence microscope (Zeis Axio Imager 2) to outline hypothalamic nuclei and count BrdU+ and Ki67+ cells.

Autofluorescence from DAPI staining (eradicated by BrdU pretreatment) was used to outline the hypothalamus at 2.5X magnification (Fig. 2.1A), whilst NeuN staining was used to outline the ventromedial nucleus (VMH), and in turn, the predicted hypothalamic nuclei boundaries according to the 'Mouse Brain in Sterotaxic co-ordinates' (Paxinos & Franklin, 2012). The following hypothalamic nuclei/regions were outlined at 5X magnification (Fig 2.1B); Median Eminence (ME), 3rd Ventricle wall (3V), Periventricular nucleus (Pe), Arcuate nucleus (Arc), Ventromedial nucleus (VMH), Dorsomedial nucleus (DMH). The Lateral hypothalamic area (LH) is attributed here to the remaining hypothalamic tissue that was not outlined.

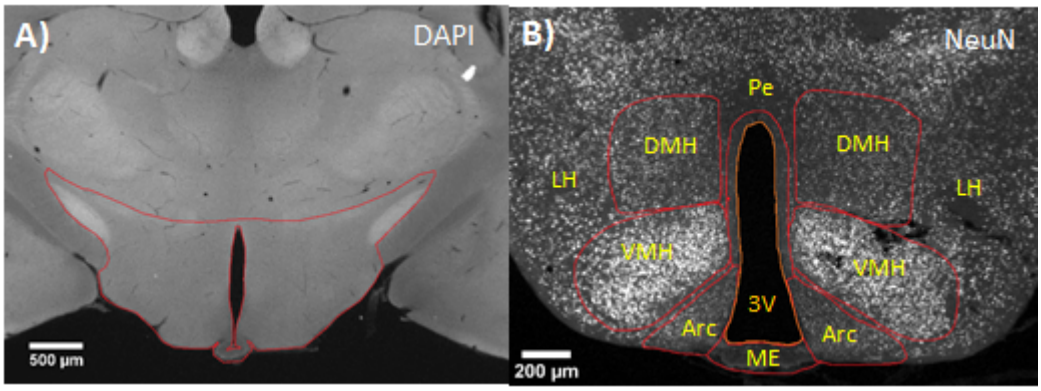

Figure 2.1. Methodology for determining the hypothalamic nuclei for BrdU+ and Ki67+ cell quantification. A) Autofluorescence observed through the DAPI filter was used to help visualize and outline the hypothalamus (note, nuclear staining with DAPI has been ablated by acid pre-treatment for BrdU immunostaining). **B)** NeuN staining was used to help identify the Bregma point of the section and hence outline the predicted boundaries of the respective nuclei/regions.

A blind-approach was adopted during the counting of BrdU+ and Ki67+ cells (under 20X magnification); the identity (control or treatment) of immunostained sections was hidden (by Sandhya Kamath) to the counter. Total number of BrdU+/Ki67+ cell numbers were counted (in the 4-6 sections) and standardised as cell densities per volume (μm^3) of brain tissue per mouse (n = number of animals used) to allow for comparisons between different mice/brains.

Statistics

Results are expressed using box plots (median and interquartile range with whiskers representing the min/max values). The Kruskal-Wallis one-way analysis of variance was used, followed by post-hoc Dunn's for pairwise comparisons within multiple groups. For comparisons between two groups, two-tailed independent samples Mann-Whitney test was used. Significance was only established when $p \leq 0.05$ (*) and satisfied a post-hoc false-discovery test [Curran-Everett, 2000]. Higher levels of significance is indicated when $p \leq 0.01$ (**) or $p \leq 0.001$ (***).

Results

Physical activity may not elicit an effect on hypothalamic cell proliferation

Using the experimental design in Figure 2.2A, BrdU and Ki67-labelling was used to analyze cell proliferation at two different time-points; the thymidine analog BrdU was injected at day 7 to incorporate into S-phase dividing cells and their progenies, whilst Ki67 expression (which is present in all phases of cell division) was immunolabelled for post-mortem to visualize actively proliferating cells at day 14 [Scholzen & Gerdes, 2000; Kuhn et al, 2007].

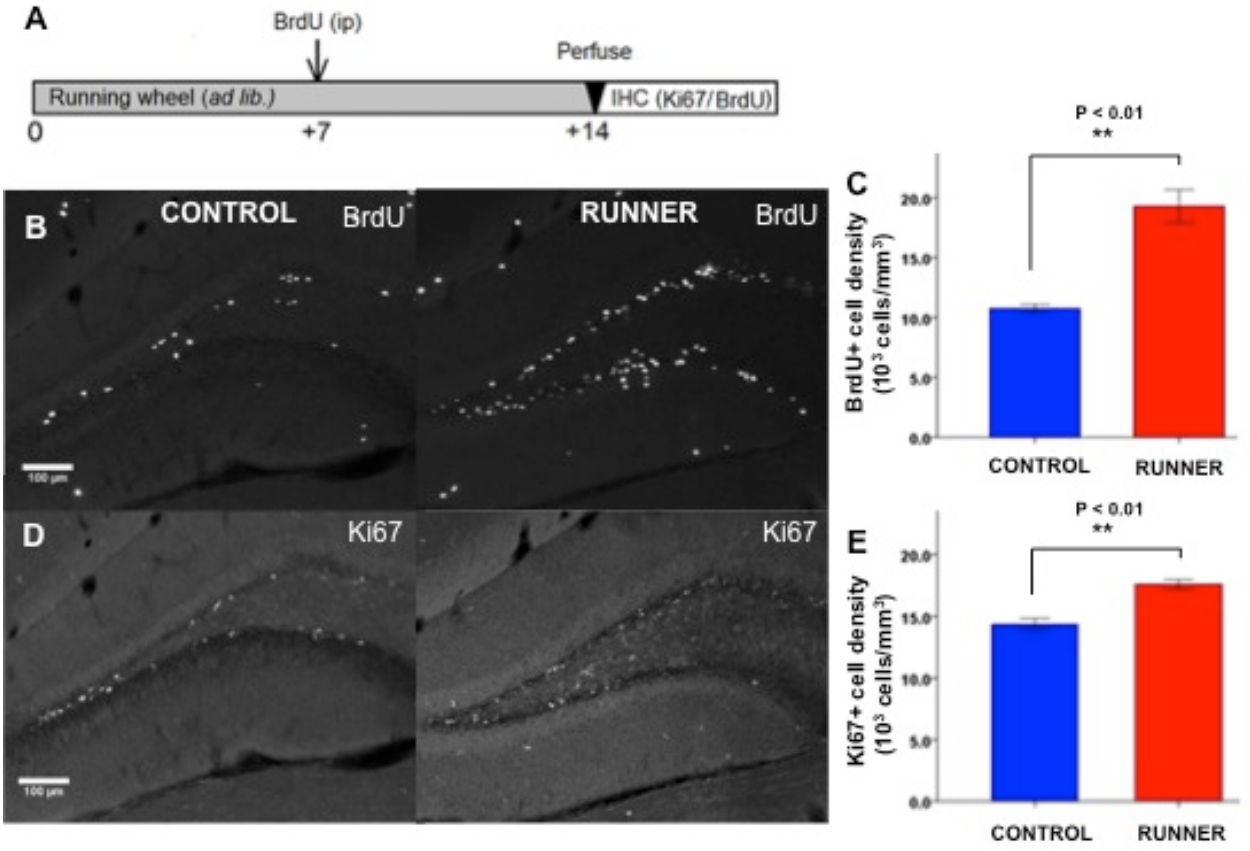

Figure 2.2 The effect of physical exercise on cell proliferation in the dentate gyrus. A) schematic of the experimental paradigm/design. Exemplar images of sections immunostained for **B)** BrdU and **D)** Ki67 are indicated. **C)** BrdU+ and **E)** Ki67+ cells were quantified and calculated as the density of positive cells per mm^3 of tissue. Significant differences detected are denoted by an asterisk and the level of significance by the number of asterisks. Runner n=8 mice, Control; n=10 mice.

Firstly, the effect of running on cell proliferation in the dentate gyrus was assessed (Fig. 2.2B-E) for confirmation that the experimental paradigm was effective, since physical exercise is known to elicit an increase in cell proliferation here [van Praag et al, 1999]. A significant increase in BrdU+ ($p<0.005$, two-tailed independent samples Mann-Whitney test; Fig. 2.2C) and Ki67+ ($p<0.005$, two-tailed independent samples Mann-Whitney test; Fig. 2.2E) cell density was seen in the dentate gyrus of 'Runner' mice. Thus, in this experiment, cell proliferation was increased in the dentate gryus after 7 and 14 days of physical exercise. This observation is in line with the reported effect of physical activity on cell proliferation and neurogenesis in the adult dentate gyrus [van Praag et al, 1999]. Of note, there is a clear difference in the magnitude of the increase in BrdU+ cells versus Ki67+ cells in 'Runner' mice. The larger increase in BrdU+ cells might be caused by the continued proliferation and/or increased survival of BrdU+ cells from day 7 until the end of the experiment, whereas Ki67+ proliferating cells were labeled and quantified within a single temporal snapshot (on day 14, post-mortem).

Figure 2.3

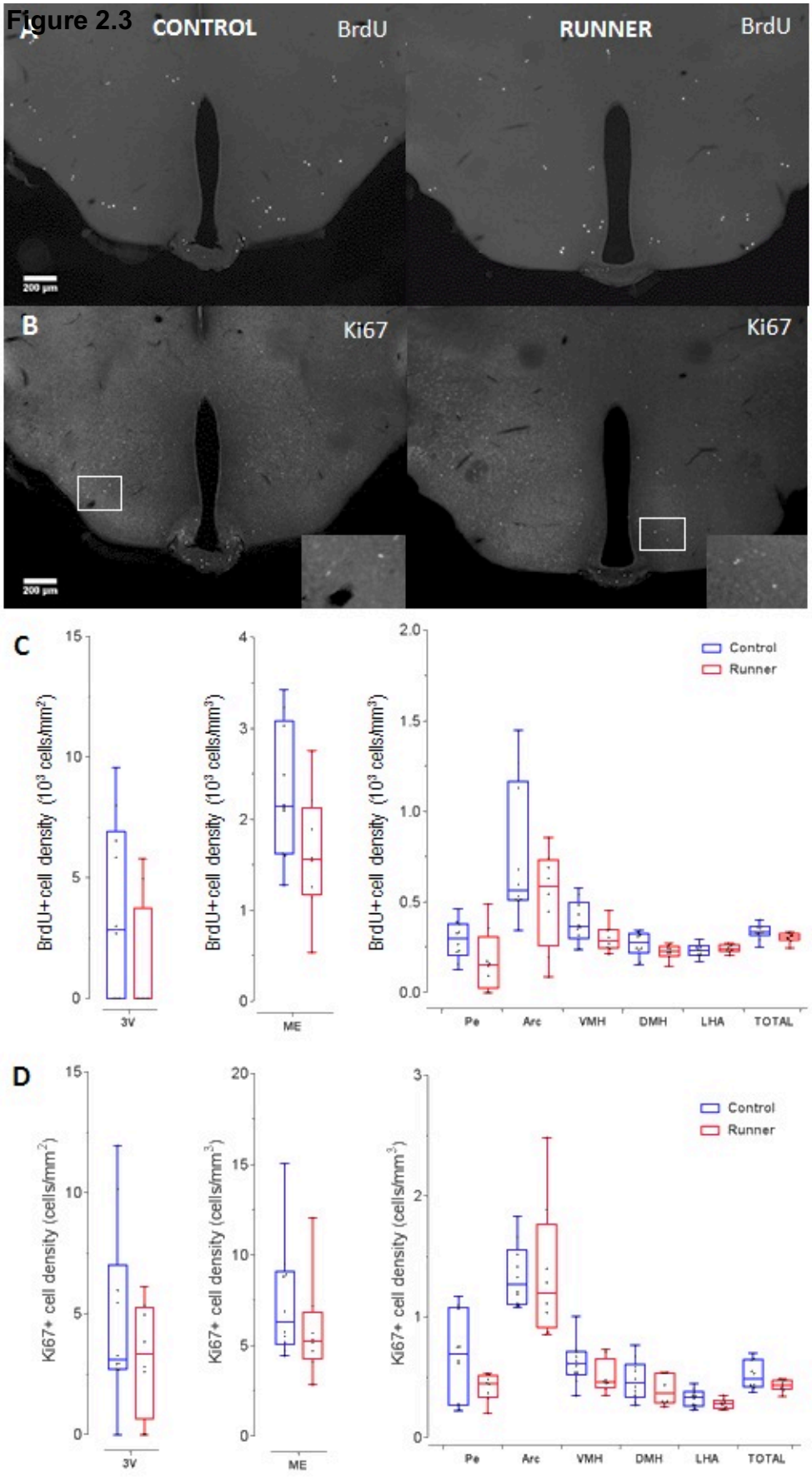
A
CONTROL
BrdU
RUNNER
BrdU
200 µm
B
Ki67
Ki67
200 µm
C
BrdU+cell density (10³ cells/mm²)
3V
BrdU+cell density (10³ cells/mm³)
ME
BrdU+cell density (10³ cells/mm³)
Control
Runner
Pe
Arc
VMH
DMH
LHA
TOTAL
D
Ki67+ cell density (cells/mm²)
3V
Ki67+ cell density (cells/mm³)
ME
Ki67+ cell density (cells/mm³)
Control
Runner
Pe
Arc
VMH
DMH
LHA
TOTAL

Figure 2.3 The effect of physical exercise on cell proliferation in the hypothalamus. Cell proliferation was also assessed in the hypothalamus of the same mice used in Fig 2.2. Exemplar images of sections immunostained for **A)** BrdU and **C)** Ki67 are indicated. **C)** Insets indicate magnified images of Ki67+ cells. **B)** BrdU+ and **D)** Ki67+ cells were quantified and calculated as the density of positive cells per mm^3.of tissue in several hypothalamic nuclei/regions (ME; median eminence, Pe; periventricular nucleus, Arc; arcuate nucleus, VMH; ventromedial nucleus, DMH; dorsomedial nucleus, LHA; lateral hypothalamic area, TOTAL; entire hypothalamus). Runner; n=8, Control; n=10.

In the hypothalamus, the effect of physical activity on cell proliferation was assessed individually in several hypothalamic nuclei/regions. This was done so as to more accurately assess this effect (if any), since it is possible that an effect on cell proliferation may be localized in specific nuclei/regions, as previously seen with exposure to other environmental/molecular stimuli [Fowler et al, 2002; Xu et al, 2005; Robins et al, 2013a; Perez-Martin et al, 2010]. The average number of hypothalamic BrdU+ cells counted per (40μm) brain section of Control and Runner mice was 41.4±1.6 and 36.6±1.8, respectively. The average number of hypothalamic Ki67+ cells counted per (40μm) brain section of Control and Runner mice was 69.4±3.2 and 57.6±2.6, respectively. Both BrdU- and Ki67-labelling indicated an apparent decrease in Runner mice. Indeed, comparison of calculated BrdU+ cell densities also indicated a decrease in the majority of hypothalamic nuclei of Runner mice, with the most notable differences seen in the median eminence, arcuate nucleus and along the 3rd ventricle (Fig. 2.3C). Comparison of Ki67+ cell densities indicated a smaller but similar decrease in Runner mice (Fig. 2.3D). However, these differences in cell density were not significant ($p>0.05$, two-tailed independent samples Mann-Whitney test) in any of the hypothalamic nuclei/regions analyzed, although some were very close (in the ME; $p=0.055$, and the cumulative total; $p=0.055$; Fig. 2.3C). Whilst the lack of statistical significance may be suggestive that 7 or 14 days of physical exercise may not have an effect on hypothalamic cell proliferation, this cannot be decisively concluded due to the high variation in the data.

Fluoxetine may not elicit an effect on hypothalamic cell proliferation

A similar experimental design was used for this experiment to assess for cell proliferation at two time-points (Fig 2.3A); the antidepressant, fluoxetine was applied daily for 21 days,

starting from day 0. BrdU was injected to assess cell proliferation on day 14, whilst Ki67 immunostaining was aimed to indicate cell proliferation at day 21.

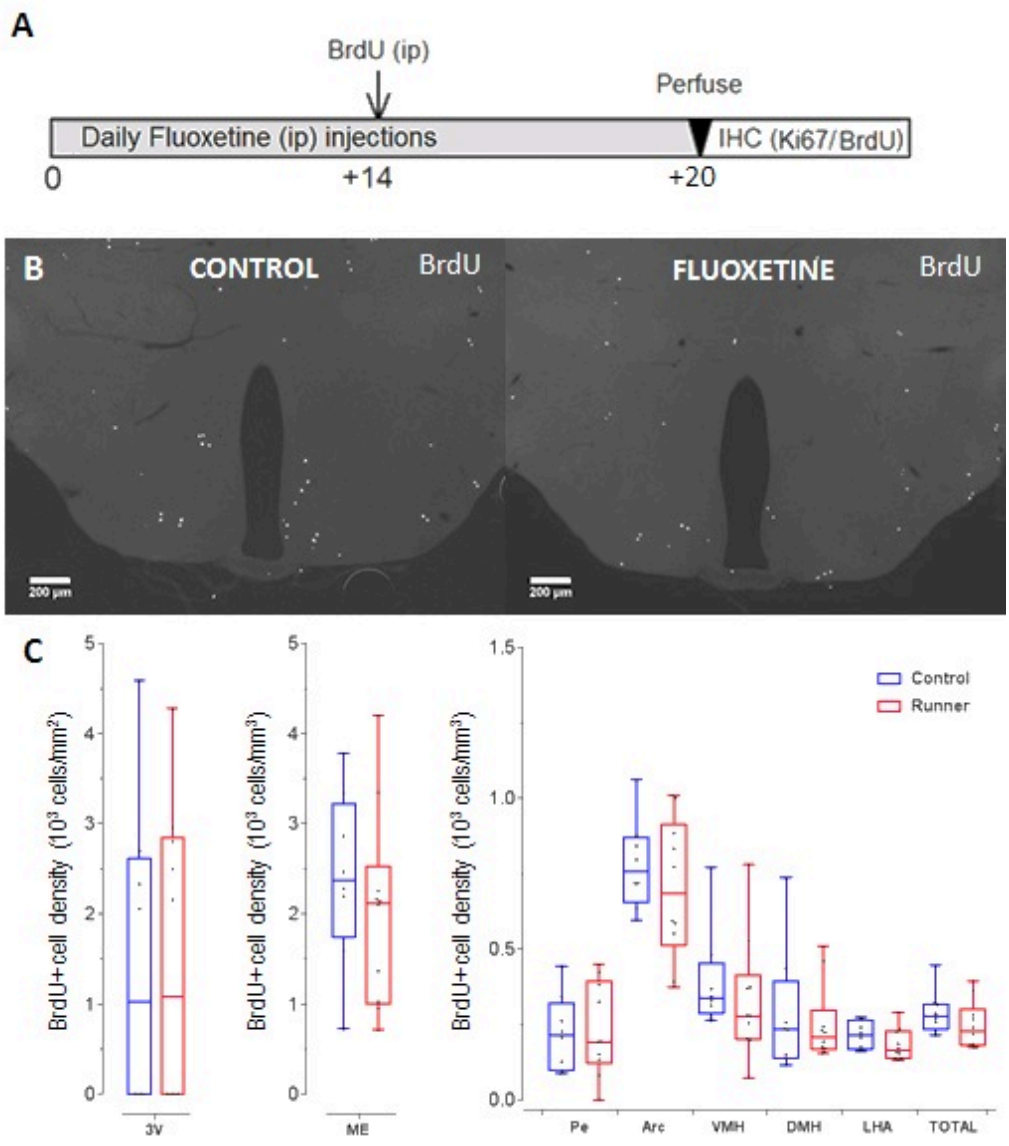

Figure 2.4 The effect of Fluoxetine on cell proliferation in the hypothalamus. A) Schematic of the experimental paradigm/design. **B)** Exemplar images of BrdU-immunostained sections are indicated. **C)** BrdU+ cell densities were quantified in several hypothalamic nuclei/regions (ME; median eminence, Pe; periventricular nucleus, Arc; arcuate nucleus, VMH; ventromedial nucleus, DMH; dorsomedial nucleus, LH; lateral hypothalamic area, HYPO; entire hypothalamus). Fluox; n=10, Control; n=8.

The average number of hypothalamic BrdU+ cells counted per (40µm) brain section of Control and fluoxetine-injected mice was 36.3±1.8 and 29.4±1.6, respectively. Although

this implies a difference, comparison of calculated BrdU+ cell densities indicated no observable difference in any of the hypothalamic nuclei (except the ME) between both groups (Fig. 2.4C). Concurrently, no significant difference in BrdU+ cell density ($p>0.05$, two-tailed independent samples Mann-Whitney test) was seen in any of the hypothalamic regions/nuclei analyzed between fluoxetine-treated or control mice (Fig 2.4C). However, similarly to physical exercise, due to the high variation in data it cannot be concluded that fluoxetine had no effect on hypothalamic cell proliferation (regardless of the lack of any significant difference in BrdU+ cell numbers).

Acesulfame-K induces elicits a divalent effect on hypothalamic cell proliferation

The effect of Acesulfame-K (Ace-K) on hypothalamic cell proliferation was assessed to test the hypothesis that tanycyte activation by Ace-K (as seen by Benford et al, 2017) could upregulate adult hypothalamic cell proliferation and neurogenesis. Ace-K (in drinking water) was given to mice *ad libitum* for 14 days. During this, BrdU was injected to assess cell proliferation on day 7, whilst Ki67 immunostaining was aimed to indicate cell proliferation at day 14 (Fig. 2.5A)

Figure 2.5

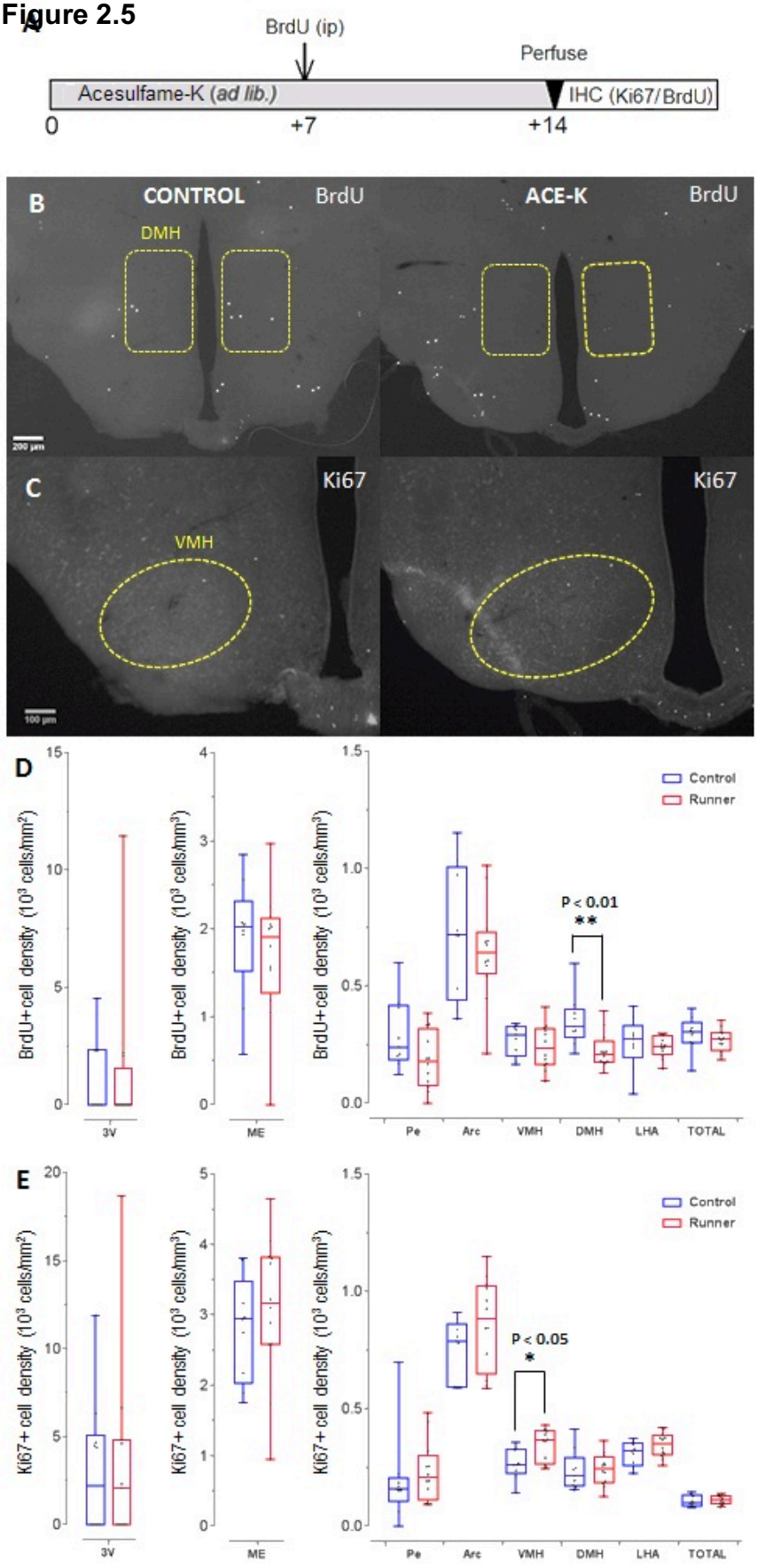
A
BrdU (ip)
Perfuse
Acesulfame-K (ad lib.)
IHC (Ki67/BrdU)
0
+7
+14
B
CONTROL
BrdU
ACE-K
BrdU
DMH
C
Ki67
Ki67
VMH
D
BrdU+cell density (10³ cells/mm²)
BrdU+cell density (10³ cells/mm³)
BrdU+cell density (10³ cells/mm³)
Control
Runner
P < 0.01
**
3V
ME
Pe
Arc
VMH
DMH
LHA
TOTAL
E
Ki67+cell density (10³ cells/mm²)
Ki67+cell density (10³ cells/mm³)
Ki67+cell density (10³ cells/mm³)
Control
Runner
P < 0.05
*
3V
ME
Pe
Arc
VMH
DMH
LHA
TOTAL

Figure 2.5 The effect of acesulfame-K on cell proliferation in the hypothalamus. A) Schematic of the experimental paradigm/design. Exemplar images of **B)** BrdU- and **C-D)** Ki67-immunostained sections are indicated. Boundaries of the arcuate nucleus, in which a change in cell proliferation was detected are outlined. **D)** BrdU+ and **E)** Ki67+ cell densities were quantified in several hypothalamic nuclei/regions (ME; median eminence, Pe; periventricular nucleus, Arc; arcuate nucleus, VMH; ventromedial nucleus, DMH; dorsomedial nucleus, LH; lateral hypothalamic area, HYPO; entire hypothalamus). Significant differences detected are denoted by an asterisk and the level of significance by the number of asterisks. Ace-K; n=11, Control; n=10.

The average number of hypothalamic BrdU+ cells counted per (40μm) brain section of Control and Ace-K-treated mice was 40.9±1.6 and 37.3±0.8, respectively. The average number of hypothalamic Ki67+ cells counted per (40μm) brain section of Control and Ace-K-treated mice was 30.9±1.2 and 34.2±1.1, respectively. Comparison of calculated BrdU+ densities indicated a small yet significant decrease in the dorsomedial hypothalamic nuclei of mice given Ace-K ($p=0.007$; two-tailed independent samples Mann-Whitney test). On the other hand, comparison of Ki67+ cell densities indicated an increase in several hypothalamic nuclei/regions upon Ace-K consumption, of which there was a small yet significant increase in the ventromedial nucleus ($p<0.05$; two-tailed independent samples Mann-Whitney test; Fig. 2.5E). These results potentially suggest that Ace-K consumption may decrease cell proliferation in the DMH within the first 7 days but then increase cell proliferation in the VMH between 7 to14 days.

Discussion

Physical exercise

In this study, physical exercise did not have any significant effect on hypothalamic cell proliferation. In contrast to these results, recent studies have since reported a positive effect of physical exercise (running) on hypothalamic cell proliferation [Li et al, 2013a; Borg et al, 2014; Niwa et al, 2015]. Using BrdU labelling, increased cell proliferation was observed at several time-points as early as 6 days from initiating voluntary physical exercise [Li et al, 2013a; Borg et al, 2014]. Another study noted an increase in cell proliferation particularly at the ependymal layer, in the arcuate nucleus and median eminence [Niwa et al, 2015]. Finally, long-term (12 weeks) voluntary physical exercise

was able to restore diminished levels of cell proliferation (indicated by Ki67-immunolabelling) in diet-induced obese mice [Laing et al, 2016].

The number of hypothalamic BrdU+ cells counted in control/sedentary mice was comparable between our study (41±2 cells per 40μm section) and of a separate study in the same species (31±5 cells per 30μm section) [Borg et al, 2014]. However, whilst Borg et al reported a 3.5-fold increase in BrdU+ cells after 7 days of physical activity, we observed no such change. Our study administered BrdU (peripherally; i.p.) at a single instance (day 7) and terminated/analysed 7 days after, whereas Borg et al [2014] continuously administered BrdU (centrally) over the 7 days of physical exercise, followed by termination/analysis 1 day after.

Although BrdU+ cell numbers in control/sedentary mice were comparable in both studies, the difference in effects observed may be due to several methodological differences. Firstly, administration of BrdU centrally (i.c.v) or peripherally (i.p) has been reported to indicate preferential BrdU uptake in different hypothalamic regions (the ventricular/periventricular and parenchymal, respectively) [Kokoeva et al, 2007]. Thus any potential effect, as reported in the ependymal layer [Niwa et al, 2015], may not have been detected in our study. Furthermore, in our study the (potential) continued proliferation of BrdU+ cells from day 7 until the end of the experiment (day 14), may have affected the BrdU+ cell numbers (i.e. to yield increased BrdU+ cells or conversely, BrdU dilution beyond detection limits could yield a decrease in BrdU+ cells) thereby not representing the exact numbers of proliferative cells on day 7. Finally, the number of BrdU+ cells could be further influenced by an effect of physical exercise on cell survival or migration from other areas from day 7 to 14 [Kuhn et al, 1996; Taupin, 2007]. Importantly, although the survival period (time from last BrdU administration to termination) was limited by Borg et al [2014] and Li et al [2013] to 1 day, BrdU was administered for several days during physical exercise (7 and 5 days, respectively), allowing the possibility of physical exercise to influence BrdU+ cell survival and/or migration, just as in our study. Our study used Ki67-immunolabelling to assess cell proliferation at the end of 14 days of physical exercise and saw no significant change in Ki67+ cells either. Ki67 is expressed and identified in cells during all active phases of the cell cycle (G1, S, G2 and mitosis) [Scholzen & Gerdes, 2000], and unequivocally

represents proliferative cells at the time of perfusion/termination on day 14. Thus, it cannot be determined if physical exercise is able to induce hypothalamic cell proliferation at any time point before day 14.

In order to understand the cause of discrepancy in results with Borg et al [2014], and effectively distinguish between the effects of physical exercise on cell proliferation and cell survival, future studies may require higher methodological stringency. Firstly, by utilizing a combination of central and peripheral delivery methods and multiple instances (injections) of BrdU administration, a high number of parenchymal and ventricular proliferating cells can be labelled, providing reliable quantitative comparison/analysis. Secondly, by minimising the time-frame of these injections and the survival period after BrdU administration (ideally to 1 day, in each respect), the influence of cell survival on BrdU+ cell numbers is very limited. Immunolabelling for endogenous proliferative markers, such as Ki67 or proliferating cell nuclear antigen (PCNA) [Ino & Chiba, 2000] would provide an effective alternative to BrdU-labelling-based proliferation studies.. Indeed, this would mean that any varied durations of physical exercise (7,14 or more days) would require separate experimental-groups. To evaluate cell survival, two time-points of analysis are required. If the ratio of BrdU+ cell numbers (late:early time points) in exercised mice are higher than that in control mice, an effect on survival may be claimed. However, this would require confirmation by assessing any changes in apoptosis with cell death markers at these time-points.

Some studies have associated an increase in observed cell proliferation with enhanced neurogenesis, indicated by an increase in BrdU+ cells expressing neuronal fate-markers (NeuN/Hu) at later time-points [Li et al, 2013a; Niwa et al, 2015], as well as increased expression of neurotrophic factors, such as EGF, FGF-2 and BDNF in exercising mice [Borg et al, 2014; Niwa et al, 2015]. These factors have been previously reported to upregulate hypothalamic cell proliferation and adult neurogenesis [Pencea et al, 2001; Xu et al, 2005; Robins et al, 2013a]. Of particular interest, physical exercise was suggested to increase tanycyte proliferation, as indicated by a semi-quantitative increase in tanycyte marker (vimentin, nestin and GFAP) expression levels and increased BrdU uptake in ependymal and subependymal layers [Niwa et al, 2015]. However, other studies on diet-induced (HFD) obese mice provide evidence that question whether neurogenesis is

indeed responsible for the metabolic changes associated with physical exercise. Although a relative increase in cell proliferation was seen in exercising obese mice, no significant change in differentiation (BrdU+/NeuN+ colocalization) was noted [Borg et al, 2014]. Furthermore, ablation of neurogenesis with the anti-mitotic drug, Ara-C, in these mice did not alter metabolic parameters (food intake, body weight, fat mass and insulin sensitivity) [Borg et al, 2014]. Instead, another study suggested that the observed metabolic changes associated with physical exercise was more due to a neuroprotective effect, whereby a shift in POMC neuronal turnover was altered by increasing cell proliferation and decreasing obesity/HFD-induced apoptosis [Laing et al, 2016]. Although, these latter studies focussed on the effect of physical exercise in (HFD-induced) obese mice and that the mechanisms by which physical activity may mediate metabolic changes may differ in healthy mice, this may provide evidence that physical exercise may not in fact, alter neurogenesis, at least in the short-term.

Fluoxetine

In our study, fluoxetine did not have any statistically significant effect on hypothalamic cell proliferation after 14 days of treatment. Fluoxetine has previously been reported to increase cell proliferation in the dentate gyrus of the hippocampus [Malberg et al, 2000; Santarelli et al, 2003; Sairanen et al, 2005]. However, this effect was not confirmed in our study as a positive control. Thus, the interpretation of our results is based on the assumption that the current experimental protocol was sufficient to induce hippocampal cell proliferation, as previously reported. Whilst it could be argued that this assumption is fair, since a significant increase in cell proliferation (BrdU+ cells) was seen as early as 11 days of daily administration at half the dose [Santarelli et al, 2003], it cannot be conclusively determined whether this effect was achieved in our study.

In contrast to our results, other studies have reported that fluoxetine upregulates hypothalamic cell proliferation [Sachs & Caron, 2014; Sousa-Ferreira et al, 2014b]. An increase in Ki67-expressing cells was seen when fluoxetine was applied to embryonic hypothalamic neurosphere cultures [Sousa-Ferreira et al, 2014b]. In a more comparable experimental paradigm, chronic application of fluoxetine (for 28 days) in mice induced an increase in BrdU uptake in the hypothalamus of adult mice [Sachs & Caron, 2014]. It was

further demonstrated in this study that this reported increase in cell proliferation was attributed to the upregulation of BDNF expression, a neuropeptide previously indicated to upregulate hypothalamic cell proliferation (and neurogenesis) [Pencea et al, 2001]. Finally, using a fate-mapping approach to label putative neural stem/progenitor cells driven by nestin expression, fluoxetine treatment also led to a two-fold increase in these labelled cells at the ependymal layer [Sachs & Caron, 2014].

Several methodological differences exist between the aforementioned study [Sachs and Caron, 2014] and the current study that may account for the difference in observed effects. First, Sachs and Caron administered fluoxetine for longer (28 days) and at a dose of 155mg/L in drinking water, whereas in our study, fluoxetine was administered for 21 days at a dose of 20mg/kg of bodyweight with i.p. injection. Thus, in our study, a maximum of 0.6mg fluoxetine was injected into mice daily (volumes no more than 0.15ml of 4mg/ml fluoxetine), whereas in the study by Sachs & Caron [2014] mice drinking any more than 4ml of 155mg/L fluoxetine would have ingested a higher dose. This is highly likely as a study indicated that average of 6ml/mouse (or 8ml/30g bodyweight) of water was drank daily by C57BL/6J mice (same background strain used in both studies) [Bachmanov et al, 2002]. Secondly, although BrdU was delivered via i.p. injection in both studies, Sachs & Caron injected BrdU multiple (three) times at a much higher concentration (100mg/kg) vs our study (once, at a dose of 50mg/kg), thus the chances of capturing proliferating cells was higher. This may be relevant as it could be argued that increased BrdU-labelling may be necessary for a more reliable statistical estimate for a detecting any significant changes. Furthermore, BrdU-labelling was done at different time-points with Sachs and Caron assessing cell proliferation after 4 weeks of fluoxetine, whilst our study assessed cell proliferation after 2 weeks of fluoxetine. Again, this may be important to note as chronic effects of fluoxetine may differ from its short-term effects [Yuan et al, 2015].

Similarly to our results with physical exercise, it could be speculated that the increased survival period (7 days) in our study may have caused for misinterpretation of cell proliferation at day 7 and overlooking an effect on cell survival. Indeed, the study by Sachs and Caron provides a more stringent assessment of cell proliferation (injecting BrdU multiple times within 24 hours) and limits the influence of cell survival and BrdU dilution in their analysis.

It should be highlighted that the current methodology in quantifying proliferative (BrdU+ and Ki67+) cells (analyzing 4-6 sections from a total of 8 immunostained sections per brain at an interval of every 4th section) was used with the following aims and benefits in mind. Firstly, to cover the entire anterior-posterior (AP) axis of the hypothalamus, given that cell proliferation may not be uniform throughout the hypothalamus. Secondly, the interval was used to minimize the possibility of re-counting the same (split) cells in separate sections, as previously highlighted (Matsuzaki et al, 2009). However, a caveat that requires consideration is that a limited number of sections were analyzed per brain. The majority of the hypothalamic nuclei analyzed in my experiments may have been too small to accurately quantify BrdU+ cells with the interval used. Indeed, this is reflected in the fact that only 4-6 sections out of 8 immunostained sections were relevant for BrdU+ cell quantification in these nuclei. Thus, by lowering the section interval (i.e. 1 in every 3 sections), more relevant sections can be analyzed (per brain) and any change in cell proliferation (in each nucleus) can be more reliably captured. This would be further aided with the suggested changes in BrdU administration methodology (described previously) to label a higher number of proliferative cells in each section.

Whilst fluoxetine treatment has been demonstrated to increase cell proliferation in the hypothalamus *in vivo* [Sachs & Caron] and hypothalamic neurospheres *in vitro* [Sousa-Ferreira et al, 2014], it did not affect the percentage of BrdU+ cells that become NeuN+ neurons or GFAP+ astrocytes *in vivo* [Sachs & Caron, 2014], and even inhibited differentiation *in vitro* [Sousa-Ferreira et al, 2014b]. It has thus been suggested that fluoxetine may only increase cell proliferation and self-renewal, but it does not alter the commitment of newly-generated cells to a neural fate [Sachs & Caron, 2014]. Indeed, a study on hippocampal neurogenesis suggested that neuronal turnover is increased upon antidepressant administration, mediated by an increase in cell proliferation as well as apoptosis [Sairanen et al, 2005]. Interestingly, although BDNF has been implicated in antidepressants' mechanism of action [Nestler et al, 2002; Castrén, 2004], it was also indicated that BDNF and its receptor (trkB) activation do not play a major role in the antidepressant-induced increase in hippocampal cell proliferation [Sairanen et al, 2005].

Acesulfame-K

Ace-K is an artificial sweetner used as a dietary substitute for sucrose in manufactured food products [Shankar et al, 2013]. Indeed, whilst Ace-K is non-nutritive, it is approximately 200 times sweeter than sucrose and can stimulate tanycytes via sweet-taste receptor activation at the ependymal layer [Benford et al, 2017]. Thus it was hypothesized that Ace-K could potentially have an effect on hypothalamic neurogenesis, through tanycyte activation.

To the best of my knowledge, this is the first study to assess the effect of artificial sweetener (Ace-K) exposure on adult hypothalamic cell proliferation. Our results may suggest that cell proliferation is initially downregulated in the dorsomedial hypothalamic nucleus (at day 7), but is recovered later (at day 14), whilst cell proliferation is upregulated in the ventromedial hypothalamic nucleus after two weeks of Ace-K consumption. Thus, a divalent effect is observed whereby initially, cell proliferation is decreased, but later increases in different hypothalamic nuclei. This observation might be explained by a similar but opposite effect seen under other dietary conditions; upon short exposure to a high fat diet, a transient increase in cell proliferation was observed in the arcuate and ventromedial nuclei [Gouaze et al, 2013], but long-term exposure resulted in differential regulation (increase in the median eminence and decrease in the arcuate nucleus) of cell proliferation [Lee et al, 2014]. Indeed, these effects of a high-fat diet can be explained; upon increased exposure to high fat diet, initially neurogenesis is induced in a neuroprotective context and generate anorexigenic POMC neurons to mediate adaptive anorectic behaviour (reduced feeding) [Gouaze et al, 2013]. Inhibition of this early onset HFD-induced neurogenesis resulted in an accelerated onset of obesity and neuroinflammation [Gouaze et al, 2013]. However, upon prolonged exposure, neurogenesis is down-regulated in the arcuate and instead upregulated in the median eminence to modify the metabolic neural circuitry and mediate changes in energy metabolism and energy storage [Li et al, 2012; Lee et al, 2012; 2014].

The opposite divalent effect of Ace-K is much more difficult to explain given the technical issues with interpreting BrdU+ cell numbers. As highlighted earlier, BrdU+ cell numbers may be influenced by ongoing cell proliferation and any change in BrdU+ cell survival and

migration into the nuclei from day 7 up until the end of the experiment (day 14). Thus, it cannot be determined if the effect seen in the dorsomedial nucleus is due to a decrease in cell proliferation, cell survival, migration or any combination of them. Ki67, on the other hand, is expressed in cells during all active phases of the cell cycle (G1, S, G2 and mitosis) [Scholzen & Gerdes, 2000], so Ki67-immunolabelling unequivocally identified proliferative cells at the time of animal perfusion on day 14. Accordingly, the increase in Ki67+ cells in the ventromedial nucleus was clearly due to an increase in cell proliferation.

Both, the ventromedial and dorsomedial nuclei host populations of gluco-sensitive neurons and have been implicated in glucose-sensing and metabolic regulation, particularly in hypoglycemia detection [Song et al, 2001; Routh et al, 2014]. Thus, these changes in cell proliferation could potentially reflect an adaptive mechanism for glucose-sensitivity, which are integral to the counterregulatory response to (Ace-K-induced) hypoglycaemia [Watts & Donovan, 2010; Routh et al, 2014]; for example, with this mechanism, neurogenesis of dorsomedial glucose-inhibited neurons may be inhibited, whilst that of glucose-excited neurons of the ventromedial nucleus may be enhanced to potentially achieve increased counterregulatory hormone (glucagon and adrenaline) release and/or activation of orexinergic (apetite-inducing) neurons in the arcuate nucleus [Verberne et al, 2014].

Summary

Our results suggest that, under the current experimental paradigm, short/mid-term exposure to physical exercise and fluoxetine may not have any effect on the number of newly-generated hypothalamic cells (whose identity was not determined), whilst Ace-K may induce a divalent effect; decreasing and increasing these cell numbers in the dorsomedial and ventromedial nuclei, respectively. However, as seen in previously-described studies, a change in cell proliferation may not necessarily equate to a change in neurogenesis. Since our studies lack phenotypic characterization of the newly-generated cells quantified, we cannot determine whether these stimuli (short/mid-term) had an effect on neurogenesis. Thus, further investigation is required to clarify this and the discrepancies between our proliferation results and of previous studies. Further-investigating the effect of Ace-K on cell proliferation, survival or migration is warranted.

Chapter 3: characterization of cells defined by a transgenic nestin promoter and their progenies in the adult hypothalamus

Background

Lineage-tracing/fate-mapping is defined as the visual identification of a cell or cell population and its progeny by a permanent labelling method [Kretzschmar & Watt, 2012]. Since the permanent labelling is inherited in all subsequent progeny, this allows for the characterization of the location, proliferative capacity and the cellular fate(s) of the source cell and its progeny [Kretzschmar & Watt, 2012]. Indeed, provided the context of adult neurogenesis, fate-mapping studies have allowed for elaborate characterization of neural stem/progenitor cells to further elucidate their cellular dynamics and mechanisms of cell fate determination/regulation [Blanpain & Simons, 2013; Imayoshi et al, 2011].

Several studies in adult neurogenesis have indeed established and adopted different transgenic mice using the genetic inducible fate-mapping approach to label neural stem/progenitor cells. One of the most abundantly used promoter sequences to drive Cre expression is that of nestin [Imayoshi et al, 2011; Dhaliwal & Lagace, 2011]. nestin is an intermediate filament protein that is expressed in neuroepithelial cells of the developing CNS and in neural stem/progenitor cells of the SVZ and SGZ in the adult brain [Lendahl et al, 1990; Zimmerman et al, 1994; Doetsch et al, 1997]. Indeed, when tamoxifen was injected in mice expressing Cre-ER under the control of the nestin promoter (Nestin-CreER mice), neural stem/progenitor cells were reporter-labelled, which gave rise to reporter-positive newborn neurons [Carlen et al, 2006; Lagace et al, 2007; Burns et al, 2007; Imayoshi et al, 2006; Chen et al, 2009; Giachino & Taylor, 2009; Dranovsky et al, 2011]. However, it should be noted that the specificity and efficiency of reporter expression in neural progenitors was seen to vary highly between transgenic mice developed by different research groups [Sun et al, 2014]; of the transgenic mice evaluated, the Nestin-CreERT2 driver mouse from the Eisch group [Lagace et al, 2007] appeared to provide the highest specificity, albeit at the cost of labeling a smaller percentage of neural progenitors. In addition to nestin, other promoter sequences of neural stem/progenitor cell-associated genes (Sox-2, GLAST, GFAP) have been used in

fate-mapping studies, demonstrating successful recombination following tamoxifen injection [Favaro et al, 2009; Mori et al, 2006; Ganat et al, 2006].

Whilst the prior studies focussed on neural stem/progenitor cells in the adult canonical neurogenic niches, it was only recently that such transgenic mice (and analogous genetic fate-mapping methods) were applied in parallel to identify and study neurogenesis and/or neural stem/progenitor cells in the postnatal and adult hypothalamus [Pierce & Xu, 2010; El Agha et al, 2012; Lee et al, 2012; Li et al, 2012; Haan et al, 2013; Robins et al, 2013a; Robins et al, 2013b; Pak et al, 2014].

In a study using the Sox2-promoter-directed Cre-expression, shortly following recombination, reporter (YFP) expression was detected in the parenchyma, indicating that another previously uncharacterized parenchymal neural stem/progenitor cell population existed in the hypothalamus [Li et al, 2012]. It was later suggested that the majority of these parenchymal Sox-2+ cells were NG2+ glia, by yet another fate-mapping study [Robins et al, 2013b]. Using the promoter from another canonical NSC/progenitor gene, nestin, both α- and β-tanycytes were successfully fate-mapped in the postnatal hypothalamus, and were later seen to differentiate into predominantly ME neurons, exhibiting a range of different neuronal subtypes [Lee et al, 2012]. Subsequent studies were able to fate-map specific subpopulations of tanycytes. Radial glial promoters such as GLAST [Robins et al, 2013a] and FGF10 [Haan et al, 2013] were used to drive CreER-expression and label α- and β- tanycytes, respectively. However, whilst both subtypes of tanycytes were indicated to exhibit neurogenic capacities, the interpretations from these two studies contradict each other, in that α-tanycytes (and not β) were explicitly proposed to retain neural stem cell properties. It should be noted however, that GLAST is also strongly expressed in astrocytes [Rothstein et al, 1994; Anderson & Swanson, 2000], and thus the contribution of GLAST+ α-tanycytes to neurogenesis is not clear. Whilst the contribution of FGF10+ β-tanycytes to neurogenesis can be appreciated, it could be hypothesized that each tanycyte subtype (α and β) may still potentially contribute towards neurogenesis (of different neuronal subtypes or in different regions) in the hypothalamus. Thus, whilst the literature clearly suggests a role for tanycytes in neurogenesis, the responsible subtype is still under debate. Meanwhile, no study as of yet, has been able to successfully fate-map the collective population of tanycytes in the adult hypothalamus.

Whilst this was achieved this in the postnatal mice [Lee et al, 2012], it has yet to be demonstrated whether nestin+ tanycytes can be fate-mapped in the adult.

The aim of this study was to characterize cells labelled under the control of a transgenic nestin promoter sequence, and assess this mouse model (Nestin-CreER^{T2}/Rosa26-lox-STOP-lox-YFP) as a suitable tool to label tanycytes and other putative neural stem/progenitor cells in the adult hypothalamus. Indeed, this mouse would provide preliminary support for the use of a similar transgenic mouse model to optogenetically stimulate tanycytes.

Methods

Animals

The following transgenic mice were purchased from Jackson Laboratory (Bar Harbour, ME, U.S.A) and bred in the animal facility at Biopolis (Singapore): Nestin-CreER^{T2} [C57BL/6-Tg(Nes-creER^{T2})KEisc/J] generated by Eisch lab [Lagace et al, 2007], ROSA26$^{loxP\text{-}STOP\text{-}LoxP\text{-}YFP}$ [B6.129X1-Gt(ROSA)26Sortm1(EYFP) Cos/J]. Nestin-CreERT2**:**ROSA26-loxP-STOP-loxP-YFP mice were obtained by breeding Nestin-CreERT2 mice with ROSA26$^{loxP\text{-}STOP\text{-}LoxP\text{-}YFP}$ mice. Only offspring positive for Cre-recombinase (Nestin-CreERT2$^{+/-}$**:**ROSA26-loxP-STOP-loxP-YFP$^{+/+}$, hereon referred to as NCE-YFP) were selected for experiments based on genotyping results.

Mice were genotyped using the following PCR primers: Nestin-CreERT2 transgene; CCG GTG AAC GTG CAA AAC AGG CTC TA (mutant forward), GAT TAA CAT TCT CCC ACC GTC AGT (mutant reverse), CTA GGC CAC AGA ATT GAA AGA TCT (wildtype forward), GTA GGT GGA AAT TCT AGC ATC ATC C (wildtype reverse). Mutant primers amplified a smaller transgenic sequence for positive identification of Cre+ mice, whilst the wildtype primers amplified a larger endogenous sequence common to both Cre+ and Cre- mice. Primers used to identify ROSA26-loxP-STOP-loxP-YFP transgene; AAA GTC GCT CTG CGT TGT TAT (common forward), AAG ACC GCG AAG AGT TTG TC (mutant reverse), GGA GCG GGA GAA ATG GAT ATG (wildtype reverse). In mice negative for the transgene, the common forward primer and the wildtype reverse primer will produce a PCR product that spans the transgene integration site within the Rosa26 locus. However,

the PCR product is too large to be amplified when the transgene is inserted and instead, DNA is amplified between the mutant reverse primer (complimentary to a portion of the transgene) and the common forward primer. Exemplar images from genotyping NCE-YFP mice with these primers is shown in Figure 3.1.

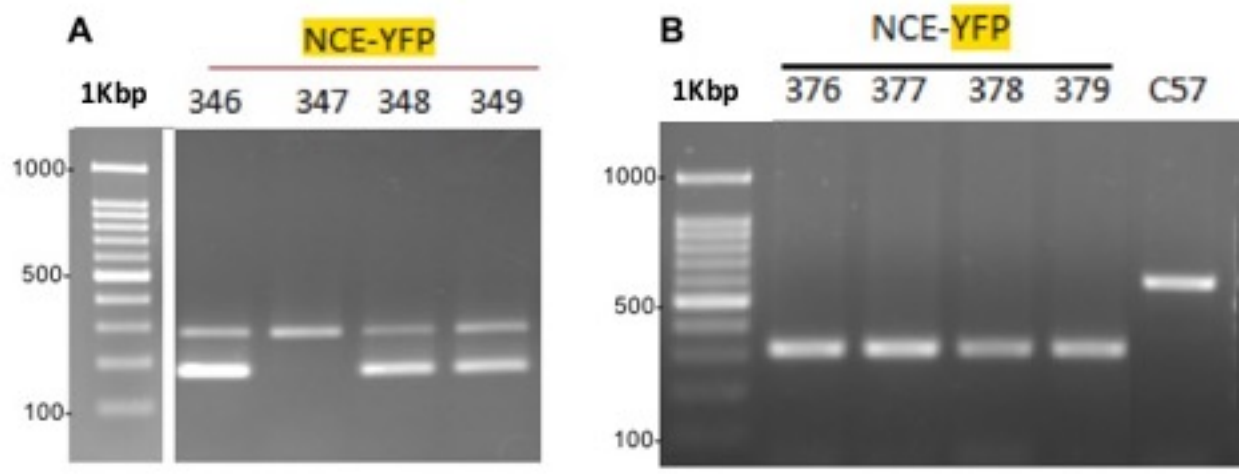

Figure 3.1 Exemplar gel electrophoresis images of PCR- genotyped NCE-YFP mice. A) Mice positive for the Nestin-CreERT2 transgene were identified by the presence of two bands at 199 bp and 324 bp (NCE-YFP 346, 348, 349), corresponding to PCR-amplified products from the separate sets of mutant and wildtype primers, respectively. Mice negative for the transgene only indicated 1 band at 324 bp (NCE-YFP 347). **B)** For the ROSA26-loxP-STOP-loxP-YFP transgene, mice homozygous for the transgene indicated only 1 band at 320 bp (NCE-YFP 376, 377, 378, 379) and wild-type mice indicated 1 band at 600 bp (C57). 1000bp, 500bp and 100bp have been labelled along the 1kb DNA ladder.

NCE-YFP mice aged 8-16 weeks-old were used for fate-mapping experiments. Although the NCE-YFP mouse line (progenies positive for Cre-recombinase) did not present any overt abnormalities, some degree of hydrocephaly was observed in some individuals (these were not used in the study) as reported previously [Forni et al, 2006].

All mice used in these studies were maintained and euthanized according to protocols approved by the Institutional Animal Care and Use Committee at the Biological Resource Centre, Agency for Science, Technology and Research (A*STAR).

Tamoxifen & BrdU injection

Tamoxifen (Sigma, T-5648) was dissolved in 90% cornoil (Sigma, C8267):10% ethanol at a concentration of 20mg/ml. To induce Cre-mediated recombination for induction of YFP expression, tamoxifen was injected into adult (8-12 weeks-old) mice intraperitoneally for 5 consecutive days at a daily dose of 100mg/kg of body weight. Following injections, mice were either perfused one day after or left to survive for different stated survival-periods prior to perfusion-fixation.

BrdU (Sigma, B5002) was dissolved in 0.9% saline at a concentration of 10mg/ml. BrdU was injected into adult mice intraperitoneally on the stated days at a dose of 50mg/kg body weight.

Tissue processing

Mice were anesthetized with a lethal dose of pentobarbital and intracardially perfused with 4% paraformaldehyde (PFA; Sigma, P-6148) in 0.1M phosphate buffer (PB). Brains were immediately post-fixated in 4% PFA solution overnight at 4 °C, and subsequently cryoprotected in 30% sucrose in 0.1M PB for at least 48 hours. Cryoprotected brains were sectioned coronally at a thickness of 40µm using a freezing microtome at -30°C (Microm HM430, Thermo Scientific, USA). Serial coronal sections were collected along the anteroposterior axis (approx. from Bregma 0 to -3.0mm) covering the hypothalamus and stored in cryoprotective solution (20% Glycerin, 30% Ethylene Glycol in 0.1M PB) at -20 °C.

Immunohistochemistry

For immunohistochemisty, a total of 8 sections were used (1 every 4 serial sections). This was appropriate to capture the majority of the hypothalamus. The free-floating method [Bachman, 2013] was used; sections were rinsed 3 times for 10 minutes in 0.1M Tris-buffered saline (TBS), incubated in blocking buffer, TBS++ (3% Donkey serum, 0.25% Triton-X100 in 0.1M TBS) for 60min, prior to incubation with primary antibody in TBS++ at 4°C for 36 hours (two nights). Following primary antibody incubation, sections were rinsed with TBS 2 times for 10min, blocked in TBS++ for 20 min, and incubated in secondary antibody in TBS++ for 4 hours at room temperature. Nuclear staining was

performed with incubation with 4',6-Diamidino-2-phenylindole-dihydrochloride (DAPI; 0.5µg/mL; Sigma, 28718-90-3) for 10 mins. Immunostained sections were rinsed with TBS 3 times for 10 minutes and mounted on glass slides with mounting medium containing polyvinyl alcohol and 1,4-diazabicyclo[2.2.2]octane (DABCO). Primary antibodies used: rabbit anti-GFP (to detect YFP) (1:400; Life Technologies, A11122), rabbit anti-Sox2 (1:1500; Millipore, AB5603), mouse anti-NeuN (1:1200; Millipore, MAB377), mouse anti-nestin (1:400; BD Pharmingen, 556309), chicken anti-vimentin (1:1200; Millipore, AB5733), rat anti-BrdU (1:400; AbD Serotec, OBT0030G). Secondary antibodies used: donkey Anti-Rat Cy3 (1:250; Jackson Immuno., 712-165-153), donkey Anti-Rabbit Alexa Fluor488 (1:250; Jackson Immuno., 711-545-152), donkey Anti-Rabbit Cy3 (Jackson Immuno, 711-165-152), donkey anti-mouse Alexa Fluor647 (1:250; Jackson Immuno., 705-605-147), donkey Anti-Mouse Cy3 (Jackson Iummuno, 715-165-151), donkey Anti-Chicken Alexa Fluor 647 (Jackson Immuno, 703-605-155).

Statistics

Results are expressed as the mean ± SEM. Comparison between two groups was done by performing a two-tailed independent samples Mann-Whitney test. The Kruskal-Wallis one-way analysis of variance was used, followed by post-hoc Dunn's for pairwise comparisons within multiple groups. Significance was only established when $p \leq 0.05$ and satisfied a post-hoc false-discovery test [Curran-Everett, 2000].

Results

YFP expression is not restricted to tanycytes

A genetic inducible fate-mapping approach was employed using the nestin promotor to target $CreER^{T2}$ expression to putative neural stem/progenitor cells and thus, permanently label these cells (with YFP) in the hypothalamus. Of these cells, tanycytes were expected to be labelled given their strong expression profile for neural stem/progenitor genes [Bennett et al, 2009; Haan et al, 2013], and their successful fate-mapping in postnatal mice [Lee et al, 2012]. Following the generation of Nestin-CreERT2:ROSA26-loxP-STOP-loxP-YFP (referred to as NCE-YFP) mice, tamoxifen was injected (daily for 5 days)

into the mice to induce Cre-recombination and initiate permanent YFP expression in nestin-expressing cells.

Firstly, the identity, location and distribution of YFP+ cells were assessed after tamoxifen-induced recombination. 1 day after the last tamoxifen injection, brains were PFA-fixed and analysed for YFP expression using an anti-GFP antibody (Fig. 3.2). Several cell-types were labelled with YFP expression, characterized by their differential morphologies. In addition to tanycytes (Fig. 3.2Ai) ventricular cuboidal ependymocytes (Fig. 3.2Aii) and parenchymal cells (Fig. 3.2A; denoted 'P') were also labelled. Of the parenchymal cells labelled, different morphologies were observed, suggesting that these may represent different cell-types; some cells indicated long and bifurcated/bipolar projections suggestive of a typical neuronal morphology (Fig. 3.2Aiii), whilst others indicated short, heavily branched projections (Fig. 3.2Aiv), reminiscent of glial cells. The observation of potential YFP+ neurons shortly after Cre-recombination was unexpected since this mouse model was intended to label solely neural stem/progenitor cells at such short survival periods (6 days after the first tamoxifen injection).

The extent of leaky Cre-activation was assessed in NCE-YFP mice that were not injected with tamoxifen. When analysed for YFP expression, NCE-YFP mice not injected with tamoxifen still indicated the presence of YFP+ cells throughout the brain, including in the hypothalamus, both at the ventricular interface and within the parenchyma, indicating some leaky Cre-activation and recombination (Fig. 3.2B, C). No sex-specific differences were seen in NCE-YFP mice not injected with tamoxifen ($p > 0.05$, two-tailed Mann-Whitney test; Fig. 3.2C). Quantification and comparison of YFP+ cells between NCE-YFP mice injected (TAM+) and not injected (TAM-) with tamoxifen indicated a significant increase in YFP+ cells at the 3rd ventricle and in the parenchyma ($p=0.01$ and 0.038, respectively; two-tailed Mann-Whitney test) of NCE-YFP (+TAM) mice, indicating that recombination at both regions occurs significantly more upon on tamoxifen administration. However, due to leaky Cre-activation, YFP+ cells might not be limited to nestin-expressing cells. YFP+ cells were predominantly found along the 3rd ventricle, at an average of 80.4±3.5 cells/section (97.3% of total hypothalamic YFP+ cells), in comparison to 2.25±0.5 cells/section (2.7%) within the hypothalamic parenchyma (Fig. 3.2D).

Figure 3.2

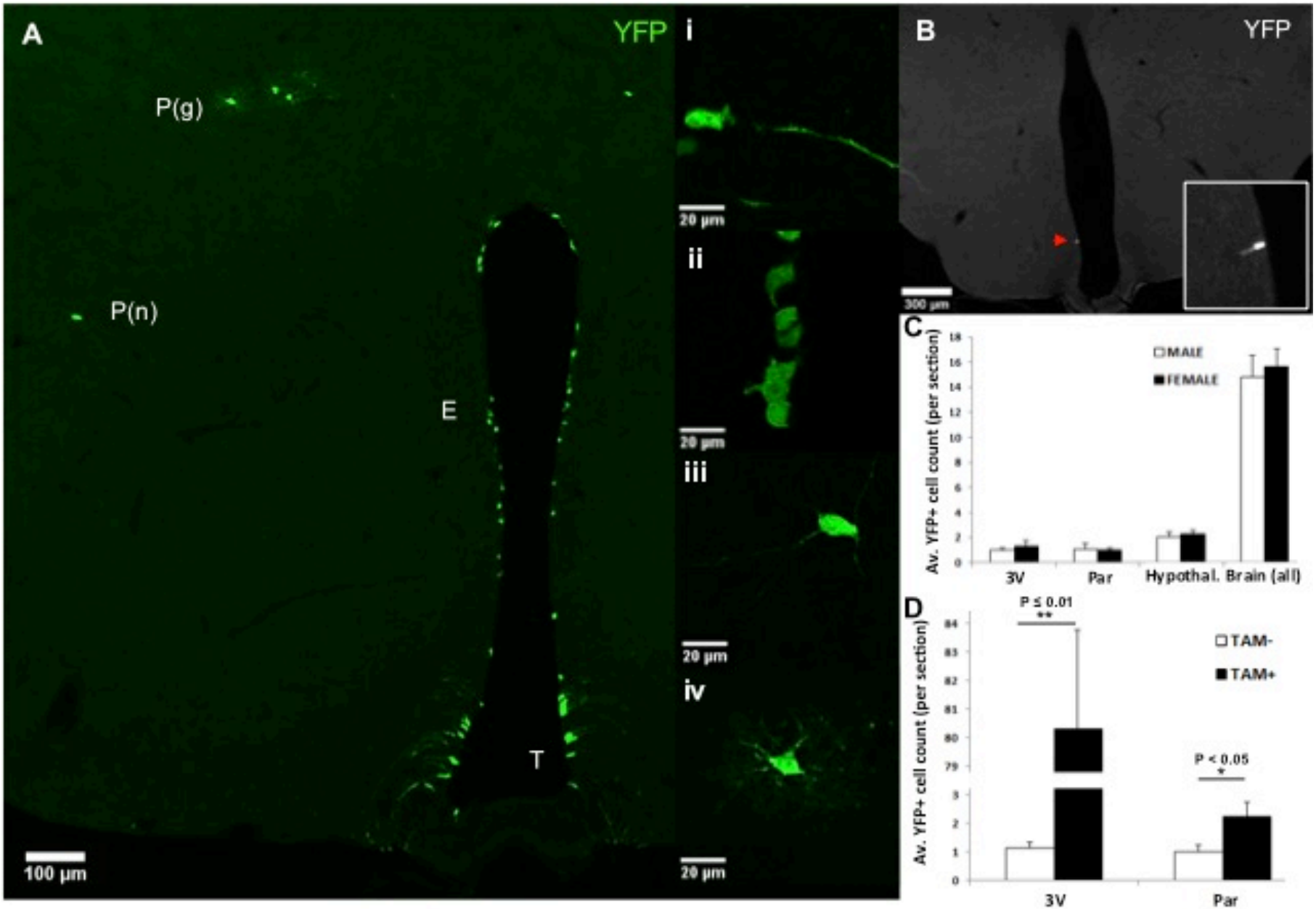
A
YFP
P(g)
P(n)
E
T
100 µm
i
20 µm
ii
20 µm
iii
20 µm
iv
20 µm
B
YFP
300 µm
C
MALE
FEMALE
Av. YFP+ cell count (per section)
3V
Par
Hypothal. Brain (all)
D
P ≤ 0.01
**
TAM-
TAM+
P < 0.05
*
Av. YFP+ cell count (per section)
3V
Par

Figure 3.2 Location, morphology and distribution of YFP+ recombined cells in the hypothalamus. In NCE-YFP mice that were sacrificed 1 day after tamoxifen injection (injected daily for 5 days). **A)** Analysis of YFP (immunostaining for YFP with anti-GFP antibody) expression revealed recombination occurring predominantly in tanycytes (labelled T; and **i**) and ependymocytes (labelled E; and **ii**) at the 3rd ventricle, and to a lesser extent in parenchymal cells that exhibit neuronal (labelled P(n) and **iii**) or glial (labelled P(g) and **iv**) morphologies. **B)** Immunohistochemical analysis of YFP expression in NCE-YFP mice not injected with tamoxifen. Inset reveals a zoom-in image of a YFP+ tanycyte. **C)** Comparison of Cre-recombination in male and female NCE-YFP mice not injected with tamoxifen reveals no difference (n=3). **D)** Comparison of YFP+ cell count (per section) in NCE-YFP mice injected (+TAM) and not injected (-TAM) indicates a significant increase in recombination at both hypothalamic regions after tamoxifen injection (n=4).

Ventricular YFP+ cells exhibited sustained neural stem/progenitor marker expression, whilst parenchymal YFP+ cells exhibited heterogeneity in marker expression

The expression of nestin, Sox-2, vimentin and NeuN was assessed in YFP+ cells at different survival periods (short; 7 days, long; 30-60 days after the last tamoxifen injection) to characterize the phenotype and identity of recombined YFP+ cells.

Nestin was predominantly expressed in the mediobasal hypothalamus, from the mediolateral regions of the 3rd ventricle down to the median eminence (Fig. 3.3). Some nestin+ cells were found residing in the parenchyma, although less abundantly (Fig. 3.3A, white arrow). It is interesting to note that in the median eminence, which exhibited robust relative expression levels, no YFP+ β2 tanycytes (and hence no recombination) was observed. In NCE-YFP mice sacrificed 7 days after tamoxifen injections, nestin co-expression was observed in 72±8% YFP+ ependymocytes (Fig. 3.3B, n= 2 animals; 55 cells counted) and in 96±2% tanycytes (Fig 3.3C, n= 2 animals; 52 cells counted). In both cases, all (100% of) YFP+ tanycytes (Fig. 3.4A, B; n= 2 animals; 31 cells counted) and YFP+ ependymocytes (Fig. 3.5A, n= 2 animals; 39 cells counted) were positive for expression of the radial glial/ependymal marker, vimentin [Schnitzer et al, 1981; Pixley et al, 1984; Sancho-Tello et al, 1995] and the canonical neural stem cell marker, Sox-2 (Fig. 3.4C, D, Fig. 3.5B; white arrowheads), but negative for the neuronal marker, NeuN (Fig. 3.4 E, F; images not shown for YFP+ ependymocytes).

On the other hand, no nestin expression was seen in any of the YFP+ parenchymal cells visualized at any survival period. An exemplar parenchymal YFP+ cell indicating no nestin expression 7 days after the last tamoxifen injection is indicated (Fig. 3.3D). Parenchymal YFP+ cells exhibited expressional heterogeneity, whereby some cells were negative for Sox-2 (30 days after tamoxifen; Fig 3.5B, yellow arrowheads), whilst others were positive (60 days after tamoxifen; Fig. 3.5C, white arrowheads). Similarly, only a small proportion of YFP+ parenchymal cells were positive for NeuN (Fig. 3.5D), even at 60 days after the last tamoxifen injection (NeuN-negative cells were not shown).

Figure 3.3 Ventricular but not parenchymal YFP+ cells exhibited continuous nestin expression. In NCE-YFP mice that were sacrificed 7 days after tamoxifen injection (injected daily for 5 days). **A)** Immunohistochemical analysis of YFP and nestin co-expression in the hypothalamus. Strong nestin expression is predominantly restricted to the medio-basal ventricular regions and the median eminence..Co-expression of YFP and Nestin (white arrowheads) is seen in **B)** tanycytes and **C)** ependymocytes, but **D)** not in neuron-like parenchymal YFP+ cells.

Figure 3.4 YFP+ Tanycytes express other neural stem/progenitor markers and do not express a neuronal marker. In NCE-YFP mice that were sacrificed 7 days (n=2) after tamoxifen injection, the expression profile of YFP+ tanycytes was assessed. YFP+ tanycytes expressed **A-B)** the radial glial marker, vimentin, the **C-D)** neural stem cell marker, Sox-2, but did not express **E-F)** the mature neuronal marker, NeuN. This gene-expression is indicative of a neural stem/progenitor-like phenotype.

Figure 3.5 YFP+ ependymocytes also express neural stem/progenitor markers, whilst parenchymal YFP+ cells exhibit phenotypic heterogeneity. In NCE-YFP mice that were sacrificed **A)** 7 (n=2) (**B-C**) 30 (n=1) and (**D**) 60 (n=1) days after tamoxifen injection, the expression profile of YFP+ ependymoctes and parenchymal cells was assessed. YFP+ ependymocytes expressed **A)** the radial glial marker, vimentin, and retained expression of the **B)** neural stem cell marker, Sox-2 (white arrowheads) after 30 days. Interestingly, parenchymal YFP+ cells indicated expressional heterogeneity whereby some **B)** were negative for Sox-2 (at 30 days; yellow arrowheads) whilst **C)** others expressed Sox-2 (after 60 days). Further heterogeneity was seen by YFP+ parenchymal cells, where **D)** NeuN co-expression was seen in some cells, where as other YFP+ cells were negative (not shown) after 60 days. White and yellow arrowheads indicate positive and negative co-localization, respectively.

Figure 3.3

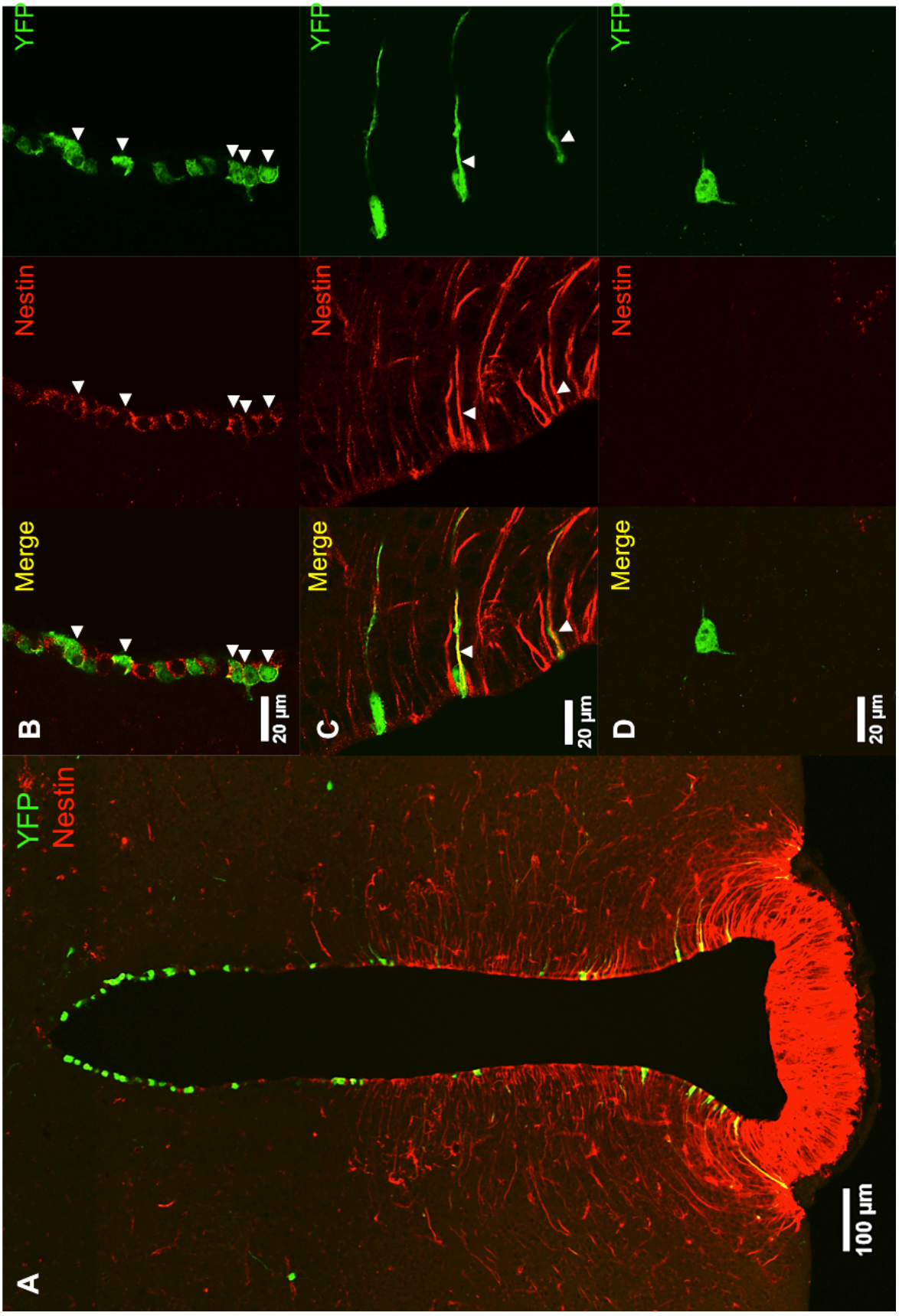

Figure 3.4

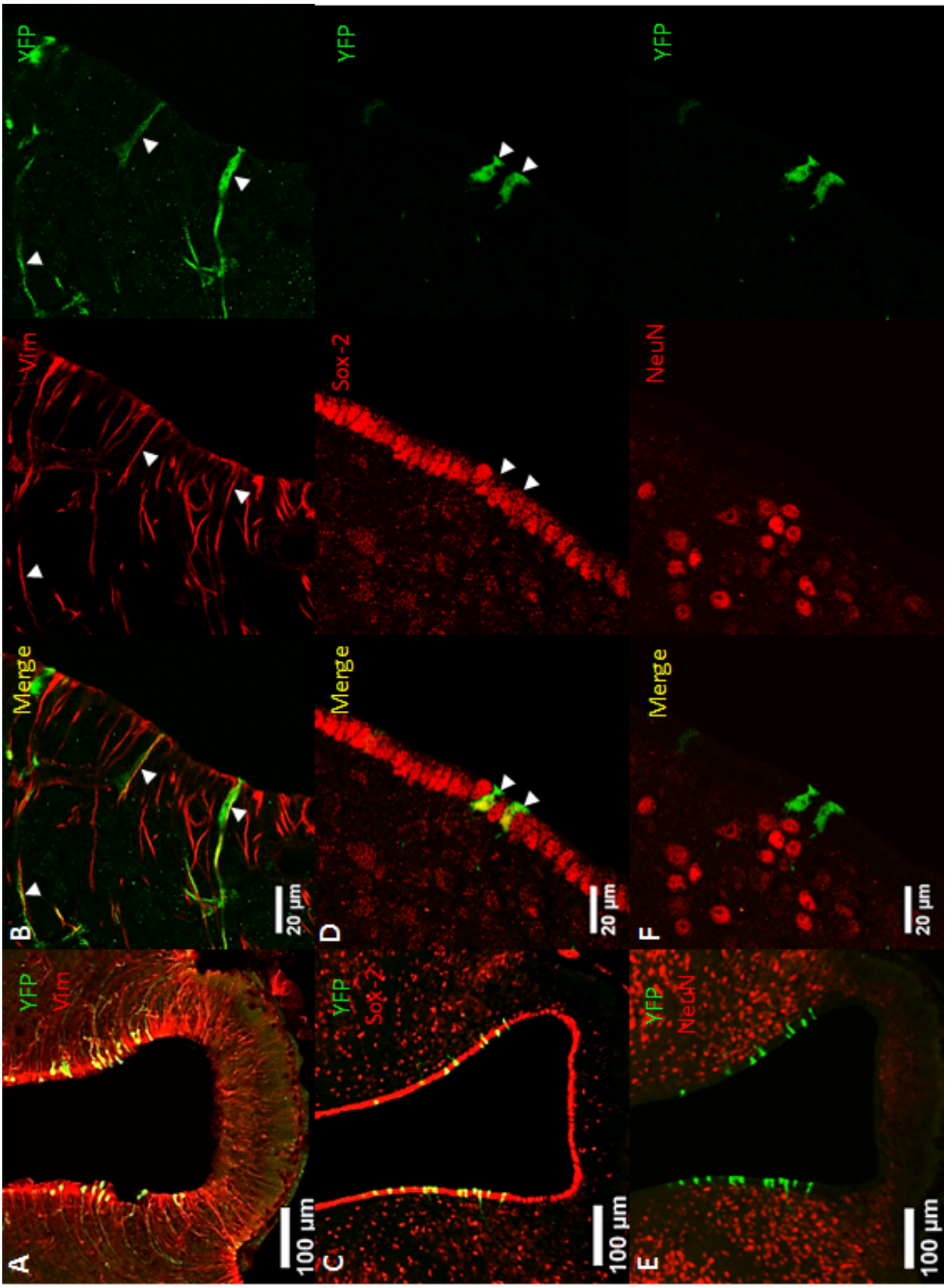
A
YFP
Vim
100 µm
B
Vim
YFP
Merge
20 µm
C
YFP
Sox-2
100 µm
D
Sox-2
YFP
Merge
20 µm
E
YFP
NeuN
100 µm
F
NeuN
YFP
Merge
20 µm

Figure 3.5

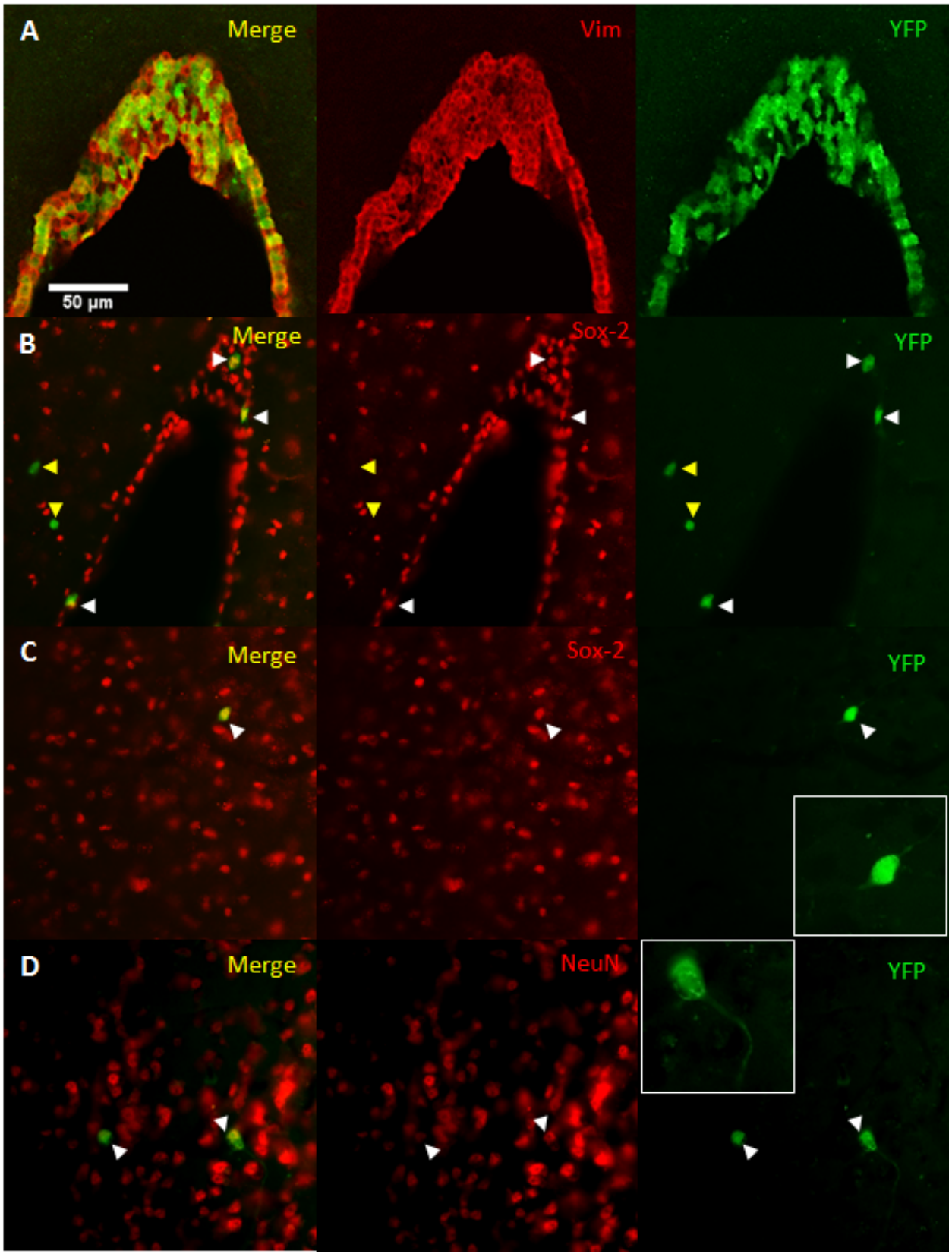
A
Merge
Vim
YFP
50 µm
B
Merge
Sox-2
YFP
C
Merge
Sox-2
YFP
D
Merge
NeuN
YFP

YFP+ tanycytes do not take up BrdU and their numbers are maintained over time

The proliferative state of YFP+ tanycytes under basal conditions was assessed with BrdU-labelling. BrdU was injected on the same days as tamoxifen (daily for 5 days, 2 hours after tamoxifen) in order to identify any dividing tanycytes within the closest time-window during/just after the induction of recombination with tamoxifen. NCE-YFP mice were then sacrificed 1 day after the last injection for analysis.

Many BrdU+ cells were found in the hypothalamic parenchyma, but none were found along the ependymal layer. Thus, no YFP+/BrdU+ tanycytes were seen (Fig. 3.6A). However, it is interesting to note that a substantial proportion of BrdU+ cells were found in the periventricular region and/or in the mediobasal region of the hypothalamus (arcuate nucleus and median eminence), to where YFP+ tanycytes were mostly seen projecting into. At higher magnification, some of these BrdU+ cells can be found in very close proximity or even contacting tanycyte cell bodies or their basal processes (Fig 3.6Bi-iii, white arrowheads).

YFP+ tanycytes were quantified over time in order to assess any change in YFP+ tanycyte numbers under basal conditions. Here, all NCE-YFP mice were injected with tamoxifen for 5 days, followed by sacrifice at one of the following survival periods- 1, 10, 30 or 60 days (n=4-5 mice/survival period; Fig. 3.7A). Comparison of quantified YFP+ tanycyte cell densities at different survival periods indicated no significant change over time (Fig. 3.7B, C; p=0.592, Kruskal-Wallis one-way ANOVA).

Comparison of quantified parenchymal YFP+ cells indicated an increasing trend over time, although these changes were not significant (Fig. 3.7D, black bars; p=0.0745, Kruskal-Wallis one-way ANOVA). Interestingly, when these YFP+ parenchymal cells were subdivided based on their morphologies (neuronal-like or glia-like), a significant increase was seen with neuronal-like YFP+ cells over time (Fig. 3.7D, white bars; p=0.0261, Kruskal-Wallis one-way ANOVA). Nevertheless, post-hoc analysis indicated no significant difference in YFP+ neuronal-like cells between any survival period, including between 1 day and 60 days post-tamoxifen (p=0.0663, Dunn's multiple comparison). YFP+ glia-like cell numbers did not appear to increase much over time and

any change seen was not significant (Fig. 3.7D, grey bars; p=0.1729, Kruskal-Wallis one-way ANOVA).

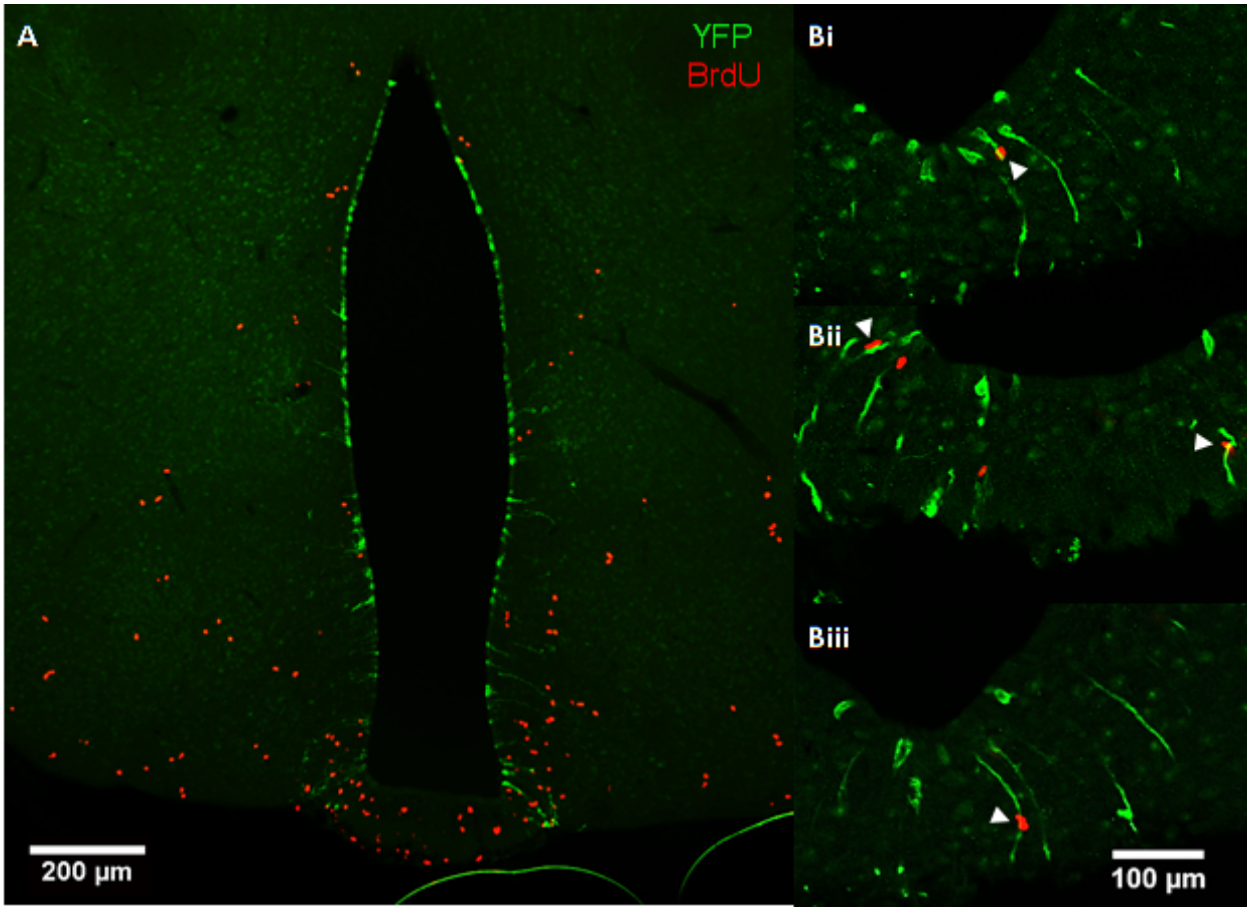

Figure 3.6 YFP+ tanycytes do not take up BrdU. In NCE-YFP mice that were sacrificed 1 day after 5 daily tamoxifen and BrdU injections, YFP+ tanycyte proliferation was assessed (n=2). **A)** Immunohistochemical analysis indicated no YFP+/BrdU+ co-localization. BrdU+ cells were mostly localized to the mediobasal hypothalamus. **B)** At higher magnification, several BrdU+ cells within the mediobasal hypothalamus indicated were in close proximity or in contact with tanycyte basal processes.

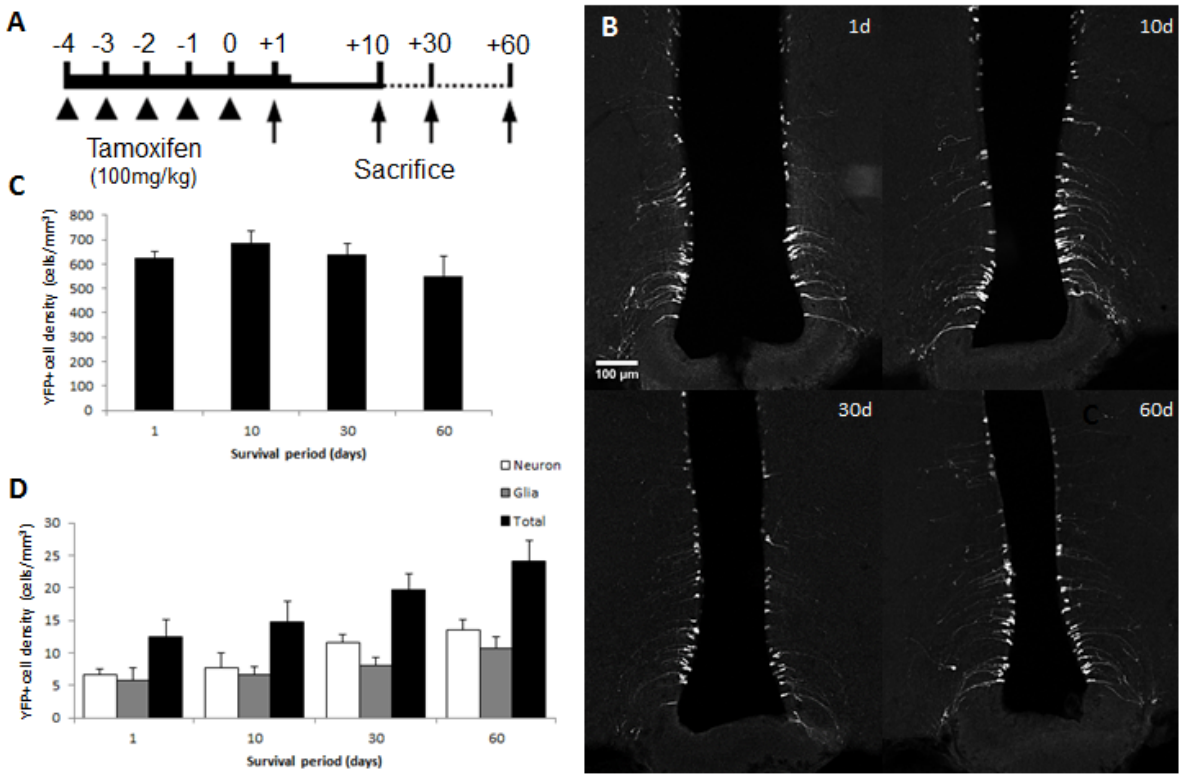

Figure 3.7 No significant change in YFP+ cell numbers was observed over time. A) NCE-YFP mice were sacrificed at varying (1, 10, 31, 60) days after tamoxifen injection. **B)** YFP+ tanycytes and parenchymal cells at different time points. Exemplar immunostained sections of the mid-portion of the hypothalamus are indicated. **C)** YFP+ tanycytes and **D)** YFP+ parenchymal cells (divided into neuron-like and glia-like cells based on their morphologies) were quantified and compared between different suvival times. No significant differences were observed in any case. 1/10-day survival, n=4; 30/60-day survival, n=5.

Discussion

A range of cell-types were labelled upon induced-recombination in NCE-YFP mice

Nestin-driven CreER^{T2} expression and subsequent activation by tamoxifen was used and intended to selectively identify and label (with permanent YFP expression) putative nestin-expressing neural stem/progenitor cells in the hypothalamus.

Tanycytes

It is not surprising to have labelled tanycytes in this model, given their previously indicated expression for nestin and suggested role in hypothalamic neurogenesis [Bennett et al, 2009; Lee et al, 2012; Haan et al, 2013; Robins et al, 2013a]. However, whilst tanycytes

of the mediolateral 3rd ventricle walls were labelled, no YFP expression was seen along the ventral ependymal layer of the 3rd ventricle, at the median eminence interface (Fig. 3.7), where β-tanycytes are seen to reside [Rodriguez et al, 2005]. This is a surprising observation given the high/strong expression of nestin observed in the median eminence and a previous study having successfully labelled β-tanycytes using the same nestin promoter-based fate mapping strategy, albeit at postnatal ages [Lee et al, 2012]. Indeed, it could be hypothesized that tamoxifen may not be accessible to β-tanycytes in adults due to their exclusive expression of impermeable tight junction complexes, which are absent in postnatal mice [Peruzzo et al, 2000; Mullier et al, 2010]. However this is unlikely due to the successful labelling of in β-tanycytes in FGF10-CreER/Rosa26-lox-STOP-lox-(reporter) adult mice [Haan et al, 2013] administered with Tamoxifen using the same injection protocol as in our experiments.

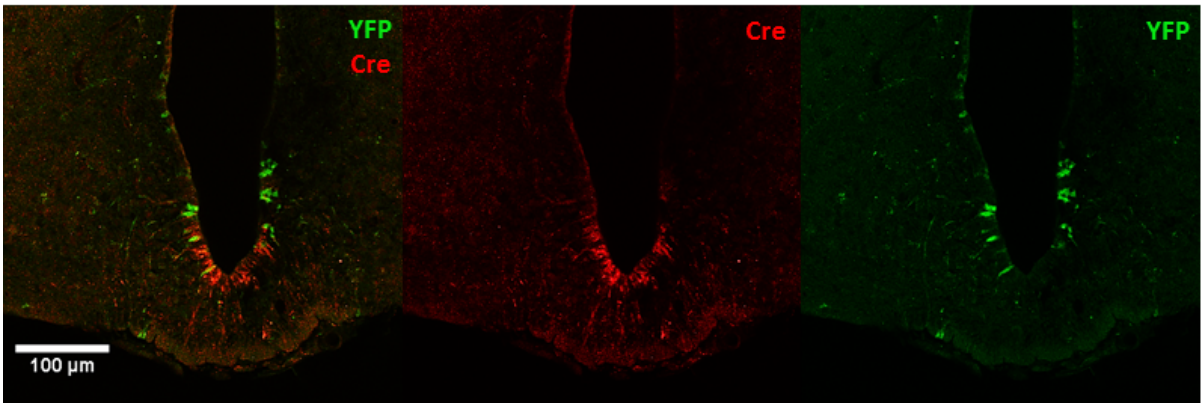

Figure 3.8 CreER^{T2} is expressed in the median eminence, but no apparent recombination/YFP expression is seen here upon tamoxifen administration. A lack of YFP expression was seen at the median eminence of NCE-YFP mice, which could not be explained. Due to the high expression of Nestin in this domain, it was expected that recombination and hence, YFP expression would have been induced here. However, the lack of YFP expression was not due to a lack of CreER^{T2} expression, as positive Cre-expression was detected with a polyclonal anti-cre antibody. This indicates that the lack of detectable YFP expression may be due to another factor specific to the median eminence.

From our study, it is currently unknown as to why there is a lack of observed YFP expression in the median eminence. Cre-expression was confirmed in the median eminence via immunostaining (Fig. 3.8), reflecting that the transgenic nestin promoter sequence (although incomplete in comparison to the endogenous sequence) was able to

drive cre-expression. Thus, upon exposure to tamoxifen it cannot be conceived as to why YFP fluorescence (and supposedly, expression) was not visualized in the median eminence. Of note, it has been previously reported that ventral tanycytes exhibit heterogeneity in gene expression profiles, in which some tanycytes were seen without nestin expression [Haan et al, 2013]. However, this does not entirely account for why there was almost exclusively no YFP expression in ME tanycytes, especially given that robust nestin immunolabelling was observed (unless this indeed, was an artifact of non-specific labelling). In order to assess whether recombination did occur in this region, it would be of interest to evaluate recombination in the genomic sequence of ME tanycytes via PCR; by using PCR primers designed to flank the loxP sites on either side of the STOP cassette, the occurrence of recombination could be confirmed (Fig. 3.9); if recombination has occurred, a smaller DNA-amplified band would be detected due to the excision of the STOP cassette, compared to the larger band produced when no cre-mediated excision/recombination has occurred. If recombination was successful in the ME, it is possible that YFP expression could be silenced (by unknown mechanisms). On the other hand, if recombination was confirmed to not occur, It could be concluded that cre-recombinase may be inhibited by unknown mechanisms from inducing recombination in the ME (note Cre-expression levels were highest as shown in Fig. 3.8).

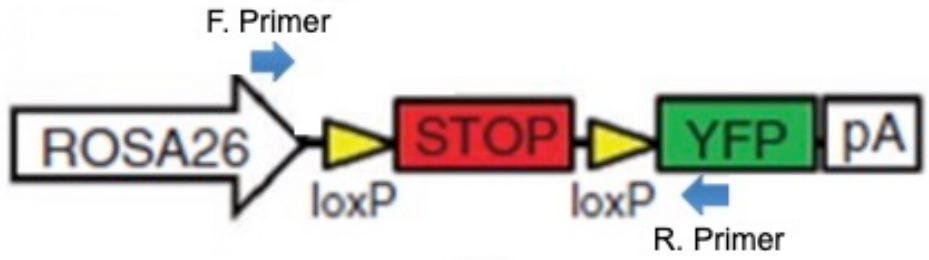

Figure 3.9 Schematic showing how recombination could be assessed in the median eminence using PCR. PCR primers (blue arrows) could be designed to flank the LoxP sequences outside of the STOP cassette (red). The forward primer (F. Primer) would overlap with the end of the ROSA26 promoter sequence, whilst the reverse primer (R. Primer) would overlap with the initial segment of the YFP transgene sequence. PCR-amplification of recombined transgenic constructs (lacking the STOP cassette) would yield a smaller PCR product than non-recombined constructs. This experiment would require genomic DNA to be extracted only from the median eminence (beta-2) tanycytes in order to avoid any false-positive identification of recombination.

Ependymocytes

In addition to tanycytes, ependymocytes were labelled with YFP expression, indicating they express nestin. Interestingly, nestin expression in ependymocytes has not been clearly described [Bruni, 1998; Didier-Bazès et al, 2001; Jiménez et al, 2014], and the few instances of reported nestin expression are circumstantial due to the lack of absolute distinction between, or specific labelling of ependymocytes versus tanycytes or subependymal astrocytes [Chouaf-Lakdar et al, 2003; Coskun et al, 2008; Chojnacki et al, 2009; Hendrickson et al, 2011]. However, our observation of positive YFP expression (confirmed by positive nestin and vimentin immunostaining) in a vast number of ependymocytes opens the question of whether these cells may also represent a hypothalamic neural stem/progenitor cell population, previously overlooked.

Subependymal astrocytes

Subependymal astrocytes have been strongly suggested as neural stem/progenitor cells, with strong resemblance to B1 cells in the subventricular neurogenic niche of the lateral ventricles [Perez-Martin et al, 2010; Rojczyk-Gołębiewska et al 2014]. Although it has yet to be clearly demonstrated in the hypothalamus, these cells may likely express nestin (since their cellular equivalent in the SVZ; B1 cells do [Doetsch et al, 1997]) and thus may also be labelled in our transgenic fate-mapping model. However, due to their overlapping localization with tanycytes, it cannot be determined if these cells were truly labelled. Furthermore, positive identification of these cells is exacerbated due to their overlapping expression of GFAP with (α) tanycytes [Robins et al, 2013a].

Potential parenchymal cell-types

In the parenchyma, several cells were noted with YFP expression and were classed into two main groups; cells that possessed highly branched processes were classed as glial-like cells, whilst those that had a relatively big cell body and very long processes (uni, bi or multipolar) were classed as neuron-like cells. Whilst the identity of these cells were not confirmed several candidates could have been labelled, based on their expression of nestin.

Glial-like

Some parenchymal YFP+ cells in our mouse model were Sox-2+. Interestingly, the majority of proliferative parenchymal cells were seen to be NG2+ glia, a large fraction of which (37%) demonstrated Sox-2 expression [Robins et al, 2013b]. Thus, it is possible that at least a proportion of parenchymal YFP+ cells may be NG2+ glia. Indeed, cultured oligodendrocytes have been reported to express nestin [Almazán et al, 2001], whilst some nestin+ cells have been seen to express oligodendrocyte markers such as NG2 and PDGFRα [Kronenberg, 2005; Koch et al, 2008]. However, the most convincing data arises from a genetic labelling study in mice using nestin to drive eGFP expression (nestin-eGFP), in which oligodendrocytes were also positively identified [Walker et al, 2010].

Astrocytes [Clarke et al, 1994; Lin et al, 1995] and microglia [Yokoyama et al, 2004; Takamori et al, 2009] have been debatably reported to express nestin although primarily upon brain injury or ischaemia [Duggal et al, 1997; Sahin et al, 1999; Yokoyama et al, 2004; Ernst & Christie, 2006; Götz et al, 2015]. One study even reported nestin expression in microglia under basal conditions [Takamori et al, 2009]. However, another study suggested that microglial progenitors, and not mature microglia expressed nestin [Elmore et al, 2014]. Similarly to microglia, whilst nestin+ pericytes and endothelial cells were reported *in vitro* [Dore-Duffy et al, 2006], it is not known whether these were nestin+ (peri)endothelial progenitor cells, and not mature (peri)endothelial cells [Suzuki et al, 2010]. Other studies assessing nestin expression in the adult CNS (either through nestin-reporter or immunodetection methods) failed to identify Nestin+ microglia or astrocytes under basal/normal conditions [Walker et al, 2010; Hendrickson et al, 2011]. Thus, it is unclear whether these cell-types may have been labelled in our study.

Neuron-like

Parenchymal YFP+ neuron-like cells were unexpected at early time points after tamoxifen injection as it was initially presumed that nestin-driven Cre-expression (and thus subsequent recombination/YFP expression) would have been limited only to neural stem/progenitor cells. However, a study has indeed reported nestin-expressing neurons, which may be a result of transient cytoskeletal remodelling as part of a neural plasticity event [Hendrickson et al, 2011]. This could potentially explain the (low) incidence of YFP+

neurons appearing as early as 1 day post-tamoxifen. Furthermore, the lack of nestin expression in YFP+ neuron-like cells might further corroborate the transience of nestin expression in neurons such as those identified by Hendrickson et al (2011).

Interestingly, another study identified nestin-expressing neuroblasts characterised by DCX expression [Batailler et al, 2014]. These DCX+ cells were seen exhibiting a unipolar or bipolar morphology with long neurites, somewhat similar to the morphology used to classify YFP+ neuron-like cells in our study. Thus, it is also possible that migrating neuroblasts may have retained nestin expression during tamoxifen-induced recombination in our Nestin-CreER mouse model and thereby were labelled with YFP expression. Indeed, as these cells matured into Hu+ neurons, DCX (and presumably nestin) expression was seen to decrease [Batailler et al, 2014], potentially substantiating the absence of nestin expression in these YFP+ cells when analysed 6 and 12 days after the first instance of induced recombination (1 and 7 day survival periods, respectively). In order to further confirm the neuronal identity and elucidate the developmental stage of YFP+ neuron-like cells (whether they are predominantly neuroblasts or mature neurons), further phenotypic analysis would be required.

Finally, the possibility that these YFP+ neuronal-like cells may be the progeny of neural stem/progenitor cells previously labelled via tamoxifen-independent recombination (prior to tamoxifen injections) or neurons exhibiting leaky Cre-expression might also be possible.

Overall, these results indicate that Cre-expression under the control of the nestin promoter and subsequently, YFP-labelling is not specific to tanycytes, as YFP+ ependymocytes and other parenchymal YFP+ cells were also seen immediately upon induced recombination. It is not clear what lineage (glial or neuronal) and cell-type(s) are comprised in this parenchymal YFP+ cell population. Thus, the possibility that any of the aforementioned cell-types may have been labelled with YFP expression in our study cannot be ruled out and would require confirmation by phenotypic characterization (co-expression analysis) with molecular markers for the respective lineages (for example, Iba-1 to identify microglia, NG2 for oligodendrocyte progenitors, GFAP for astrocytes, DCX for neuroblasts and NeuN or Hu for neurons).

Increased parenchymal YFP+ cells may not solely originate from YFP+ tanycytes

Over time an increasing trend was observed with YFP+ parenchymal cells (an approximate two-fold increase in both YFP+ neuron-like and glial-like cells after a 60-day survival period, in comparison to 1 day post-tamoxifen). This temporal increase may be suggestive of hypothalamic neurogenesis, as suggested previously [Pencea et al, 2001; Kokoeva et al, 2007; Robins et al, 2013a; Sousa-Ferreira et al, 2014a]. Furthermore, at longer survival-times (60 days), some YFP+ neuronal-like cells co-expressed NeuN, confirming their neuronal identity. It is tempting to hypothesize that this gradual increase in YFP+ neurons may, in part, be due to the migration of YFP+ tanycyte progeny into the parenchyma. Indeed, with YFP+ tanycytes numbers maintained over time, it could be further speculated that YFP+ tanycytes may potentially divide asymmetrically to generate YFP+ migrating neuroblasts (which, similarly to some YFP+ cells in our study, have also been seen to express Sox-2 [Batailler et al, 2014]) and contribute towards the increasing number of YFP+ new-born neurons, as suggested by other fate-mapping studies [Lee et al, 2012; Haan et al, 2013; Robins et al, 2013a]. Similarly, the increase in YFP+ glia may potentially be attributable to YFP+ tanycytes, as previously shown [Robins et al, 2013a]. However, although the observation of YFP+/NeuN+ cells (at 60 days post-tamoxifen) confirms that some of these YFP+ neuron-like cells are indeed mature neurons, it is not known whether these cells were derived from YFP+ tanycytes or YFP+ neuroblasts/neurons labelled upon induced recombination. Thus, these results do not unequivocally demonstrate that these YFP+ neurons were derived from tanycytes.

YFP+ tanycytes may not serve as the only source of YFP+ neurons, as other cell-types have been shown to demonstrate neurogenic capacities as well. One study indicated that NG2+ oligodendrocyte progenitor cells (OPCs) are highly proliferative under basal conditions and can generate neurons and oligodendrocytes in the adult hypothalamus [Robins et al, 2013b]. Given that NG2+ OPCs were previously seen to express nestin [Walker et al, 2010], the contribution of these cells to the increase in parenchymal YFP+ neuron-like and glial-like cells cannot be overlooked. Indeed, a subpopulation of NG2+ glia were also positive for Sox-2 expression [Robins et al, 2013b], potentially explaining the heterogeneous population of YFP+/Sox-2$^-$ and YFP+/Sox-2+ cells in our study. However, it should be noted that whilst NG2+ OPCs were capable of neurogenesis, they

were predominantly gliogenic towards the oligodendrocyte lineage and not able to generate astrocytes [Robins et al, 2013b]. Having observed higher numbers of YFP+ neuron-like cells compared to YFP+ glial-like cells, and YFP+ cells morphologically similar to astrocytes, it is possible that both tanycytes and NG2+ glia may contribute toward adult neurogenesis under basal conditions. However, using our fate-mapping approach, the two populations (and their progeny) cannot be distinguished and therefore their separate progeny cannot be distinguished from each other either. Finally, whilst reactive astrocytes and microglia have been described to play supportive roles in adult neurogenesis, any capacity as multipotent neural stem/progenitor cells are only adopted under brain injury conditions [Sato, 2015; Götz et al 2015]. Considering that adult neurogenesis was assessed under basal/normal conditions (with tamoxifen not having any positive neuroinflammatory nor neurogenic effect [Sun et al, 2013; Rotheneichner et al, 2017]), the contribution of these cells is unlikely. However as previously described, subependymal astrocytes have been previously suggested as candidate neural stem/progenitor cells in the hypothalamus [Perez-Martin et al, 2010; Rojczyk-Gołębiewska et al 2014], although no studies have provided any direct evidence yet for a role in adult hypothalamic neurogenesis.

A clear limitation of using the NCE-YFP mouse to selectively label and fate-map tanycytes comprises the fact that nestin expression and subsequent YFP-labelling upon inducible recombination is seen in several cell-types in addition to tanycytes. Similarly to nestin, Sox-2 expression is not restricted to ventricular cells as seen in both, our study and in a similar fate-mapping mouse model [Li et al, 2012]. Thus, the use of generic neural progenitor promoters such as Sox-2 or nestin to drive Cre-expression is not sufficiently specific in this fate-mapping approach. Instead, it could be suggested to use other radial glial-specific promoters such as FGF10 [Hajihosseini et al, 2008; Haan et al, 2013] or Rax [Miranda-Angulo et al, 2014; Pak et al, 2014] to drive Cre-expression in tanycytes. Whilst the FGF10-CreER mouse only allowed for fate-mapping of ventral β-tanycytes [Haan et al, 2013], it is possible that the Rax-CreER mouse may prove more useful in labelling more subpopulations (α- and β- subtypes) of tanycytes and providing results that could further clarify our speculations from the current study.

On the other hand, an alternative fate-mapping approach could be adopted using nestin to drive Cre-expression and hence specificity of labelling. The Brainbow approach is a relatively recent development that allows for the multicolour-labelling of a cellular population specified by a single promoter, in which each cell is differentially labelled with different fluorescent protein (XFP) expression [Livet et al, 2007; Weissman et al, 2011]. In this approach, the Cre/lox system is used to induce stochastic recombination of the Brainbow construct, comprising of 3-4 XFPs sequentially flanked with different lox-sequence variants (only recognizable by Cre in identical pairs). Upon Cre-mediated recombination, differential XFP expression can be stochastically triggered whereby each individual cell will randomly express a single XFP from the Brainbow construct and adopt a colour [Weissman et al, 2011]. The diversity of colours adopted by each cell can be greatly expanded by using multiple copies of the Brainbow construct to generate combinatorial XFP expression. Here, each Brainbow construct will express an XFP independently of each other, and the differential combinations (and ratios) of XFPs expressed together will determine different hues/colours [Weissman & Pan, 2015]. As a result, the Brainbow approach allows for detailed visualization of the morphologies of closely associated/densely packed cells and their interactions. Furthermore, given that these multicolour labels are inheritable, the progeny of labelled cells can be tracked according to their unique ‘colour barcode’ [Weissman & Pan, 2015]. Thus, although this method was classically applied to label neurons and investigate their network connectivity [Livet et al, 2007], more recent studies have made use of this method to fate-map stem cells and their progeny in the brain as well as in other organs [Snippert et al, 2010; Calzolari et al, 2015]. Similarly, the Nestin-CreER driver construct could be used in conjunction with the Brainbow construct to label putative hypothalamic neural stem/progenitor cells with different colours and allow for the fate-mapping of individual cells (including, parenchymal and ependymal cell-types) within the entire cell population. Furthermore, by being able to distinguish between adjacent cells, this approach may even help determine if subependymal astrocytes are also labelled and if there is any interaction between these cells and tanycytes during neurogenesis.

YFP+ Tanycytes do not actively proliferate

No BrdU uptake was seen in any YFP+ tanycyte (or YFP-negative tanycytes) after 5 days of injection. This is consistent with a failure to label with BrdU tanycytes in other studies (injecting up to 7-8 days) [Hajihosseini et al, 2008; Haan et al, 2013]. Furthermore, when tracked over time, YFP+ tanycyte numbers/densities did not change significantly. In contrast, a majority (80%) of BrdU+ cells were identified as NG2+ glia by another study [Robins et al, 2013b]. These results are suggestive that tanycytes may not have the capacity to proliferate. Whilst, other studies were able to identify BrdU+ tanycytes albeit with increased survival periods (after 9-15 days of BrdU administration) [Haan et al, 2013], it could be argued that this increased survival period may also increase the possibility that the actively dividing cell may have given rise to daughter (progenitor) cells that may later differentiate into tanycytes.

It should also be highlighted that the aforementioned studies administered BrdU via peripheral delivery methods (either intraperitoneally and/or via drinking water), which preferentially label proliferative cells in the parenchyma [Kokoeva et al, 2007; Sousa-Ferreira et al, 2014a]. A previous study has indicated the stark difference in BrdU-labelling preference in the hypothalamus using peripheral versus central delivery methods, whereby the latter delivery method preferentially labelled ventricular and periventricular proliferative cells [Kokoeva et al, 2007]. Indeed, using central delivery methods (such as intracerebroventricular infusion) BrdU+ tanycytes have been successfully reported (in survival periods as early as 2 days after BrdU administration) [Chouaf-Lakdar, et al, 2003; Cifuentes et al, 2011]. Thus, it would be recommendable to use central-delivery methods when investigating the basal proliferative capacity of tanycytes in the future.

It is possible that tanycytes may represent a quiescent or rarely-dividing adult neural stem/progenitor pool under basal conditions [Li & Clevers, 2010; Wang et al, 2011b] that may require stimulation from external stimuli/growth factors, as seen for hippocampal quiescent neural stem cells [Lugert et al, 2010]. Whilst BrdU+ tanycytes have been reported under basal conditions, the frequency of such observations is low [Xu et al, 2005]. Indeed, increased tanycyte proliferation (BrdU uptake) has been demonstrated with FGF-2 and IGF-1 [Xu et al, 2005; Robins et al, 2013a; Perez-Martin et al, 2010].

Quiescent NSCs may re-enter their cell cycles less frequently than active NSCs and thus, when BrdU is administered briefly, actively proliferating cells (such as NG2+ glia) are more likely to take up available BrdU [Li & Clevers, 2010; Wang et al, 2011b; Sousa-Ferreira et al, 2014a].

Studies on other stem cell niches have suggested the presence of separate pools of quiescent and 'active' (proliferative) stem cells. Using BrdU-labelling and/or histone2B-labelling (with GFP) to label hematopoietic stem cells (HSCs), a biphasic dilution of these labels was seen, whereby rapid-proliferating HSCs exhibited fast label-dilution whilst quiescent HSCs retained these labels over extended periods [Wilson et al, 2008; Foudi et al, 2009]. These quiescent HSCs were predominantly located near the vasculature (arterioles) of the bone marrow endosteum, but upon activation by, for example injury [Wilson et al, 2008], would migrate to the sinusoidal region where they are induced to proliferate [Kunisaki et al, 2013]. It is interesting to note the parallel between this stem cell niche and that of tanycytes; both populations are located in close proximity to the blood circulation and exhibit reactive proliferative capacity (in response to injury or growth factors, respectively). Thus, the possibility that tanycytes may represent a quiescent population of hypothalamic neural stem cells that exhibit a reactive neurogenic potential (activated only by external stimuli/growth factors) cannot be ruled out.

Summary

Using the nestin promoter sequence to drive Cre-expression in a fate-mapping mouse model, tanycytes were successfully labelled. However, this labelling method is not specific to tanycytes, as other cell-types were also labelled shortly following tamoxifen-induced recombination. Thus, any changes in YFP+ cell numbers and their phenotype over time cannot be indisputable evidence for tanycytes' role in neurogenesis using this mouse model. Nevertheless, it could be argued that since the vast majority of YFP+ cells were limited to the ependymal layer, it may be possible to use the Nestin-CreER driver mouse in manipulation experiments and attribute an effect to tanycytes and ependymal cells.

Chapter 4: Optogenetic stimulation of nestin-expressing cells induced an increase in newly-generated cells

Background

Purinergic signalling in Tanycytes

Tanycytes can sense and respond to nutrients in the CSF, such as glucose [Frayling et al, 2011; Orellana et al, 2012; Benford et al, 2017]. This is mediated by a purinergic signalling mechanism, driven by changes in intracellular calcium [Dale, 2011]. When glucose, amino acids or other molecules associated with the drive to feed (such as ATP, histamine or acetylcholine), bind to their respective receptors on tanycytes, a large increase in intracellular calcium is observed [Frayling et al, 2011; Lazutkaite et al, 2017]. This calcium signal is then seen to propagate along the tanycyte layer through both, short- and long-range feedforward signalling mechanisms [Bolborea & Dale, 2013]; increased intracellular calcium in stimulated tanycytes can diffuse into adjoining tanycytes via gap junctions [Orellana et al, 2012], whilst simultaneously, the increase in intracellular calcium concentration triggers the extracellular release of ATP, which in turn can activate P2Y1 receptors (hereon referred to as P2Y1R) and stimulate further increases in intracellular calcium in surrounding tanycytes [Frayling et al, 2011; Benford et al, 2017]. As a result of the propagating calcium signal, a wave of extracellular ATP release ensues [Dale, 2011; Bolborea & Dale, 2013]. Initiation and propagation of the calcium signal and ATP in tanycytes is illustrated in Fig 4.1.

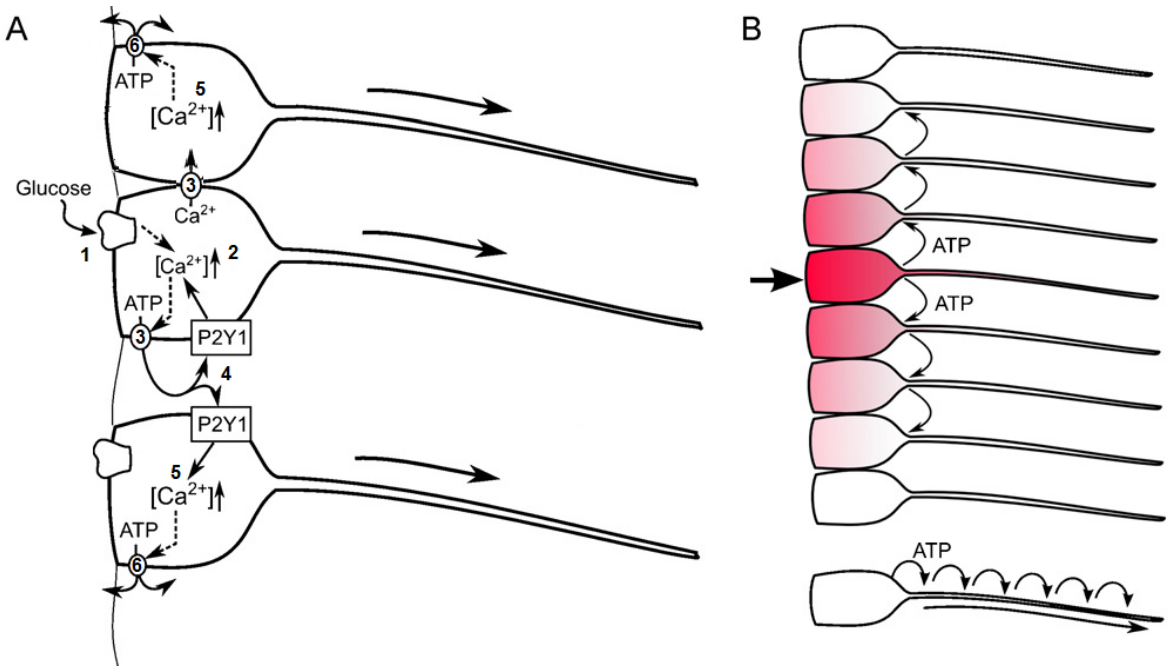

Figure 4.1. Initiation and propagation of calcium and ATP signalling in tanycytes. A) Suggested mechanism by Dale (2011): Stimulation by agonists, such as glucose (1), leads to the release of calcium from intracellular stores, resulting in an increased cytosolic concentration (2). This leads to the extracellular release of ATP whilst, simultaneously, increased calcium can diffuse into neighbouring tanycytes via gap junctions (3). Extracellular ATP binds to and activates P2Y1 receptors on surrounding tanycytes to stimulate (further) calcium influx (4). The resulting increased intracellular calcium in neighbouring and surrounding tanycytes again leads to ATP release (5) and reiteration of the described signalling pathway. **B)** As highlighted, the resulting feed-forward signalling cascade, leads to the propagation of extracellular ATP along the tanycyte layer and amplification of the response (above). In addition, the ATP signal may also be propagated along its basal projections into the parenchyma (below). Adapted from Dale, 2011.

Purinergic signalling in neural stem/progenitor cells

Interestingly, intracellular calcium waves, ATP release and purinergic activation of the P2Y1 receptor have been previously implicated in neural stem/progenitor cell proliferation, migration and/or differentiation and thus, neurogenesis [Weissman et al, 2004; Lecca et al, 2016; Tang & Illes, 2017].

SVZ-derived neural progenitor cells cultured as neurospheres expressed purinergic receptors, including P2Y1R, and exhibited transient calcium waves upon stimulation by ATP [Mishra et al, 2006; Lin et al, 2007]. When P2Y1R agonists were applied, cell

proliferation was seen to be enhanced [Mishra, et al, 2006; Lin et al, 2007; Boccazzi et al, 2014]. Concurrently, injection of ATP into the murine lateral ventricle yielded increased proliferation of neural progenitors and transit-amplifying cells [Suyama et al, 2012]. Indeed, upon application of the P2Y1R antagonist, MRS2179, cell proliferation decreased [Mishra et al, 2006; Suyama et al, 2012]. Similarly, inhibition of the calcium wave with inhibitors or calcium chelators negated any ATP-induced cell proliferation [Ryu et al, 2003; Heo & Han, 2006]. Further corroboration of the proliferative role of ATP is seen in mice deficient for the ectoenzyme, NTPDase (responsible for extracellular nucleoside triphosphate degradation) whereby increased cell proliferation was observed in the classical neurogenic niches, the SGZ and SVZ [Gampe et al, 2015]. It has been indicated that the source of extracellular ATP (and other nucleotide bi/triphosphates) are neural stem/progenitor cells themselves, including NSC niche astrocytes [Lin et al, 2007; Cao et al, 2013].

In addition to cell proliferation, P2Y1R activation was also associated with increased cell migration and differential cell fate. An increase in the cortical actin cytoskeleton and in cell-spreading was observed in cultured adult murine neural stem cells when nucleotides (ATP) and EGF were applied [Grimm et al, 2010]. Furthermore, in another study, blockade of P2Y1R in cultured neurospheres from embryonic striata resulted in decreased proliferation and migratory distances [Scemes et al, 2003]. Indeed, in the embryonic brain, radial glial cells have been suggested to release ATP to coordinate proliferation and cell migration [Weissman et al, 2004]. With regards to cell fate determination, sustained P2Y1R activation has been reported to lead to astrogliosis, yielding increased parenchymal astrocytes [Boccazzi et al, 2014], whilst the loss of purinergic signalling led to the onset of neuronal differentiation and maturation [Lin et al, 2007].

Using optogenetics to stimulate intracellular calcium waves and ATP release

Whilst electrophysiology was classically used as one of the principal methods used to study neurons and neural networks, the development of genetically encoded light-sensitive tools and thus the prevalence of the optogenetics field has revolutionized neuroscience [Fenno et al, 2011; Zeng & Madisen, 2012; Hausser, 2014]. A key feature

of optogenetics comprises the ability to target expression of these light-sensitive tools in specific cell types and even sub-cellular compartments, enabling high-resolution investigation of the nervous system at several levels, from the synaptic level to intact neural circuits underlying complex behaviours [Hausser, 2014]. Whilst optogenetic tools include optical indicators such as genetically encoded calcium or voltage sensors, and optical actuators such as light-sensitive membrane channels or pumps, the latter has the capacity to manipulate neuronal activity, including in live animals [Zeng & Madisen, 2012]. Indeed, studies have demonstrated the ability to activate [Nagel et al, 2003; Boyden et al, 2005] as well as silence [Han & Boyden, 2007; Chow et al, 2010] neurons with high spatiotemporal precision using different engineered microbial opsins and/or pumps [Zeng & Madisen, 2012]. Two widely-used microbial opsins are the channelrhodopsin variants, Channelrhodopsin-1 (ChR1) and Channelrhodopsin-2 (ChR2), isolated from an algal species, *Chlamydomonas reinhardtii* [Nagel et al, 2002; Nagel et al, 2003]. Both are non-selective for cations such as sodium, potassium and calcium, and allow their flux across the cell membrane when illuminated with blue light at 470nm [Lin et al, 2009; Kato et al, 2012]. Indeed, being encoded by a single gene and possessing rapid on/off kinetics in response to blue light makes these ideal optogenetic actuators for neuronal depolarization/activation [Repina et al, 2017].

Although optogenetics was originally applied to control neuronal activity, it is now being used in order to manipulate additional cell-types and biological systems [Yawo et al, 2013]. More recently, optogenetic activation of astrocytes has been pursued in order to demonstrate their role in synaptic modulation and plasticity [Gradinaru et al, 2009; Gourine et al, 2010; Sasaki et al, 2012; Chen et al, 2013; Li et al, 2013b; Perea et al, 2014]. Optogenetic stimulation of astrocytes in the brainstem induced increased intracellular calcium, leading to the release of ATP, which in turn triggered depolarization of retrotrapezoid nucleus (RTN) neurons, increasing respiratory activity [Gourine et al, 2010]. Similarly, in another study, photo-activated brainstem astroglia released ATP, activating rostral ventrolateral medulla neurons resulting in increased sympathetic nerve activity and arterial blood pressure and heart rate [Marina et al, 2013]. Interestingly, optogenetic activation of (other) glia and/or the elevation of intracellular calcium was also

associated with glutamate release, which has been implicated in glia-to-neuron signalling and neuronal excitotoxicity [Sasaki et al, 2012; Beppu et al, 2014].

Aim

Since tanycytes exhibit a chemosensory role via purinergic signalling and P2Y1R activation, and is suggested to have a role as a neural stem/progenitor cells in adult hypothalamic neurogenesis, I hypothesized that these functions are associated. Indeed, given that the optogenetic stimulation of glia/astrocytes triggers intracellular calcium waves and ATP release (similarly to tanycytes upon chemosensory stimulation), this study aims to assess whether optogenetic stimulation of tanycytes can induce the same effect, and whether this in turn may affect cell proliferation and neurogenesis in the adult hypothalamus.

Methods

Animals

The following transgenic mice were purchased from Jackson Laboratory (Bar Harbour, ME, U.S.A) and bred in the animal facility at Biopolis (Singapore): Nestin-CreER^{T2} [C57BL/6-Tg(Nes-creER^{T2})KEisc/J], ROSA26$^{loxP\text{-}STOP\text{-}LoxP\text{-}ChR2\text{-}YFP}$ [B6.Cg-Gt(ROSA)26Sortm32(CAG-COP4*H134R/EYFP)Hze/J]. Nestin-CreERT2:ROSA26-loxP-STOP-LoxP-ChR2-YFP mice were obtained by breeding Nestin-CreERT2 mice with ROSA26$^{loxP\text{-}STOP\text{-}LoxP\text{-}ChR2\text{-}YFP}$. Only offspring positive for Cre-recombinase (Nestin-CreERT2$^{+/-}$: ROSA26-loxP-STOP-LoxP-ChR2-YFP$^{+/+}$, hereon referred to as NCE-ChR2Y) mouse colonies were selected for experiments based on genotyping results. Mice were genotyped as described in the previous chapter (same primers). Genotyping was carried out by animal facility staff of Biological Research Centre (BRC), A*STAR, Singapore and/or by animal facility staff at the University of Warwick, UK.

All mice used in these studies were maintained and euthanized according to protocols either approved by the Institutional Animal Care and Use Committee at the Biological Resource Centre, Agency for Science, Technology and Research (A*STAR), Singapore, or by the Animal Welfare and Ethical Review Board of the University of Warwick and the UK Home Office.

In vitro validation

Tamoxifen injection

Tamoxifen (Sigma, T-5648) was dissolved in 90% corn oil (Sigma, C8267):10% ethanol at a concentration of 20mg/ml. To induce Cre-mediated recombination for induction of ChR2-YFP expression, tamoxifen was injected into adult (8-12 weeks-old) mice intraperitoneally for 5 consecutive days at a daily dose of 100mg/kg of body weight.

Acute slice preparation

1-4 days after tamoxifen injection, mice (of either sex) were humanely sacrificed by cervical dislocation in accordance with schedule 1 of the Animals (scientific procedures) act 1986. The brain was rapidly dissected and placed in ice-cold artificial cerebrospinal fluid (aCSF; 124mM NaCl, 26mM $NaHCO_3$, 1.25mM NaH_2PO_4, 3mM KCl, 2mM $CaCl_2$, 3mM $MgSO_4$, 10mM glucose saturated with 95% O2/5% CO_2) with additional 10mM $MgSO_4$. Coronal sections 300μm thick were prepared from the hypothalamus using a vibrating microtome (Microm HM650). Each section was subsequently dissected along the midline separating the third ventricle and incubated in 35-6^{o}C aCSF for 30-60 minutes to allow for recovery of adenine nucleotide levels [zur Nedden et al, 2011]. Slices were then transferred and stored in 1mM glucose aCSF at room temperature for the remainder of the experiment.

Calcium imaging and optogenetic stimulation

Hypothalamic slices were loaded with the ratiometric Ca^{2+} indicator Fura-8 AM (12.5 μg/mL in 0.125% DMSO and 0.025% pluronic) for 90 minutes in 10mM glucose aCSF. Fura-8-loaded slices were transferred to a flow chamber with circulating 1mM glucose aCSF (at 37^{o}C) and imaged under a Scientifica Slicescope via an Olympus 60x water immersion objective (NA 1.0). Images were captured with a Hamamatsu ImageEM EM-CCD camera. A ratiometric image of Fura-8 fluorescence was achieved by illumination at 350nm and 415nm via LEDs of the appropriate wavelength and suitable bandpass filters (Cairn Research).

Optogenetic stimulation was performed by flashing blue light (470nm at 0.5Amps on the OptoLED light source module, Cain Research; 20/50 millisecond cycle of ON/OFF) for 29 iterations followed by image acquisition of Fura-8 fluorescence. The duration of stimulation varied from 5-20 cycles of the described algorithm.

Metafluor imaging was used to control illumination (all wavelengths) and acquisition of images. Recordings were made at room temperature (25-28^{o}C), and the flow chamber was perfused at 3-4 ml/minute.

Data analysis & statistics

Analysis was performed using ImajeJ. Fura-8-loaded tanycytes and/or other (parenchymal) cells of interest were outlined as regions of interest (ROI) and the mean pixel intensity at 365nm and 415nm of each ROI calculated. The emission ratios for F_{365}/F_{415} (no units) were then calculated. Peak response magnitudes were calculated by subtracting the average baseline value (from at least 5 images) from the maximum change in relative fluorescence intensity. Only ROIs that indicated a change from baseline of >0.015 was considered a minimum value at which a response was observed. The mean value from each brain slice was produced and used for statistical analysis.

Results are expressed using box plots (median and interquartile range with whiskers representing the min/max range). The Kruskal-Wallis one-way analysis of variance was used, followed by post-hoc Dunn's for pairwise comparisons within multiple groups. For comparisons between two groups, two-tailed independent samples Mann-Whitney test was used. Significance was only established when $p \leq 0.05$ (*) and satisfied a post-hoc false-discovery test [Curran-Everett, 2000].

In vivo opto-stimulation experiment

Fibre optic stub implantation

All surgeries were performed by Dr Paul Anderson. Mice were anaesthetised with 3% isoflurane (1L/min O_2 flow rate), their heads shaved and secured on a stereotaxic rig. Local anaesthetic (lignocain; 2.5mg/ml, 0.4ml/kg body weight subcutaneous) and analgesic (buprenorphine; 0.03mg/ml, 1.7ml/kg body weight subcutaneous) was applied

under the skin. Eye lubricant cream was applied and incision site sterilized with 70% ethanol and iodine wipes. An incision was made through the midline of the scalp and the cranium exposed by holding back the skin with clamps. The skull surface was cleaned with sterile saline and allowed to dry. A small hole (< 1 mm diameter) was drilled at 1.5 mm posterior to bregma and 0.25 mm lateral (right) of bregma. A fiber optic stub (245 µm diameter, 0.37 NA, 5.2 mm long with 1.25 mm diameter Zirconia ferrule: Doric Lenses, part no: MFC_200/245-0.37_5.2mm_ZF1.25_FLT) was inserted slowly (~1 mm/min) into the first hole made using a stereotaxic arm, finally allowing the ferrule to rest on the cranium. Finally, dental cement was applied across the cranium (covering the anchoring screws) and onto the lower portion of the implant, avoiding any contact with the skin, to result in a small pyramidal mound over the cranium with 3-5 mm of the ferrule clean of cement for unobstructed connection with the light cable. Once the dental cement was dried, the scalp was sutured around the implant and the animal allowed to recover in its housing cage whilst kept warm with a heat lamp. Animals were allowed to recover from surgery and given antibiotics and analgesia in drinking water for 3 days following surgery, whilst monitoring body weight and animal condition closely to ensure health of the animal.

Tamoxifen & BrdU injection

Tamoxifen (Sigma, T-5648) was dissolved in 90% corn oil (Sigma, C8267):10% ethanol at a concentration of 20mg/ml. To induce Cre-mediated recombination for induction of YFP expression, tamoxifen was injected into adult (8-12 weeks-old) mice intraperitoneally for 5 consecutive days at a daily dose of 100mg/kg of body weight. BrdU (Sigma, B5002) was dissolved in 0.9% saline at a concentration of 10mg/ml. BrdU was injected into adult mice intraperitoneally on the stated days at a dose of 50 or 100 mg/kg body weight (see below).

Tamoxifen and BrdU injections were performed distinctly according to two different optogenetic-stimulation experiments (refer to Figures 4.7A and 4.9A).

Short term opto-stimulation: Tamoxifen was injected for 5 consecutive days. Mice were then opto-stimulated and injected with BrdU (100 mg/kg body weight, after the last opto-stimulation each day) daily for the next 7 days.

Long term opto-stimulation: Tamoxifen and BrdU (50 mg/kg body weight) injections were performed on the same days for 5 consecutive days. Mice were opto-stimulated daily for the next 28 days.

Optogenetic stimulation

Mice with fiber optic stubs implanted were connected to an optic fibre cable and opto-stimulated with blue light (470nm, LED) twice a day (gap of 4-6 hours) with the following protocol: 20ms/50ms ON/OFF cycle for 70s every 15minutes for a total of 3 times. The duration of opto-stimulation (days) varied according to two different opto-stimulation experiments (refer to Figures 4.7A and 4.9A); short-term opto-stimulation was performed for 7 days, whilst long-term opto-stimulation was performed for 28 days.

A light intensity of 15.9 milliwatts was used to deliver an estimated light intensity of 3-5 milliwatts (at a depth range of 0.75-0.9mm) to the lateral 3rd ventricle walls, according to the the brain tissue light transmission calculator (Stanford Optogenetics Resource centre; http://web.stanford.edu/group/dlab/cgi-bin/graph/chart.php).

Tissue processing

Mice were anesthetized with a lethal dose of pentobarbital and intracardially perfused with 4% paraformaldehyde (PFA; Sigma, P-6148) in 0.1M phosphate buffer (PB). Brains were immediately post-fixated in 4% PFA in 0.1M PB overnight at 4 °C, and subsequently cryoprotected in 30% sucrose in 0.1M PB for at least 48 hours. Cryoprotected brains were sectioned coronally at a thickness of 40µm using a freezing microtome at -30°C (Microm HM430, Thermo Scientific, USA). Serial coronal sections were collected along the anteroposterior axis covering the hypothalamus and stored in cryoprotective solution (20% Glycerin, 30% Ethylene Glycol in 0.1M PB) at -20 °C.

Immunohistochemistry

For multiple immunohistochemistry, 8 sections were used (1 every 4 serial sections). This was appropriate to capture the majority of the hypothalamus. The free-floating method [Bachman, 2013] was used; sections were rinsed 3 times for 10 minutes in 0.1M Tris-buffered saline (TBS), incubated in blocking buffer, TBS++ (3% Donkey serum, 0.25%

Triton-X100 in TBS) for 60min, prior to incubation with primary antibody in TBS++ at 4°C for 36 hours (two nights). Following primary antibody incubation, sections were rinsed with TBS 2 times for 10min, blocked in TBS++ for 20 min, and incubated in secondary antibody in TBS++ for 4 hours at room temperature. Nuclear staining was performed with incubation with 4',6-Diamidino-2-phenylindole-dihydrochloride (DAPI; 0.5µg/mL; Sigma, 28718-90-3) for 10 mins. Immunostained sections were rinsed with TBS 3 times for 10 minutes and mounted on glass slides with mounting medium, polyvinyl alcohol (PVA)-DABCO. Primary antibodies used: rabbit anti-GFP (1:400; Life Technologies, A11122), mouse anti-NeuN (1:1200; Millipore, MAB377), rat anti-BrdU (1:400; AbD Serotec, OBT0030G). Secondary antibodies used: donkey Anti-Rat Cy3 (1:250; Jackson Immuno., 712-165-153), donkey Anti-Rabbit 488 (1:250; Jackson Immuno., 711-545-152), donkey anti-mouse 647 (1:250; Jackson Immuno., 705-605-147).

Statistics

From immunostained slides, 6-8 sections were selected based on their location (mid-caudal hypothalamus), from Bregma -1.22mm to -2.18mm, and analysed for BrdU+ and YFP+ cell quantification. Selected sections were imaged/viewed under the epifluorescence microscope (Zeis Axio Imager 2) to count BrdU+ and YFP+ cells (under a 20x objective). Hypothalamic regions were outlined as described previously; using NeuN immunostaining the ventromedial nucleus was used to predict hypothalamic nuclei boundaries according to the 'Mouse Brain in Sterotaxic co-ordinates' (Paxinos & Franklin, 2012). BrdU+ and YFP+ cell counts were quantified as a function of cell density (per mm^2 or mm^3 of hypothalamic tissue).

Results are expressed either using box plots (median and interquartile range with whiskers representing the min/max range) or bar charts (mean with whiskers representing standard error of the mean). For comparisons between two groups, two-tailed independent samples Mann-Whitney test was used. Significance was only established when $p \leq 0.05$ (*) and satisfied a post-hoc false-discovery test [Curran-Everett, 2000].

Results

An optogenetic approach was used to stimulate tanycytes. Similarly to the NCE-YFP mice, a Cre-inducible double-transgenic mouse model was used to conditionally express a channelrhodopsin-2 variant, ChR2(H134R) [Nagel et al, 2005] and YFP (as a fusion protein) under the constitutive, CMV early enhancer/chicken β-actin (CAG) promoter in Nestin-expressing tanycytes. CreERT2 expression was driven under the nestin promoter. Thus, when tamoxifen is injected into Nestin-CreERT2:ROSA26-loxP-STOP-loxP-CAG-ChR2-EYFP (referred to as NCE-ChR2Y) mice, CreERT2 is allowed to excise the lox-STOP-lox codon upstream of ChR2-YFP and initiate permanent expression in tanycytes.

ChR2-YFP expression in NCE-ChR2Y mice is not exclusively restricted to tanycytes.

Given the observation that YFP expression in a parallel fate-mapping transgenic mouse (NCE-YFP; chapter 2) was not exclusively restricted to tanycytes in the hypothalamus, the specificity of ChR2-YFP expression was assessed shortly after tamoxifen-induced recombination.

NCE-ChR2Y mice exhibited a similar YFP expression pattern to that seen in NCE-YFP mice; additional cell-types other than tanycytes were found to be YFP+. 3 days after tamoxifen injection, YFP immunofluorescence was predominantly observed at the ependymal layer, specifically in many ependymocytes and tanycytes lining the lateral walls of the 3rd ventricle (Fig. 4.2A). YFP+ cells were also identified in the parenchyma exhibiting both, neuronal- and glial-like morphologies, albeit at much lower numbers than ependymal YFP+ cells (Fig. 4.2A, C, D; yellow asterisk/arrows). Over a prolonged survival period (30 days after tamoxifen), YFP expression is still predominantly observed at the ependymal layer (Fig. 4.2B). Interestingly, some tanycytes at the ventral wall of the 3rd ventricle were also seen to express YFP (Fig. 4.2B, E; green arrows).

Figure 4.2

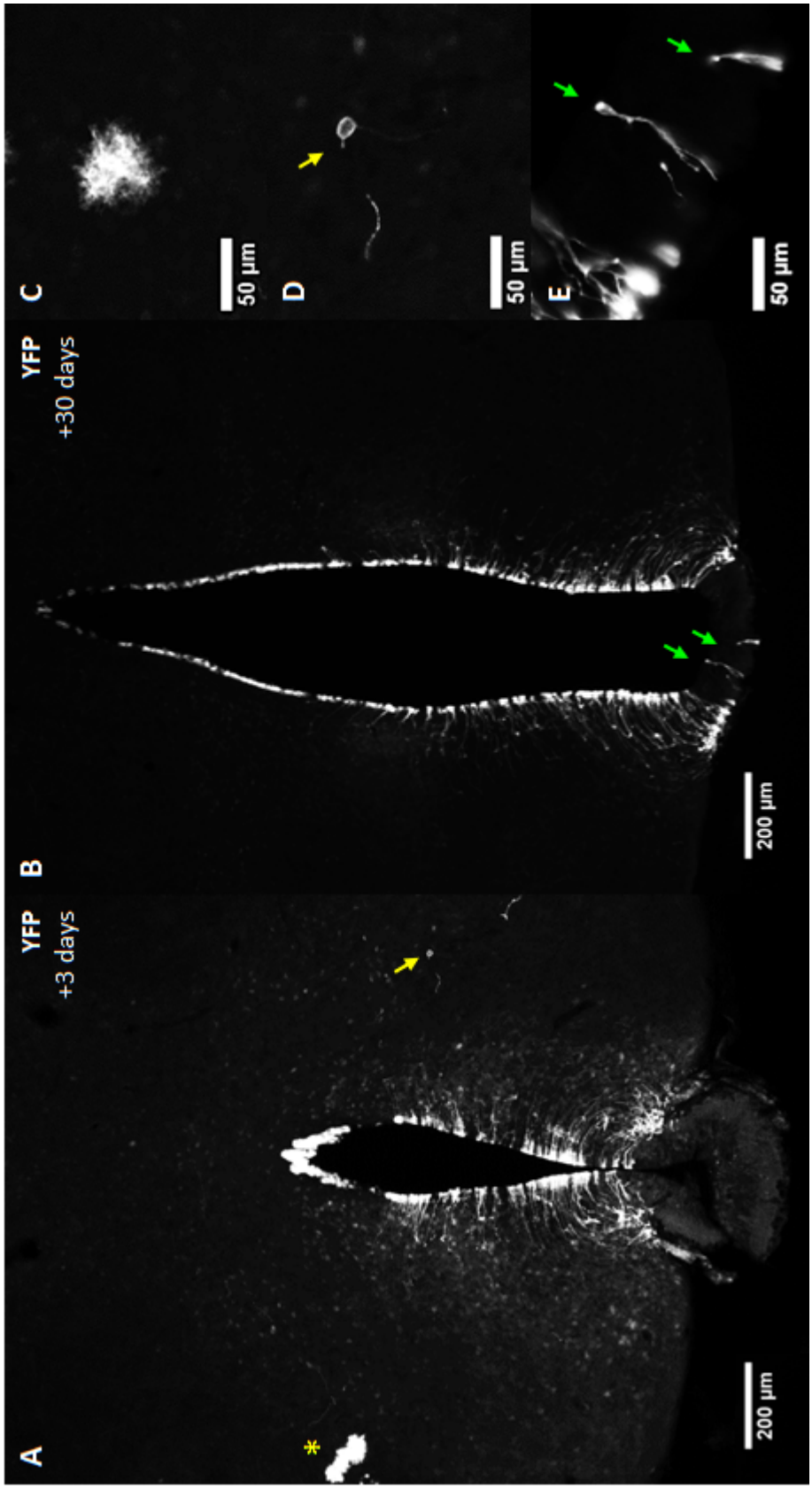

Figure 4.2. ChR2-YFP expression is not restricted to tanycytes. Analysis of ChR2 expression was performed by immunostaining for YFP **A)** 3 days after tamoxifen injection, YFP+ cells were observed in the ependymal layer of the lateral 3rd ventricle walls and in the parenchyma (indicated by yellow). **B)** 30 days after tamoxifen injection, YFP expression is still predominantly observed at the ependymal layer, albeit also along the ventral 3rd ventricle wall (green arrows). **C-D)** Parenchymal YFP+ cells were identified morphologically as glial (C, , another example shown by yellow asterisk in A) or neuronal (D, yellow arrow in A). **E)** Magnified images of YFP+ tanycytes observed along the ventral 3rd ventricle wall 30 days after tamoxifen injection (green arrows in B). (n=2).

In vitro validation

Tanycytes expressing Chr2-YFP are responsive to optogenetic stimulation

Firstly, the ability of ChR2-expressing tanycytes to respond to optic stimulation and induce increases in intracellular calcium was validated in tamoxifen-injected (TAM+) NCE-ChR2Y brain slices using calcium imaging. This was achieved by measuring changes in intracellular calcium concentration with a calcium-sensitive fluorescent ratiometric dye, Fura-8 AM [AAT Bioquest, 2017]. This dye, like Fura-2 AM [Martinez et al, 2016, 2017], is membrane permeable and able to cross the cell membrane, and once intracellular, is de-esterified to membrane-impermeable Fura-8 (referred to as dye-loading). Calcium-bound fura-8 has an excitation wavelength of 354 nm, whilst calcium-free fura-8 has an excitation wavelength of 415 nm. By measuring the intensity of fluorescence emitted by calcium-bound and calcium-free FURA-8, a ratiometric image and value can be generated (354nm/415nm; Figure 4.3B). Indeed, changes in cytosolic calcium are indicated by fluctuations of this ratio. Thus, changes in cytosolic calcium was measured in tanycytes in response to optogenetic (opto-) stimulation.

Inspection of YFP fluorescence indicated that a heterogeneous population of ChR2-YFP+ and ChR2-YFP- tanycytes existed; not all tanycytes expressed ChR2-YFP (Fig 4.3A). Nevertheless, upon opto-stimulation, an immediate and robust increase in intracellular calcium was observed along the tanycyte layer (Fig 4.3C, D). The nature of this response was transient, as intracellular calcium levels were typically restored to baseline levels immediately after opto-stimulation. In response to 100μM ATP (applied through the perfusion medium), a delayed yet similar transient response was seen (Fig. 4.3E). Opto-

stimulation of ChR2+ ependymocytes did not appear to elicit an intracellular calcium response (data not shown).

Quantification of the calcium response in acute brain slices of (TAM+) NCE-ChR2Y mice indicated that opto-stimulation yielded an increase in cytosolic calcium in 86±3% of recorded tanycytes (Fig. 4.4A), with an average peak response magnitude of 0.044±0.004 (Fig. 4.4B). Indeed, calcium responses elicited in tanycytes were reproducible as there was no significant differences between average peak response magnitudes of the first, second or third instance of sequential opto-stimulation (given a 15-20min recovery interval) in the same brain slice (Kruskal-Wallis ANOVA, followed by post-hoc Dunn's multiple comparisons test; Fig 4.4C). Interestingly however, the duration of the calcium response was seen to depend on the duration of light stimulation, with a significant increase in response duration observed between 5 to 20 ($p=0.0043$), and 10 to 20 ($p=0.0002$) cycles of the optostimulation protocol (Kruskal-Wallis ANOVA, followed by post-hoc Dunn's multiple comparisons test; Fig. 4.4D).

Calcium responses induced by 100μM ATP (0.058±0.009) were comparable to those induced optogenetically (0.044±0.004); no significant difference was observed in average peak response magnitudes of either treatment (Two-tailed Mann-Whitney test; Fig 4.4B). Similarly, no significant difference was seen in the average percentage of tanycytes that responded to ATP or opto-stimulation (Two-tailed Mann-Whitney test; Fig 4.4A).

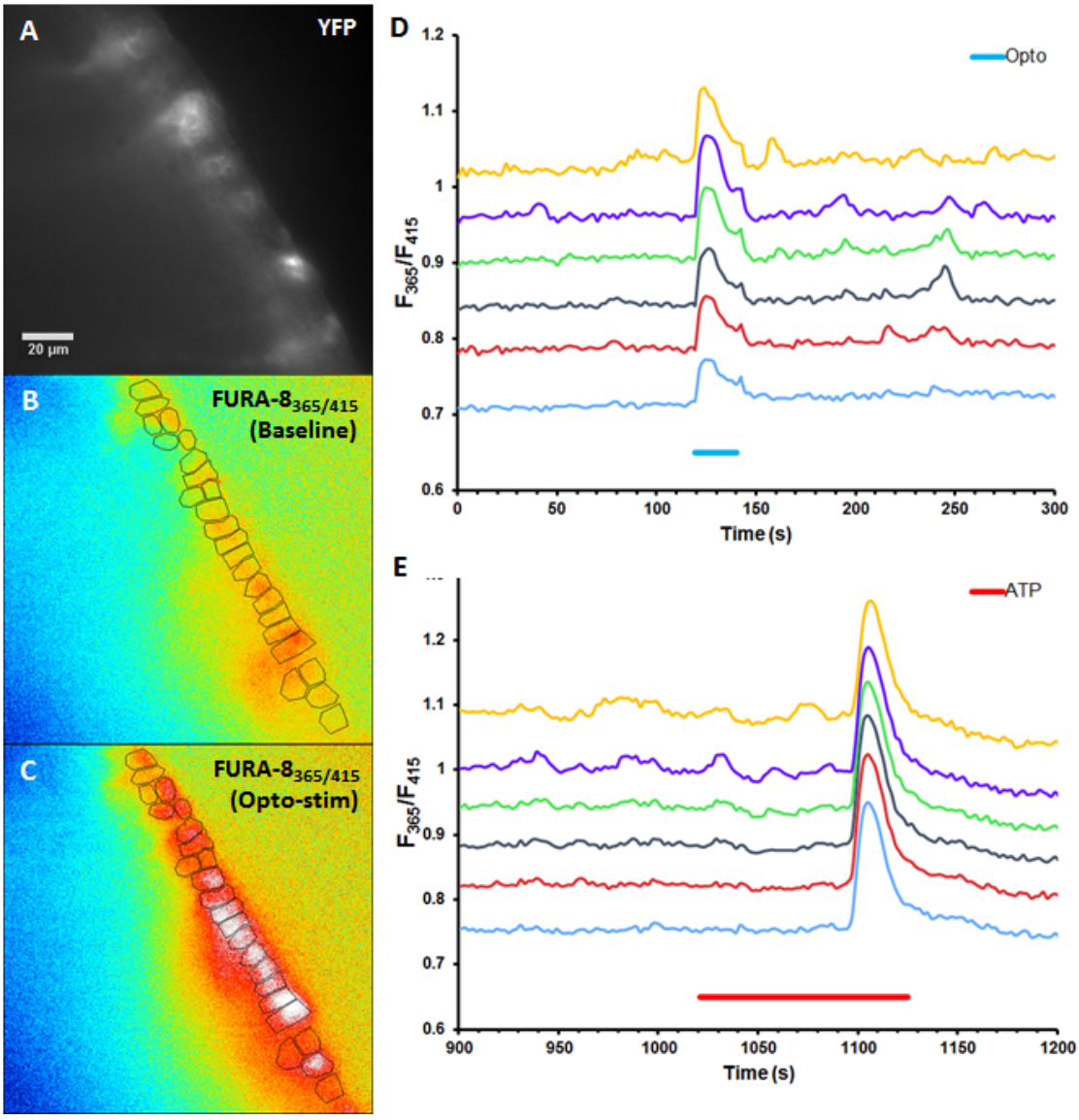

Figure 4.3. ChR2-expressing tanycytes evoked calcium responses to optogenetic stimulation. A) Representative image of YFP fluorescence observed, indicating the heterogeneity of ChR2-EYFP expression in the tanycyte population. **B)** Overlaying image indicating ratiometric Fura-8 in tanycytes (cell bodies outlined in black) under baseline conditions. Colour intensity (from low to high: Blue-green-yellow-red-white,) indicates the relative concentration of calcium-bound to calcium-free Fura-8. **C)** Overlaying image indicating ratiometric Fura-8 in tanycytes upon opto-stimulation (at a time-point where all tanycytes reached a peak response). **D)** Temporal graph indicating ratiometric Fura-8 fluctuations in individual tanycytes (indicated by separate coloured traces) upon opto-stimulation; a large transient increase in intracellular calcium was observed that lasts for the duration of optical stimulation. **E)** Temporal graph indicating ratiometric Fura-8 fluctuations upon application of 100µM ATP via the bath medium. A delayed but robust transient intracellular calcium response was seen.

Figure 4.4

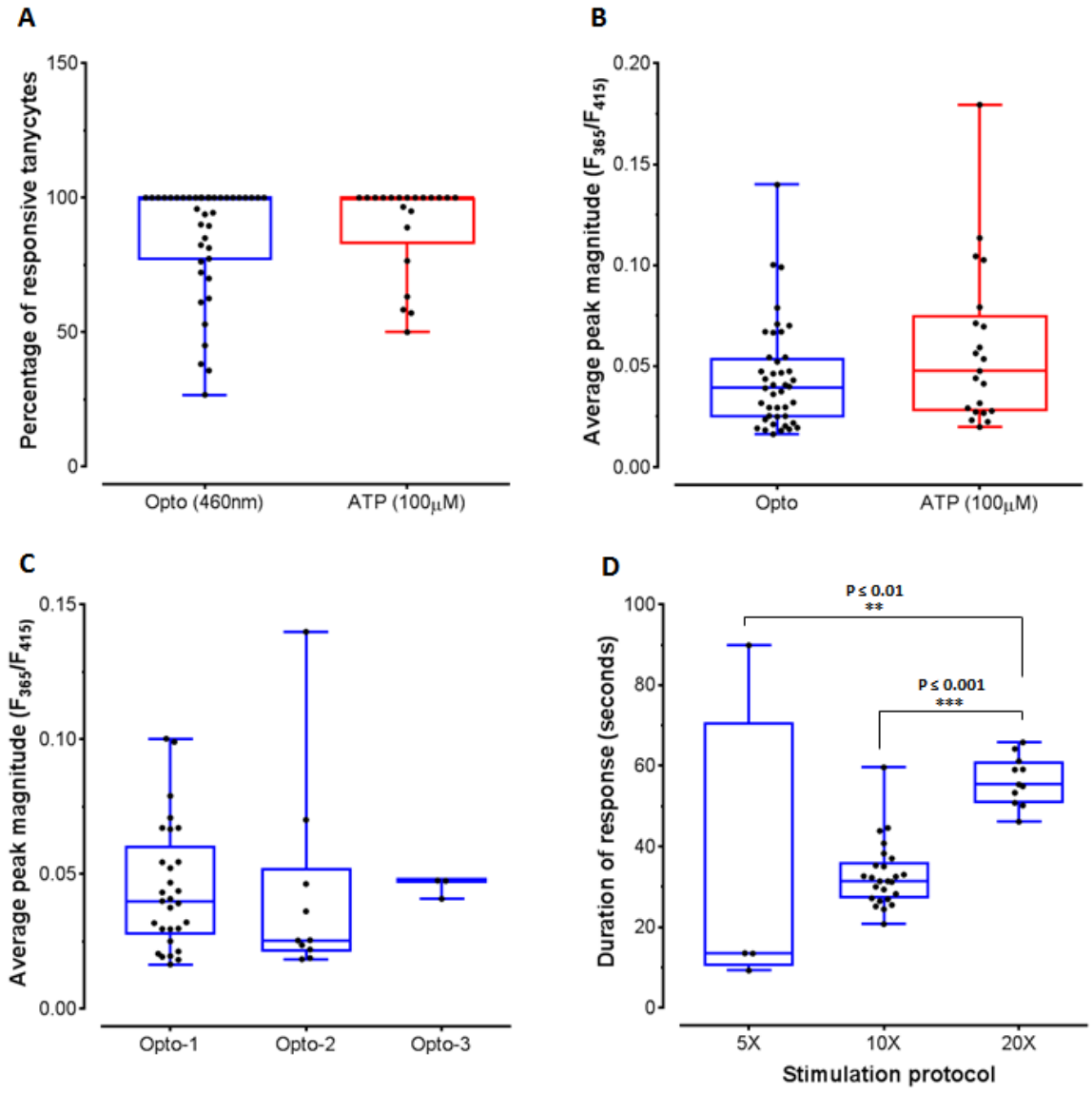
A
Percentage of responsive tanycytes
150
100
50
0
Opto (460nm)
ATP (100μM)
B
Average peak magnitude (F365/F415)
0.20
0.15
0.10
0.05
0.00
Opto
ATP (100μM)
C
Average peak magnitude (F365/F415)
0.15
0.10
0.05
0.00
Opto-1
Opto-2
Opto-3
D
Duration of response (seconds)
100
80
60
40
20
0
P ≤ 0.01
**
P ≤ 0.001
***
5X
10X
20X
Stimulation protocol

Figure 4.4. Quantification and measurement of calcium responses in tanycytes induced by optogenetic stimulation and 100μM ATP. Data is expressed as box (median and interquartile range) and whisker (min/max value) plots. Individual data points are also indicated **A)** The percentage of responsive tanycytes to opto-stimulation and ATP were quantified as a percentage of all tanycytes recorded. A similar percentage of tanycytes were seen to respond to both treatments. **B)** Average tanycyte peak response magnitudes in response to opto-stim and ATP were calculated for each brain slice and compared. A similar average peak magnitude was observed between both treatments. **C)** No significant difference was seen between average peak response magnitudes at the first, second or third instance of multiple opto-stimulations. **D)** The duration of the intracellular calcium response significantly increased with increasing duration of optostimulation. Each cycle of opto-stimulation consisted of 29 flashes of blue light (470nm, at 20ms/50ms cycles of ON/OFF) followed by acquisition of Fura-8 fluorescence. Slices were thus stimulated for a minimum of 5 cycles and maximum of 20 cycles of opto-stimulation. Opto-stim slices: n=42 (Opto-1, n=29; Opto-2, n=10; Opto-3, n=3; 5X, n=5; 10X, n=26; 20X, n=11); ATP-infused slices: n=21.

Parenchymal cells in close proximity to YFP+ tanycytes also responded to optogenetic stimulation

Next, we tested if optogenetic stimulation of tanycytes and subsequent ATP release could affect the intracellular calcium levels of parenchymal cells loaded with Fura-8. This was done to test the hypothesis that tanycytes may be capable of propagating purinergic signalling to parenchymal cells in a similar manner as astrocytes [Cao et al, 2013], as this may indicate an additional role by which tanycytes may regulate parenchymal neural stem/progenitor cell proliferation, migration and hence, neurogenesis [Oliveira et al, 2016; Tang & Illes, 2017].

Parenchymal (ChR2-YFP-) cells loaded with Fura-8 were outlined and ratiometric changes in Fura-8 fluorescence intensity were measured. Upon opto-stimulation, some parenchymal cells in the vicinity of ChR2-YFP+ tanycytes exhibited a heterogeneous range of intracellular calcium responses (Fig. 4.5A-D); whilst some responses were almost immediate (Fig. 4.5C, D), others were delayed for as long as 400 seconds after opto-stimulation (Fig. 4.5B; red trace). In addition, the duration of these responses also varied greatly, with some requiring approximately 100 seconds or less to return to baseline (Fig. 4.5A, B, C; red traces), whilst others required 300 seconds or more (Fig. 4.5B, C; yellow traces). Some calcium responses did not return to a clear baseline (Fig. 4.5D).

This led to the speculation that the heterogeneity in calcium responses observed may be due to the stimulation of a range of different parenchymal cell-types (of neuronal and glial lineage) and/or due to varying distances from ChR2-YFP+ tanycytes.

In order to determine whether the proximity of parenchymal cells to YFP+ tanycytes affected their response to optogenetic stimulation, the minimum distance from the cell-edge of Fura-8 outlined parenchymal cell bodies (both, responsive and non-responsive to opto-stimulation) to the cell-edge of YFP+ tanycytes (including their basal projections) was measured in the XY plane of captured images (Fig. 4.6A, B, D). Indeed, the majority of parenchymal cells that were responsive to opto-stimulation were significantly closer on average (7±1µm; Mean ±SEM) to YFP+ tanycytes and/or the tanycyte layer, in comparison to non-responsive parenchymal cells (18±1µm; $p<0.0001$; Two-tailed Mann-Whitney test; Fig 4.6D). Interestingly, in some instances, opto-responsive parenchymal cells were seen to exhibit different response latencies depending on their distance to YFP+ tanycyte cell bodies (Fig. 4.6A-C); a more immediate calcium response was generated in cells closer to, whereas a more delayed response was seen further away from the YFP+ tanycyte cell body.

Finally, it has been generally postulated that neuronal soma are bigger than that of glial cells [Purves et al, 2001; von Bartheld et al, 2016]. Thus, in order to crudely classify whether the opto-responsive parenchymal cells were of a particular neural lineage (neuronal or glial), the cross-sectional area of Fura-8 loaded parenchymal cells were measured and compared. No statistical difference was detected between the mean cross-sectional area of opto-responsive (89±7 μm^2) and non-responsive (73±5 μm^2) parenchymal cells ($p=0.078$, Two-tailed Mann-Whitney test; Fig. 4.6E). Indeed, the cross-sectional areas of opto-responsive parenchymal cells were as diverse as those that did not respond to opto-stimulation.

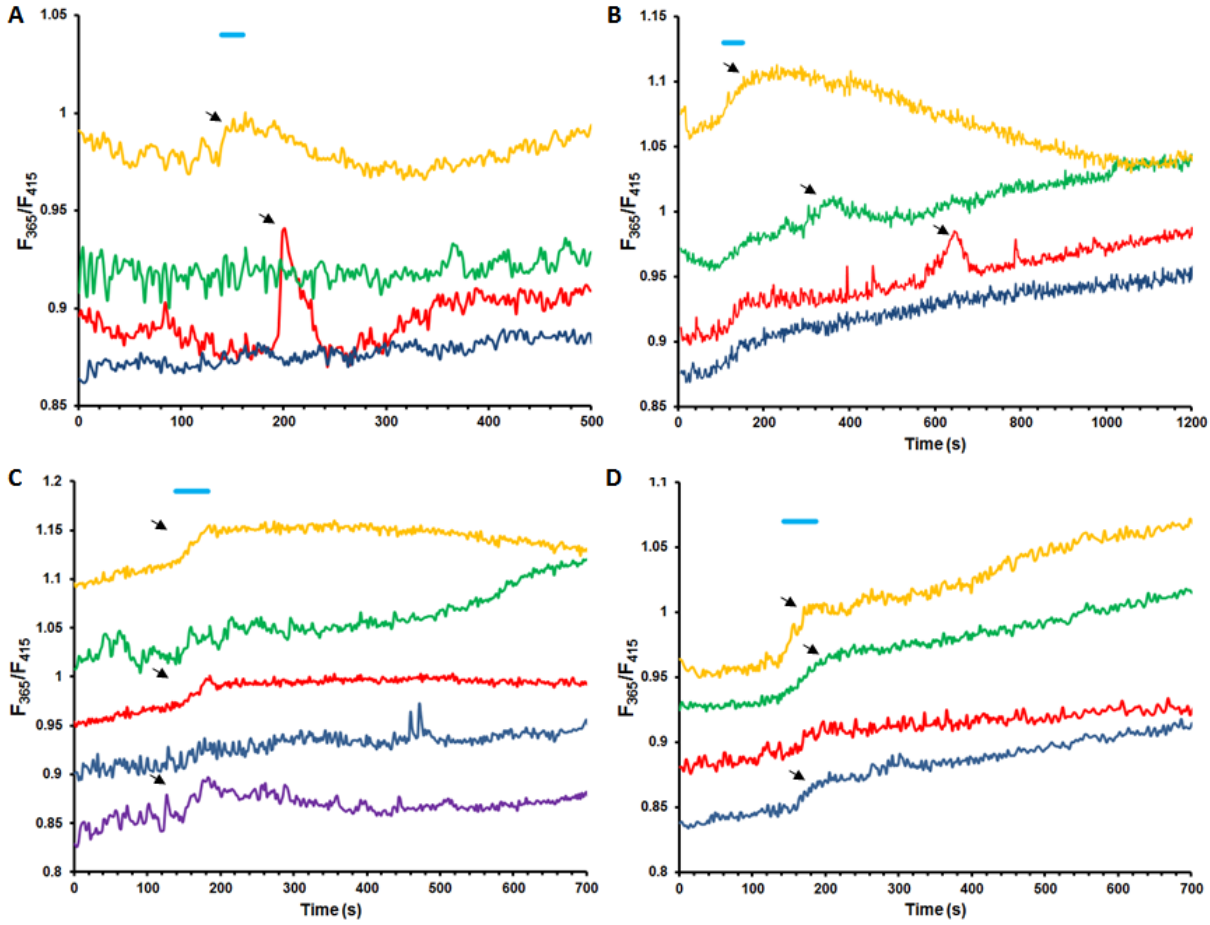

Figure 4.5. Fura-8-loaded parenchymal cells exhibited heterogeneous intracellular calcium responses to opto-stimulation. A-D) Exemplar graphs indicate temporal fluctuations of Fura-8 fluorescence ratio in individual parenchymal cells (indicated by separate coloured traces) upon 10X (A, B) or 20X (C, D) opto-stimulation. Arrows indicate cells and fluctuations considered to be responsive and calcium responses, respectively. Heterogeneity in responses was seen whereby different latencies and durations of intracellular calcium responses were seen upon/after opto-stimulation. Some responses do not return to baseline levels. Due to the high variability in responses observed and small sample size (n=6), quantified analysis of responses was not possible.

Figure 4.6

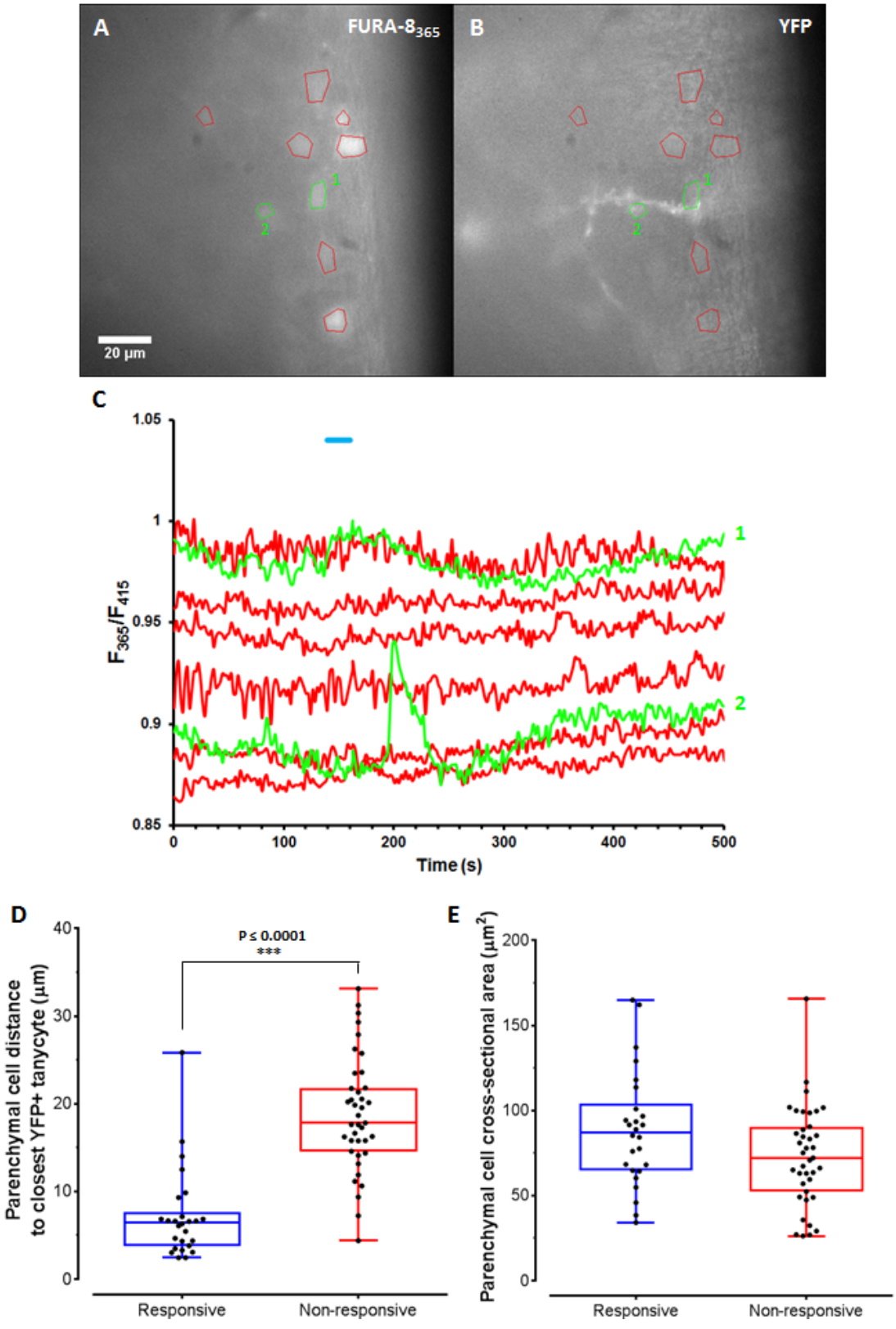
A
FURA-8365
B
YFP
1
2
20 µm
C
1.05
1
0.95
0.9
0.85
F365/F415
0
100
200
300
400
500
Time (s)
1
2
D
P ≤ 0.0001
***
Parenchymal cell distance to closest YFP+ tanycyte (µm)
40
30
20
10
0
Responsive
Non-responsive
E
Parenchymal cell cross-sectional area (µm2)
200
150
100
50
0
Responsive
Non-responsive

Figure 4.6. Parenchymal cells exhibited calcium responses and different response latencies depending on their proximity to ChR2-YFP+ tanycytes. A-B) Parenchymal cells loaded with Fura-8 (A) were measured for their cross-sectional area and minimum distance to ChR2-YFP+ tanycyte cell bodies and/or their basal processes (B). Opto-responsive cells are outlined and numbered in green. Non-responsive cells are outlined in red. Overlaying images were used. **C)** Temporal graph indicating ratiometric Fura-8 fluctuations in parenchymal cells upon opto-stimulation. Responsive cells are represented as green traces. Note that the parenchymal cell proximal (1) to the YFP+ tanycyte cell body exhibits an immediate calcium response, in comparison to the delayed calcium response by the distal parenchymal cell (2). **D-E)** Data is expressed as box (median and interquartile range) and whisker (min/max range) plots. Individual data points are also indicated **D)** Opto-responsive parenchymal cells were significantly closer to YFP+ tanycytes than non-responsive parenchymal cells. **E)** No significant difference was seen between the size of opto-responsive parenchymal cells and non-responsive parenchymal cells. Slices: n=5 (Opto-responsive cells: n=26; non-responsive cells: n=39)

In vivo characterization and experiments

Given the demonstration that ChR2-expressing tanycytes can be optogenetically stimulated to generate intracellular calcium waves along the tanycyte layer to the same effect as agonists such as ATP, the effect of their opto-stimulation on neurogenesis was tested *in vivo*. This was achieved by the chronic implantation of an optic-fibre stub into the dorsal hypothalamus, allowing for illumination of blue light (470nm) on ChR2+ cells of the 3rd ventricle. It should be noted that all mice (control and opto-stimulated) were implanted with optic-fibre stubs to minimise any differential effect due to implantation surgery. Accordingly, experiments were devised to investigate the effect of tanycyte opto-stimulation on cell proliferation, survival and differentiation in the adult hypothalamus.

Short-term opto-stimulation of hypothalamic ChR2-YFP+ cells did not alter cell proliferation or YFP+ cell numbers.

We then proceeded to investigate whether opto-stimulation of ChR2-YFP+ cells affected cell proliferation in the hypothalamus. In order to assess an effect on cell proliferation, a short-term opto-stimulation experiment was designed, whereby BrdU was injected (100mg/kg) daily alongside optogenetic stimulation for 7 days (Fig. 4.7A). Cell proliferation was analysed by immunohistochemical quantification of BrdU+ cells in the whole hypothalamus as well as in distinct regions; at the ependymal layer of the 3rd ventricle, at the underlying subependymal layer and in the periventricular area (here,

defined as parenchymal tissue immediately surrounding the ependymal and subependymal layers and extending out as far as 50 μm from the 3rd ventricle). YFP+ tanycytes were quantified as a cell density per area of the 3rd ventricle (multiplying the length of the ependymal layer by the thickness of the immunostained section), whilst YFP+ parenchymal (neuron- and glial-like) cells were quantified as a cell density per volume of parenchymal tissue throughout the hypothalamus.

Upon opto-stimulation, no visual nor statistical difference in BrdU+ cell density was observed in the hypothalamic regions measured (3V; p=0.8182, Subepend; p=0.8182, PeA; p=0.5887, HYPO; p=0.8182, Two-tailed Mann-Whitney test; Fig. 4.7B, C). However, a significant increase was found in BrdU+ cells located in close proximity (within 10μm) to YFP+ tanycytes and their projections in opto-stimulated brains. (p=0.0087; Two-tailed Mann-Whitney test; Fig. 4.8A; white arrows, B). No BrdU uptake (co-localization) was seen in YFP+ tanycytes (data not shown) and no significant difference was seen in the densities of YFP+ tanycytes (p=0.132) or YFP+ parenchymal (neuron-like; p=0.4848, glial-like; p=0.5887) cells between control and opto-stimulated brains (Two-tailed Mann-Whitney test; Fig. 4.8C, D).

Figure 4.7. Short-term opto-stimulation of hypothalamic ChR2-YFP+ cells did not change BrdU+ cell numbers. A) Following optic fibre-implantation surgery (day -3), NCE-ChR2Y mice were given daily tamoxifen injections (day 0-4), followed by opto-stimulation (twice daily, 4-6 hour interval; day 5-11) and BrdU injections (100mg/kg ip; immediately after last opto-stimulation; day 5-11) daily for 7 days prior to perfusion-fixation (day 11; 2-4 hours after last BrdU injection) and subsequent immunohistochemical analysis. **B)** Representative immunostaining images indicated comparable BrdU uptake in control and opto-stimulated mice. BrdU+ cells were quantified in the following regions, as illustrated: 3rd ventricle ependymal layer (3V; orange single-cell layer in direct contact with the ventricle), subependymal layer (Subepend; blue single-cell layer immediately underlying the 3V ependymal layer), Periventricular area (PeA; defined here as 50μm of parenchyma immediately surrounding the perimeter of the 3rd ventricle; outlined in yellow). **C)** Data is expressed as box (median and interquartile range) and whisker (min/max range) plots. The mean (plus sign) and individual data points (black points) are also indicated. Horizontal labels on the graphs correspond to those regions illustrated in B. Total hypothalamus (HYPO) was also analyzed. Mice used: n=6 for either treatment.

Figure 4.7

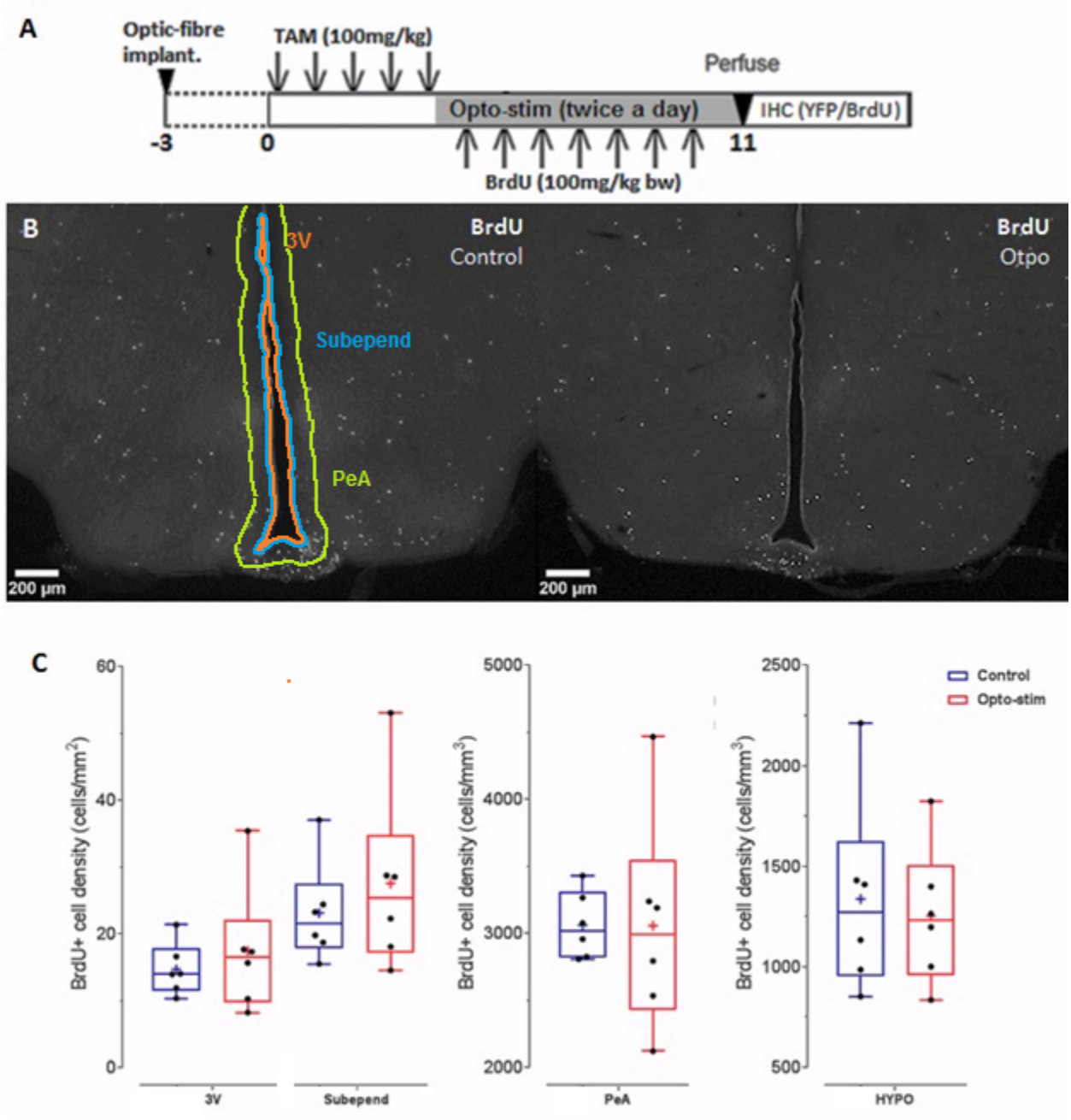
A
Optic-fibre implant.
TAM (100mg/kg)
Perfuse
Opto-stim (twice a day)
IHC (YFP/BrdU)
-3
0
11
BrdU (100mg/kg bw)
B
3V
Subepend
PeA
BrdU
Control
BrdU
Otpo
200 µm
200 µm
C
Control
Opto-stim
BrdU+ cell density (cells/mm2)
BrdU+ cell density (cells/mm3)
BrdU+ cell density (cells/mm3)
3V
Subepend
PeA
HYPO

Figure 4.8

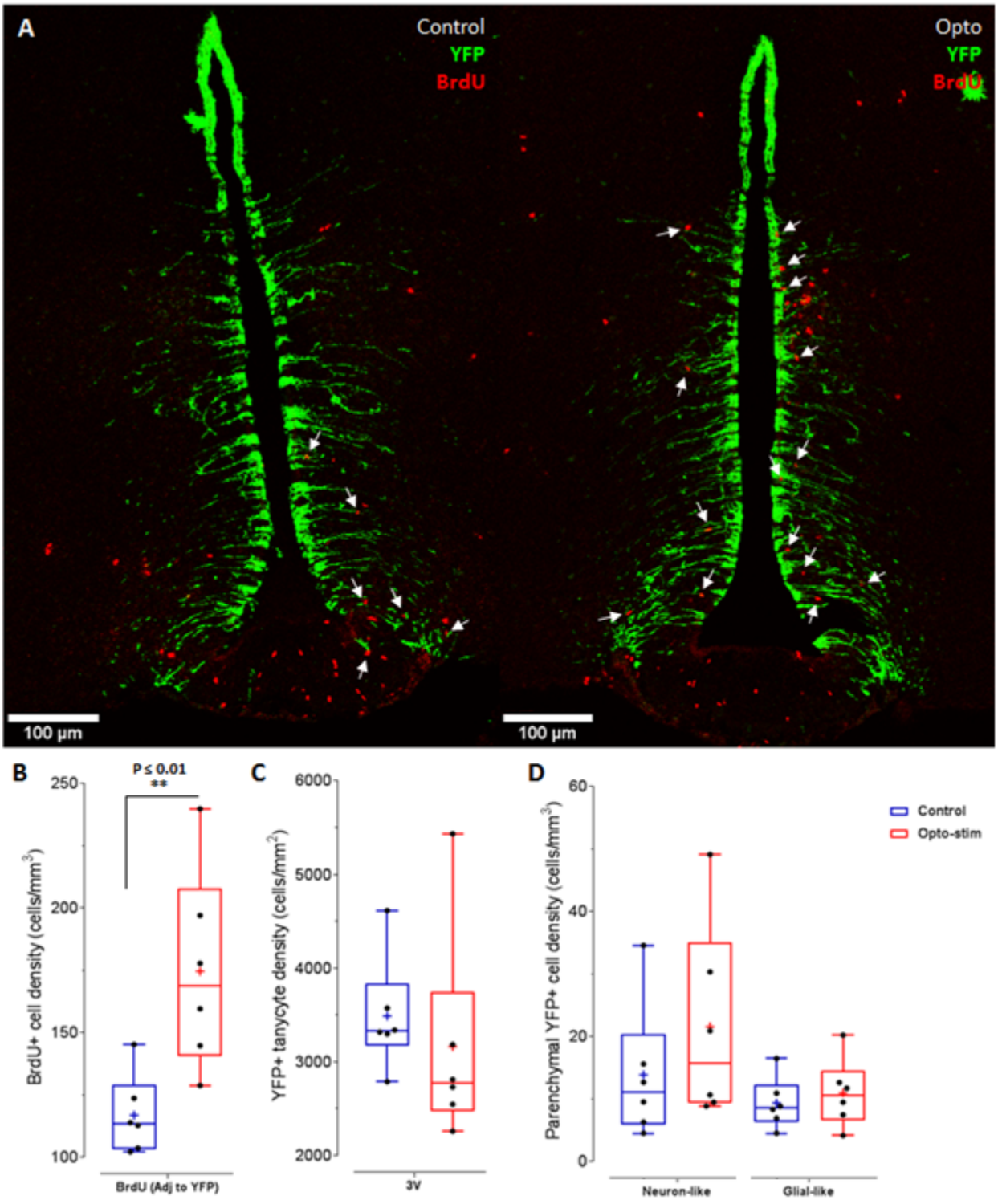
A
Control
YFP
BrdU
Opto
YFP
BrdU
100 µm
100 µm
B
P≤ 0.01
**
BrdU+ cell density (cells/mm3)
250
200
150
100
BrdU (Adj to YFP)
C
YFP+ tanycyte density (cells/mm2)
6000
5000
4000
3000
2000
3V
D
Parenchymal YFP+ cell density (cells/mm3)
60
40
20
0
Neuron-like
Glial-like
Control
Opto-stim

Figure 4.8. Short-term opto-stimulation of hypothalamic ChR2-YFP+ cells did not change YFP+ cell numbers but increased BrdU+ cells in close proximity. A) Representative immunofluorescence images indicated visually comparable numbers of YFP+ tancytes (green) and BrdU+ cells (red). **B)** Upon opto-stimulation, a significant increase was seen in the number of BrdU+ cells in close proximity to YFP+ tanycytes (indicated with white arrows in **A**). No change was seen in quantified YFP+ cells, including **C)** tancytes or **D)** parenchymal cells. Data is expressed as box (median and interquartile range) and whisker (min/max values) plots. The mean (plus sign) and individual data points (black points) are also indicated. Mice used: n=6 for either treatment.

Long-term opto-stimulation of hypothalamic ChR2-YFP+ cells did not significantly increase cell survival or differentiation.

We next proceeded to investigate whether opto-stimulation of ChR2-YFP+ cells affected cell survival and differentiation in the hypothalamus. Thus, a long-term opto-stimulation experiment was designed, whereby BrdU was injected daily (50mg/kg) alongside tamoxifen for 5 days prior to opto-stimulation. Tamoxifen-injected NCE-ChR2Y mice were then opto-stimulated for 28 days prior to analysis (Fig. 4.9A). In this experiment, BrdU was used to label post-mitotic cells at the onset of opto-stimulation. BrdU+ quantification was performed as previously described, albeit in additional hypothalamic regions/nuclei; the ependymal layer of the 3rd ventricle (3V), the median eminence (ME), the periventricular nucleus (Pe), the ventromedial nucleus (VMH) and dorsomedial nucleus (DMH). YFP+ cell quantification was performed as described previously.

Upon opto-stimulation, an increasing trend in average BrdU+ cell densities was seen in some hypothalamic regions, most notably along the 3rd ventricle, in the periventricular and arcuate nuclei (Fig. 4.9B, C). However, these differences were not statistically significant (3V; p=0.7, Arc; p=0.4, Pe; p=0.4; two-tailed Mann-Whitney test). When BrdU+ cells in close proximity (within 10 μm) to YFP+ tanycytes were counted (Fig. 4.10A, B), almost a two-fold increase was seen in opto-stimulated brains, although this difference was not statistically significant (p=0.2; Two-tailed Mann-Whitney test).

Quantification and comparison of YFP+ cells indicated an observable increase upon opto-stimulation, albeit lacking statistical significance (two-tailed Mann-Whitney test). Approximately, a two-fold increase in the mean density of YFP+ tanycytes (p=0.2) was seen in opto-stimulated mice compared to control mice (Fig. 4.10C). Similarly, opto-

stimulation induced almost a three-fold increase in the mean density of YFP+ neuronal- (p=0.2) and glial-like (p=0.7) cells, respectively (Fig. 4.10D).

When parenchymal YFP+ cells were assessed for expression of the neuronal marker, NeuN, the majority of neuronal-like YFP+ cells were positive for NeuN (Fig. 4.11A, B). Glial-like YFP+ cells did not express NeuN (Fig. 4.11C). Indeed, quantification of YFP+/NeuN+ and YFP+/NeuN- cells (Fig. 4.11D) indicated a similar magnitude of difference as seen for YPF+ neuronal-like and glial-like cell densities (Fig. 4.10D). However, these differences were not statistically significant (both,YFP+/NeuN- and YFP+/NeuN+; p=0.4, two-tailed Mann-Whitney test).

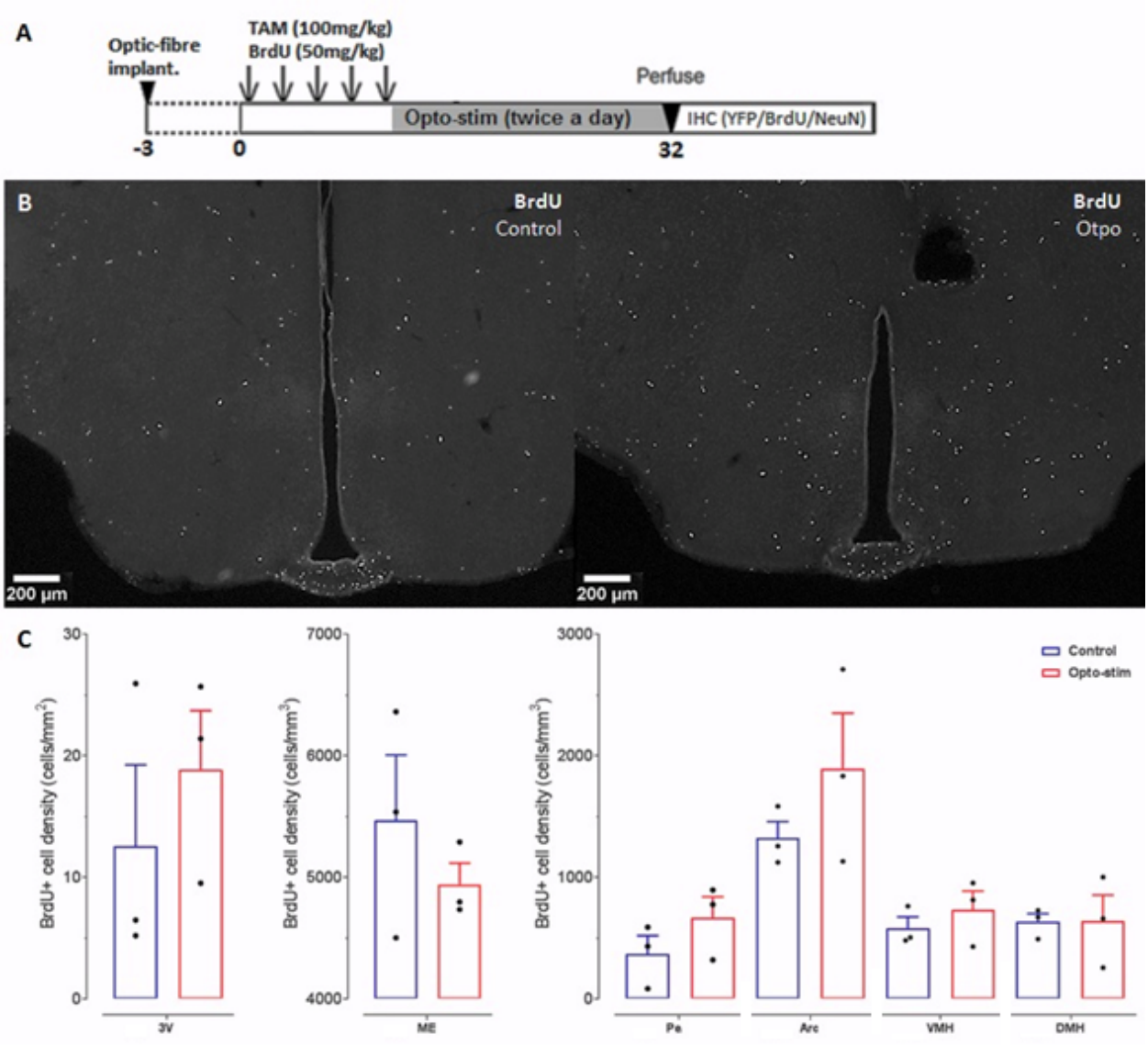

Figure 4.9. Long-term opto-stimulation of hypothalamic ChR2-YFP+ did not significantly increase hypothalamic BrdU+ cell numbers. A) Experimental plan: Following optic fibre-implantation surgery (day -3), NCE-ChR2Y mice were given daily injections of tamoxifen (100mg/kg) and BrdU (50mg/kg) for 5 days (day 0-4; 6 hour interval between tamoxifen and BrdU injections). Mice were then opto-stimulated (twice daily, 4-6 hour interval; day 5-32) for 28 days prior to perfusion-fixation (day 32; 2-4 hours after last optostimulation) and subsequent immunohistochemical analysis. **B)** Representative immunostaining images indicated increased BrdU uptake in opto-stimulated mice. **C)** Mean BrdU+ cell numbers are indicated as histograms (whiskers representing standard error of the mean). Individual data points (black points) are also indicated. Although an increasing trend in BrdU+ cells can be seen in opto-stimulated brains, these differences were not statistically significant in any of the hypothalamic regions analysed (3V; 3rd ventricle ependymal layer, ME; median eminence, Pe; periventricular nucleus, Arc; arcuate nucleus, VMH; ventromedial nucleus, DMH; dorsomedial nucleus). Mice used: n=3 for either treatment.

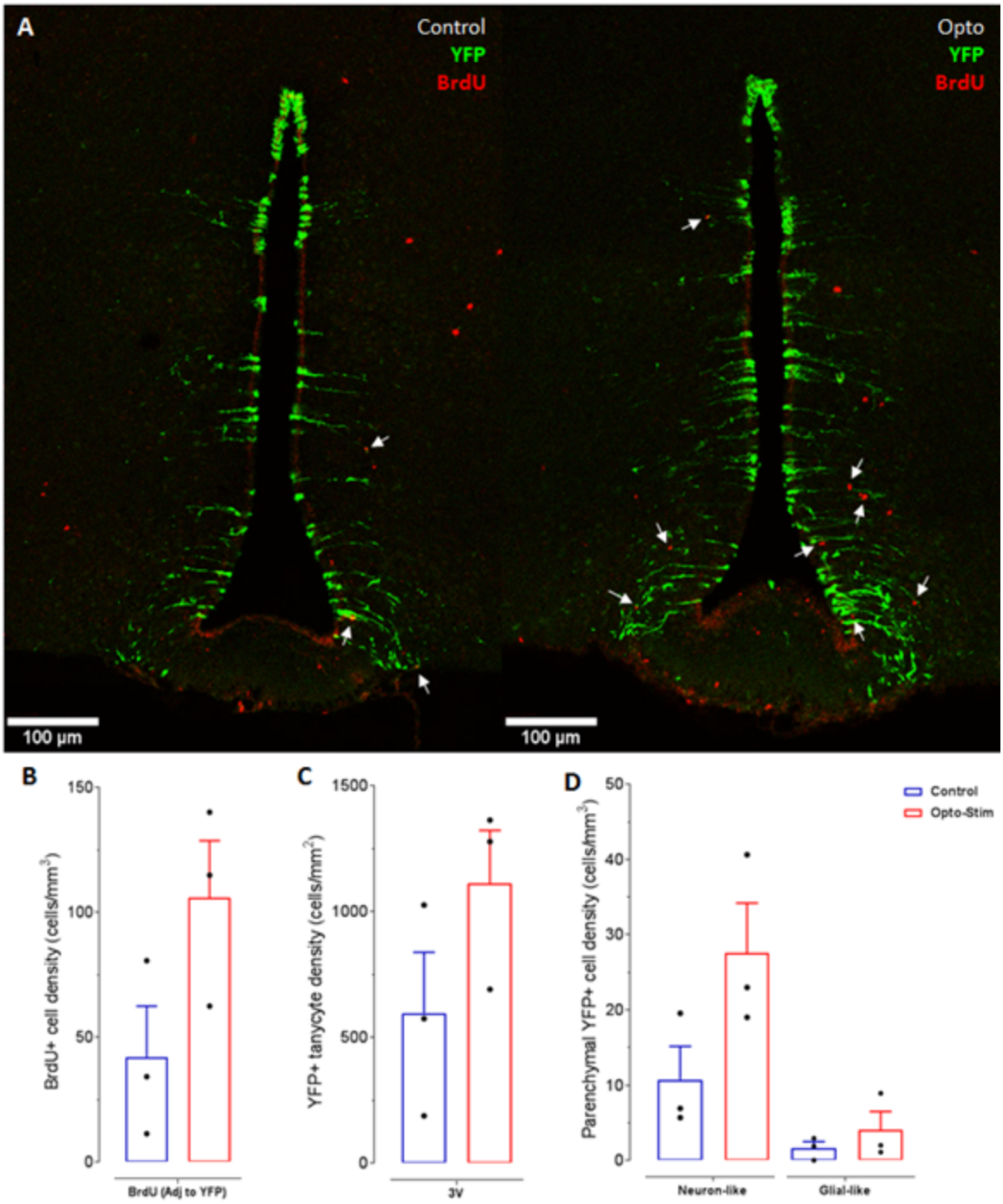

Figure 4.10. Long-term opto-stimulation of hypothalamic ChR2-YFP+ cells did not significantly increase YFP+ cell numbers or BrdU+ cells in close proximity. A) Representative immunofluorescence images indicated increased numbers of YFP+ tancytes (green) and close-proximity BrdU+ cells (white arrows) in optostimulated brains. However, upon quantification and statistical comparison, no significant increase was seen in the number of **B)** BrdU+ cells in close proximity to YFP+ tanycytes, **C)** YFP+ tanycytes or **D)** YFP+ parenchymal cells. Data is expressed as histograms indicating the mean with whiskers representing standard error of the mean. Individual data points (black points) are also indicated. Mice used: n=3 for either treatment.

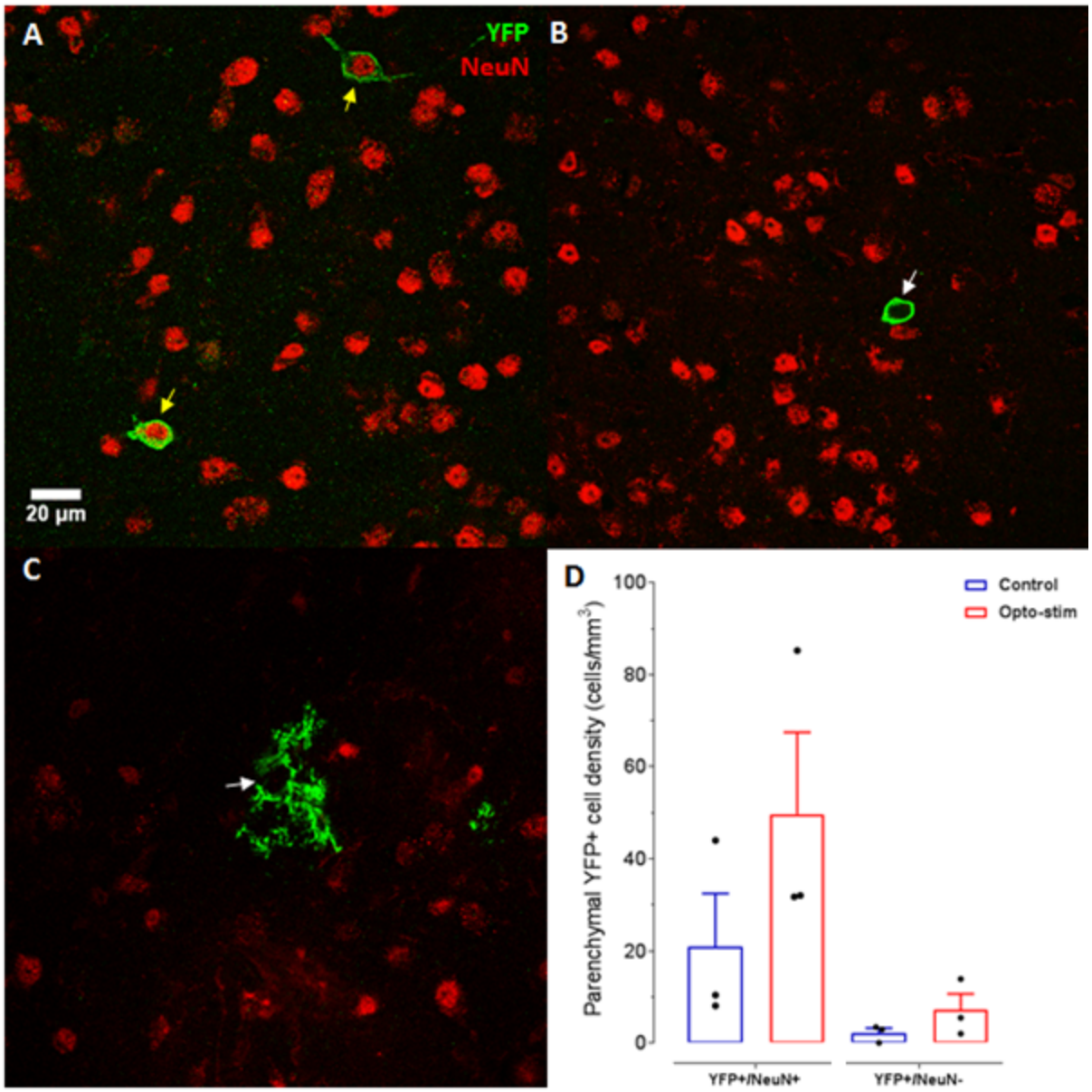

Figure 4.11. Long-term opto-stimulation of hypothalamic ChR2-YFP+ cells did not significantly increase YFP+ neurons or non-neuronal YFP+ cells. Representative immunofluorescence images assessing parenchymal YFP+ cell co-localization with the pan neuronal marker, NeuN. **A)** Whilst the majority of YFP+ cells exhibiting neuronal morphologies co-expressed NeuN, **B)** some did not. **C)** glial-like YFP+ cells did not co-express NeuN. **D)** Quantification of YFP+/NeuN+ double-positive and YFP+/NeuN- cells indicated an increase in both populations in opto-stimulated brains. However, these differences were not statistically significant. Data is expressed as histograms indicating the mean with whiskers representing standard error of the mean. Individual data points (black points) are also indicated. Mice used: n=3 for either treatment.

To summarize the results from this chapter, in brain slices of NCE-ChR2Y mice optic stimulation of ChR2-expressing tanycytes elicited intracellular calcium waves that permeated the tanycyte layer in a similar intensity as 100μM ATP (when applied via the perfusion medium). In addition, opto-stimulation led to heterogeneous intracellular calcium responses in parenchymal cells, which was dependent on their close proximity (within 10μm) of ChR2-expressing tanycytes. Expression of ChR2 in NCE-ChR2Y mice was not restricted to tanycytes, indicating ChR2-expressing cells in the parenchyma as early as 3 days after tamoxifen injection. *In vivo* optogenetic stimulation of ChR2-expressing cells in the hypothalamus for 7 days significantly increased the number of dividing (BrdU+) cells in the close vicinity of ChR2-expressing tanycytes, but did not alter overall hypothalamic cell proliferation. Finally, although long-term *in vivo* optogenetic stimulation (for 28 days) did not significantly increase the survival of (BrdU+) post-mitotic cells, the number of YFP+ tanycytes or YFP+ parenchymal (neuronal and non-neuronal/glial) cells, an increasing trend (in all of the above) was observed, warranting further investigation/replication.

Discussion

Optogenetic stimulation in acute brain slices induced calcium responses in tanycytes reminiscent of those elicited by ATP

In this study, we have demonstrated that (ChR2-expressing) tanycytes can be stimulated optogenetically to elicit reproducible intracellular calcium waves in the tanycyte layer, as previously shown with glucose or ATP [Frayling et al, 2011]. Indeed, since opto-stimulation also led to the propagation of this intracellular calcium signal along the tanycyte layer, including in surrounding tanycytes that did not express ChR2, it can be inferred that optogenetic stimulation also led to the extracellular release of ATP. This interpretation can supported by assessing the effect of opto-stimulation on the calcium response and its propagation in the presence of P2Y1R inhibitors such as MRS2179 or MRS2500 [Frayling et al, 2011; Suyama et al, 2012], since propagation of the calcium response along the tanycyte layer is ATP-dependent [Frayling et al, 2011; Benford et al, 2017].

In order to confirm (and measure) ATP release from ChR2(YFP)+ tanycytes upon optostimulation, a range of imaging methods could be applied [Rajendran et al, 2016]. For example, fluorescent analogs of ATP, such as methylanthraniloyl-ATP could be used to assess vesicular ATP release from ChR2+ tanycytes *in vitro* (i.e. brain slices), as previously done for dopaminergic neurons [Ho et al, 2015]. For *in vivo* imaging, the luciferase-luciferin system has been used commonly as a genetically encoded ATP imaging assay [Manfredi et al, 2002] and has been successfully modified for extracellular ATP measurement [Praetorius & Leipziger, 2009]. However, some fallbacks include the requirement of administering exogenous substrate for detection, low signal (luminescence) yield and lack of absolute quantitation [Rajendran et al, 2016]. More recently, genetically encoded fluorescent protein-based ATP sensors such as ATeams [Imamura et al, 2009; Conely et al, 2017], QUEENs [Yaginuma et al, 2014] and PercevalHT [Berg et al, 2009; Tantama et al, 2013] have since been developed and/or re-engineered to overcome these fallbacks; these sensors primarily utilize fluorescence resonance energy transfer (FRET) to provide ratiometric measurements of changes in ATP levels and do not require addition of any substrate [Rajendran et al, 2016].

ChR2-expressing ependymocytes however, were not seen to respond to optostimulation. This is an unexpected result, as ChR2 stimulation should have allowed for calcium influx and thus a cytosolic change in intracellular calcium. However, it is possible that insufficient calcium influx may have occurred (partly due to the non-selective gating of ChR2 [Lin et al, 2009; Kato et al, 2012]) to trigger the feed-forward loop of purinergic signalling and amplification of the calcium response as seen in tanycytes. Indeed, such minimal changes in intracellular calcium may have either been undetected by Fura-8, or insufficient to classify as a response from the analysis (only ratiometric changes of ≥0.015 were considered a calcium response). To date, studies have only detected P2X7 expression in ependymocytes of the lateral ventricle and spinal cord, and predominantly mediate purinergic signaling via this receptor [Genzen et al, 2009; Gomez-Villafuertes et al, 2015; Marichal et al, 2016], however this has yet to be determined for hypothalamic ependymocytes.

When 100μM ATP was applied to acute brain slices via perfusion, a delayed transient calcium response was observed, whereas when ATP was applied focally (via puffer

pipette) [Frayling et al, 2011], immediate calcium responses were observed. It is considered that the delay in response was due to the time-delay in the delivery of ATP to acute brain slices.

Comparison of calcium responses generated by optogenetic (opto-) stimulation and ATP in tanycytes indicated a similar transient nature, further suggesting that the signalling mechanisms underlying these responses in both treatments are alike. Indeed, opto-stimulation also generated relatively similar (peak) response magnitudes (75% as high in amplitude as) to 100μM ATP. This may suggest that opto-stimulation of ChR2-expressing tanycytes in NCE-ChR2Y mice may induce a similar magnitude of an effect/extracellular ATP release to 100uM ATP. However, it could be argued that the magnitude of opto-stimulated responses may be overestimated due to the following reasons. Firstly, the actual concentration of ATP that triggered calcium responses from our study is not known (but likely less than 100μM) due to dilution when applied into the flow chamber (already containing aCSF). Secondly, it is possible that application of excessive ATP concentrations may generate saturated calcium responses, given that a peak concentration of only ~5μM extracellular ATP was sufficient to trigger responses endogenously (by glucose application) [Frayling et al, 2011]. Thus, it cannot be claimed that optogenetic stimulation can induce comparable calcium responses to 100μM ATP. Thus, in order to accurately estimate the extracellular concentration of ATP released after opto-stimulation, it would be suggested to compare such responses with lower (more physiological) concentrations of ATP (5-10μM). This would give a more accurate measure of the relative potency of opto-generated responses in tanycytes. Indeed, intracellular calcium levels and extracellular ATP levels strongly determine NSC/progenitor behaviour [Glaser et al, 2013]. Thus, it would be essential as to not induce non-physiological levels of calcium influx in tanycytes and potentially induce a different signalling pathway from endogenous activation [Frayling et al, 2011].

Optogenetic stimulation of tanycytes could induce downstream signalling in parenchymal cells

In addition to tanycytes, intracellular calcium responses were also detected in some parenchymal cells of unknown cellular identity (Fig. 4.6). Although ChR2 expression was

absent in these cells, the proximity of these cells to ChR2-expressing tanycytes greatly modulated their capability to respond to opto-stimulation, suggesting that ChR2+ tanycytes may be capable of signalling to parenchymal cells in the close vicinity via ATP release. In support of this theory, another unpublished study indicated that selective optogenetic stimulation of tanycytes with a calcium-permeable channelrhodopsin (CaTCh) induced ATP-dependent depolarization and increased spontaneous synaptic firing of arcuate orexigenic and anorexigenic neurons [Bolborea et al, unpublished data]. Furthermore, several studies have indicated that tanycytes signal to peptidergic neurons in the arcuate nucleus via lactate release [Cortes-Campos et al, 2011; Elizondo-Vega et al, 2016; Uranga et al, 2017; Barahona et al, 2018]. In addition to neurons, tanycytes may also signal to act on parenchymal glia (including astrocytes and oligodendroglia) via purinergic signalling to regulate a host of processes, including glial-neuron communication and/or neurogenesis [Lohr et al, 2014; Rivera et al, 2016; Lecca et al, 2016; Tang & Illes, 2017].

Calcium responses generated by parenchymal cells were heterogeneous, exhibiting different response latencies and durations. These differential response dynamics may be indicative of the heterogeneity in cell-types (both neurons and glia) that tanycytes may potentially signal to. This interpretation (albeit highly speculative) is supported by the variability in the cell soma sizes of responsive parenchymal cells. On the other hand, the distance of these opto-responsive parenchymal cells from the tanycyte layer may also play a contributing factor to the heterogeneity in responses latencies; in some instances, parenchymal cells located at increased distances from the cell bodies of ChR2-expressing tanycytes indicated increasing response latencies. However, due to the lack of quantitative analysis to demonstrate this relationship and the lack of any cell-type (morphological or gene-expression) characterization of these parenchymal cells, the factors underlying their heterogeneity in calcium responses and their cellular identity cannot be determined from the results of this study.

The possibility that the blue light may have had a direct (aberrant) effect on these ChR2Y-negative parenchymal cells is unlikely since in control brain slices (in which no tamoxifen was injected and ChR2 expressed) no intracellular calcium changes were seen (data not shown).

Tanycytes represent the majority of opto-responsive hypothalamic cells, albeit non-specific ChR2 expression

Upon, inducible cre-recombination, ChR2 expression (represented by YFP visualization) was seen in tanycytes of the lateral 3rd ventricle walls, indicating successful ChR2 expression in subpopulations of all tanycyte sub-types (α1, α2 and β1) except β2 tanycytes. However, YFP expression was not exclusively restricted to tanycytes, with additional positive cells being identified in the parenchyma (resembling neurons and glia) as early as 3 days after inducible cre-recombination. As with NCE-YFP mice, Cre-recombinase expression was driven under the control of the nestin promoter. In addition to tanycytes [Rodriguez et al, 2005; Lee et al, 2012; Haan et al, 2013], nestin-expression (transient or sustained) has been reported in a range of cell-types, including ependymocytes [Chouaf-Lakdar et al, 2003; Hendrickson et al, 2011], some neurons [Hendrickson et al, 2011] and more debatably, in oligodendrocytes (and/or their progenitors), microglia and (reactive) astrocytes [Clarke et al, 1994; Takamori et al, 2009; Walker et al, 2010; Hendrickson et al, 2011; Elmore et al, 2014]. Thus, it is possible that upon inducible cre-recombination, in addition to tanycytes, these cells may have attained ChR2 expression and potentially have had an effect on neurogenesis upon optogenetic stimulation. Indeed, due to leaky cre-expression and/or activity, non-nestin-expressing cells have been seen in NCE-YFP (without tamoxifen). Therefore, leakiness in Cre-activity prior to tamoxifen-induced recombination may have potentially caused additional hypothalamic cells to express ChR2, although this is likely minimal (based on our observations of very few YFP+ cells in NCE-YFP mice that were not injected with tamoxifen).

Although the effects of optogenetic stimulation might not be solely attributed to ChR2+ tanycyte stimulation, the vast majority (98.2%) of light-responsive ChR2-YFP+ cells (excluding ependymocytes) were seen to be tanycytes; an average of 3162±248 YFP+ tanycytes (per mm^2) were estimated along the surface area of the 3rd ventricle in comparison to 21±7 neuronal-like and 11±2 glial-like YFP+ cells (per mm^3) of the hypothalamic parenchyma 7 days after tamoxifen injection (n=6; Fig. 4.8C, D). Ependymocytes were excluded from this calculation since they were not seen to elicit clear responses (if any) to opto-stimulation in acute brain slices. Since the ChR2+

tanycyte population represents an overwhelming proportion to ChR2+ parenchymal cells, it could be speculated/argued that the effects seen upon *in vivo* optogenetic stimulation could have been mostly a result of tanycyte stimulation.

Short-term in vivo optogenetic stimulation of nestin-expressing hypothalamic cells

Opto-stimulation of nestin+ cells in the hypothalamus for 7 days did not significantly change the overall number of BrdU+ cells, nor the number of YFP+ cells (tanycytes or parenchymal). This may suggest that short-term opto-stimulation and consequently, short-term purinergic signalling was not sufficient to induce any apparent change in hypothalamic cell proliferation overall. However, a significant increase in BrdU+ cells in the close vicinity of YFP+ tanycytes (and/or their basal processes) was seen in opto-stimulated brains. The contradicting observations of no overall change in BrdU+ cells but an increase in BrdU+ cells near YFP+ tanycytes may be explained by 2 possibilities that are not mutually exclusive. Firstly, opto-stimulation may have induced a spatial redistribution of BrdU+ cells within the hypothalamus, which may be suggestive of an effect on newborn (BrdU+) cell migration. Secondly, this increase in BrdU+ cells may simply represent an increase in cell proliferation (and survival during the 7-day period). However, it should be noted that the increase in BrdU+ cells near YFP+ tanycytes in opto-stimulated brains (~50 cells/mm^3, Fig. 4.8B) was comparatively miniscule to the total number of BrdU+ cells quantified in the whole hypothalamus (~1250-1300 cells/mm^3, Fig. 4.7C, HYPO histogram). Thus, it could be argued that this small (yet clear) effect may have been shadowed by collective quantification and comparison of all BrdU+ cells in the whole hypothalamus.

ATP release and purinergic signalling have been shown to regulate neural stem/progenitor cell proliferation, migration and survival by a multitude of studies [reviewed in Lecca et al, 2016 & Tang & Illes, 2017]. ATP has particularly been seen to act on P2Y1 receptors to induce cell proliferation and migration in neural stem/progenitor cell populations [Weissman et al, 2004; Suyama et al, 2012; Santiago & Scemes, 2012; Cao et al, 2013; Boccazzi et al, 2014]. In the case that the increase in BrdU+ cells near YFP+ tanycytes may have been predominantly due to increased cell proliferation (and survival), the cell-type from which these newborn cells arose from is not known, but

several candidate progenitor populations can be proposed. Firstly, the expression of P2Y1 receptors in tanycytes might imply their opto-induced proliferation and migration of newborn cells along YFP+ tanycytes, in a similar fashion seen by radial glia during cortical development [Weissman et al, 2004; Ulrich et al, 2012]. Given that these BrdU+ cells were not YFP+, it can be inferred that they may not be the progeny of YFP+ tanycytes, but potentially of YFP-negative tanycytes. However, this is unlikely as no change in BrdU+ tanycytes (at the 3rd ventricle) was seen. Alternatively, the source of these BrdU+ cells could arise from subependymal astrocytes, which have been previously suggested to represent a potential subpopulation of hypothalamic neural stem/progenitor cells [Perez-Martin et al, 2010; Rojczyk-Gołębiewska et al, 2014], although their expression profile of purinergic (P2Y1) receptors has yet to be investigated. Finally, opto-stimulation may have resulted in the purinergic activation of parenchymal progenitor populations such as NG2+ oligodendrocyte precursor cells (OPCs), which also express P2Y1 receptors and have previously shown to exhibit modest neurogenic potential under basal conditions [Agresti et al, 2005; Robins et al, 2013b].

On the other hand, if the increase in BrdU+ cells near YFP+ tanycytes was more due to a spatial redistribution of (and not necessarily an increase in) hypothalamic BrdU+ cells, this might be explained by the recruitment of reactive cells (such as astrocytes and/or OPCs). Such cells are recruited along increasing gradients of extracellular ATP concentrations in response to neuroinflammatory/ischaemic conditions [Di Virgilio et al, 2009; Feng et al, 2015, Ulrich et al, 2012]. Indeed, it could be speculated that opto-stimulation of ChR2(YFP)+ tanycytes in particular could have potentially led to the excessive release of ATP, and recruitment of such reactive cells to mediate/regulate neurogenesis [Robel et al, 2011; Ulrich et al, 2012; Lecca et al, 2016]. The effect of opto-stimulation on OPC/astrocyte recruitment could be confirmed by assessing for co-localization of BrdU with oligodendrocytic (NG2) and astrocytic (S100b) markers. An increase in the proportion of double-labelled cells would reflective this.

Of note, BrdU+ cells in close proximity to YFP+ tanycytes were not quantified in specific hypothalamic regions/nuclei (but just as a density within the hypothalamic parenchyma). Given the possibility that optogenetic stimulation may induce recruitment and/or proliferation of reactive cells such as subependymal astrocytes and/or OPCs, it would be

interesting to assess any change in these BrdU+ cell (near-YFP+-tanycytes) numbers in particular hypothalamic regions such as the subependymal layer, the periventricular area and parenchymal nuclei between opto-stimulated and control mice. Similarly, (all) BrdU+ cells could be quantified in specific (arcuate, ventromedial, dorsomedial, lateral) hypothalamic nuclei in order to provide a higher-resolution analysis of the effect of short-term opto-stimulation on parenchymal cell proliferation. In conjunction with co-localization analysis of OPC and astroglial markers (NG2 and GFAP, respectively), the source of these BrdU+ cells could be further determined. To conclude, optogenetic stimulation of ChR2+ cells may have increased parenchymal cell proliferation and/or migration near tanycytes, although the identity of these cells has yet to be determined.

Long-term in vivo optogenetic stimulation of nestin-expressing hypothalamic cells

Due to a small sample size (n=3 mice per treatment), the observations made from long-term opto-stimulation experiments can only be considered as preliminary and speculative. Understandably, as data variance was high for the small sample size, any differences observed could not be reliably assessed for statistical significance. Nevertheless, visual and quantitative analysis indicated noteworthy differences in BrdU+ and YFP+ cells between opto-stimulated and control (non-stimulated) mice.

A trend of increase in BrdU+ cells was seen at the 3rd ventricle ependymal layer, the periventricular and arcuate nuclei, suggesting a potential increase in cell survival and/or proliferation in these regions. Concurrently, a two-fold increase in YFP+ tanycytes numbers in opto-stimulated brains may also reflect increased longevity and/or proliferation of these cells during the 4 weeks. Indeed, BrdU was administered prior to opto-stimulation, thus labelling post-mitotic cells at the onset of opto-stimulation. However, whilst BrdU+ numbers may reflect an increase in cell survival, further proliferation of these cells could also result in an increase in BrdU+ cell numbers. Therefore, it cannot be specified whether an increase in BrdU+ cells, if any, was due to increased cell proliferation or survival of BrdU-labelled cells. The identity of these BrdU+ cells has yet to be elucidated. Furthermore, it has yet to be determined if the increase in parenchymal BrdU+ cell proliferation/survival was also accompanied by increased differentiation into neuronal or glial cell fates.

As with short-term opto-stimulation, the number of BrdU+ cells which were close to YFP+ tanycytes increased. Whilst the reason(s) underlying this increase is not known (whether it is due to increased cell proliferation, survival and/or migration, or whether, the increase in YFP+ tanycytes may simply increase the probability for BrdU+ cells to be located nearby), it suggests that opto-stimulation of ChR2+ tanycytes may be responsible for the observed effect. Thus, the (optogenetic) induction of purinergic signalling (ATP release) in tanycytes to induce an increase in cell proliferation, survival and/or migration is indicative of a potential role tanycytes may play in neurogenesis.

Cross-comparison of BrdU+ cells (in close proximity to YFP+ cells) between short- and long-term opto-stimulation experiments would have given further indication as to whether an increase in cell proliferation and/or survival is seen over time. However comparisons between these experiments cannot be made due to differences in BrdU administration concentrations, timing (before or during opto-stimulation) and durations; in short-term experiments, double the BrdU concentration (100mg/kg) was applied for 7 days, in comparison to long-term (50mg/kg for 5 days). Thus, for instance, although it may appear that fewer BrdU+ cells near YFP+ tanycytes were seen in the long-term (compared to short-term) opto-stimulated brains (Fig. 4.9C, Fig. 4.10B), this may not be the case.

The increases in YFP+ neurons and non-neuronal (likely a heterogeneous population of glia and migrating neuroblasts) cells upon opto-stimulation may potentially reflect tanycytes' reported involvement in neurogenesis (and gliogenesis), whereby tanycytes and/or their progeny were suggested to migrate and differentiate into neurons and astroglia [Lee et al, 2012; Haan et al, 2013; Robins et al, 2013a]. Although it has been argued that tanycytes represent the vast majority of light-responsive ChR2+ cells in the hypothalamus, the possibility that the increase in YFP+ parenchymal cells may have been in part due to opto-stimulation of other ChR2+ cell-populations cannot be ignored. Indeed, parenchymal NG2+ OPCs have previously been identified with nestin expression [Walker et al, 2010] and reported to retain modest neuro- and gliogenic capacity in the hypothalamus [Robins et al, 2013b], potentially mediated by purinergic signalling [Agresti et al, 2005; Lecca et al, 2016], although no nestin+ parenchymal YFP+ cells were identified in NCE-YFP mice (Chapter 2) Since subependymal cells have been reported to express nestin [Holmin, 1997], hypothalamic subependymal astrocytes (another potential

neural stem/progenitor population), may have also expressed ChR2-YFP+ and thus, their contribution to YFP+ neurons and/or glia cannot be overlooked. Finally, studies have shown that optogenetic stimulation of neuronal activity can modulate/induce neurogenic activity in different brain/neurogenic regions [Paez-Gonzalez P, 2014; Song et al, 2012; 2013; 2017]. This raises a similar possibility with optogenetic stimulation of (the few) ChR2+ neurons in the hypothalamus. Further work needs to be performed to test whether selective opto-stimulation of tanycytes and of these separate parenchymal cell populations could independently affect cell proliferation and neurogenesis.

Summary

An optogenetic approach was used to investigate the mechanistic link between tanycytes' chemosensory and neurogenic roles by assessing the effect of tanycyte stimulation on adult hypothalamic neurogenesis; ChR2 was used to induce intracellular calcium responses as seen upon endogenous tanycyte stimulation. Using calcium imaging on brain slices *in vitro,* we demonstrated that ChR2-expressing tanycytes could elicit robust calcium responses and interestingly, signal to proximal parenchymal cells, presumably via ATP release. Whilst short-term opto-stimulation of cells under the transgenic nestin promoter (predominantly tanycytes) was able to induce cell proliferation/survival/migration, we found a trend that long-term opto-stimulation was able to induce an increase in labelled neurons and glia derived from putative hypothalamic neural stem/progenitor cells. Thus hypothalamic neurogenesis may potentially be stimulated by optically inducing calcium signalling.

General summary of discussion

Given that the results obtained in this project have been thoroughly discussed in their respective chapters, this section will focus on the potential impact of this project's findings on our current understanding of adult hypothalamic neurogenesis, the major methodological caveats of our experiments and future studies that can address these issues and build on our findings further.

Regulation of adult hypothalamic neurogenesis by extrinsic stimuli

In this project, we first investigated the effect of three external factors (physical exercise, fluoxetine and acesulfame-K; Ace-K) on hypothalamic cell proliferation and survival with the intention of identifying/elucidating potential (external) regulatory factors of adult hypothalamic neurogenesis. Our results indicated no change in hypothalamic cell proliferation and/or survival upon short/mid-term exposure (2-3 weeks) to physical exercise or fluoxetine. In the case of Ace-K exposure (2 weeks), some mixed effects on cell proliferation and/or survival were seen (decrease in the DMH, increase in the VMH), although these changes were relatively miniscule. Thus, our data suggests that short/mid-term exposure to these extrinsic factors may not induce a substantial change in cell proliferation, which in turn may not be sufficient to alter neurogenesis levels.

The levels of basal cell proliferation and neurogenesis in the hypothalamus has been noted to be lower than that of the canonical neurogenic niches for the hippocampus (SGZ) and the olfactory bulb (SVZ) [Kokoeva et al, 2007; Lee & Blackshaw, 2012; Robins et al, 2013a]. This may indicate the level to which these regions exhibit constitutive plasticity and require modification of the neuronal circuitry underlying their respective physiological functions. Indeed, it has been previously suggested that neurogenesis in the hippocampus and olfactory bulb may serve as an adaptive mechanism for discriminating between similar or ambiguous stimuli to allow for dynamic refinement of the contextual and perceptual (olfactory) memory to these stimuli in a complex environment [Sahay et al, 2011; Migaud et al, 2016]. Thus, it is understandable that a high rate of neurogenesis and neuronal turnover is required to fulfil this demand. However, the hypothalamus, being a major regulatory centre for several (basic yet crucial) homeostatic functions may not require such constant and dynamic refinement/modification of the neuronal networks

regulating these processes. Instead it would be more plausible that these neuronal networks, for example of feeding, are established prenatally [Bouret & Simerly, 2006; Padilla et al, 2010] and mostly modified/adjusted during postnatal periods, during which, high levels of neurogenesis and turnover are seen [Lee et al, 2012; McNay et al, 2012; Haan et al, 2013]. Adult neurogenesis may thus serve to gradually/slowly refine these neuronal networks upon long-term changes in the environment. This may explain why some studies, using long exposure periods, were able to see an increase in cell proliferation in response to physical exercise and fluoxetine [Sachs & Caron, 2014, Niwa et al, 2015].

In contrast to our results however, other reports have been published indicating that the adult hypothalamus is malleable enough to exhibit short-term changes in cell proliferation upon exposure to several different external stimuli, including physical exercise, dietary changes (to HFD) and heat exposure [Matsuzaki et al, 2009; Li et al, 2013a; Borg et al, 2014; Gouaze et al, 2013]. Indeed, an absence of an observed effect in our study might reflect an ineffective BrdU-labelling methodology. Whilst a single pulse of BrdU delivered peripherally has proven sufficient for detecting and assessing cell proliferation in the canonical neurogenic niches, the use of this method in the hypothalamus appears to have some limitations. Peripheral and central BrdU delivery methods have shown to differentially label proliferative cells in the hypothalamus, reflecting a potential variability in BrdU permeability throughout the hypothalamus [Kokoeva et al, 2007; Cifuentes et al, 2011; Lee et al, 2012; Sousa-Ferreira et al, 2014a]. Thus, it is possible that in our studies, a single peripheral pulse of BrdU may have proven insufficient to label a high number of proliferative cells to detect a change in cell proliferation. It would be suggested to use multiple peripheral (intraperitoneal) and central (intracerebroventricular) injections in future studies to label parenchymal and ventricular proliferative cells more effectively.

In relation to the concern of insufficient BrdU-labelling with a single BrdU-pulse, this also raises the possibility of high variance in the number of BrdU+ cells in the respective nuclei/regions between mice (of the same experimental treatment). Indeed, one way to assess for the extent of variance would be to separately quantify and assess the variance in BrdU+ cell numbers between left and right brain hemispheres.

Increased cell proliferation induced upon short-term exposure however, may not necessarily reflect increased neurogenesis; some of these studies indicated no significant change in adult-born (BrdU+/NeuN+) neurons generated immediately after short-term (6-13 days) exposure to physical exercise or heat [Matsuzaki et al, 2009; Li et al, 2013a]. Similarly, upon short/mid-term exposure to HFD (15-21 days), an initial/transient increase in cell proliferation was seen (after 3 days), but there was no increase in neuronal fate rate (BrdU+/NeuN+ cell number) [Gouaze et al, 2013]. Interestingly, the cell-types that were seen to proliferate upon HFD onset were of astroglial (GFAP+) and microglial (Iba-1+) lineage. Indeed, it was suggested that amplification of these cell-types was required for the shift in the maturation/specification of newborn neurons to anorectic POMC neurons as an adaptive mechanism to regulate food/energy intake upon the onset of HFD [Gouaze et al, 2013].

On the other hand, prolonged exposure to these external stimuli has indeed demonstrated a regulatory effect on hypothalamic neurogenesis. Heat and physical activity, both increased the number of adult-born (BrdU+/Neun+) neurons after 33-53 days of exposure [Matsuzaki et al, 2009; Li et al, 2013a], whilst HFD induced a divalent effect: increasing the number of adult-born (BrdU+/Hu+) neurons in the median eminence (of female mice), whilst decreasing these numbers in arcuate nucleus (of both sexes) after 33 days of exposure [Lee et al, 2014]. Interestingly, some studies did not see any change in adult-born neurons even after exposure to external stimuli such as physical activity (for 33 days) or fluoxetine (for 28 days) [Borg et al, 2014; Sachs & Caron, 2014], potentially suggesting that longer periods of exposure/treatment may be required to reliably increase the number and/or survival of adult-born neurons. Thus, it seems that short-term exposure to external stimuli may induce changes in the maturation and integration of newborn neurons to adapt to these external/environmental changes and that increased generation and/or survival of these newborn neurons may require longer exposure.

Genetic labelling of putative hypothalamic neural stem/progenitor cells

We used an inducible genetic labelling approach (Nestin-CreER:Rosa-lox-STOP-lox-YFP) that has been used previously to study the canonical neurogenic niches [Carlen et al, 2006; Lagace et al, 2007; Burns et al, 2007; Imayoshi et al, 2006; Chen et al, 2009;

Giachino & Taylor, 2009] to identify and characterize adult neural stem/progenitor cells in the hypothalamus. Whilst tanycytes and ependymocytes were predominantly labelled, other reporter-positive cells were also seen in the parenchyma shortly after induced-recombination, reinforcing the notion that several putative neural stem/progenitor cell populations may exist in the hypothalamus [Li et al, 2012; Lee & Blackshaw, 2012; Sousa-Ferreira et al, 2014a]. Indeed, temporal analysis indicated an increasing trend in reporter-labelled cells in the parenchyma, supporting previous literature reporting the migration of neural progenitors into the hypothalamic parenchyma [Xu et al, 2005; Haan et al, 2013; Robins et al, 2013a]. However, potential amplification of labelled parenchymal neural stem/progenitor cells cannot be ruled out.

However, it remains to be determined what cell-types may comprise these parenchymal reporter-labelled cells following induced-recombination. To that effect, it has yet to be clearly demonstrated if this genetic labelling approach exclusively labels for hypothalamic neural progenitor cells. Thus, further phenotypic analysis (co-expression studies) would help to elucidate the identity of these labelled cells and their potential as neural progenitors. In the case that the labelled parenchymal cells may represent neural stem cells and/or progenitors, such as NG2+ glia [Robins et al, 2013b] or Dcx+ neuroblasts [Batailler et al, 2014], this model may be of further use in allowing the investigation of the effects of external factors and genetic manipulation (deletion) on hypothalamic neural stem/progenitor cell behaviour (migration, proliferation, self-renewal and cell fate), as recently reported in a similar mouse model (Nestin-CreERT2;CAG-tdTomato) [Chaker et al, 2016]. Given that hypothalamic neural stem/progenitor cells may likely constitute a heterogeneous population, it would also be interesting to assess if there is a difference in effects seen between those labelled under the control of other regulatory (promoter) sequences of generic neural stem/progenitor genes, such as Sox-2.

Optogenetic stimulation of putative hypothalamic neural stem/progenitor cells

We used a similar genetically inducible mouse model (Nestin-CreER:Rosa-lox-STOP-lox-ChR2-YFP) with the aim to induce expression of channelrhodopsin in tanycytes and investigate the effect of their optogenetic stimulation on hypothalamic neurogenesis. However, as with the previous mouse model, given that the Nestin-CreER driver construct

did not label tanycytes exclusively, the effects observed cannot be unequivocally attributed to tanycyte stimulation, especially if parenchymal cells expressing ChR2 may be neural stem/progenitor cells. Upon short-term optogenetic stimulation, we observed an increase in cell proliferation in the close vicinity of ChR2-expressing tanycytes, potentially suggesting that tanycytes may regulate parenchymal progenitor cell proliferation or migration. Interestingly, long-term stimulation indicated an increasing trend in YFP-labelled tanycytes and parenchymal (neuron-like and glia-like) cells, potentially indicative of increased tanycyte proliferation and neurogenesis. These results may thus support the notion above that long-term and not short-term stimulation (by changes in the external environment/stimuli) may upregulate neurogenesis.

Although these results are not conclusive, our results provide interesting preliminary data for future investigation and corroboration. It would be of particular interest to assess whether selective optogenetic stimulation of tanycytes could indeed reiterate our results and induce increased cell proliferation and neurogenesis. Other studies have reported the development and use of Cre-driver mice under the expression of radial glia-specific promoters, such as FGF10 or Rax, that confer substantial specificity to tanycytes [Hajohosseini et al, 2008; Haan et al, 2013; Miranda-Angulo et al, 2014; Pak et al, 2014]. Accordingly, promoter sequences of these, or other tanycyte-specific genes such as Raldh1 [Shearer et al, 2012; Stoney et al, 2016], could be used to drive CreER-expression. Following from this, similar optogenetic experiments could be carried out to address whether β-tanycytes or α-tanycytes may differentially contribute towards adult neurogenesis using CreER driver lines to label the respective subpopulations. Whilst FGF10-CreER has proven specific for β-tanycytes [Haan et al, 2013], Raldh1 may present a more suitable candidate to specify Cre-expression in α-tanycytes [Shearer et al, 2012]. Indeed, whilst optogenetic stimulation with ChR2 was shown to induce modest calcium responses in tanycytes from our *in vitro* validation experiments, a more robust calcium response could potentially be elicited by the use of a more calcium-permeable channelrhodopsin variant, such as CatCh [Kleinlogel et al, 2011]. Finally, it would be of great interest in further investigating the functional consequences of tanycyte-mediated neurogenesis on hypothalamic functions in addition to feeding and energy metabolism [Lee et al, 2012; Haan et al, 2013; Goodman & Hajihosseini, 2015] through behavioural

studies. Thus, it may also be of use to consider other less invasive strategies, such as chemogenetic approaches that make use of designer receptors exclusively activated by designer drugs (DREADDs), to stimulate tanycytes for long and sustained periods of time [Roth, 2016; Smith et al, 2016].

We rationalized using an optogenetic strategy for tanycyte stimulation based on the notion that neurogenic induction may comprise of a common mechanism to tanycyte chemosensation; optogenetic stimulation may elicit intracellular calcium waves/signalling similarly to that elicited by purinergic stimulation of P2Y1 receptors upon chemosensation of ATP and other nutritional signals [Frayling et al, 2011; Benford et al, 2017]. Indeed, whilst purinergic signalling has been implicated in progenitor cell proliferation in neurogenic niches such as the SGZ and SVZ [Gampe et al, 2015], it is not clear if optogenetic stimulation may have induced neurogenesis via purinergic signalling in our experiments. Thus, it would be of interest in assessing whether tanycyte (and the collectively, hypothalamic neural stem/progenitor cell) proliferation and hypothalamic neurogenesis might be regulated by purinergic signalling through gene silencing (shRNA mediated RNA interference of P2Y1 receptors to inhibit purinergic signalling) or gene deletion (of NTDPase 2 to induce overstimulation of purinergic signalling) studies.

Concluding remarks

In this thesis, I first identified acesulfame-K as a novel external factor regulating the number of newly-generated cells in the adult hypothalamus, which may potentially affect neurogenesis in the long-term. Second, I developed and characterized a mouse model (NCE-YFP) predominantly labeling ependymal cells of the 3rd ventricle, including tanycytes. This model may serve useful in visualizing the effect of external factors/stimuli or genetic manipulation on putative hypothalamic neural stem/progenitor cell behaviour. Finally, based on the NCE-YFP mouse model, I have generated a optogenetic mouse model (NCE-ChR2Y) and successfully validated its application to stimulate tanycytes. Furthermore, I provided preliminary evidence to suggest that optogenetic stimulation of putative hypothalamic neural stem cells and/or progenitors can modulate adult neurogenesis. This novel optogenetic strategy may prove useful in future studies aiming to elucidate the differential contribution of distinct neural progenitor populations to adult hypothalamic neurogenesis and the functional/behavioural consequences of their manipulation. To conclude, our findings suggest that adult hypothalamic neurogenesis is regulated slowly, on a long-term basis to reliably adapt to fluctuating stimuli in the external environment.

References

Agresti C, Meomartini ME, Amadio S, Ambrosini E, Volonté C, Aloisi F, Visentin S. (2005). ATP regulates oligodendrocyte progenitor migration, proliferation, and differentiation: involvement of metabotropic P2 receptors. Brain Res. Rev. 48, 157-165.

Ahlfeld J, Filser S, Schmidt F, Wefers AK, Merk DJ, Glaß R, Herms J, Schüller U. (2017). Neurogenesis from Sox2 expressing cells in the adult cerebellar cortex. Sci Rep. 7, 6137.

Allen Institute Brain Atlas. [ONLINE] Available at: http://mouse.brain-map.org/static/atlas [Accessed: 03 July 2017].

Almazán G, Vela JM, Molina-Holgado E, Guaza C. (2001). Re-evaluation of nestin as a marker of oligodendrocyte lineage cells. Microsc. Res. Tech. 52, 753-765.

Altman J, Das GD. (1965). Autoradiographic and histological evidence of postnatal hippocampal neurogenesis in rats. J. Comp. Neurol. 124, 319–335.

Altman J, Das GD. (1966). Autoradiographic and histological studies of postnatal neurogenesis. I. A longitudinal investigation of the kinetics, migration and transformation of cells incorporating tritiated thymidine in neonate rats, with special reference to postnatal neurogenesis in some brain regions. J Comp Neurol. 126, 337-89

Altman J. (1969). Autoradiographic and histological studies of postnatal neurogenesis. IV. Cell proliferation and migration in the anterior forebrain, with special reference to persisting neurogenesis in the olfactory bulb. J. Comp. Neurol. 137, 433–457.

Altman J, Bayer SA. (1986). The development of the rat hypothalamus. Adv Anat Embryol Cell Biol. 100, 1–173.

Alvarez-Buylla A, García-Verdugo JM, Tramontin AD. (2001). A unified hypothesis on the lineage of neural stem cells. Nat. Rev. Neurosci. 2, 287–293.

Alvarez-Buylla A, Garcia-Verdugo JM. (2002). Neurogenesis in adult subventricular zone. J. Neurosci. 22, 629-634.

Alvarez-Buylla A, Lim DA. (2004). For the long run: Maintaining germinal niches in the adult brain. Neuron. 41, 683–686.

Alvarez-Buylla A, Nottebohm F. (1988). Migration of young neurons in adult avian brain. Nature. 335, 353–354.

Alvarez-Buylla A, Seri B, Doetsch F. (2002). Identification of neural stem cells in the adult vertebrate brain. Brain Res. Bull. 57, 751–758.

Anderson CM, Swanson RA, (2000). Astrocyte glutamate transport: Review of properties, regulation, and physiological functions. Glia. 32, 1–14.

Anthony TE, Heintz N. (2008). Genetic lineage tracing defines distinct neurogenic and gliogenic stages of ventral telencephalic radial glial development. Neural Dev. 3, 30.

Arellano JI, Harding B, Thomas JL. (2018). Adult Human Hippocampus: No New Neurons in Sight. Cereb Cortex. 28, 2479-2481.

Askew K, Li K, Olmos-Alonso A, Garcia-Moreno F, Liang Y, Richardson P, Tipton T, Chapman MA, Riecken K, Beccari S, Sierra A, Molnár Z, Cragg MS, Garaschuk O, Perry VH, Gomez-Nicola

D. (2017). Coupled Proliferation and Apoptosis Maintain the Rapid Turnover of Microglia in the Adult Brain. Cell Rep. 18, 391-405.

Bachman J. (2013). Immunohistochemistry on freely floating fixed tissue sections. Methods Enzymol. 533, 207-15.

Bachmanov AA, Reed DR, Beauchamp GK, Tordoff MG. (2002). Food intake, water intake, and drinking spout side preference of 28 mouse strains. Behav Genet. 32, 435-43.

Bakos J, Zatkova M, Bacova Z, Ostatnikova D. (2016). The Role of Hypothalamic Neuropeptides in Neurogenesis and Neuritogenesis. Neural Plast. 2016, 3276383.

Balland E, Dam J, Langlet F, Caron E, Steculorum S, Messina A, Rasika S, Falluel-Morel A, Anouar Y, Dehouck B, Trinquet E, Jockers R, Bouret SG, Prévot V. (2014). Hypothalamic tanycytes are an ERK-gated conduit for leptin into the brain. Cell Metab. 19, 293–301.

Bao AM, Swaab DF. (2018). The art of matching brain tissue from patients and controls for postmortem research. Handb Clin Neurol. 150, 197-217.

Barahona MJ, Llanos P, Recabal A, Escobar-Acuña K, Elizondo-Vega R, Salgado M, Ordenes P, Uribe E, Sepúlveda FJ, Araneda RC, García-Robles MA. (2018). Glial hypothalamic inhibition of GLUT2 expression alters satiety, impacting eating behavior. Glia. 66, 592-605.

Barden N. (2004). Implication of the hypothalamic-pituitary-adrenal axis in the physiopathology of depression. J. Psychiatry Neurosci. 29, 185-193.

Barkho BZ, Munoz AE, Li X, Li L, Cunningham LA, Zhao X. (2008). Endogenous matrix metalloproteinase (MMP)-3 and MMP-9 promote the differentiation and migration of adult neural progenitor cells in response to chemokines. Stem Cells. 26, 3139–3149.

Barrack DS, Thul R, Owen MR. (2015). Modelling cell cycle synchronisation in networks of coupled radial glial cells. J. Theor. Biol. 377, 85-97.

Barres BA, Raff MC. (1993). Proliferation of oligodendrocyte precursor cells depends on electrical activity in axons. Nature. 361, 258-60.

Batailler M, Droguerre M, Baroncini M, Fontaine C, Prevot V, Migaud M. (2014). DCX-expressing cells in the vicinity of the hypothalamic neurogenic niche: A comparative study between mouse, sheep, and human tissues. J. Comp. Neurol. 522, 1966–1985.

Batailler M, Derouet L, Butruille L, Migaud M. (2015). Sensitivity to the photoperiod and potential migratory features of neuroblasts in the adult sheep hypothalamus. Brain Struct. Funct. 221, 3301–3314.

Bauer S, Patterson PH. (2005). The cell cycle-apoptosis connection revisited in the adult brain. J. Cell Biol. 171, 641–650.

Bedard A, Cossette M, Lévesque M, Parent A. (2002). Proliferating cells can differentiate into neurons in the striatum of normal adult monkey. Neurosci. Lett. 328, 213–216.

Belluardo N, Wu G, Mudo G, Hansson AC, Pettersson R, Fuxe K. (1997). Comparative localization of fibroblast growth factor receptor-1, -2, and -3 mRNAs in the rat brain: In situ hybridization analysis. J. Comp. Neurol. 379, 226–246.

Belluzzi O, Benedusi M, Ackman J, LoTurco JJ. (2003). Electrophysiological differentiation of new neurons in the olfactory bulb. J. Neurosci. 23, 10411–10418.

Benford H, Bolborea M, Pollatzek E, Lossow K, Hermans-Borgmeyer I, Liu B, Meyerhof W, Kasparov S, Dale N. (2017). A sweet taste receptor-dependent mechanism of glucosensing in hypothalamic tanycytes. Glia. 65, 773-789.

Bennett L, Yang M, Enikolopov G, Iacovitti L. (2009). Circumventricular organs: A novel site of neural stem cells in the adult brain. Mol. Cell. Neurosci. 41, 337–347.

Beppu K, Sasaki T, Tanaka KF, Yamanaka A, Fukazawa Y, Shigemoto R, Matsui K. (2014). Optogenetic countering of glial acidosis suppresses glial glutamate release and ischemic brain damage. Neuron. 81, 314-320

Berg J, Hung YP, Yellen G (2009). A genetically encoded fluorescent reporter of ATP:ADP ratio. Nat Methods. 6, 161-6.

Berger UV, Hediger MA. (2001). Differential distribution of the glutamate transporters GLT-1 and GLAST in tanycytes of the third ventricle. J. Comp. Neurol. 433, 101-114.

Berkey CS, Rockett HR, Field AE, Gillman MW, Colditz GA. (2004). Sugar-added beverages and adolescent weight change. Obes. Res. 12, 778-788.

Bernier PJ, Bedard A, Vinet J, Levesque M, Parent A. (2002). Newly generated neurons in the amygdala and adjoining cortex of adult primates. Proc. Natl. Acad. Sci. USA. 99, 11464–11469.

Berridge MJ. (1997). Elementary and global aspects of calcium signalling. J. Exp. Biol. 200, 315–319.

Bes-Rastrollo M, Sayon-Orea C, Ruiz-Canela M, Martinez-Gonzalez MA. (2016). Impact of sugars and sugar taxation on body weight control: A comprehensive literature review. Obesity (Silver Spring). 24, 1410-1426.

Biebl M, Cooper CM, Winkler J, Kuhn HG. (2000). Analysis of neurogenesis and programmed cell death reveals a self-renewing capacity in the adult rat brain. Neurosci Lett. 291, 17-20.

Blanpain C, Simons BD. (2013). Unravelling stem cell dynamics by lineage tracing. Nat. Rev. Mol. Cell. Biol. 14, 489-502.

Boccazzi M, Rolando C, Abbracchio MP, Buffo A, Ceruti S. (2014). Purines regulate adult brain subventricular zone cell functions: Contribution of reactive astrocytes. Glia. 62, 428–439.

Bolborea M, Benford H, Dale N. (2014-2017). Hypothalamic tanycytes mediate context–dependent modulation of the arcuate neuronal network controlling appetite. Unpublished report in possession of M Bolborea, Coventry.

Bolborea M, Dale N. (2013). Hypothalamic tanycytes: Potential roles in the control of feeding and energy balance. Trends Neurosci. 36, 91–100

Boldrini M, Fulmore CA, Tartt AN, Simeon LR, Pavlova I, Poposka V, Rosoklija GB, Stankov A, Arango V, Dwork AJ, Hen R, Mann JJ. (2018). Human Hippocampal Neurogenesis Persists throughout Aging. Cell Stem Cell. 22, 589-599.

Bond AM, Ming GL, Song H. (2015). Adult Mammalian Neural Stem Cells and Neurogenesis: Five Decades Later. Cell Stem Cell. 17, 385-95.

Bonfanti L. (2006). PSA-NCAM in mammalian structural plasticity and neurogenesis. Prog. Neurobiol. 80, 129–164.

Borg ML, Lemus M, Reichenbach A, Selathurai A, Oldfield BJ, Andrews ZB, Watt MJ. (2014). Hypothalamic neurogenesis is not required for the improved insulin sensitivity following exercise training. Diabetes. 63, 3647-3658.

Boulland JL, Mastrangelopoulou M, Boquest AC, Jakobsen R, Noer A, Glover JC, Collas P. (2013). Epigenetic regulation of nestin expression during neurogenic differentiation of adipose tissue stem cells. Stem Cells Dev. 22, 1042-1052.

Bouret SG, Simerly RB. (2006). Developmental programming of hypothalamic feeding circuits. Clin. Genet. 70, 295–301

Bovetti S, Hsieh YC, Bovolin P, Perroteau I, Kazunori T, Puche AC. (2007). Blood vessels form a scaffold for neuroblast migration in the adult olfactory bulb. J Neurosci. 27, 5976–5980.

Boyden ES, Zhang F, Bamberg E, Nagel G, Deisseroth K. (2005). Millisecond-timescale, genetically targeted optical control of neural activity. Nat. Neurosci. 8, 1263-1268.

Branda CS, Dymecki SM. (2004). Talking about a revolution: The impact of site-specific recombinases on genetic analysis in mice. Dev. Cell. 6, 7–28.

Braun N, Sévigny J, Mishra SK, Robson SC, Barth SW, Gerstberger R, Hammer K, Zimmermann H. (2003). Expression of the ecto-ATPase NTPDase2 in the germinal zones of the developing and adult rat brain. Eur. J. Neurosci. 17, 1355–1364.

Braun SM, Jessberger S. (2014). Adult neurogenesis: Mechanisms and functional significance. Development. 141, 1983-1986.

Brennan P, Keverne EB. (2015). Biological complexity and adaptability of simple mammalian olfactory memory systems. Neurosci. Biobehav. Rev. 50, 29–40.

Breton-Provencher V, Lemasson M, Peralta MR 3rd, Saghatelyan A. (2009). Interneurons produced in adulthood are required for the normal functioning of the olfactory bulb network and for the execution of selected olfactory behaviors. J Neurosci. 29, 15245-57.

Breunig JJ, Arellano JI, Macklis JD, Rakic P. (2007). Everything that glitters isn't gold: A critical review of postnatal neural precursor analyses. Cell. Stem Cell. 1, 612–627.

Bruni JE. (1998). Ependymal development, proliferation, and functions: A review. Microsc. Res. Tech. 41, 2-13.

Bruni JE, Clattenburg RE, Millar E. (1983). Tanycyte ependymal cells in the third ventricle of young and adult rats: A Golgi study. Anat Anz. 153, 53–68.

Burns KA, Ayoub AE, Breunig JJ, Adhami F, Weng WL, Colbert MC, Rakic P, Kuan CY. (2007). Nestin-CreER mice reveal DNA synthesis by nonapoptotic neurons following cerebral ischemia-hypoxia. Cereb. Cortex. 17, 2585–2592.

Calzolari F, Michel J, Baumgart EV, Theis F, Götz M, Ninkovic J4. (2014). Fast clonal expansion and limited neural stem cell self-renewal in the adult subependymal zone. Nat Neurosci. 18, 490-2.

Cao X, Li LP, Qin XH, Li SJ, Zhang M, Wang Q, Hu HH, Fang YY, Gao YB, Li XW, Sun LR, Xiong WC, Gao TM, Zhu XH. (2013). Astrocytic adenosine 5′-triphosphate release regulates the proliferation of neural stem cells in the adult hippocampus. Stem Cells. 31, 1633–1643

Carlén M, Meletis K, Barnabé-Heider F, Frisén J. (2006). Genetic visualization of neurogenesis. Exp. Cell. Res. 312, 2851–2859.

Castrén E. (2004). Neurotrophic effects of antidepressant drugs. Curr. Opin. Pharmacol. 4, 58-64.

Cavaliere F, Donno C, D'Ambrosi N. (2015). Purinergic signaling: A common pathway for neural and mesenchymal stem cell maintenance and differentiation. Front Cell Neurosci. 9, 211.

Chaker Z, George C, Petrovska M, Caron JB, Lacube P, Caillé I, Holzenberger M. (2016). Hypothalamic neurogenesis persists in the aging brain and is controlled by energy-sensing IGF-I pathway. Neurobiol. Aging. 41, 64-72.

Chen J, Kwon CH, Lin L, Li Y, Parada LF. (2009). Inducible site-specific recombination in neural stem/progenitor cells. Genesis. 47, 122–131.

Chen J, Tan Z, Zeng L, Zhang X, He Y, Gao W, Wu X, Li Y, Bu B, Wang W, Duan S. (2013). Heterosynaptic long-term depression mediated by ATP released from astrocytes. Glia. 61, 178–191.

Chojnacki AK, Mak GK, Weiss S. (2009). Identity crisis for adult periventricular neural stem cells: subventricular zone astrocytes, ependymal cells or both? Nat. Rev. Neurosci. 10, 153-163.

Chouaf-Lakhdar L, Fèvre-Montange M, Brisson C, Strazielle N, Gamrani H, Didier-Bazès M. (2003). Proliferative activity and nestin expression in periventricular cells of the adult rat brain. Neuroreport. 14, 633–636.

Chow BY, Han X, Dobry AS, Qian X, Chuong AS, Li M, Henninger MA, Belfort GM, Lin Y, Monahan PE, Boyden ES. (2010). High-performance genetically targetable optical neural silencing by light-driven proton pumps. Nature. 463, 98-102

Cifuentes M, Pérez-Martín M, Grondona JM, López-Ávalos MD, Inagaki N, Granados-Durán P, Rivera P, Fernández-Llebrez P. (2011). A comparative analysis of intraperitoneal versus intracerebroventricular administration of bromodeoxyuridine for the study of cell proliferation in the adult rat brain. J Neurosci Methods. 201, 307-14.

Cipriani S, Ferrer I, Aronica E, Kovacs GG, Verney C, Nardelli J, Khung S, Delezoide AL, Milenkovic I, Rasika S, Manivet P, Benifla JL, Deriot N, Gressens P, Adle-Biassette H. (2018). Hippocampal Radial Glial Subtypes and Their Neurogenic Potential in Human Fetuses and Healthy and Alzheimer's Disease Adults. Cereb Cortex. 28, 2458-2478.

Clarke SR, Shetty AK, Bradley JL, Turner DA. (1994). Reactive astrocytes express the embryonic intermediate neurofilament nestin. Neuroreport. 5, 1885-1888.

Clelland CD, Choi M, Romberg C, Clemenson GD Jr, Fragniere A, Tyers P, Jessberger S, Saksida LM, Barker RA, Gage FH, Bussey TJ. (2009). A functional role for adult hippocampal neurogenesis in spatial pattern separation. Science. 325, 210-3.

Conley JM, Radhakrishnan S, Valentino SA, Tantama M. (2017). Imaging extracellular ATP with a genetically-encoded, ratiometric fluorescent sensor. PLoS One. 12, e0187481.

Cong WN, Wang R, Cai H, Daimon CM, Scheibye-Knudsen M, Bohr VA, Turkin R, Wood WH 3rd, Becker KG, Moaddel R, Maudsley S, Martin B. (2013). Long-term artificial sweetener acesulfame potassium treatment alters neurometabolic functions in C57BL/6J mice. PLoS One. 8, e70257.

Coppola A, Liu ZW, Andrews ZB, Paradis E, Roy MC, Friedman JM, Ricquier D, Richard D, Horvath TL, Gao XB, Diano S. (2007). A central thermogenic-like mechanism in feeding regulation: An interplay between arcuate nucleus T3 and UCP2. Cell Metab. 5, 21–33.

Cortés-Campos C, Elizondo R, Llanos P, Uranga RM, Nualart F, García MA. (2011). MCT expression and lactate influx/efflux in tanycytes involved in glia-neuron metabolic interaction. PLoS One. 6, e16411.

Coskun V, Wu H, Blanchi B, Tsao S, Kim K, Zhao J, Biancotti JC, Hutnick L, Krueger RC Jr, Fan G, de Vellis J, Sun YE. (2008). CD133+ neural stem cells in the ependyma of mammalian postnatal forebrain. Proc. Natl. Acad. Sci. USA. 105, 1026-1031.

Curran-Everett D. (2000). Multiple comparisons: Philosophies and illustrations. Am. J. Physiol. Regul. Integr. Comp. Physiol. 279, R1-8.

Dale N. (2011). Purinergic signaling in hypothalamic tanycytes: Potential roles in chemosensing. Semin. Cell. Dev. Biol. 22, 237–244.

Datla KP, Mitra SK, Bhattacharya SK. (1991). Serotonergic modulation of footshock induced aggression in paired rats. Indian J. Exp. Biol. 29, 631-635.

Dayer AG, Ford AA, Cleaver KM, Yassaee M, Cameron HA. (2003). Short-term and long-term survival of new neurons in the rat dentate gyrus. J Comp Neurol. 460, 563-72.

Dayer AG, Cleaver KM, Abouantoun T, Cameron HA. (2005). New GABAergic interneurons in the adult neocortex and striatum are generated from different precursors. J. Cell. Biol. 168, 415–427.

Dennis CV, Suh LS, Rodriguez ML, Kril JJ, Sutherland GT. (2016). Human adult neurogenesis across the ages: An immunohistochemical study. Neuropathol Appl Neurobiol. 42, 621-638.

Desai M, Li T, Ross MG. (2011). Fetal hypothalamic neuroprogenitor cell culture: Preferential differentiation paths induced by leptin and insulin. Endocrinology 152, 3192–3201.

Dhaliwal J, Lagace DC. (2011). Visualization and genetic manipulation of adult neurogenesis using transgenic mice. Eur. J. Neurosci. 33, 1025–1036.

Di Virgilio F, Ceruti S, Bramanti P, Abbracchio MP. (2009). Purinergic signalling in inflammation of the central nervous system. Trends Neurosci. 32, 79–87.

Didier-Bazès M, Chouaf-Lakhdar L, Dutuit M, Aguera M, Belin MF. (2001). Cell lineage of the subcommissural organ secretory ependymocytes: Differentiating role of the environment. Microsc Res Tech. 52, 461-467.

Djogo T, Robins SC, Schneider S, Kryzskaya D, Liu X, Mingay A, Gillon CJ, Kim JH, Storch KF, Boehm U, Bourque CW, Stroh T, Dimou L, Kokoeva MV. (2016). Adult NG2-Glia Are Required for Median Eminence-Mediated Leptin Sensing and Body Weight Control. Cell Metab. 23, 797-810.

Doetsch F, García-Verdugo JM, Alvarez-Buylla A. (1997). Cellular composition and three-dimensional organization of the subventricular germinal zone in the adult mammalian brain. J Neurosci. 17, 5046-61.

Doetsch F, García-Verdugo JM, Alvarez-Buylla A. (1999). Regeneration of a germinal layer in the adult mammalian brain. Proc. Natl. Acad. Sci. USA. 96, 11619–11624.

Dore-Duffy P, Katychev A, Wang X, Van Buren E. (2006). CNS microvascular pericytes exhibit multipotential stem cell activity. J. Cereb. Blood Flow Metab. 5, 613-624.

Dranovsky A, Picchini AM, Moadel T, Sisti AC, Yamada A, Kimura S, Leonardo ED, Hen R. (2011). Experience dictates stem cell fate in the adult hippocampus. Neuron. 70, 908-23.

Duggal N, Schmidt-Kastner R, Hakim AM, (1997). Nestin expression in reactive astrocytes following focal cerebral ischemia in rats. Brain Res. 768, 1–9.

Dymecki SM. (1996). Flp recombinase promotes site-specific DNA recombination in embryonic stem cells and transgenic mice. Proc Natl Acad Sci U S A. 93, 6191–6196.

El Agha E, Al Alam D, Carraro G, MacKenzie B, Goth K, De Langhe SP, Voswinckel R, Hajihosseini MK, Rehan VK, Bellusci S. (2012). Characterization of a novel fibroblast growth factor 10 (Fgf10) knock-in mouse line to target mesenchymal progenitors during embryonic development. PLoS One. 7, e38452.

Elizondo-Vega R, Cortés-Campos C, Barahona MJ, Carril C, Ordenes P, Salgado M, Oyarce K, García-Robles ML. (2016). Inhibition of hypothalamic MCT1 expression increases food intake and alters orexigenic and anorexigenic neuropeptide expression. Sci Rep. 6, 33606.

Elmore MR, Najafi AR, Koike MA, Dagher NN, Spangenberg EE, Rice RA, Kitazawa M, Matusow B, Nguyen H, West BL, Green KN. (2014). Colony-stimulating factor 1 receptor signaling is necessary for microglia viability, unmasking a microglia progenitor cell in the adult brain. Neuron. 82, 380-397.

Eriksson PS, Perfilieva E, Björk-Eriksson T, Alborn AM, Nordborg C, Peterson DA, Gage FH. (1998). Neurogenesis in the adult human hippocampus. Nat. Med. 4, 1313–1317.

Ernst C, Christie BR. (2006). The putative neural stem cell marker, nestin, is expressed in heterogenous cell types in the adult rat neocortex. Neuroscience. 138, 183–188

Evans J, Sumners C, Moore J, Huentelman MJ, Deng J, Gelband CH, Shaw G. (2002). Characterization of mitotic neurons derived from adult rat hypothalamus and brain stem. J. Neurophysiol. 87, 1076–1085.

Favaro R, Valotta M, Ferri AL, Latorre E, Mariani J, Giachino C, Lancini C, Tosetti V, Ottolenghi S, Taylor V, Nicolis SK. (2009). Hippocampal development and neural stem cell maintenance require Sox2-dependent regulation of Shh. Nat. Neurosci. 12, 1248–1262.

Feil R, Wagner J, Metzger D, Chambon P. (1997). Regulation of Cre recombinase activity by mutated estrogen receptor ligand-binding domains. Biochem. Biophys. Res. Commun. 237, 752–757.

Feng JF, Gao XF, Pu YY, Burnstock G, Xiang Z, He C. (2015). P2X7 receptors and Fyn kinase mediate ATP-induced oligodendrocyte progenitor cell migration. Purinergic Signal. 11, 361–369.

Fenno L, Yizhar O, Deisseroth K. (2011). The development and application of optogenetics. Annu. Rev. Neurosci. 34, 389-412.

Forni PE, Scuoppo C, Imayoshi I, Taulli R, Dastrù W, Sala V, Betz UA, Muzzi P, Martinuzzi D, Vercelli AE, Kageyama R, Ponzetto C. (2006). High levels of Cre expression in neuronal progenitors cause defects in brain development leading to microencephaly and hydrocephaly. J. Neurosci. 26, 9593–9602.

Foudi A, Hochedlinger K, Van Buren D, Schindler JW, Jaenisch R, Carey V, Hock H. (2009). Analysis of histone 2B-GFP retention reveals slowly cycling hematopoietic stem cells. Nat Biotechnol. 27, 84-90.

Fowler CD, Liu Y, Ouimet C, Wang Z. (2002). The effects of social environment on adult neurogenesis in the female prairie vole. J. Neurobiol. 51, 115–128.

Franklin KBJ, Paxinos G. (2012). The mouse brain in stereotaxic coordinates. 4th edition. San Diego: Academic Press.

Frayling C, Britton R, Dale N. (2011). ATP-mediated glucosensing by hypothalamic tanycytes. J. Physiol. 589, 2275–2286.

Fuente-Martín E, García-Cáceres C, Granado M, de Ceballos ML, Sánchez-Garrido MÁ, Sarman B, Liu ZW, Dietrich MO, Tena-Sempere M, Argente-Arizón P, Díaz F, Argente J, Horvath TL, Chowen JA. (2012). Leptin regulates glutamate and glucose transporters in hypothalamic astrocytes. J Clin Invest. 122, 3900-13.

Fura-8™, AM | AAT Bioquest, Inc. 2018. Fura-8™, AM | AAT Bioquest, Inc. [ONLINE] Available at: https://www.aatbio.com/products/fura-8-am. [Accessed 22 January 2018].

Gage FH, Coates PW, Palmer TD, Kuhn HG, Fisher LJ, Suhonen JO, Peterson DA, Suhr ST, Ray J. (1995). Survival and differentiation of adult neuronal progenitor cells transplanted to the adult brain. Proc. Natl. Acad. Sci. USA. 92, 11879-11883.

Gage FH. (2000). Mammalian neural stem cells. Science. 287, 1433–1438.

Gampe K, Stefani J, Hammer K, Brendel P, Pötzsch A, Enikolopov G, Enjyoji K, Acker-Palmer A, Robson SC, Zimmermann H. (2015). NTPDase2 and purinergic signaling control progenitor cell proliferation in neurogenic niches of the adult mouse brain. Stem Cells. 33, 253–264.

Ganat YM, Silbereis J, Cave C, Ngu H, Anderson GM, Ohkubo Y, Ment LR, Vaccarino FM. (2006). Early postnatal astroglial cells produce multilineage precursors and neural stem cells in vivo. J. Neurosci. 26, 8609–8621.

Garcia M, Millán C, Balmaceda-Aguilera C, Castro T, Pastor P, Montecinos H, Reinicke K, Zúñiga F, Vera JC, Oñate SA, Nualart F. (2003). Hypothalamic ependymal-glial cells express the glucose transporter GLUT2, a protein involved in glucose sensing. J. Neurochem. 86, 709–724.

Garzotto D, Giacobini P, Crepaldi T, Fasolo A, De Marchis S. (2008). Hepatocyte growth factor regulates migration of olfactory interneuron precursors in the rostral migratory stream through Met-Grb2 coupling. J Neurosci. 28, 5901–5909.

Ge S, Yang CH, Hsu KS, Ming GL, Song H. (2007) A critical period for enhanced synaptic plasticity in newly generated neurons adult brain. Neuron. 54, 559–566.of the

Ge S, Pradhan DA, Ming GL, Song H. (2007). GABA sets the tempo for activity-dependent adult neurogenesis. Trends Neurosci. 30, 1–8.

Genzen JR, Platel JC, Rubio ME, Bordey A. (2009). Ependymal cells along the lateral ventricle express functional P2X(7) receptors. Purinergic Signal. 5, 299-307.

Giachino C, Taylor V. (2009). Lineage analysis of quiescent regenerative stem cells in the adult brain by genetic labelling reveals spatially restricted neurogenic niches in the olfactory bulb. Eur. J. Neurosci. 30, 9–24.

Gil-Perotín S, Duran-Moreno M, Cebrián-Silla A, Ramírez M, García-Belda P, García-Verdugo JM. (2013). Adult neural stem cells from the subventricular zone: a review of the neurosphere assay. Anat Rec (Hoboken). 296,1435-52.

Gilyarov AV. (2008). Nestin in central nervous system cells. Neurosci. Behav. Physiol. 38, 165-169.

Glaser T, Resende RR, Ulrich H. (2013). Implications of purinergic receptor-mediated intracellular calcium transients in neural differentiation. Cell Commun. Signal. 11, 12.

Goldman SA & Nottebohm F. (1983). Neuronal production, migration, and differentiation in a vocal control nucleus of the adult female canary brain. Proc Natl Acad Sci USA. 80, 2390–2394.

Golic KG, Lindquist S. (1989). The FLP recombinase of yeast catalyzes site-specific recombination in the Drosophila genome. Cell. 59, 499–509.

Gomez-Villafuertes R, Rodríguez-Jiménez FJ, Alastrue-Agudo A, Stojkovic M, Miras-Portugal MT, Moreno-Manzano V. (2015). Purinergic receptors in spinal cord-derived ependymal stem/progenitor cells and their potential role in cell-based therapy for spinal cord injury. Cell Transplant. 24, 1493–1509.

Gonzalez AM, Logan A, Ying W, Lappi DA, Berry M, Baird A. (1994). Fibroblast growth factor in the hypothalamic–pituitary axis: differential expression of fibroblast growth factor-2 and a high affinity receptor. Endocrinology. 134, 2289–2297.

Goodman T, Hajihosseini MK. (2015). Hypothalamic tanycytes - Masters and servants of metabolic, neuroendocrine, and neurogenic functions. Front Neurosci. 9, 387.

Götz M, Sirko S, Beckers J, Irmler M. (2015). Reactive astrocytes as neural stem or progenitor cells: In vivo lineage, In vitro potential, and Genome-wide expression analysis. Glia. 63, 1452–1468

Gouaze A, Brenachot X, Rigault C, Krezymon A, Rauch C, Nédélec E, Lemoine A, Gascuel J, Bauer S, Pénicaud L, Benani A. (2013). Cerebral cell renewal in adult mice controls the onset of obesity. PLoS One. 8, e72029.

Gould E, Reeves AJ, Graziano MS, Gross CG. (1999). Neurogenesis in the neocortex of adult primates. Science. 286, 548–552.

Gould E. (2007). How widespread is adult neurogenesis in mammals? Nat. Rev. Neurosci. 8, 481–488.

Gourine AV, Kasymov V, Marina N, Tang F, Figueiredo MF, Lane S, Teschemacher AG, Spyer KM, Deisseroth K, Kasparov S. (2010) Astrocytes control breathing through pH-dependent release of ATP. Science. 329, 571–575.

Gradinaru V, Mogri M, Thompson KR, Henderson JM, Deisseroth K. (2009). Optical deconstruction of parkinsonian neural circuitry. Science. 324, 354–359.

Grandel H, Brand M. (2013). Comparative aspects of adult neural stem cell activity in vertebrates. Dev. Genes. Evol. 223, 131–147.

Grimm I, Ullsperger SN, Zimmermann H. (2010). Nucleotides and epidermal growth factor induce parallel cytoskeletal rearrangements and migration in cultured adult murine neural stem cells. Acta Physiol. 199, 181–189.

Gropp E, Shanabrough M, Borok E, Xu AW, Janoschek R, Buch T, Plum L, Balthasar N, Hampel B, Waisman A, Barsh GS, Horvath TL, Brüning JC. (2005). Agouti-related peptide-expressing neurons are mandatory for feeding. Nat. Neurosci. 8, 1289–1291.

Grote HE, Hannan AJ. (2007). Regulators of adult neurogenesis in the healthy and diseased brain. Clin Exp Pharmacol Physiol. 34, 533-45.

Haan N, Goodman T, Najdi-Samiei A, Stratford CM, Rice R, El Agha E, Bellusci S, Hajihosseini MK. (2013). Fgf10-expressing tanycytes add new neurons to the appetite/energy-balance regulating centers of the postnatal and adult hypothalamus. J. Neurosci. 33, 6170–6180.

Hajihosseini MK, De Langhe S, Lana-Elola E, Morrison H, Sparshott N, Kelly R, Sharpe J, Rice D, Bellusci S. (2008). Localization and fate of Fgf10-expressing cells in the adult mouse brain implicate Fgf10 in control of neurogenesis. Mol. Cell. Neurosci. 37, 857-868.

Hack I, Bancila M, Loulier K, Carroll P, Cremer H. (2002). Reelin is a detachment signal in tangential chain-migration during postnatal neurogenesis. Nat Neurosci. 5, 939–945.

Hamilton DL, Abremski K. (1984). Site-specific recombination by thebacteriophage P1 lox-Cre system. Cre-mediated synapsis of two lox sites. J Mol Biol. 178, 481–486.

Han JH, Kushner SA, Yiu AP, Hsiang HL, Buch T, Waisman A, Bontempi B, Neve RL, Frankland PW, Josselyn SA. (2009). Selective erasure of a fear memory. Science. 323, 1492–1496.

Han X, Boyden ES. (2007). Multiple-color optical activation, silencing, and desynchronization of neural activity, with single-spike temporal resolution. PLoS One. 2, e299

Hartfuss E, Galli R, Heins N, Götz M. (2001). Characterization of CNS precursor subtypes and radial glia. Dev Biol. 229, 15-30.

Hausser M. (2014). Optogenetics: The age of light. Nat. Methods. 11, 1012-1014.

Hawken PA, Jorre TJ, Rodger J, Esmaili T, Blache D, Martin GB. (2009). Rapid induction of cell proliferation in the adult female ungulate brain (Ovis aries) associated with activation of the reproductive axis by exposure to unfamiliar males. Biol Reprod. 80, 1146–1151.

Hendrickson ML, Rao AJ, Demerdash ON, Kalil RE. (2011). Expression of nestin by neural cells in the adult rat and human brain. PLoS One. 6, e18535.

Heo JS, Han HJ. (2006). ATP stimulates mouse embryonic stem cell proliferation via protein kinase C, phosphatidylinositol 3-kinase/Akt, and mitogen-activated protein kinase signaling pathways. Stem Cells. 24, 2637–2648.

Ho T, Jobling AI, Greferath U, Chuang T, Ramesh A, Fletcher EL, Vessey KA. (2015). Vesicular expression and release of ATP from dopaminergic neurons of the mouse retina and midbrain. Front Cell Neurosci. 9, 389.

Holmin S. (1997). Adult nestin-expressing subependymal cells differentiate to astrocytes in response to brain injury. Eur J Neurosci. 9, 65-75.

Horstmann E. (1954) Die Faserglia des Selachiergehirns. Z Zellforsch. 39, 588 – 617

Horvath TL, Chowen JA. (2012). Leptin regulates glutamate and glucose transporters in hypothalamic astrocytes. J. Clin. Invest. 122, 3900–3913.

Hoyer D, Jacobson LH. (2013). Orexin in sleep, addiction and more: Is the perfect insomnia drug at hand? Neuropeptides. 47, 477-488.

Hu H, Tomasiewicz H, Magnuson T, Rutishauser U. (1996). The role of polysialic acid in migration of olfactory bulb interneuron precursors in the subventricular zone. Neuron. 16, 735–743.

Huang L, DeVries GJ, Bittman EL. (1998). Photoperiod regulates neuronal bromodeoxyuridine labeling in the brain of a seasonally breeding mammal. J. Neurobiol. 36, 410–420.

Imamura H, Nhat KP, Togawa H, Saito K, Iino R, Kato-Yamada Y, Nagai T, Noji H. (2009). Visualization of ATP levels inside single living cells with fluorescence resonance energy transfer-based genetically encoded indicators. Proc Natl Acad Sci U S A. 106, 15651–15656.

Imayoshi I, Ohtsuka T, Metzger D, Chambon P, Kageyama R. (2006). Temporal regulation of Cre recombinase activity in neural stem cells. Genesis. 44, 233-8.

Imayoshi I, Sakamoto M, Kageyama R. (2011). Genetic methods to identify and manipulate newly born neurons in the adult brain. Front Neurosci. 5, 64

Ino H, Chiba T. (2000). Expression of proliferating cell nuclear antigen (PCNA) in the adult and developing mouse nervous system. Brain Res. Mol. Brain Res. 78, 163–174.

Indra AK, Warot X, Brocard J, Bornert JM, Xiao JH, Chambon P, Metzger D. (1999). Temporally-controlled site-specific mutagenesis in the basal layer of the epidermis: Comparison of the recombinase activity of the tamoxifen-inducible Cre-ER(T) and Cre-ER(T2) recombinases. Nucleic. Acids Research. 27, 4324–4327.

Jiménez AJ, Domínguez-Pinos MD, Guerra MM, Fernández-Llebrez P, Pérez-Fígares JM. (2014). Structure and function of the ependymal barrier and diseases associated with ependyma disruption. Tissue Barriers. 2, e28426.

Johnson AK, Gross PM. (1993). Sensory circumventricular organs and brain homeostatic pathways. FASEB J. 7, 678–686.

Kandasamy M, Rosskopf M, Wagner K, Klein B, Couillard-Despres S, Reitsamer HA, Stephan M, Nguyen HP, Riess O, Bogdahn U, Winkler J, von Hörsten S, Aigner L. (2015). Reduction in subventricular zone-derived olfactory bulb neurogenesis in a rat model of Huntington's disease is accompanied by striatal invasion of neuroblasts. PLoS One. 10, e0116069.

Kaneko N, Sawada M, Sawamoto K. (2017). Mechanisms of neuronal migration in the adult brain. J Neurochem. 141, 835-847.

Kaplan MS, Bell DH. (1984). Mitotic neuroblasts in the 9-day-old and 11-month old rodent hippocampus. J. Neurosci. 4, 1429–1441.

Kaplan MS, Hinds JW. (1977). Neurogenesis in the adult rat: Electron microscopic analysis of light radioautographs. Science. 197, 1092–1094.

Kaplan MS, McNelly NA, Hinds JW. (1985) Population dynamics of adult-formed granule neurons of the rat olfactory bulb. J. Comp. Neurol. 239, 117–125.

Kato HE, Zhang F, Yizhar O, Ramakrishnan C, Nishizawa T, Hirata K, Ito J, Aita Y, Tsukazaki T, Hayashi S, Hegemann P, Maturana AD, Ishitani R, Deisseroth K, Nureki O. (2012). Crystal structure of the channelrhodopsin light-gated cation channel. Nature. 482, 369–374.

Kempermann G, Kuhn HG, Gage FH. (1998). Experience-induced neurogenesis in the senescent dentate gyrus. J Neurosci. 18, 3206-12.

Kempermann G, van Praag H, Gage FH. (2000). Activity-dependent regulation of neuronal plasticity and self repair. Prog Brain Res.127, 35-48.

Kempermann G. (2012). New neurons for 'survival of the fittest'. Nat. Rev. Neurosci. 13, 727-736.

Kempermann G, Gage FH, Aigner L, Song H, Curtis MA, Thuret S, Kuhn HG, Jessberger S, Frankland PW, Cameron HA, Gould E, Hen R, Abrous DN, Toni N, Schinder AF, Zhao X, Lucassen PJ, Frisén J. (2018). Human Adult Neurogenesis: Evidence and Remaining Questions. Cell Stem Cell. 23, 25-30.

Kiel MJ, He S, Ashkenazi R, Gentry SN, Teta M, Kushner JA, Jackson TL, Morrison SJ. (2007). Haematopoietic stem cells do not asymmetrically segregate chromosomes or retain BrdU. Nature. 449, 238-42.

Kim WR, Park OH, Choi S, Choi SY, Park SK, Lee KJ, Rhyu IJ, Kim H, Lee YK, Kim HT, Oppenheim RW, Sun W. (2009). The maintenance of specific aspects of neuronal function and behavior is dependent on programmed cell death of adult-generated neurons in the dentate gyrus. Eur J Neurosci. 29, 1408-21.

Kim WR, Sun W. (2011). Programmed cell death during postnatal development of the rodent nervous system. Dev Growth Differ. 53, 225-35.

Klein C, Butt SJ, Machold RP, Johnson JE, Fishell G. (2005). Cerebellum- and forebrain-derived stem cells possess intrinsic regional character. Development. 132, 4497-508.

Kleinlogel S, Feldbauer K, Dempski RE, Fotis H, Wood PG, Bamann C, Bamberg E. (2011). Ultra light-sensitive and fast neuronal activation with the Ca²+-permeable channelrhodopsin CatCh. Nat Neurosci. 14, 513-8.

Koch JD, Miles DK, Gilley JA, Yang CP, Kernie SG. (2008). Brief exposure to hyperoxia depletes the glial progenitor pool and impairs functional recovery after hypoxic-ischemic brain injury. J. Cerebral Blood Flow Metab. 28, 1294–1306.

Kokoeva MV, Yin H, Flier JS. (2005). Neurogenesis in the hypothalamus of adult mice: Potential role in energy balance. Science. 310, 679–683.

Kokoeva MV, Yin H, Flier JS. (2007). Evidence for constitutive neural cell proliferation in the adult murine hypothalamus. J. Comp. Neurol. 505, 209–220.

Kretzschmar K, Watt FM. (2012). Lineage tracing. Cell. 148, 33-45.

Kriegstein A, Alvarez-Buylla A. (2009). The glial nature of embryonic and adult neural stem cells. Annu. Rev. Neurosci. 32, 149–184.

Kronenberg G, Wang LP, Synowitz M, Gertz K, Katchanov J, Glass R, Harms C, Kempermann G, Kettenmann H, Endres M. (2005). Nestin-expressing cells divide and adopt a complex electrophysiologic phenotype after transient brain ischemia. J. Cerebral Blood Flow Metab. 25, 1613–1624.

Kuhn HG. (2015). Control of Cell Survival in Adult Mammalian Neurogenesis. Cold Spring Harb Perspect Biol. 7, a018895.

Kuhn HG, Dickinson-Anson H, Gage FH. (1996). Neurogenesis in the dentate gyrus of the adult rat: Age-related decrease of neuronal progenitor proliferation. J. Neurosci. 16, 2027–2033.

Kuhn HG, Biebl M, Wilhelm D, Li M, Friedlander RM, Winkler J. (2005). Increased generation of granule cells in adult Bcl-2-overexpressing mice: a role for cell death during continued hippocampal neurogenesis. Eur J Neurosci. 22, 1907-15.

Kukekov VG, Laywell ED, Suslov O, Davies K, Scheffler B, Thomas LB, O'Brien TF, Kusakabe M, Steindler DA. (1999). Multipotent stem/progenitor cells with similar properties arise from two neurogenic regions of adult human brain. Exp. Neurol. 156, 333–344.

Kunisaki Y, Bruns I, Scheiermann C, Ahmed J, Pinho S, Zhang D, Mizoguchi T, Wei Q, Lucas D, Ito K, Mar JC, Bergman A, Frenette PS. (2013). Arteriolar niches maintain haematopoietic stem cell quiescence. Nature. 502, 637-43.

Lagace DC, Whitman MC, Noonan MA, Ables JL, DeCarolis NA, Arguello AA, Donovan MH, Fischer SJ, Farnbauch LA, Beech RD, DiLeone RJ, Greer CA, Mandyam CD, Eisch AJ. (2007). Dynamic contribution of nestin-expressing stem cells to adult neurogenesis. J. Neurosci. 27, 12623–12629.

Laing BT, Do K, Matsubara T, Wert DW, Avery MJ, Langdon EM, Zheng D, Huang H. (2016). Voluntary exercise improves hypothalamic and metabolic function in obese mice. J. Endocrinol. 229, 109-122.

Lakso M, Sauer B, Mosinger B Jr, Lee EJ, Manning RW, Yu SH, MulderKL, Westphal H. (1992). Targeted oncogene activation by site-specific recombination in transgenic mice. Proc Natl Acad Sci USA. 89, 6232–6236.

Langlet F, Mullier A, Bouret SG, Prevot V, Dehouck B. (2013). Tanycyte-like cells form a blood-cerebrospinal fluid barrier in the circumventricular organs of the mouse brain. J. Comp. Neurol. 521, 3389–3405.

Langlet F. (2014). Tanycytes: A gateway to the metabolic hypothalamus. J Neuroendocrinol. 26, 753-760.

Lawson LJ, Perry VH, Gordon S. (1992). Turnover of resident microglia in the normal adult mouse brain. Neuroscience. 48, 405-15.

Lazarini F, Lledo PM. (2011). Is adult neurogenesis essential for olfaction? Trends Neurosci. 34, 20–30.

Lazutkaite G, Soldà A, Lossow K, Meyerhof W, Dale N. (2017). Amino acid sensing in hypothalamic tanycytes via umami taste receptors. Mol. Metab. 6, 1480-1492.

Lecca D, Fumagalli M, Ceruti S, Abbracchio MP. (2016). Intertwining extracellular nucleotides and their receptors with Ca2+ in determining adult neural stem cell survival, proliferation and final fate. Philos. Trans. R. Soc. Lond. B. Biol. Sci. 371, pii: 20150433.

Lee A, Kessler JD, Read TA, Kaiser C, Corbeil D, Huttner WB, Johnson JE, Wechsler-Reya RJ. (2005). Isolation of neural stem cells from the postnatal cerebellum. Nat Neurosci. 8, 723-9.

Lee DA, Blackshaw S. (2012). Functional implications of hypothalamic neurogenesis in the adult mammalian brain. Int. J. Dev. Neurosci. 30, 615–621.

Lee DA, Bedont JL, Pak T, Wang H, Song J, Miranda-Angulo A, Takiar V, Charubhumi V, Balordi F, Takebayashi H, Aja S, Ford E, Fishell G, Blackshaw S. (2012). Tanycytes of the hypothalamic median eminence form a diet-responsive neurogenic niche. Nat. Neurosci. 15, 700–702.

Lee DA, Yoo S, Pak T, Salvatierra J, Velarde E, Aja S, Blackshaw S. (2014). Dietary and sex-specific factors regulate hypothalamic neurogenesis in young adult mice. Front. Neurosci. 8, 157.

Lendahl U, Zimmerman L, McKay RD. (1990). CNS stem cells express a new class of intermediate filament protein. Cell. 60, 585–595.

Lepousez G, Lledo PM. (2013). Odor discrimination requires proper olfactory fast oscillations in awake mice. Neuron. 80, 1010–1024.

Leuchtweis J, Boettger MK, Niv F, Redecker C, Schaible HG. (2014). Enhanced neurogenesis in the hippocampal dentate gyrus during antigen-induced arthritis in adult rat--a crucial role of immunization. PLoS One. 2014 Feb 21;9(2):e89258. doi: 10.1371/journal.pone.0089258. eCollection 2014.

Levin BE, Magnan C, Dunn-Meynell A, Le Foll C. (2011). Metabolic sensing and the brain: Who, what, where, and how? Endocrinology. 152, 2552–2557.

Li G, Matsuzki K, Wang Y, Zhao N, Yang M, Shido O. (2013a). Voluntary exercise promotes proliferation and differentiation of adult rat hypothalamus progenitor cells. Nan Fang Yi Ke Da Xue Xue Bao. 33, 1099-106.

Li D, Agulhon C, Schmidt E, Oheim M, Ropert N. (2013b). New tools for investigating astrocyte-to-neuron communication. Front Cell Neurosci. 7, 193.

Li J, Tang Y, Cai D. (2012). IKKb/NF-jB disrupts adult hypothalamic neural stem cells to mediate a neurodegenerative mechanism of dietary obesity and pre-diabetes. Nat. Cell. Biol. 14, 999–1012.

Li L, Clevers H. (2010). Coexistence of quiescent and active adult stem cells in mammals. Science. 327, 542-545.

Lie DC, Dziewczapolski G, Willhoite AR, Kaspar BK, Shults CW, Gage FH. (2002). The adult substantia nigra contains progenitor cells with neurogenic potential. J. Neurosci. 22, 6639–6649.

Lin RC, Matesic DF, Marvin M, McKay RD, Brüstle O. (1995). Re-expression of the intermediate filament nestin in reactive astrocytes. Neurobiol. Dis. 2, 79-85

Lin JH, Takano T, Arcuino G, Wang X, Hu F, Darzynkiewicz Z, Nunes M, Goldman SA, Nedergaard M. (2007). Purinergic signaling regulates neural progenitor cell expansion and neurogenesis. Dev. Biol. 302, 356–366.

Lin JY, Lin MZ, Steinbach P, Tsien RY. (2009). Characterization of engineered channelrhodopsin variants with improved properties and kinetics. Biophys J. 96, 1803–1814.

Livet J, Weissman TA, Kang H, Draft RW, Lu J, Bennis RA, Sanes JR, Lichtman JW. (2007). Transgenic strategies for combinatorial expression of fluorescent proteins in the nervous system. Nature. 450, 56-62.

Lledo PM, Alonso M, Grubb MS. (2006). Adult neurogenesis and functional plasticity in neuronal circuits. Nat. Rev. Neurosci. 7, 179-193.

Lohr C, Grosche A, Reichenbach A, Hirnet D. (2014). Purinergic neuron-glia interactions in sensory systems. Pflugers Arch. 466, 1859-72.

Lois C, Garcia-Verdugo JM, Alvarez-Buylla A. (1996). Chain migration of neuronal precursors. Science. 271, 978–981.

Lugert S, Basak O, Knuckles P, Haussler U, Fabel K, Götz M, Haas CA, Kempermann G, Taylor V, Giachino C. (2010). Quiescent and active hippocampal neural stem cells with distinct morphologies respond selectively to physiological and pathological stimuli and aging. Cell Stem Cell. 6, 445-56.

Magavi SS, Mitchell BD, Szentirmai O, Carter BS, Macklis JD. (2005). Adult-born and preexisting olfactory granule neurons undergo distinct experience-dependent modifications of their olfactory responses in vivo. J. Neurosci. 25, 10729–10739.

Malberg JE, Eisch AJ, Nestler EJ, Duman RS. (2000). Chronic antidepressant treatment increases neurogenesis in adult rat hippocampus. J Neurosci. 20, 9104–9110.

Manfredi G, Yang L, Gajewski CD, Mattiazzi M. (2002). Measurement of ATP in mammalian cells. Methods. 26, 317–326.

Marichal N, Fabbiani G, Trujillo-Cenóz O, Russo RE. (2016). Purinergic signalling in a latent stem cell niche of the rat spinal cord. Purinergic Signal. 12, 331-341.

Marina N, Tang F, Figueiredo M, Mastitskaya S, Kasimov V, Mohamed-Ali V, Roloff E, Teschemacher AG, Gourine AV, Kasparov S. (2013). Purinergic signalling in the rostral ventro-lateral medulla controls sympathetic drive and contributes to the progression of heart failure following myocardial infarction in rats. Basic Res. Cardiol. 108, 317.

Markakis EA, Palmer TD, Randolph-Moore L, Rakic P, Gage FH. (2004). Novel neuronal phenotypes from neural progenitor cells. J. Neurosci. 24, 2886–2897.

Martínez M, Martínez NA, Silva WI. (2017). Measurement of the intracellular calcium concentration with Fura-2 AM using a fluorescence plate reader. Bio-protocol. 7, e2411.

Martinez NA, Ayala AM, Martinez M, Martinez-Rivera FJ, Miranda JD, Silva WI. (2016). Caveolin-1 regulates the P2Y2 receptor signaling in human 1321N1 astrocytoma cells. J. Biol. Chem. 291, 12208-12222.

Maswood N, Sarkar J, Uphouse L. (2008). Modest effects of repeated fluoxetine on estrous cyclicity and sexual behavior in Sprague Dawley female rats. Brain Res. 1245, 52-60.

Mathew TC. (2008). Regional analysis of the ependyma of the third ventricle of rat by light and electron microscopy. Anat. Histol. Embryol. 37, 9–18.

Mathieu P, Battista D, Depino A, Roca V, Graciarena M, Pitossi F. (2010). The more you have, the less you get: the functional role of inflammation on neuronal differentiation of endogenous and transplanted neural stem cells in the adult brain. J Neurochem. 112, 1368-85

Matsuzaki K, Katakura M, Hara T, Li G, Hashimoto M, Shido O. (2009). Proliferation of neuronal progenitor cells and neuronal differentiation in the hypothalamus are enhanced in heat-acclimated rats. Pflugers Arch. 458, 661–673.

Matute C, Torre I, Pérez-Cerdá F, Pérez-Samartín A, Alberdi E, Etxebarria E, Arranz AM, Ravid R, Rodríguez-Antigüedad A, Sánchez-Gómez M, Domercq M. (2007). P2X(7) receptor blockade prevents ATP excitotoxicity in oligodendrocytes and ameliorates experimental autoimmune encephalomyelitis. J. Neurosci. 27, 9525–9533.

McGuirk J, Muscat R, Willner P. (1992). Effects of chronically administered fluoxetine and fenfluramine on food intake, body weight and the behavioural satiety sequence. Psychopharmacology (Berl). 106, 401-407.

McNay DE, Briançon N, Kokoeva MV, Maratos-Flier E, Flier JS. (2012). Remodeling of the arcuate nucleus energy-balance circuit is inhibited in obese mice. J. Clin. Invest. 122, 142–152.

Mendez-David I, Hen R, Gardier AM, David DJ. (2013). Adult hippocampal neurogenesis: An actor in the antidepressant-like action. Ann Pharm. Fr. 71, 143-149.

Metzger D, Chambon P. (2001). Site- and time-specific gene targeting in the mouse. Methods. 24, 71–80.

Migaud M, Batailler M, Segura S, Duittoz A, Franceschini I, Pillon D. (2010). Emerging new sites for adult neurogenesis in the mammalian brain: A comparative study between the hypothalamus and the classical neurogenic zones. Eur. J. Neurosci. 32, 2042–2052.

Migaud M, Batailler M, Pillon D, Franceschini I, Malpaux B. (2011). Seasonal changes in cell proliferation in the adult sheep brain and pars tuberalis. J. Biol. Rhythms. 26, 486–496.

Migaud M, Butrille L, Batailler M. (2014). Seasonal regulation of structural plasticity and neurogenesis in the adult mammalian brain: focus on the sheep hypothalamus. Front Neuroendocrinol. 37, 146-57.

Migaud M, Butruille L, Duittoz A, Pillon D, Batailler M. (2016). Adult neurogenesis and reproductive functions in mammals. Theriogenology. 86, 313-23.

Ming GL, Song H. (2005). Adult neurogenesis in the mammalian central nervous system. Ann. Rev. Neurosci. 28, 223–250.

Ming GL, Song H. (2011). Adult neurogenesis in the mammalian brain: Significant answers and significant questions. Neuron. 70, 687–702.

Miranda-Angulo AL, Byerly MS, Mesa J, Wang H, Blackshaw S. (2014). Rax regulates hypothalamic tanycyte differentiation and barrier function in mice. J Comp Neurol. 522, 876-99.

Mirzadeh Z, Merkle FT, Soriano-Navarro M, Garcia-Verdugo JM, Alvarez-Buylla A. (2008). Neural stem cells confer unique pinwheel architecture to the ventricular surface in neurogenic regions of the adult brain. Cell. Stem Cell. 3, 265–278.

Mirzadeh Z, Kusne Y, Duran-Moreno M, Cabrales E, Gil-Perotin S, Ortiz C, Chen B, Garcia-Verdugo JM, Sanai N, Alvarez-Buylla A. (2017). Bi- and uniciliated ependymal cells define continuous floor-plate-derived tanycytic territories. Nat. Commun. 8,13759.

Mishra SK, Braun N, Shukla V, Füllgrabe M, Schomerus C, Korf HW, Gachet C, Ikehara Y, Sévigny J, Robson SC, Zimmermann H. (2006). Extracellular nucleotide signaling in adult neural stem cells: Synergism with growth factor-mediated cellular proliferation. Development 133, 675–684.

Moraes JC, Coope A, Morari J, Cintra DE, Roman EA, Pauli JR, Romanatto T, Carvalheira JB, Oliveira AL, Saad MJ, Velloso LA. (2009). High-fat diet induces apoptosis of hypothalamic neurons. PLoS One. 4, e5045.

Mori T, Tanaka K, Buffo A, Wurst W, Kühn R, Götz M. (2006). Inducible gene deletion in astroglia and radial glia – A valuable tool for functional and lineage analysis. Glia. 54, 21–34.

Morshead CM, Reynolds BA, Craig CG, McBurney MW, Staines WA, Morassutti D, Weiss S, van der Kooy D. (1994). Neural stem cells in the adult mammalian forebrain: A relatively quiescent subpopulation of subependymal cells. Neuron. 13, 1071-1082.

Mouret A, Lepousez G, Gras J, Gabellec MM, Lledo PM. (2009). Turnover of newborn olfactory bulb neurons optimizes olfaction. J Neurosci. 29, 12302–12314.

Mullier A, Bouret SG, Prevot V, Dehouck B. (2010). Differential distribution of tight junction proteins suggests a role for tanycytes in blood–hypothalamus barrier regulation in the adult mouse brain. J. Comp. Neurol. 518, 943–962.

Murase S & Horwitz AF. (2002). Deleted in colorectal carcinoma and differentially expressed integrins mediate the directional migration of neural precursors in the rostral migratory stream. J Neurosci. 22, 3568–3579.

Musselman LP, Fink JL, Narzinski K, Ramachandran PV, Hathiramani SS, Cagan RL, Baranski TJ. (2011). A high-sugar diet produces obesity and insulin resistance in wild-type Drosophila. Dis. Model Mech. 4, 842-849.

Nabeshima K, Inoue T, Shimao Y, Sameshima T. (2002). Matrix metalloproteinases in tumor invasion: role for cell migration. Pathol Int. 52, 255-64.

Nagel G, Ollig D, Fuhrmann M, Kateriya S, Musti AM, Bamberg E, Hegemann P. (2002). Channelrhodopsin-1: A light-gated proton channel in green algae. Science. 296, 2395-2398.

Nagel G, Szellas T, Huhn W, Kateriya S, Adeishvili N, Berthold P, Ollig D, Hegemann P, Bamberg E. (2003). Channelrhodopsin-2: A directly light-gated cation-selective membrane channel. Proc. Natl. Acad. Sci. USA. 100, 13940-13945.

Nagel G, Brauner M, Liewald JF, Adeishvili N, Bamberg E, Gottschalk A. (2005). Light activation of channelrhodopsin-2 in excitable cells of Caenorhabditis elegans triggers rapid behavioral responses. Curr. Biol. 15, 2279-2284.

Nagy A. (2000). Cre recombinase: The universal reagent for genome tailoring. Genesis. 26, 99–109.

Nestler EJ, Barrot M, DiLeone RJ, Eisch AJ, Gold SJ, Monteggia LM. Neurobiology of depression. (2002). Neuron. 34, 13-25.

Ng KL, Li JD, Cheng MY, Leslie FM, Lee AG, Zhou QY. (2005). Dependence of olfactory bulb neurogenesis on prokineticin 2 signaling. Science. 308, 1923–1927.

Niwa A, Nishibori M, Hamasaki S, Kobori T, Liu K, Wake H, Mori S, Yoshino T, Takahashi H. (2015). Voluntary exercise induces neurogenesis in the hypothalamus and ependymal lining of the third ventricle. Brain Struct Funct. 221, 1653-66.

Nolte C, Matyash M, Pivneva T, Schipke CG, Ohlemeyer C, Hanisch UK, Kirchhoff F, Kettenmann H. (2001). GFAP promoter-controlled EGFP-expressing transgenic mice: a tool to visualize astrocytes and astrogliosis in living brain tissue. Glia. 33, 72-86.

Nottebohm F. (2004). The road we travelled: Discovery, choreography, and significance of brain replaceable neurons. Ann. N.Y. Acad. Sci. 1016, 628–658.

Novak CM, Burghardt PR, Levine JA. (2012). The use of a running wheel to measure activity in rodents: Relationship to energy balance, general activity, and reward. Neurosci. Biobehav. Rev. 36, 1001-1014.

Oliveira Á, Illes P, Ulrich H. (2016). Purinergic receptors in embryonic and adult neurogenesis. Neuropharmacology. 104, 272-281.

Orban PC, Chui D, Marth JD. (1992). Tissue- and site-specific DNA recombination in transgenic mice. Proc Natl Acad Sci USA. 89, 6861–6865

Orellana JA, Sáez PJ, Cortés-Campos C, Elizondo RJ, Shoji KF, Contreras-Duarte S, Figueroa V, Velarde V, Jiang JX, Nualart F, Sáez JC, García MA. (2012). Glucose increases intracellular free Ca2+ in tanycytes via ATP released through connexin 43 hemichannels. Glia. 60, 53–68.

Padilla SL, Carmody JS, Zeltser LM. (2010). Pomc-expressing progenitors give rise to antagonistic neuronal populations in hypothalamic feeding circuits. Nat. Med. 16, 403–405

Paez-Gonzalez P, Asrican B, Rodriguez E, Kuo CT. (2014). Identification of distinct $ChAT^{+}$ neurons and activity-dependent control of postnatal SVZ neurogenesis. Nat. Neurosci. 17, 934-942.

Pak T, Yoo S, Miranda-Angulo AL, Wang H, Blackshaw S. (2014). Rax-CreERT2 knock-in mice: A tool for selective and conditional gene deletion in progenitor cells and radial glia of the retina and hypothalamus. PLoS One. 9, e90381.

Palmer TD, Willhoite AR, Gage FH. (2000). Vascular niche for adult hippocampal neurogenesis. J. Comp. Neurol. 425, 479–494.

Paratcha G, Ibáñez CF, Ledda F. (2006). GDNF is a chemoattractant factor for neuronal precursor cells in the rostral migratory stream. Mol Cell Neurosci. 31, 505-14.

Pariante CM, Lightman SL. (2008). The HPA axis in major depression: Classical theories and new developments. Trends Neurosci. 31, 464-468.

Pastrana E, Silva-Vargas V, Doetsch F. (2011). Eyes wide open: a critical review of sphere-formation as an assay for stem cells. Cell Stem Cell. 8, 486-98.

Paton JA, Nottebohm FN. (1984). Neurons generated in the adult brain are recruited into functional circuits. Science. 225, 1046–1048.

Pencea V, Bingaman KD, Wiegand SJ, Luskin MB. (2001). Infusion of brain-derived neurotrophic factor into the lateral ventricle of the adult rat leads to new neurons in the parenchyma of the striatum, septum, thalamus, and hypothalamus. J. Neurosci. 21, 6706–6717.

Perea G, Yang A, Boyden ES, Sur M. (2014). Optogenetic astrocyte activation modulates response selectivity of visual cortex neurons in vivo. Nat. Commun. 5, 3262.

Perez-Martín M, Cifuentes M, Grondona JM, López-Avalos MD, Gómez-Pinedo U, García-Verdugo JM, Fernández-Llebrez P. (2010). IGF-I stimulates neurogenesis in the hypothalamus of adult rats. Eur. J. Neurosci. 31, 1533–1548.

Peruzzo B, Pastor FE, Blázquez JL, Schöbitz K, Peláez B, Amat P, Rodríguez EM. (2000). A second look at the barriers of the medial basal hypothalamus. Exp. Brain Res. 132, 10–26.

Peruzzo B, Pastor FE, Blázquez JL, Amat P, Rodríguez EM. (2004). Polarized endocytosis and transcytosis in the hypothalamic tanycytes of the rat. Cell. Tissue Res. 317, 147–164.

Pierce AA, Xu AW. (2010). De novo neurogenesis in adult hypothalamus as a compensatory mechanism to regulate energy balance. J Neurosci. 30, 723-30.

Pixley SK, De Vellis J, (1984). Transition between immature radial glia and mature astrocytes studied with a monoclonal antibody to vimentin. Brain Res. 317, 201–209.

Pixley SK, Kobayashi Y, de Vellis J. (1984). A monoclonal antibody against vimentin: Characterization. Brain Res. 317, 185-199.

Praetorius HA, Leipziger J. (2009). ATP release from non-excitable cells. Purinergic Signal. 5, 433-46.

Prevot V, Bellefontaine N, Baroncini M, Sharif A, Hanchate NK, Parkash J, Campagne C, de Seranno S. (2010). Gonadotrophin-releasing hormone nerve terminals, tanycytes and neurohaemal junction remodelling in the adult median eminence: Functional consequences for reproduction and dynamic role of vascular endothelial cells. J. Neuroendocrinol. 22, 639–649.

Purves D, Augustine GJ, Fitzpatrick D, Katz LC, LaMantia A-S, McNamara JO, Williams SM. (2001). Neuroscience. 2nd ed. Sunderland (MA): Sinauer Associates.

Rajendran M, Dane E, Conley J, Tantama M. (2016). Imaging Adenosine Triphosphate (ATP). Biol Bull. 231, 73-84.

Ramon Y Cajal S. (1913). Degeneration and Regeneration of the Nervous System. London: Oxford University Press; (Transl. by May RM, 1928).

Raymond AD, Kucherepa NN, Fisher KR, Halina WG, Partlow GD. (2006). Neurogenesis of oxytocin-containing neurons in the paraventricular nucleus (PVN) of the female pig in 3 reproductive states: Puberty gilts, adult gilts and lactating sows. Brain Res. 1102, 44-51.

Ren X, Zhou L, Terwilliger R, Newton SS, de Araujo IE. (2009). Sweet taste signaling functions as a hypothalamic glucose sensor. Front Integr. Neurosci. 3, 1–15.

Repina NA, Rosenbloom A, Mukherjee A, Schaffer DV, Kane RS. (2017). At light speed: Advances in optogenetic systems for regulating cell signaling and behavior. Annu. Rev. Chem. Biomol. Eng. 8, 13-39.

Reynolds BA, Rietze RL. (2005). Neural stem cells and neurospheres–reevaluating the relationship. Nat. Methods. 2, 333–336.

Reynolds BA, Weiss S. (1992). Generation of neurons and astrocytes from isolated cells of the adult mammalian central nervous system. Science. 255, 1707–1710.

Reynolds BA, Weiss S. (1996). Clonal and population analyses demonstrate that an EGF-responsive mammalian embryonic CNS precursor is a stem cell. Dev. Biol. 175, 1-13.

Ridet JL, Malhotra SK, Privat A, Gage FH. (1997). Reactive astrocytes: Cellular and molecular cues to biological function. Trends Neurosci. 20, 570–577.

Rivera A, Vanzulli I, Butt AM. (2016). A Central Role for ATP signalling in glial interactions in the CNS. Curr. Drug Targets. 17, 1829-1833.

Rizzoti K, Lovell-Badge R. (2017). Pivotal role of median eminence tanycytes for hypothalamic function and neurogenesis. Mol. Cell. Endocrinol. 445, 7-13.

Robel S, Berninger B, Gotz M. (2011). The stem cell potential of glia: lessons from reactive gliosis. Nat Rev Neurosci. 12, 88–104.

Robins SC, Villemain A, Liu X, Djogo T, Kryzskaya D, Storch KF, Kokoeva MV. (2013). Extensive regenerative plasticity among adult NG2-glia populations is exclusively based on self-renewal. Glia. 61, 1735-1747.

Robins SC, Stewart I, McNay DE, Taylor V, Giachino C, Goetz M, Ninkovic J, Briancon N, Maratos-Flier E, Flier JS, Kokoeva MV, Placzek M. (2013). A-Tanycytes of the adult hypothalamic third ventricle include distinct populations of FGF-responsive neural progenitors. Nat. Commun. 4, 2049.

Robins SC, Trudel E, Rotondi O, Liu X, Djogo T, Kryzskaya D, Bourque CW, Kokoeva MV. (2013). Evidence for NG2-glia derived, adult-born functional neurons in the hypothalamus. PLoS One. 8, e78236.

Rochefort C, Gheusi G, Vincent JD, Lledo PM. (2002). Enriched odor exposure increases the number of newborn neurons in the adult OB and improves odor memory. J. Neurosci. 22, 2679–2689.

Rodriguez EM, Blázquez JL, Pastor FE, Peláez B, Peña P, Peruzzo B, Amat P. (2005). Hypothalamic tanycytes: A key component of brain–endocrine interaction. Int. Rev. Cyt. 247, 89–164.

Rojczyk-Gołębiewska E, Pałasz A, Wiaderkiewicz R. (2014). Hypothalamic subependymal niche: A novel site of the adult neurogenesis. Cell. Mol. Neurobiol. 34, 631-642.

Rolando C, Taylor V. (2014). Neural stem cell of the hippocampus: Development, physiology regulation, and dysfunction in disease. Curr. Top Dev. Biol.107,183–206.

Roth BL. (2016). DREADDs for Neuroscientists. Neuron. 2016 Feb 17; 89(4):683-94.

Rotheneichner P, Romanelli P, Bieler L, Pagitsch S, Zaunmair P, Kreutzer C, König R, Marschallinger J, Aigner L, Couillard-Després S. (2017). Tamoxifen Activation of Cre-Recombinase Has No Persisting Effects on Adult Neurogenesis or Learning and Anxiety. Front Neurosci. 11, 27.

Rothstein JD, Martin L, Levey AI, Dykes-Hoberg M, Jin L, Wu D, Nash N, Kuncl RW. (1994). Localization of neuronal and glial glutamate transporters. Neuron. 13, 713–725.

Routh VH, Hao L, Santiago AM, Sheng Z, Zhou C. (2014). Hypothalamic glucose sensing: making ends meet. Front Syst Neurosci. 8, 236.

Rutzel H, Schliebler, TH. (1980). Prenatal and early postnatal development of the glial cells in the median eminence of the rat. Cell Tissue Res. 211, 117–137.

Ryu JK, Choi HB, Hatori K, Heisel RL, Pelech SL, McLarnon JG, Kim SU. (2003). Adenosine triphosphate induces proliferation of human neural stem cells: Role of calcium and p70 ribosomal protein S6 kinase. J Neurosci Res. 72, 352–362.

Sachs BD, Caron MG. (2014). Chronic fluoxetine increases extra-hippocampal neurogenesis in adult mice. Int. J. Neuropsychopharmacol. 18, pii: pyu029.

Sahara S, O'Leary DD. (2009). Fgf10 regulates transition period of cortical stem cell differentiation to radial glia controlling generation of neurons and basal progenitors. Neuron. 63, 48-62.

Sahay A, Wilson DA, Hen R. (2011). Pattern separation: A common function for new neurons in hippocampus and olfactory bulb. Neuron. 70, 582–588.

Sahin Kaya S, Mahmood A, Li Y, Yavuz E, Chopp M. (1999). Expression of nestin after traumatic brain injury in rat brain. Brain Res. 840, 153-157.

Sairanen M, Lucas G, Ernfors P, Castrén M, Castrén E. (2005). Brain-derived neurotrophic factor and antidepressant drugs have different but coordinated effects on neuronal turnover, proliferation, and survival in the adult dentate gyrus. J. Neurosci. 25, 1089-1094.

Sakurai T, Amemiya A, Ishii M, Matsuzaki I, Chemelli RM, Tanaka H, Williams SC, Richardson JA, Kozlowski GP, Wilson S, Arch JR, Buckingham RE, Haynes AC, Carr SA, Annan RS, McNulty DE, Liu WS, Terrett JA, Elshourbagy NA, Bergsma DJ, Yanagisawa M. (1998). Orexins and orexin receptors: A family of hypothalamic neuropeptides and G protein-coupled receptors that regulate feeding behavior. Cell. 92, 573– 585.

Salgado M, Tarifeño-Saldivia E, Ordenes P, Millán C, Yañez MJ, Llanos P, Villagra M, Elizondo-Vega R, Martínez F, Nualart F, Uribe E, de Los Angeles García-Robles M. (2014). Dynamic localization of glucokinase and its regulatory protein in hypothalamic tanycytes. PLoS One. 9, e94035.

Salvatierra J, Lee DA, Zibetti C, Duran-Moreno M, Yoo S, Newman EA, Wang H, Bedont JL, de Melo J, Miranda-Angulo AL, Gil-Perotin S, Garcia-Verdugo JM, Blackshaw S. (2014). The LIM homeodomain factor Lhx2 is required for hypothalamic tanycyte specification and differentiation. J Neurosci. 34, 16809-20.

Sanchez E, Vargas MA, Singru PS, Pascual I, Romero F, Fekete C, Charli JL, Lechan RM. (2009). Tanycyte pyroglutamyl peptidase II contributes to regulation of the hypothalamic-pituitary-thyroid axis through glial-axonal associations in the median eminence. Endocrinology. 150, 2283–2291.

Sancho-Tello M, Vallés S, Montoliu C, Renau-Piqueras J, Guerri C. (1995). Developmental pattern of GFAP and vimentin gene expression in rat brain and in radial glial cultures. Glia. 15, 157–166.

Sanders NM, Dunn-Meynell AA, Levin BE. (2004). Third ventricular alloxan reversibly impairs glucose counterregulatory responses. Diabetes. 53, 1230–1236.

Santarelli L, Saxe M, Gross C, Surget A, Battaglia F, Dulawa S, Weisstaub N, Lee J, Duman R, Arancio O, Belzung C, Hen R. (2003). Requirement of hippocampal neurogenesis for the behavioral effects of antidepressants. Science. 301, 805-809.

Santiago MF, Scemes E. (2012). Neuroblast migration and P2Y1 receptor mediated calcium signalling depend on 9-O-acetyl GD3 ganglioside. ASN Neuro. 4, 357–369.

Saper CB, Lowell BB. (2014). The hypothalamus. Curr. Biol. 24, R1111-6.

Sasaki T, Beppu K, Tanaka KF, Fukazawa Y, Shigemoto R, Matsui K. (2012). Application of an optogenetic byway for perturbing neuronal activity via glial photostimulation. Proc. Natl. Acad. Sci. USA. 109, 20720–20725.

Sato K. (2015). Effects of Microglia on Neurogenesis Glia. 63, 1394–1405

Scemes E, Duval N, Meda P. (2003). Reduced expression of P2Y1 receptors in connexin43-null mice alters calcium signaling and migration of neural progenitor cells. J. Neurosci. 23, 11444–11452.

Schmidt-Hieber C, Jonas P, Bischofberger J. (2004). Enhanced synaptic plasticity in newly generated granule cells of the adult hippocampus. Nature. 429, 184–187.

Schnitzer J, Franke WW, Schachner M. (1981). Immunocytochemical demonstration of vimentin in astrocytes and ependymal cells of developing and adult mouse nervous system. J Cell Biol. 90, 435-447.

Scholzen T, Gerdes J. (2000). The Ki-67 protein: From the known and the unknown. J. Cell. Physiol. 182, 311-322.

Schwartz MW, Woods SC, Porte D Jr, Seeley RJ, Baskin DG. (2000). Central nervous system control of food intake. Nature. 404, 661-671.

Sekerková G, Ilijic E, Mugnaini E. (2004). Bromodeoxyuridine administered during neurogenesis of the projection neurons causes cerebellar defects in rat. J. Comp. Neurol. 470, 221–239.

Seri B, García-Verdugo JM, McEwen BS, Alvarez-Buylla A. (2001). Astrocytes give rise to new neurons in the adult mammalian hippocampus. J. Neurosci. 21, 7153–7160.

Shankar P, Ahuja S, Sriram K. (2013). Non-nutritive sweeteners: Review and update. Nutrition. 29, 1293-1299.

Shearer KD, Stoney PN, Nanescu SE, Helfer G, Barrett P, Ross AW, Morgan PJ, McCaffery P. (2012). Photoperiodic expression of two RALDH enzymes and the regulation of cell proliferation by retinoic acid in the rat hypothalamus. J Neurochem. 122, 789-99.

Sidman RL, Miale IL, Feder N. (1959). Cell proliferation and migration in the primitive ependymal zone: An autoradiographic study of histogenesis in the nervous system. Exp. Neurol. 1, 322–333.

Simpson KA, Martin NM, Bloom SR. (2009). Hypothalamic regulation of food intake and clinical therapeutic applications. Arq Bras Endocrinol Metabol. 53, 120-8.

Singer BH, Gamelli AE, Fuller CL, Temme SJ, Parent JM, Murphy GG. (2011). Compensatory network changes in the dentate gyrus restore long-term potentiation following ablation of neurogenesis in young-adult mice. Proc Natl Acad Sci USA. 108, 5437–5442.

Smith KS, Bucci DJ, Luikart BW, Mahler SV. (2016). DREADDS: Use and application in behavioral neuroscience. Behav Neurosci. 130, 137-55.

Snippert HJ, van der Flier LG, Sato T, van Es JH, van den Born M, Kroon-Veenboer C, Barker N, Klein AM, van Rheenen J, Simons BD, Clevers H. (2010). Intestinal crypt homeostasis results from neutral competition between symmetrically dividing Lgr5 stem cells. Cell. 143, 134–144.

Snyder JS. (2018). Questioning human neurogenesis. Nature. 555, 315-316.

Snyder JS, Kee N, Wojtowicz JM. (2001). Effects of adult neurogenesis on synaptic plasticity in the rat dentate gyrus. J Neurophysiol. 85, 2423-31.

Solek CM, Ekker M. (2012). Cell lineage tracing techniques for the study of brain development and regeneration. Int. J. Dev. Neurosci. 30, 560-569.

Song J, Zhong C, Bonaguidi MA, Sun GJ, Hsu D, Gu Y, Meletis K, Huang ZJ, Ge S, Enikolopov G, Deisseroth K, Luscher B, Christian KM, Ming GL, Song H. (2012). Neuronal circuitry mechanism regulating adult quiescent neural stem-cell fate decision. Nature. 489, 150-154.

Song J, Sun J, Moss J, Wen Z, Sun GJ, Hsu D, Zhong C, Davoudi H, Christian KM, Toni N, Ming GL, Song H. (2013). Parvalbumin interneurons mediate neuronal circuitry-neurogenesis coupling in the adult hippocampus. Nat. Neurosci. 16, 1728-1730.

Song M, Yu SP, Mohamad O, Cao W, Wei ZZ, Gu X, Jiang MQ, Wei L. (2017). Optogenetic stimulation of glutamatergic neuronal activity in the striatum enhances neurogenesis in the subventricular zone of normal and stroke mice. Neurobiol. Dis. 98, 9-24.

Song Z, Levin BE, McArdle JJ, Bakhos N, Routh VH. (2001). Convergence of pre- and postsynaptic influences on glucosensing neurons in the ventromedial hypothalamic nucleus. Diabetes. 50, 2673–2681.

Sorrells SF, Paredes MF, Cebrian-Silla A, Sandoval K, Qi D, Kelley KW, James D, Mayer S, Chang J, Auguste KI, Chang EF, Gutierrez AJ, Kriegstein AR, Mathern GW, Oldham MC, Huang EJ, Garcia-Verdugo JM, Yang Z, Alvarez-Buylla A. (2018). Human hippocampal neurogenesis drops sharply in children to undetectable levels in adults. Nature. 555, 377-381.

Sousa-Ferreira L, Almeida LP, Cavadas C. (2014). Role of hypothalamic neurogenesis in feeding regulation. Trends Endocrinol Metab. 25, 80–88.

Spalding KL, Bergmann O, Alkass K, Bernard S, Salehpour M, Huttner HB, Boström E, Westerlund I, Vial C, Buchholz BA, Possnert G, Mash DC, Druid H, Frisén J. (2013). Dynamics of hippocampal neurogenesis in adult humans. Cell. 153, 1219–1227.

Spassky N, Merkle FT, Flames N, Tramontin AD, García-Verdugo JM, Alvarez-Buylla A. (2005). Adult ependymal cells are postmitotic and are derived from radial glial cells during embryogenesis. J. Neurosci. 25, 10–18.

Sorrells SF, Paredes MF, Cebrian-Silla A, Sandoval K, Qi D, Kelley KW, James D, Mayer S, Chang J, Auguste KI, Chang EF, Gutierrez AJ, Kriegstein AR, Mathern GW, Oldham MC, Huang EJ, Garcia-Verdugo JM, Yang Z, Alvarez-Buylla A. (2018). Human hippocampal neurogenesis drops sharply in children to undetectable levels in adults. Nature. 555, 377-381.

Stoney PN, Helfer G, Rodrigues D, Morgan PJ, McCaffery P. (2016). Thyroid hormone activation of retinoic acid synthesis in hypothalamic tanycytes. Glia. 64, 425-39.

Sun X, Ji C, Hu T, Wang Z, Chen G. (2013). Tamoxifen as an effective neuroprotectant against early brain injury and learning deficits induced by subarachnoid hemorrhage: possible involvement of inflammatory signaling. J Neuroinflammation. 10, 157.

Sun MY, Yetman MJ, Lee TC, Chen Y, Jankowsky JL. (2014). Specificity and efficiency of reporter expression in adult neural progenitors vary substantially among nestin-CreER(T2) lines. J Comp Neurol. 522, 1191-208.

Suyama S, Sunabori T, Kanki H, Sawamoto K, Gachet C, Koizumi S, Okano H. (2012), Purinergic signaling promotes proliferation of adult mouse subventricular zone cells. J Neurosci. 32, 9238-47.

Suzuki S, Namiki J, Shibata S, Mastuzaki Y, Okano H. (2010). The Neural Stem/Progenitor Cell Marker Nestin Is Expressed in Proliferative Endothelial Cells, but Not in Mature Vasculature. J Histochem Cytochem. 58, 721–730

Takamori Y, Mori T, Wakabayashi T, Nagasaka Y, Matsuzaki T, Yamada H. (2009). Nestin-positive microglia in adult rat cerebral cortex. Brain Res. 1270, 10-8.

Tang Y, Illes P. (2017). Regulation of adult neural progenitor cell functions by purinergic signaling. Glia. 65, 213-230

Tantama M, Martínez-François JR, Mongeon R, Yellen G. (2013). Imaging energy status in live cells with a fluorescent biosensor of the intracellular ATP-to-ADP ratio. Nat Commun. 4, 2550.

Taupin, P. (2007). BrdU immunohistochemistry for studying adult neurogenesis: Paradigms, pitfalls, limitations, and validation. Brain Res. Rev. 53, 198–214.

Tavazoie M, Van der Veken L, Silva-Vargas V, Louissaint M, Colonna L, Zaidi B, Garcia-Verdugo JM, Doetsch F. (2008). A specialized vascular niche for adult neural stem cells. Cell. Stem Cell. 3, 279–288.

Thaler JP, Yi CX, Schur EA, Guyenet SJ, Hwang BH, Dietrich MO, Zhao X, Sarruf DA, Izgur V, Maravilla KR, Nguyen HT, Fischer JD, Matsen ME, Wisse BE, Morton GJ, Horvath TL, Baskin DG, Tschöp MH, Schwartz MW. (2012). Obesity is associated with hypothalamic injury in rodents and humans. J. Clin. Invest. 122, 153–162.

The Jackson Laboratory. [ONLINE] Available at: https://www2.jax.org/protocolsdb/f?p=116:5:0::NO:5:P5_MASTER_PROTOCOL_ID,P5_JRS_CODE:22392,016261 [Accessed: 05 September 2018].

Theodosis DT, Koksma JJ, Trailin A, Langle SL, Piet R, Lodder JC, Timmerman J, Mansvelder H, Poulain DA, Oliet SH, Brussaard AB. (2006). Oxytocin and estrogen promote rapid formation of functional GABA synapses in the adult supraoptic nucleus. Mol. Cell. Neurosci. 31, 785–794.

Thomzig A, Laube G, Prüss H, Veh RW. (2005). Pore-forming subunits of K-ATP channels, Kir6.1 and Kir6.2, display prominent differences in regional and cellular distribution in the rat brain. J. Comp. Neurol. 484, 313–330.

Ulrich H, Abbracchio MP, Burnstock G. (2012). Extrinsic purinergic regulation of neural stem/progenitor cells: Implications for CNS development and repair. Stem Cell Rev. 8, 755–767

Uranga RM, Millán C, Barahona MJ, Recabal A, Salgado M, Martinez F, Ordenes P, Elizondo-Vega R, Sepúlveda F, Uribe E, García-Robles MLÁ. (2017). Adenovirus-mediated suppression of hypothalamic glucokinase affects feeding behavior. Sci Rep. 7, 3697.

van Praag H, Christie BR, Sejnowski TJ, Gage FH. (1999). Running enhances neurogenesis, learning, and long-term potentiation in mice. Proc. Natl. Acad. Sci. USA. 96, 13427-13431.

van Praag H, Schinder AF, Christie BR, Toni N, Palmer TD, Gage FH. (2002). Functional neurogenesis in the adult hippocampus. Nature. 415, 1030-1034.

Verberne AJ, Sabetghadam A, Korim WS. (2014). Neural pathways that control the glucose counterregulatory response. Front Neurosci. 8, 38.

Vescovi AL, Parati EA, Gritti A, Poulin P, Ferrario M, Wanke E, Frölichsthal-Schoeller P, Cova L, Arcellana-Panlilio M, Colombo A, Galli R. (1999). Isolation and cloning of multipotential stem cells from the embryonic human CNS and establishment of transplantable human neural stem cell lines by epigenetic stimulation. Exp. Neurol. 156, 71−83.

Vivar C, Potter MC, van Praag H. (2013). All about running: Synaptic plasticity, growth factors and adult hippocampal neurogenesis. Curr. Top Behav. Neurosci. 15, 189-210.

von Bartheld CS, Bahney J, Herculano-Houzel S. (2016). The search for true numbers of neurons and glial cells in the human brain: A review of 150 years of cell counting. J. Comp. Neurol. 524, 3865-3895.

Walker AS, Goings GE, Kim Y, Miller RJ, Chenn A, Szele FG. (2010). Nestin reporter transgene labels multiple central nervous system precursor cells. Neural Plast. 2010, 894374.

Wang X, Lee JE, Dorsky RI. (2009). Identification of Wnt-responsive cells in the zebrafish hypothalamus. Zebrafish. 6, 49–58.

Wang TW, Zhang H, Gyetko MR, Parent JM. (2011a). Hepatocyte growth factor acts as a mitogen and chemoattractant for postnatal subventricular zone-olfactory bulb neurogenesis. Mol Cell Neurosci. 48, 38–50.

Wang YZ, Plane JM, Jiang P, Zhou CJ, Deng W. (2011b). Concise review: Quiescent and active states of endogenous adult neural stem cells: identification and characterization. Stem Cells. 29, 907-912.

Watts AG, Donovan CM. (2010). Sweet talk in the brain: glucosensing, neural networks, and hypoglycemic counterregulation. Front Neuroendocrinol. 31, 32-43.

Weiss S, Dunne C, Hewson J, Wohl C, Wheatley M, Peterson AC, Reynolds BA. (1996). Multipotent CNS stem cells are present in the adult mammalian spinal cord and ventricular neuroaxis. J. Neurosci. 16, 7599–7609.

Weissman TA, Riquelme PA, Ivic L, Flint AC, Kriegstein AR. (2004). Calcium waves propagate through radial glial cells and modulate proliferation in the developing neocortex. Neuron. 43, 647–661.

Weissman TA, Sanes JR, Lichtman JW, Livet J. (2011). Generating and imaging multicolor Brainbow mice. Cold Spring Harb Protoc. 2011 (7), 763–769.

Weissman TA, Pan YA. (2015). Brainbow: new resources and emerging biological applications for multicolor genetic labeling and analysis. Genetics. 199, 293-306.

Whitman MC, Greer CA. (2009). Adult neurogenesis and the olfactory system. Prog. Neurobiol. 89, 162–175.

Wilson A, Laurenti E, Oser G, van der Wath RC, Blanco-Bose W, Jaworski M, Offner S, Dunant CF, Eshkind L, Bockamp E, Lió P, Macdonald HR, Trumpp A. (2008). Hematopoietic stem cells

reversibly switch from dormancy to self-renewal during homeostasis and repair. Cell. 135, 1118-29.

Wu W, Wong K, Chen J, Jiang Z, Dupuis S, Wu JY, Rao Y. (1999). Directional guidance of neuronal migration in the olfactory system by the protein Slit. Nature. 400, 331–336.

Xu Y, Tamamaki N, Noda T, Kimura K, Itokazu Y, Matsumoto N, Dezawa M, Ide C. (2005). Neurogenesis in the ependymal layer of the adult rat 3rd ventricle. Exp. Neurol. 192, 251–264.

Yaginuma H, Kawai S, Tabata KV, Tomiyama K, Kakizuka A, Komatsuzaki T, Noji H, Imamura H. (2014). Diversity in ATP concentrations in a single bacterial cell population revealed by quantitative single-cell imaging. Sci Rep. 4, 6522.

Yamashita S, Katsumata O. (2017). Heat-Induced Antigen Retrieval in Immunohistochemistry: Mechanisms and Applications. Methods Mol Biol. 1560, 147-161

Yang L, Qi Y, Yang Y. (2015). Astrocytes control food intake by inhibiting AGRP neuron activity via adenosine A1 receptors. Cell Rep. 11, 798-807

Yang Q. (2010). Gain weight by "going diet?" Artificial sweeteners and the neurobiology of sugar cravings: Neuroscience 2010. Yale J. Biol. Med. 83, 101-108.

Yang SB, Tien AC, Boddupalli G, Xu AW, Jan YN, Jan LY. (2012). Rapamycin ameliorates age-dependent obesity associated with increased mTOR signaling in hypothalamic POMC neurons. Neuron. 75, 425–436.

Yawo H, Asano T, Sakai S, Ishizuka T. (2013) Optogenetic manipulation of neural and non-neural functions. Dev. Growth Differ. 55, 474-490.

Yokoyama A, Yang L, Itoh S, Mori K, Tanaka J. (2004). Microglia, a potential source of neurons, astrocytes, and oligodendrocytes. J. Glia. 45, 96-104.

Yoo S, Blackshaw S. (2018). Regulation and function of neurogenesis in the adult mammalian hypothalamus. Prog Neurobiol. 170, 53-66.

Yuan TF, Arias-Carrion O. (2011). Adult neurogenesis in the hypothalamus: Evidence, functions and implications. CNS Neurol. Disord. Drug Targets. 10, 433–439.

Yuan TF, Paes F, Arias-Carrión O, Ferreira Rocha NB, de Sá Filho AS, Machado S. (2015). Neural Mechanisms of Exercise: Anti-Depression, Neurogenesis, and Serotonin Signaling. CNS Neurol Disord Drug Targets. 14, 1307-11.

Zeng H, Madisen L. (2012). Mouse transgenic approaches in optogenetics. Prog. Brain Res. 196, 193-213.

Zhang G, Li J, Purkayastha S, Tang Y, Zhang H, Yin Y, Li B, Liu G, Cai D. (2013). Hypothalamic programming of systemic ageing involving IKK-beta, NF-kappaB and GnRH. Nature. 9, 211–216.

Zhao C, Deng W, Gage FH. (2008). Mechanisms and functional implications of adult neurogenesis. Cell. 132, 645-660.

Zhao C, Teng EM, Summers RG Jr, Ming GL, Gage FH. (2006). Distinct morphological stages of dentate granule neuron maturation in the adult mouse hippocampus. J. Neurosci. 26, 3-11.

Zhao M, Momma S, Delfani K, Carlen M, Cassidy RM, Johansson CB, Brismar H, Shupliakov O, Frisen J, Janson AM. (2003). Evidence for neurogenesis in the adult mammalian substantia nigra. Proc. Natl. Acad. Sci. USA. 100, 7925–7930.

Zimmerman L, Parr B, Lendahl U, Cunningham M, McKay R, Gavin B, Mann J, Vassileva G, McMahon A. (1994). Independent regulatory elements in the nestin gene direct transgene expression to neural stem-cells or muscle precursors. Neuron. 12, 11–24.